UNIVERSITY OF LONDON

Imperial College of Science and Technology

Department of Physics, Applied Optics Section.

# AN EXPERIMENTAL STUDY OF SOME MATHEMATICAL MODELS OF THE VISUAL MACH EFFECT.

by

RACHANEE LEELAWONGS

Thesis submitted for the Ph.D. degree

## ABSTRACT

Some of the mathematical models of the Mach effect which have been proposed since Mach's time are reviewed and numerically calculated, to obtain the predicted subjective luminance distributions from an abrupt edge and from the edges of various luminance gradients and contrasts. A new model is proposed and the model of Fry is modified. Both of these models give substantially the same subjective distribution for the same viewed luminance distribution, even though they propose different forms of inhibitory response due to distance from points lying around a particular point on the retina.

The visual Mach effect has been studied on an abrupt aluminized edge on a clear glass plate and on various luminance gradients and contrasts on the photographic edge gradients which are produced with a variety of profiles. The characteristics of the bands seen on the edges have been measured under incoherent illumination.

When the widths, positions, and brightnesses of the observed bands were compared with those calculated from mathematical models as well as with those predicted by Ludvigh's second derivative theory of perception of visual Mach bands, some agreements between them were obtained. Some

models predict bright bands approximately in the same positions as the minima of the second derivative of the luminance distribution with respect to the distance along the retina.

It has been found that the individual variations in seeing the Mach pattern are great. This makes it a difficult task to decide as to exactly which model is in the best agreement with experimental results.

CONTENTS


| | | Page |
|---|---|---|
| ABSTRACT .. .. .. .. | | 1 |
| CHAPTER I | THE PERCEPTION OF THE MACH EFFECT. | |
| 1:1 | Introduction to Mach Bands .. | 6 |
| 1:2 | Factors Affecting the Perception of Bands .. .. .. | 14 |
| 1:3 | The Visual Paths .. .. | 32 |
| 1:4 | The Retinal Mechanisms .. .. | 35 |
| 1:5 | Predictions on the Locations of Mach Bands .. .. .. | 49 |
| CHAPTER II | MATHEMATICAL MODELS OF THE MACH EFFECT. | |
| 2:1 | Introduction.. .. .. | 55 |
| 2:2 | Mach's Model.. .. .. | 60 |
| 2:3 | Fry's Model .. .. .. | 66 |
| 2:4 | The Model of Hartline and Ratliff .. | 72 |
| 2:5 | Taylor's Model .. .. | 75 |
| 2:6 | O'Brien's Model .. .. | 82 |
| 2:7 | Békésy's Model .. .. | 86 |
| 2:8 | Discussion .. .. .. | 93 |

| | | Page |
|---|---|---|
| CHAPTER III | THE MACH EFFECT AT AN ABRUPT EDGE. | |
| 3:1 | Introduction .. .. | 108 |
| 3:2 | The Physical Distribution of Illumination in an Edge Image and its Derivatives .. .. | 116 |
| 3:3 | The Visual Mach Bands.. .. | 125 |
| 3:4 | The Mach Bands Predicted by Mathematical Models .. .. | 136 |
| 3:5 | Discussion.. .. .. | 147 |
| CHAPTER IV | CALCULATIONS OF THE VISUAL IMAGES OF EXPERIMENTALLY PRODUCED GRADIENTS. | |
| 4:1 | General .. .. .. | 152 |
| 4:2 | The Production of Graded Luminance Distributions .. .. | 163 |
| 4:3 | The Retinal Image Distribution and its Derivatives .. .. | 172 |
| 4:4 | Theoretical Subjective Luminance Distributions .. .. | 189 |
| CHAPTER V | AN EXPERIMENTAL STUDY OF GRADED LUMINANCE PROFILES. | |
| 5:1 | Introduction .. .. | 202 |
| 5:2 | The Apparatus .. .. | 205 |
| 5:3 | Measurements and Results .. | 213 |
| 5:4 | Discussion.. .. .. | 231 |

| | | Page |
|---|---|---|
| CHAPTER VI | DISCUSSION AND CONCLUSION. | 235 |
| APPENDIX A | The Intensity of the Edge Image and its Derivatives. .. .. | 246 |
| APPENDIX B | Computer Programmes. .. .. | 251 |
| REFERENCES. | .. .. .. | 259 |
| ACKNOWLEDGEMENTS. | .. .. .. | 264 |


———:::::::::———

# CHAPTER I

## THE PERCEPTION OF THE MACH EFFECT.

### 1:1. Introduction to Mach Bands.

When a field in which a luminance gradient exists between two uniform bright and dark areas is viewed under suitable conditions, a bright line will be perceived at the contrast border between the gradient and the higher luminance level and a dark line at the junction of the gradient and the lower luminance level. The lines can also be seen in a less steep luminance gradient, but the bright and the dark lines are somewhat weaker and less distinct. It is not essential that the field of view be the one mentioned above, a bright or a dark line may be visible where there is an inflection in the light curve . The phenomenon is purely subjective since it cannot be detected by any light detector; physical measurement of the luminance involved shows no luminance higher or lower than the two between which the gradient exists. These lines are known as 'Mach bands' after Ernst Mach, an Austrian physicist, psychologist and philosopher, who first observed them in 1865.

One who is familiar with the phenomenon can observe the bands easily at the edges of almost any shadow cast on a fairly uniform surface by an object in the sunlight. The transition from the umbra to the graded penumbra provides a dark band; the transition from the penumbra to the fully illuminated area provides a bright band. Even indoors, Mach bands can be seen at the edge of a shadow cast on a piece of white paper by an object held close to the paper under a lamp which provides the necessary extended source of light. The bright line, however , is more prominent than the dark one.

Mach (1865,1866 a-b,1868 a-b,1906) regarded this phenomenon as a 'simultaneous contrast phenomenon'. Much work had been carried out with some assisstance from his son. The results can be summarized as follows:

1). On rotating a disc with a certain shape of white or dark sectors on a dark or white background respectively with a sufficient angular velocity, he noted that at every point where the intensity distribution had an inflection, a brighter or a darker line than the surroundings would be perceived. The location of the line was roughly determined by the point of inflection of the light distribution. The point where the inflection was concave towards the axis

representing the distance along the retina showed a bright line while the point of convex inflection showed a dark line as illustrated in figure 1:1. Point A on the luminance distribution curve, concave towards the abscissa, gives a subjective bright band. A subjective dark band is seen at B where the inflection is convex towards the abscissa.

2). The phenomenon was purely subjective since the physical intensity distribution calculated by using the Talbot-Plateau law did not show any higher or lower intensity at the point where the bright or the dark line was seen. Thus Mach concluded that the cause was not in the object, but in the visual mechanism of the eye.

3). The bands were observed under the electric spark light from a Leyden jar, which is rapid enough to eliminate eye-movement; it was inferred that the phenomenon did not result from eye-movement. Mach suggested that the phenomenon was based on a reciprocal action of the neighbouring areas of the retina; the neighbouring retina elements had a physical relation to one another. The intensity of sensation of an area could be different for equal intensities of illumination of the area, due to the influence of its neighbours.

4). The bands were very distinctly seen when their

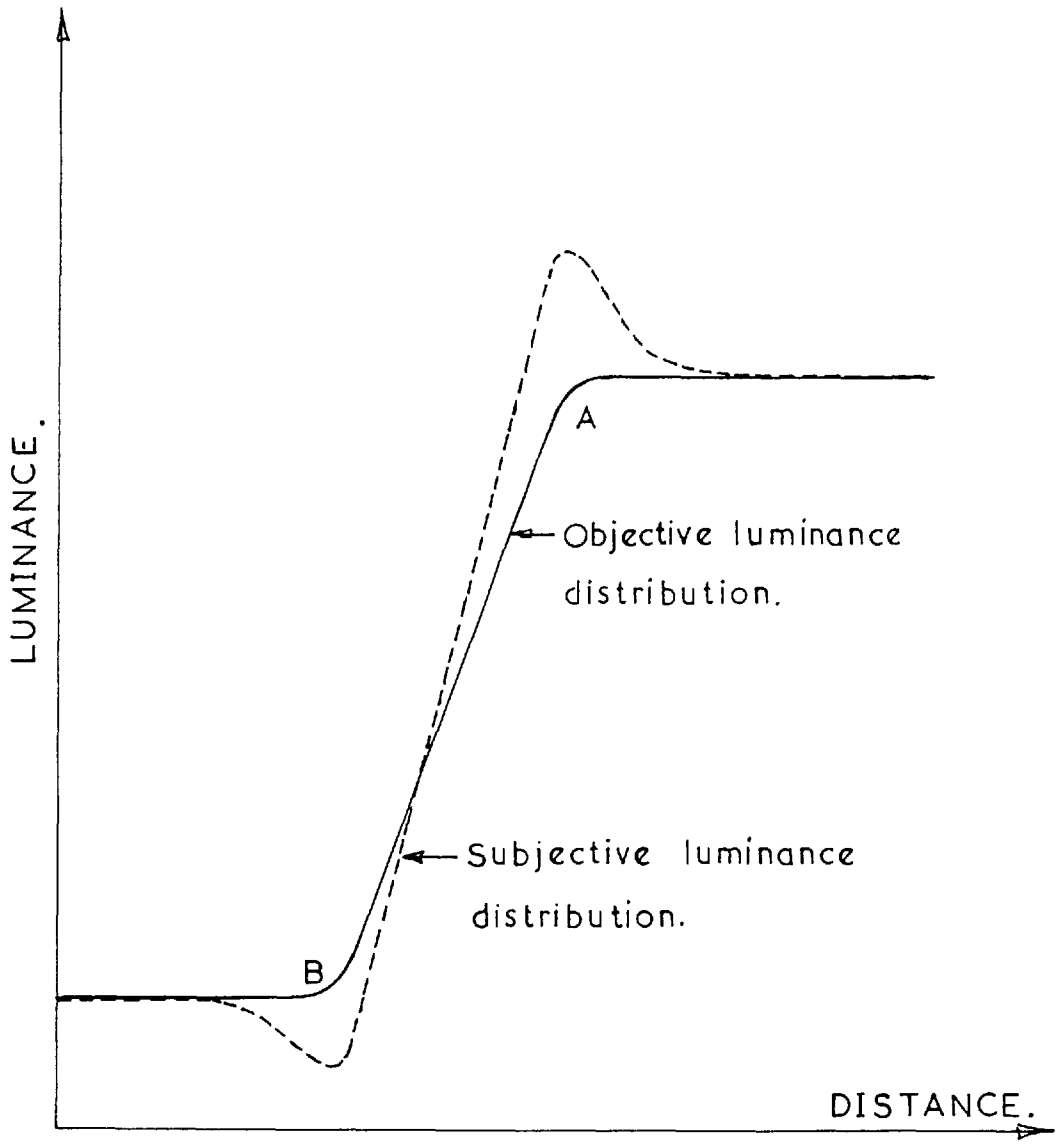



Fig. I:I. Diagrammatic representation of the Mach phenomenon.

images were fixated on the fovea, but they would disappear when the fixation point of the eye was about three degrees to one side.

5). Mach suggested a relation between retinal illumination and sensation of the form,

$$F = a \log\left(\frac{I}{b} \pm \frac{k}{I}(d^2I/dx^2)\right), \quad \ldots\ldots\ldots (1:1)$$

where I is the objective brightness at the retinal coordinate x; F is the sensation ; a, b, and k are constants; and the upper sign holds for a negative value of $d^2I/dx^2$.The equation was considered to be verified from the following observed facts:-

a). In observing bright and dark lines in bright sunshine, twilight and candle light, Mach found that the lines remained equally distinct, that is, the lines remained unchanged when the light curve $I = f(x)$ was changed to $I = q.f(x)$.

b). The lines disappeared when the light curve $I = f(x)$ was changed to $I = p + f(x)$, where p is positive and large.

c). The distinctness of the line was an increasing function of $d^2I/dx^2$.

Furthermore, he noted that even though the lines were visible on the rotating disc, the brightening and darkening were insignificant and the disturbance due to

the surrounding conditions too great to permit accurate measurements. The facts were about as well represented if the equation was;

$$F = a \log \left( \frac{I}{b} - \frac{k}{rI} \right), \qquad \ldots\ldots\ldots(1:2)$$

where r is the radius of curvature of the light curve at the point involved.

Both equations 1:1 and 1:2 are only approximate; they are no longer valid when $d^2I/dx^2$ becomes very large, or when r is very small.

6). In 1868, another expression for the sensation was derived by Mach from the assumption that the two retinal points had a smaller reciprocal action on one another if they were further away from each other. The expression is;

$$F_p = I_p \cdot \frac{I_p \sum \phi(r) \triangle v}{\sum I_j \, \phi(r) \triangle v}, \qquad \ldots\ldots\ldots(1:3)$$

where $I_p$ is the retinal distribution at a particular point p. $I_j$ signifies the intensity on each of the several separate neighbouring points j, each of a small area $\triangle v$. $\phi(r)$ is a funtion of the reciprocal action between two retinal points and is determined by the distance between them.

From this equation, another expression was derived,

$$F = I \cdot \frac{I}{I + \frac{k}{2} \left( \frac{d^2I}{dx^2} + \frac{d^2I}{dy^2} \right)}, \qquad \ldots\ldots\ldots(1:4)$$

where k is a constant.

When the diameter W of the pupil of the eye was introduced,

$$F = WI. \frac{I}{I + \frac{k}{2}\left(\frac{d^2I}{dx^2} + \frac{d^2I}{dy^2}\right)}. \qquad .....(1:5)$$

If the intensity of the illumination was increased p fold,

$$F' = \frac{W}{p}.pI. \frac{pI}{pI + \frac{pk}{2}\left(\frac{d^2I}{dx^2} + \frac{d^2I}{dy^2}\right)} = F . \qquad .....(1:6)$$

If the intensity of illumination was increased by an amount a,

$$F' = \frac{WI}{a+I}.(a+I). \frac{a + I}{a+I+ \frac{k}{2}\left(\frac{d^2I}{dx^2} + \frac{d^2I}{dy^2}\right)} , \qquad .....(1:7)$$

and if a became large, the influence of the second derivative term would diminish.

From these equations it can be seen that it is not only I which influences the sensation but also its second derivatives. And since the structure of the retina is not everywhere uniform and equally fine, the equations are not universal; they can only be regarded as an approximate representation of the phenomenon.

The effect has been investigated widely in detail since the beginning of this century. McDougall(1903),Thouless (1922-3), and Ludvigh(1953) used the same method as Mach in

order to produce artificial luminance gradients and studied the characteristics of the bands. Ludvigh showed that the amount of the change in flux density or illumination energy on the retina has little effect upon the appearance of the bands; the lowest derivative of flux density with respect to the retinal distance which is significant for perception of the bands is the second. Fiorentini, Jeanne and Toraldo di Francia (1955), McCollough (1955), Hartwig (1958) and Fiorentini (1956) have studied the effect by observing the luminance distribution of a penumbral shadow of an illuminated straight edge. Every observer reported only one bright and one dark band seen in the dark and bright regions respectively.

Looking through a microscope onto a slide of an aluminized straight edge, Watrasiewicz (1963) was able to see at least one bright and two dark bands on the dark side of the edge. He called them " the multiple Mach bands". The effect has been shown to play an important role in the microscopy where small sharp-edged particles are observed; the visual bands occurring on the edge of the image can cause an error in sizing. Furthermore, they can give rise to spurious detail in the image.

It was found that the multiple Mach bands

could also be seen when one looked directly at a knife edge through an eye pupil of which the size was restricted to be under a certain value ( Leelawongs 1964 ).

Many factors, found both in microscopic and macroscopic vision, influence the widths, positions, brightnesses and occurrence of the bands. Many mathematical expressions have been proposed to predict the phenomenon. So far, they are not very successful since the mechanism of the eye is highly complicated. A number of hypotheses explaining various mechanisms for the perception of the bands have been proposed which will be discussed later.

## 1:2 Factors Affecting the Perception of Bands.

Several factors are found to influence the phenomenon. The various ways in which the object is illuminated together with the distribution over it of the light intensity will be considered, and also many factors of the eye which influence the effect will be discussed.

It is well known that the wavelength of light used to illuminate the object has an influence on the sensitivity of the eye. In low intensity or scotopic vision, the sensitivity of the eye is a maximum to light of wavelength 0.510 micron; the maximum is at 0.555 micron in

wavelength in high intensity or photopic vision. Figure 1:2 shows the effect of changing the wavelength of the light, microscopically observed on a sharp border between dark and bright fields by Watrasiewicz (1963). The changes in the locations and the widths of the bands are noted. In the figure, the abscissa units are the dimensionless units in diffraction theory, defined by

$$Z = \frac{2\pi}{\lambda}(N.A)\eta \quad , \qquad \ldots\ldots\ldots\ldots\ldots\ldots\ldots(1:8)$$

where $\eta$ is actual distance in the object space, (N.A) is the numerical aperture of the objective, and $\lambda$ is the wavelength of light used.

From the figure, it is obvious that an exact conclusion on the relation between the nature of the effect and the wavelength still cannot be drawn.

The mode of illumination of the object is another important factor, as shown in figure 1:3, where S can be regarded as a measure of the degree of coherence; it is the ratio between the numerical aperture of the condenser and that of the objective. Thus, S = infinity, and S = 0 correspond to a complete incoherence and perfect coherence respectively. When S has a finite value the illumination is partially coherent.

It was found that the bright band shifts to

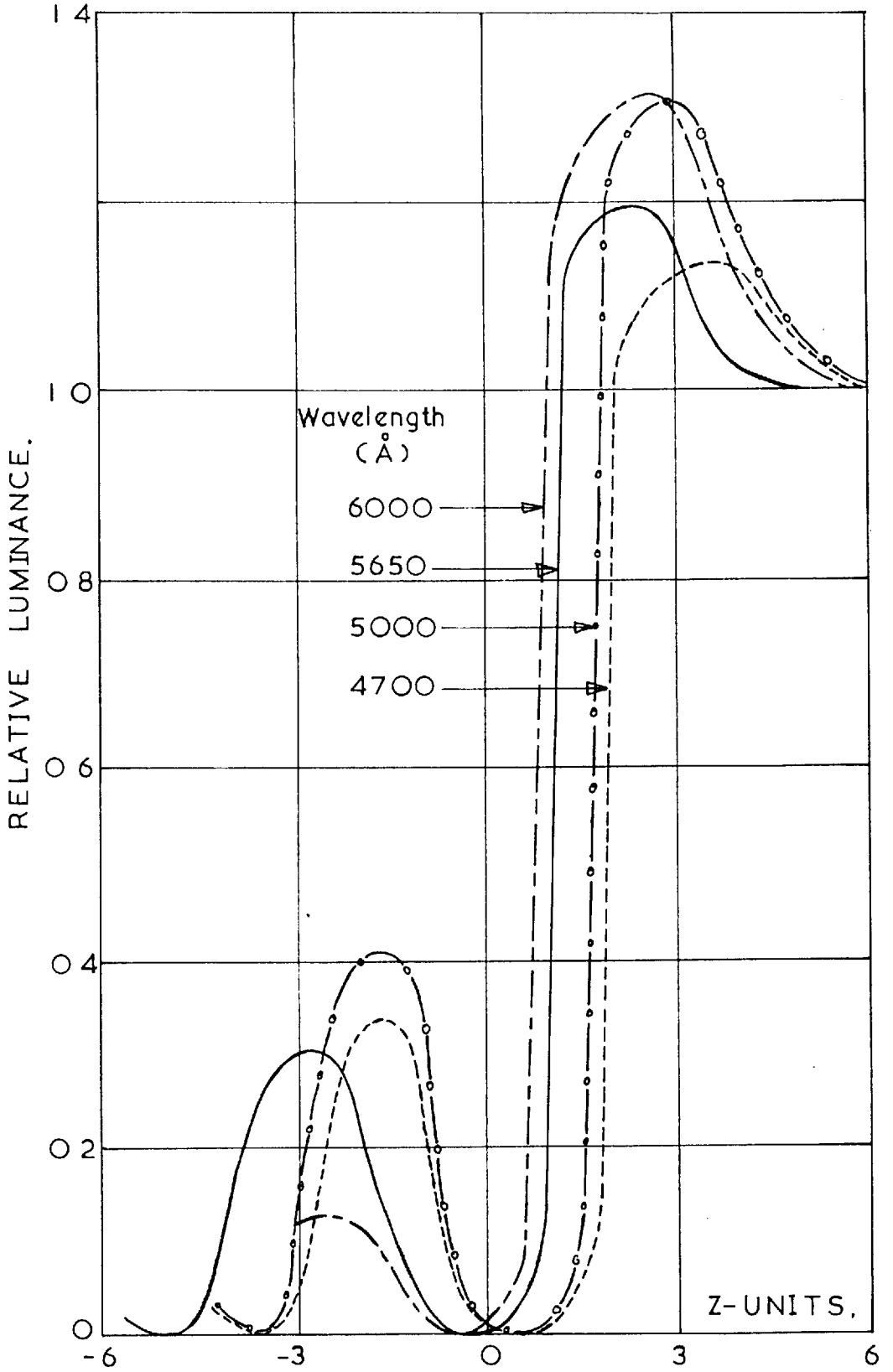



Fig. 1:2. Effect of wavelength of light on the Mach phenomena. (Watrasiewicz 1963).

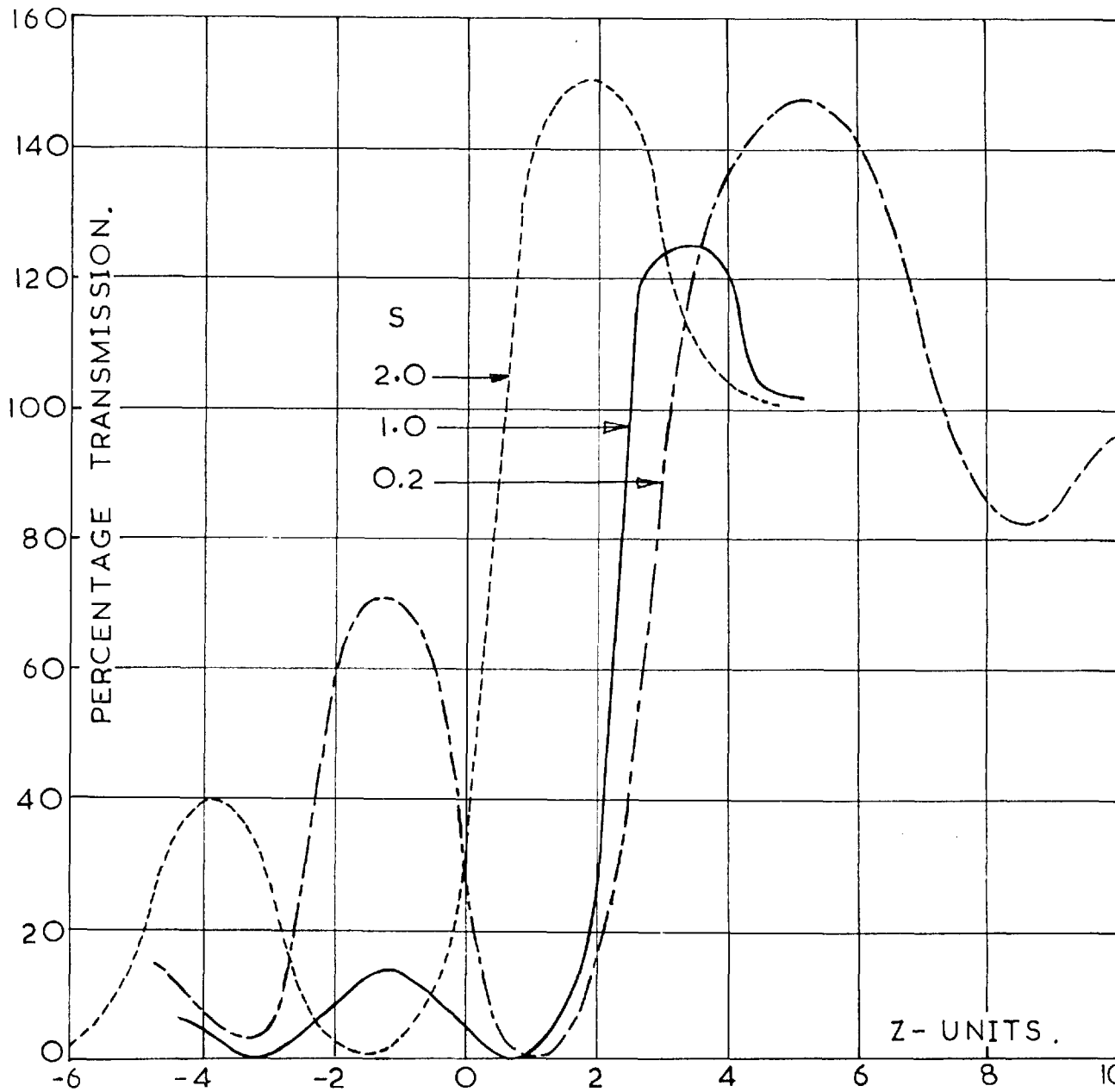



Fig. 1:3. Influence of mode of illumination (S) on the Mach effect. (Charman and Watrasiewicz 1964).

the dark side of the geometrical edge when the mode of illumination is changed from coherence to an incoherence.

The influence of the intensity distribution in the object on the phenomenon has been studied by many observers. It has been concluded that the exact appearance of the bands in any case is dependent upon the luminance level, the luminance gradient and the contrast between the object and the surroundings. This is contradictory to Mach's result who found no change in the distinctness of the subjective impression when observing the dark and bright bands on the rotating disc at various luminance levels. However, when the detailed response of the eye to these factors is considered it can be seen that several changes are involved at the same time. The luminance level can cause changes in the visual acuity and sensitivity of the eye. The visual acuity of the eye is improved with increase in the level of the illumination. Furthermore, the luminosity curve for scotopic or low intensity vision ( luminance level below 10 candelas per square metre) is different from that for photopic or high intensity vision (luminance level above 100 candelas per square metre ). According to the duplicity theory, high intensity vision is mediated through the cones, and low intensity vision through the rods. Thus a change in perception is expected

when a change in the luminance level occurs.

Ercoles and Fiorentini (1959) noted that bands are not visible at low luminance levels and the threshold of the perception for the dark band is higher than that for the bright band.The ratio required for the visibility of the dark band is about four times greater than that for the bright band. Furthermore, in 1955, Mc Collough found that the width of the bright band decreases and that it shifts towards the dark side of the edge as the luminance is increased, while the luminance gradient remains constant. At higher luminance level, the width of the band tends to a constant value. When the luminance gradient is increased and the luminance level is held constant, the width of the bright band will decrease. In 1958, Fiorentini and Radici reported that the luminance gradient must exceed a certain minimum for the bands to be perceived. The minimum value of the luminance gradient at which the bands disappear depends on the luminance level and the contrast of the object. When the luminance difference between the dark and the bright areas of the object is increased the bands become narrower. Similarly, when the slope of the luminance gradient is increased the bands will be narrower and more distinct and, according to these authors, they will disappear when the slope becomes an abrupt one.In fact, when one looks at a

sharp transition or an abrupt edge, owing to the diffraction and aberrations of the eye, the image appearing on the retina will not have the same transition of luminance as that of the object. It yields a slope which is not infinite. Under suitable conditions of observation, the Mach bands can be seen. This will be discussed in more detail in Chapter III.

Lowry and DePalma (1961) also showed how the widths of the bands change when the luminance gradient is altered, but little change in amplitudes is noted. This is shown in figure 1:4; the bright band is more pronounced than the dark one. They also concluded that for a really sharp transition edge the eye may not be able to distinguish any band differing in apparent luminance from the objective luminance. The effect of contrast was also studied by Ronchi, Bittini and Adachi in 1963; they observed that the visibility or the sharpness of the bands varies according to the contrast of the object.

As has been mentioned, the eye itself is an essential factor in such subjective phenomena. Diffraction and aberrations of the eye cause blurring of the retinal image. Furthermore, the image itself has some movements on the retina even if we attempt to fix the eye steadily on an object. This is owing to involuntary movements of the

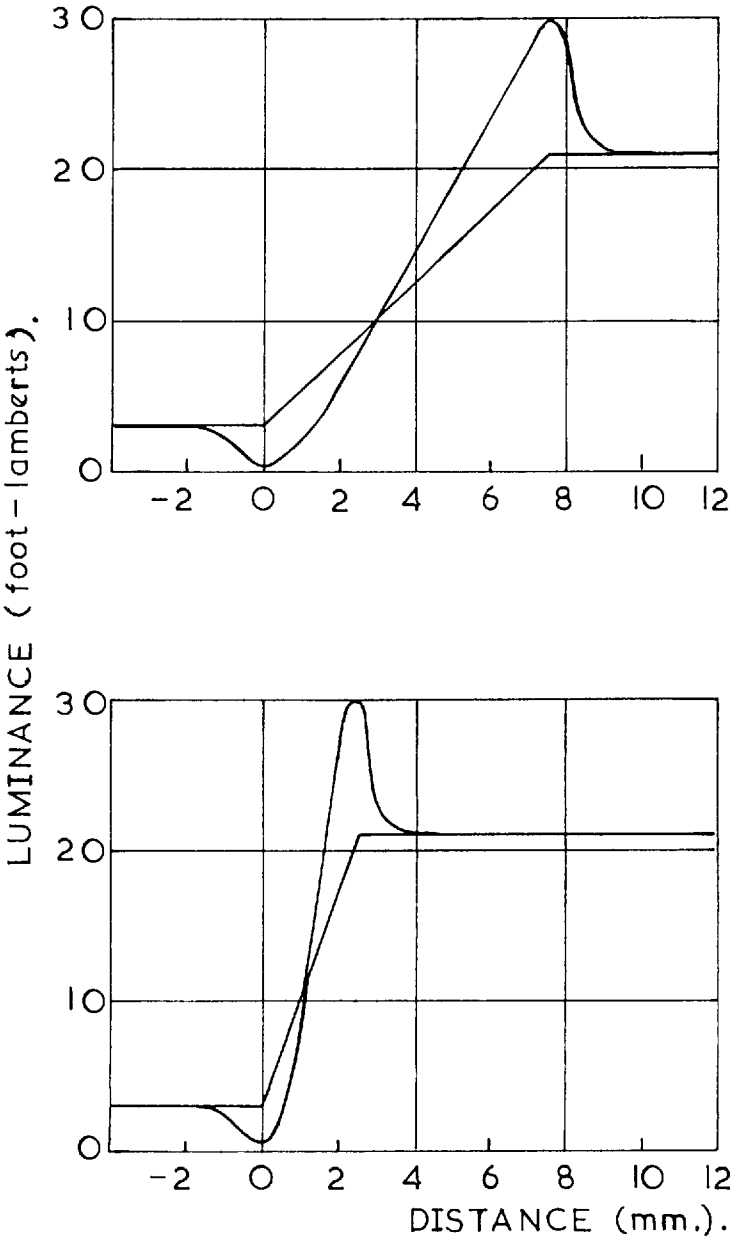



Fig. 1:4. Influence of luminance gradient on the visual Mach bands (Lowry and De Palma 1961).

eye. These involuntary movements have been widely investigated by many observers, such as, Ditchburn and Ginsborg (1953), Fender (1955), and Ditchburn (1955) who used a lens tightly contacted to the eye reflecting a light beam onto a recording apparatus. The movements are divided into three types; i) tremors, ii) flicks or sacades, and, iii) drifts. The effect of tremors is to move the retinal image back and forth 30 to 100 times per second. The shifts produced by tremors are very small. The mean amplitude of tremors corresponds to a displacement smaller than the width of a single receptor in the fovea, while the maximum amplitudes correspond to two or three receptor widths. The drifts make the image shift slowly across a few cones. Cornsweet (1956) suggested that the drifts are not under direct visual control since the drift rates measured during fixation are essentially identical to the drift rates recorded while the subject is in total darkness. However, the effect of the flicks is to bring the image of the observed object back to the centre of the fixation area, where the visual acuity is highest, when it has been shifted away by drifts. Flicks are so rapid and large that they would be expected to produce a considerable amount of blur in the perceived image. These three involuntary movements will continually shift the image of the object being fixated to and fro across a number

of receptors.

Mach himself reported the presence of the bands with spark illumination. In 1960, Keesey, observing the effect of eye movements on visual acuity, showed that human acuity is neither enhanced nor impaired by involuntary eye movements which occur during a short observation of a test object; the contours are perceived clearly in motionless objects during the first critical few seconds of viewing. Thomas (1963,1965) was able to measure the threshold of bands at exposures as brief as 0.01 second. Moreover, in 1966, Matthews showed that the bright band is seen on a photographic edge, with a luminance of 3400 millilamberts (about $10^4 cd/m^2$) in the brighter field and luminance of 250 millilamberts ($\simeq 800$ $cd/m^2$) in the darker field, even for exposures of 0.002 second. These results confirm that the eye movements are not essential for the formation of the bands.

However, in 1952, Cheatham investigated the effect of movement of the retina on the visibility of the bands. He observed that the sharp contours take a finite time to be perceived ; the time needed is from 0.03 to 0.1 second when the luminance level decreases from 0.46 millilambert ($\simeq 1.46$ $cd/m^2$) to 0.0046 millilambert ($\simeq 0.015$ $cd/m^2$). However, the conditions under which the bands were

studied by each of these three observers differed in the luminance level and the luminance gradient, not to mention possibly other factors. The luminance in Matthews's case was about $10^4$ candelas per square metre (photopic range) while in Thomas's case, it was 34 candelas per square metre (mesopic range) and in Cheatham's case, 1.46 to 0.015 candelas per square metre (scotopic range).

Fiorentini and Ercoles (1957) also observed the bands with a stabilized image on the retina, using apparatus on the same principle as that used by Ditchburn and Ginsborg (1953). They found that the bands which are clearly seen at the beginning of the observation disappear in 5 to 10 seconds and fail to reappear unless the eye makes a very sharp movement which possibly destroys stabilization. Furthermore they noticed that, with an oscillating target showing Mach bands perpendicular to the line of sight, the eye tends to follow the oscillations when the frequency of the movement is low. Thus, the visibility of the Mach bands is then improved significantly by slow oscillatory movements of the observed pattern. Using the same method, Bittini, Ercoles, Fiorentini, Ronchi and Toraldo diFrancia (1960) reported that for any given angular amplitude of motion, visibility at first increases with increasing frequency of motion until a maximum value is reached; it then decreases with increasing frequency. For several amplitudes, the larger the amplitude used

the larger the maximum width of the gradient needed in order to produce just-visible bands. In stabilized retinal images, Riggs, Ratliff, Cornsweet and Cornsweet(1953) noted that the contours gradually fade from view. The normally viewed bands tend to disappear also, but their disappearance times are generally much longer than those for the properly stabilized images.

Many reports on the Mach effect have mentioned the influence of retinal illumination on the appearance of the bands. The retinal illumination has been defined as the product of the object luminance and the area of the eye pupil. Thus, a study of the changes in the appearance of the bands due to changes in the retinal image can be carried out by varying either the object luminance or the size of the eye pupil. Figure 1:5 shows the influence of the retinal illumination on the widths and locations of the bands macroscopically observed through an eye pupil of 0.52 millimetre diameter on an incoherently illuminated knife edge by Leelawongs in 1964.

The unit of retinal illumination was called by Troland in 1922, a "photon", but this was later changed to 'troland' by the Colorimetry Committee of the Optical Society of America. One troland corresponds to a luminance of 1 candela per square metre seen through a pupil of 1 square

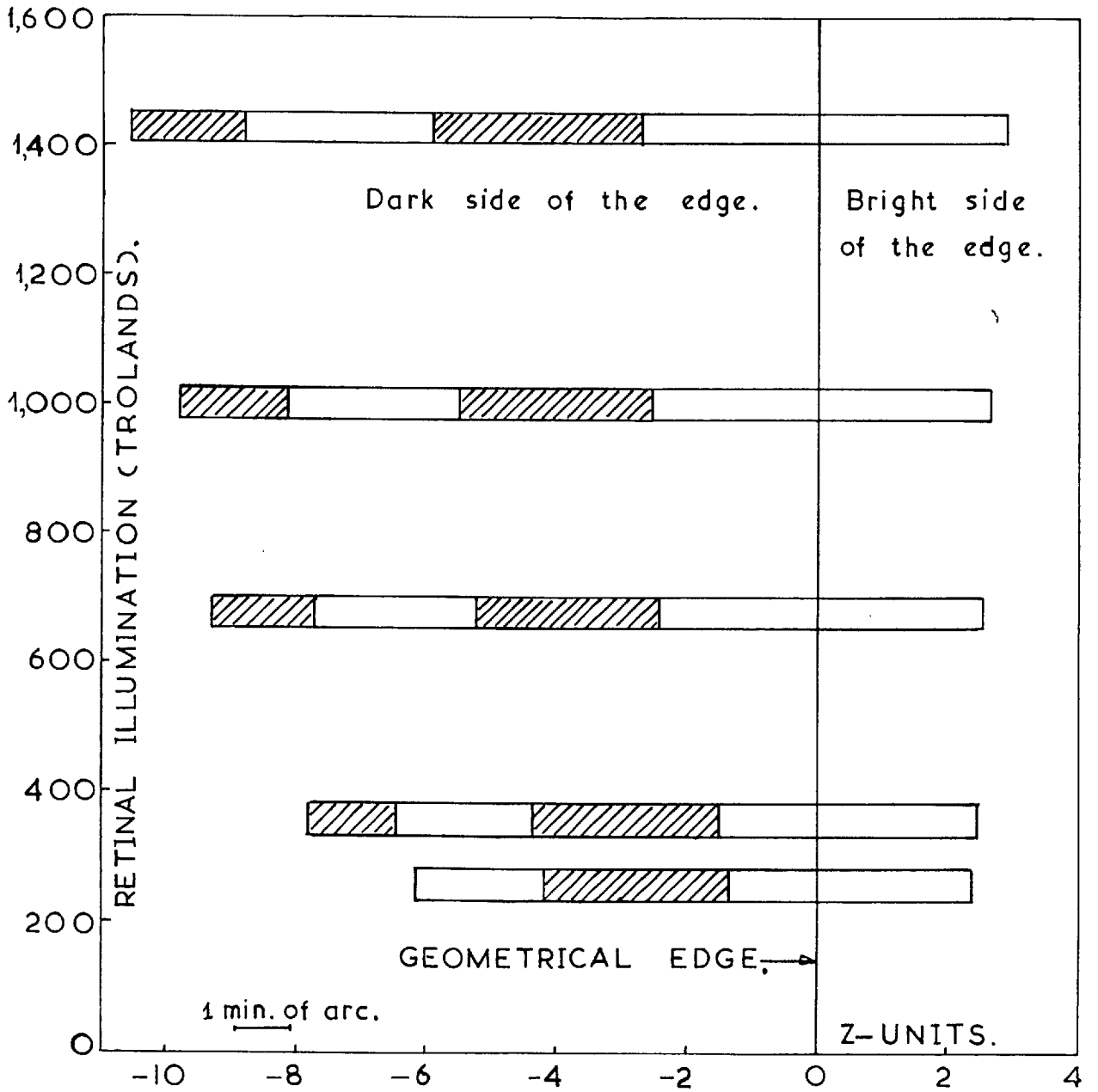



Fig. 1:5. Effect of retinal illumination on the widths and positions of Mach bands (Leelawongs 1964).

millimetre area, or to a luminance of one equivalent lux seen through a pupil of one millimetre radius. Therefore, the photopic range of luminance level refers to the level above $10^3$ trolands, and the level below 10 trolands occurs in scotopic vision.

Mach bands are also affected when the linear scale of the distribution of the retinal illumination is changed owing to a change in either the eye-piece power in microscopic vision or the pupil size in the macroscopic vision, even if the retinal illumination is kept constant. Figure 1:6 shows the influence of the eye-piece power reported by Charman and Watrasiewicz (1964), while figure 1:7 shows the influence of the pupil size on visual Mach bands. The bands in the latter case were observed on the edge of an incoherently illuminated razor blade. Looking through various sizes of apertures, without any intervening optics; more bands were obtained when the eye pupil was decreased in size. From the figure, it can be seen that Mach bands represent details smaller than the formal resolution limit of the eye.

When an object in the form of a step function (half-plane object) is presented to the eye, without any optics lying between, the distribution of the image can be determined from the convolution of the object intensity

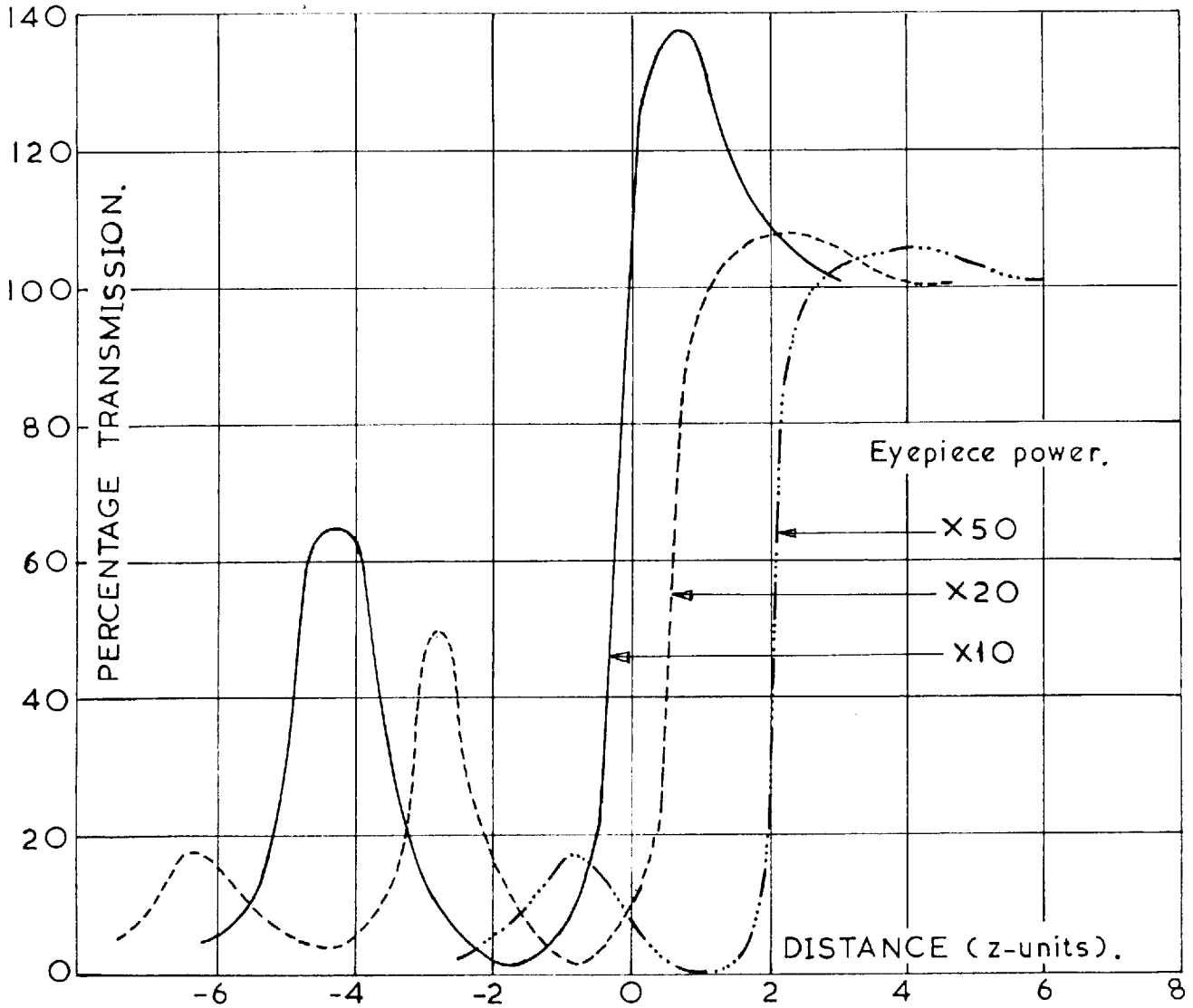



Fig. 1:6. Effect of eyepiece power on the subjective luminance distribution of the microscopic image of a straight edge. (Charman and Watrasiewicz 1964).

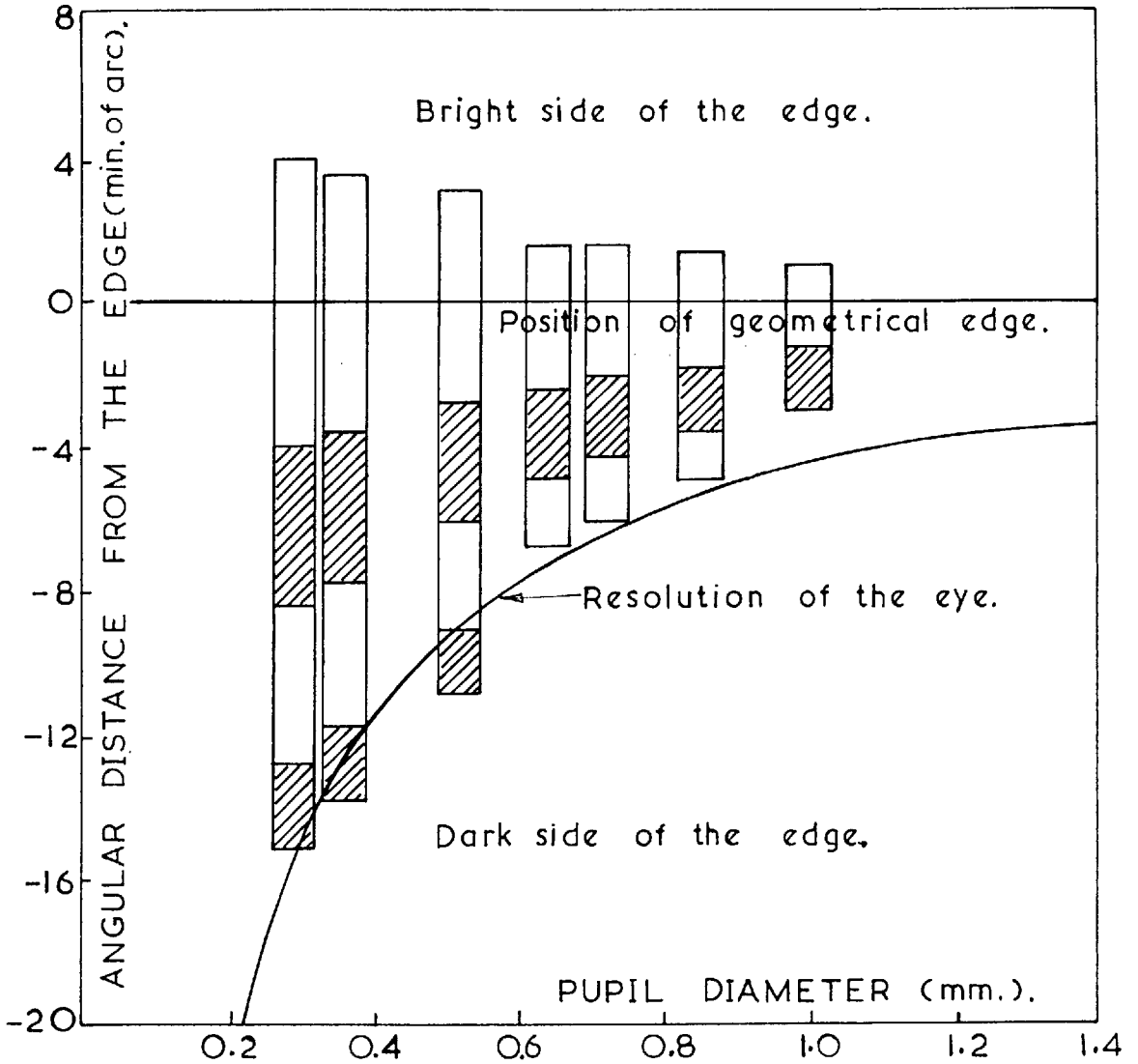



Fig. 1:7. Influence of eye pupil diameter on the widths and positions of Mach bands observed in incoherent light; retinal illumination 682 trolands. (Leelawongs 1964).

distribution with a line spread function of the eye. This line spread function will change as the size of the eye pupil is changed, the larger the pupil size the smaller the spread in the function along the retinal distance, as shown in figure 1:8 where the line spread functions for various pupil diameters are computed. Therefore, the image distribution from the convolution of a step function with a line spread function of a smaller eye pupil is broader than the one obtained from the convolution of the same step function distribution with a line spread function of a larger eye pupil. That is, when the diameter of the pupil increases the inflection points in the retinal image profile come close together and, therefore, the Mach pattern shrinks. With larger pupils, those inflections may come too close to be effective in producing the bands. Besides this, more scattered light reaches the receptors causing the effect of inflections in the luminance distribution curve to be diminished.

In microscopic vision, an increase of eye-piece power increases the scale of the retinal image. Therefore, the image contour covers a greater number of receptors than before and a greater number of neural units are involved in the interaction. The bright bands, thus, should appear less bright because of the greater inhibitory effect.

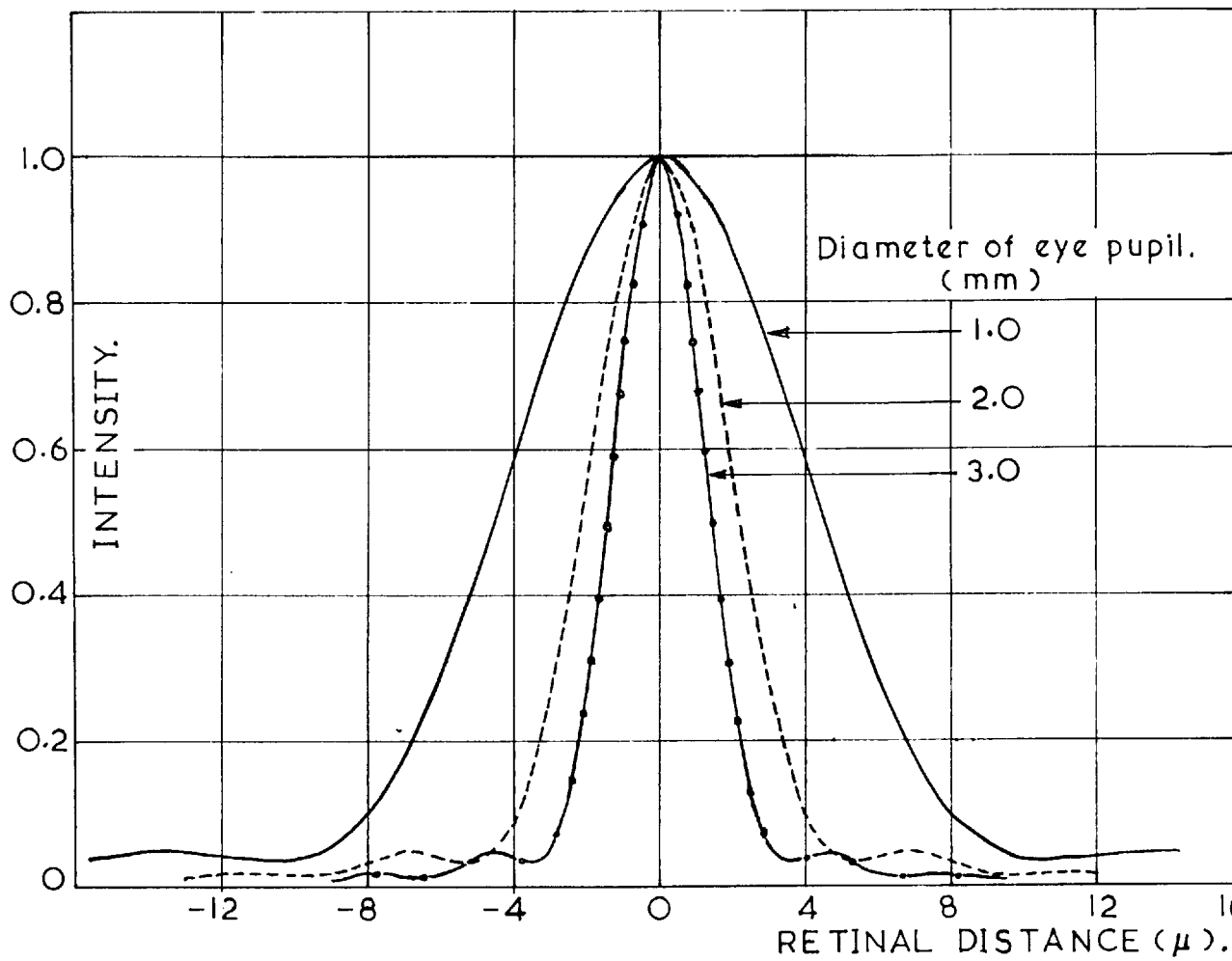



Fig. 1:8. Effect of the size of eye pupil on line spread function.

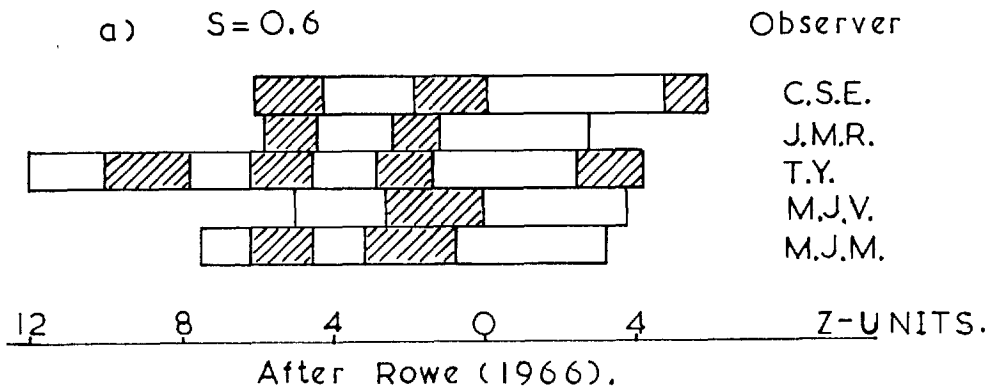
Furthermore, many observers have noticed that the characteristics of the bands also change from individual to individual. The differences are great, as shown in figures 1:9a and 1:9b. In both figures, the bands were obsered microscopically with S= 0.60 by Rowe(1966), and S= 1 by Watrasiewicz (1964), respectively.

With the parameters mentioned above, it is obvious that to elucidate theoretically the exact locations, widths, and brightnesses of the bands is an extremely difficult job.

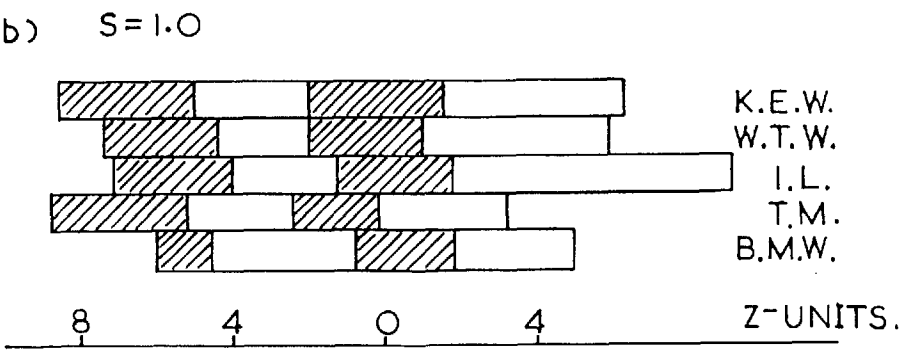
## 1:3 The Visual Paths.

The essentials for perception of the visual stimuli from the outside world can be listed as follows: 1). the physical process by which the external physical stimulus reaches the rod and cone receptors in the retina, and, 2). the physiological process which deals with the transformation of the light energy into the nervous energy and with the transmission of the resulting afferent nervous impulses to the brain.

The retina consists of many layers of elements of various structures and functions. Curiously enough, their arrangement is inverted. The light falling on the retina reaches the sensitive nerve cells only after it has pene-




After Rowe (1966).




After Watrasiewicz (1964).

Fig. 1:9. Individual variations. (Shaded areas are dark bands).

-trated all the layers of the retina, which are, fortunately, transparent. The sensitive nerve cells or visual receptors are of two kinds, known as rods and cones. The light energy is relayed through the bipolar cells to the ganglion cells whose axons form the fibres of the optic nerve. The impulses elicited from the retina are then conveyed to the brain through the nerve fibres which spread out over the surface of the retina and run along the optic nerve.

Electrical impulses in the ganglion cell stage can be measured when t h e r e is activity. But, the actual mechanism that transforms light energy into electric energy in the retina is not yet clearly understood.

The visual pulses from each eye which pass along the optic nerve meet each other at the optic chiasma, and here, the fibres from the retina of each eye divide. The fibres from the temporal half of the left retina and the nasal half of the right retina join and go along the optic tract to the left side of the brain, while the fibres from the nasal half of the left retina and the temporal half of the right retina also join and go to the right side of the brain.

The central nervous system which is situated in the brain is also still imperfectly understood. It continually receives signals from the nerve fibres. The system

contains altogether some $10^{10}$ neurons. Most of them are in the cerebral cortex. Each neuron is an independent cell consisting of one cell body which contains the cell nucleus, a long fibre called an axon, which will pass out the materials synthesized in the cell body, and, several receiving branches called dendrites. Impulses travel from one neuron to the others through dendrites and it is found that they are electric in nature. Figure 1:10 shows a schematic diagram of the visual paths from the eye to the brain.

It is believed that the impulses received from both eyes are co-ordinated in the brain. Then, the visual pattern is interpreted by the mind.

## 1:4 The Retinal Mechanisms.

Many workers on the Mach phenomena have tried to explain the mechanisms which cause the formation of the bands. They postulated that these mechanisms might be located in the retina. Some suggested an inhibiting mechanism which is electrical in character, and some explained that it is owing to diffusion of some substances from one region of the retina to another.

At Mach's time it was not possible to study directly the neural events in the retina. He obtained indirect evidence from his psychophysical experiments. The

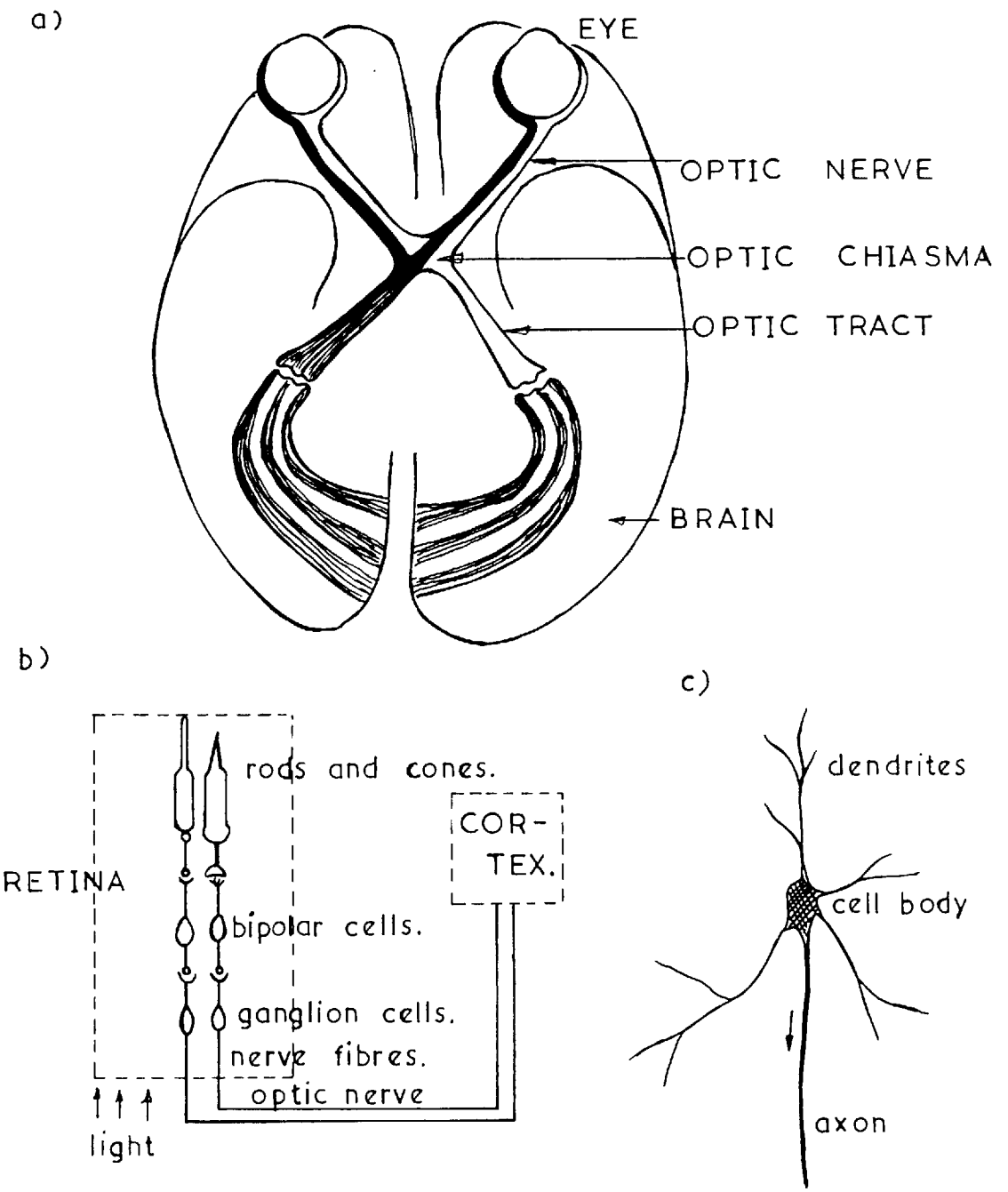



Fig. 1:10. a) and b). Schematic representations of the visual system.

c). A neural in the cortex.

phenomenon was explained on the basis of a reciprocal action of the neighbouring areas of the retina. He assumed that the central excitatory area was surrounded by an inhibitory area. Since the points nearest to one another predominantly exerted the greatest influence upon each other, the magnitude of the reciprocal influence would diminish with distance. It was probably an exponential function, decreasing rapidly at first and then more slowly as shown in figure 1:11. However, the magnitude of the influence at the excitatory area and in the inhibitory surroundings were proportional to the intensity at the central element.

In 1933, Granit, on studying the electrophysiology of the retina and the optic nerve of the cat's eye, deduced that the mechanism for inhibition was an electrical effect. He was able to analyse the response which was generated by a potential difference between the front and the back of the retina into three components. The first component was not connected with the discharge in the optic nerve and was present only in the dark adapted eye. The second component was connected with the discharge of impulses through the optic nerve. The third one was associated with the inhibition of impulses but was not associated with either the photochemical reaction of the photoreceptors or the discharge of the impulses in the photoreceptor axons.

THE DIMINUTION OF INHIBITION WITH DISTANCE.

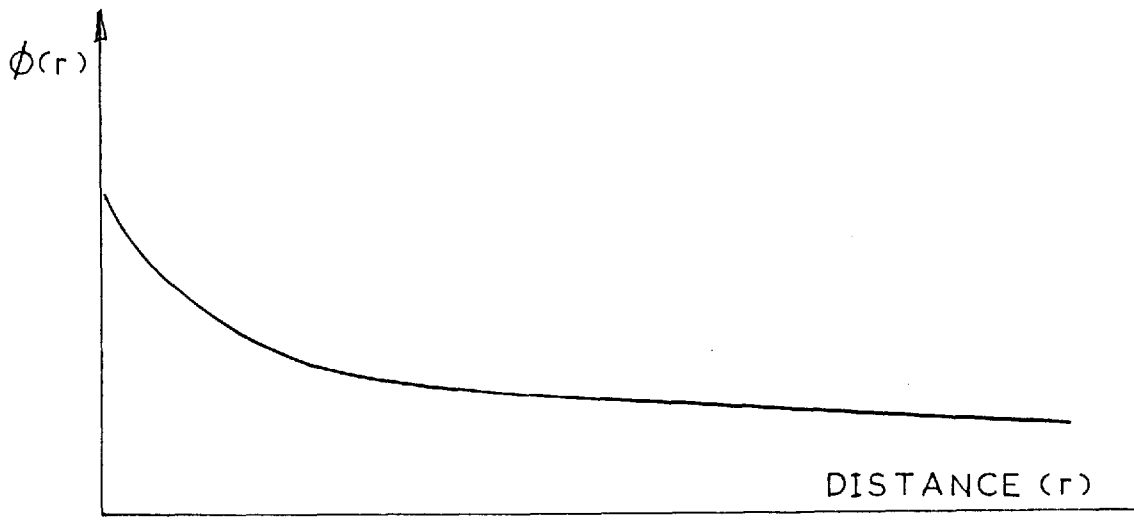



Fig.1:11. After Mach (1865).

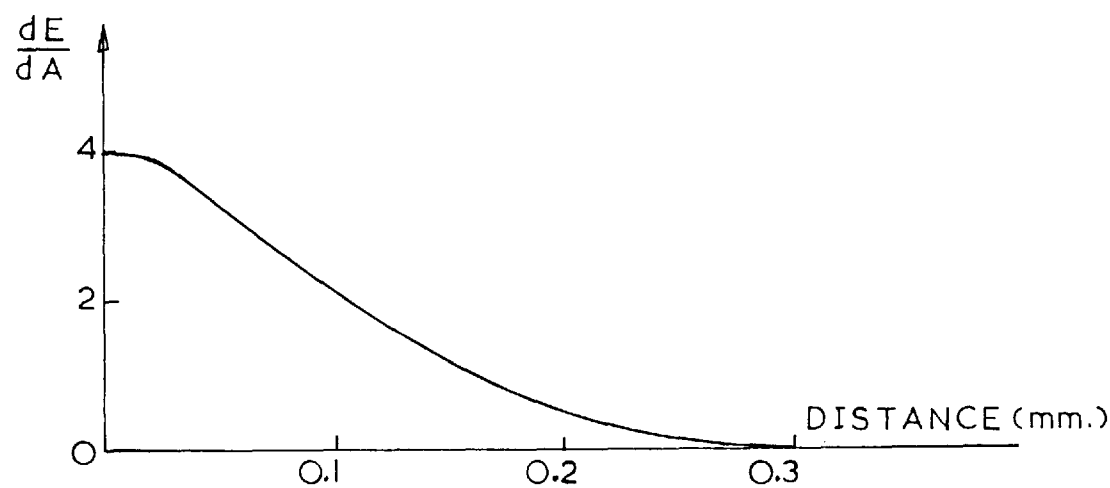



Fig.1:12. After Fry (1948).

The frequency response of a ganglion cell axon recorded with a micro-electrode could be enhanced or inhibited by causing a current to flow through the eyeball from an external source, depending upon the direction of the current flow.

In 1935, Granit and Thermal worked on the Hungarian frog which they found to be the most suitable preparation for comparing retinal action potential with the discharge in the nerve. They found that the latent period of discharge in the nerve consisted of two phases; an inhibitory phase and the latent period of the excitation. A third factor might be added, that is, the duration of the initial photochemical process, of which nothing was known.

Granit's assumption was confirmed by Schouten and Ornstein in 1939. They proposed the following hypothesis: " When the retina is illuminated there is induced at the illuminated part and also in the surrounding area, an electric state which manifests itself to the light-sense by a diminished sensitivity". An experiment to demonstrate subjectively the inhibitory and enhancing effect produced by the electric current was carried out in which the right eye could perceive only a test field and glare light from a light source, while the left eye saw only a comparison field which was placed adjacent to the test field. No light

from the light source was allowed to fall upon the eye in the beginning and the two fields were matched under this condition. When the glare source was switched on, the test field suddenly appeared to be much darker than the comparison field. After short times of exposure the brightness quickly returned to its original value. With a pupillometer, they proved that this effect, viz; the drop in brightness, was not because the pupil of the illuminated eye was narrower than that of the other eye, because when one eye was illuminated both pupils changed to the same extent and with the same dependence upon time.

Hartline (1938) reported that three types of ganglion cell axons which formed the optic nerve existed in the eye of the frog. They were as follows:

1). Those which were either silent or discharged very slowly under steady illumination but responded vigorously when the illumination was increased. The responses were called "on" responses.

2). Those which yielded a burst of impulses when the light was turned on, no further activity as the light stayed on, and a final burst after the light was turned off. They were called "on-off" responses.

3). Those which would remain completely inactive during maintained illumination and then yielded a burst when the light was turned off. They were termed "off"

responses.

He pointed out that the "on-off" and "off" responses might be the result of the complex interplay of excitatory and inhibitory influences by showing that the experimental manipulation of these influences could yield transient responses.

In 1940, Ludvigh assumed that three different sets of elements existed in the retina. One was for the perception of contours and it consisted of "on-off" elements which would mediate contour perception, while the other two were involved in the illumination level and discrimination of brightness. Owing to eye movement, the "on-off" element would be maximally excited in the vicinity of regions where the first derivative of illumination was a maximum, but the rate of change of the excitation of "on-off" elements would be a maximum where the second derivative was a maximum.

The photochemical process in the retina was considered as a mechanism of the eye for the perception of the contours by Byram in 1944. He explained that in the absence of any eye movement, the receptors at either side of the border between the bright and the dark areas would adapt themselves to the respective levels, and the rates of the photochemical reactions would become the same in the two regions. There would be no brightness discrimination

after having reached such a steady state of adaptation. The movement of the eye would change the equilibrium of the photochemical reaction rates between two sides and make the rate of reaction on the side of the border where the illumination was higher greater than on the other side.

Fry published his hypothesis in 1948. He proposed the interactions between the retino-cortical pathways as mechanisms for inhibition and frequency-equalization. The mechanisms for the inhibition were located at a very low level in the retino-cortical transmission system; when any point in the retina was stimulated not only the excitation which spread to adjacent retino-cortical pathways was stimulated but also the inhibiting potential which inhibited activity over a wide area centred around the point stimulated; this would diminish with increasing distance from it as shown in figure 1:12. The magnitude of the potential difference at each point in the field was proportional to the magnitude of the stimulus. The potentials at any point produced by stimulation of a number of surrounding points were additive. Furthermore, the inhibition depended on the potential difference; the greater the potential difference the greater the inhibition. The frequency-equalizing mechanism, however, would operate at a higher level to equalize the frequencies in adjacent pathways, except at contrast

borders where the mechanism tended to smooth out the frequencies on the two sides of the border.

Lateral inhibition in the retina was postulated for the perception of Mach bands by Green in 1957. He assumed that there were two sets of elements which were responsible for the percept presented by the retina; the first set whose response was proportional to the level E of local stimulation and the second set whose response was proportional to $\bar{E}$, the mean of E over a certain area of the retina. The response from the second set of elements inhibited the response from the first set, so that the resulting response would depend on $E - \bar{E}$. A contour would be perceived where the first derivative of $E - \bar{E}$ with respect to distance had a sharp variation.

In 1958, Green also concluded that the second and the fourth derivatives of the retinal illumination were important in the occurrence of the bands.

Hartline et al (1954, 1956, 1957, 1958) performed a series of experiments on the eye of the horseshoe crab , Limulus, which is a compound eye containing approximately 800 to 1000 ommatidia(receptor units). Each ommatidium contains approximately a dozen cells; the nerve fibres arise from the ommatidia in small bundles and come together to form the optic nerve. The discharge of impulses of the single fibres dissected from the optic nerve were recorded

by means of microelectrodes. They found that there were inhibitory influences exerted mutually among the receptor units. If two groups of receptors were illuminated together the total inhibition they exerted on a test receptor near them would depend on the combined inhibitory influences of the two groups. If those two groups were widely separated in the eye, their total inhibitory influence on the test receptor would equal the sum of the inhibitory influences they each produced separately. If the two groups were close enough together to interact, each group would inhibit the activity of the other and hence reduce its inhibitory influence; their effect was usually less than the sum of their separate effects. Moreover, the disinhibition could happen when the test receptor was illuminated such that it could only inhibit one of the other two receptors. Then the frequency discharge of the other would decrease due to the partial release from inhibition of the first receptor which was now inhibited by the test receptor. Thus, the frequency of the discharge of impulses in a single optic nerve fibre decreased and could be even stopped by illuminating areas of the eye in the neighbourhood of the sensory element from which the fibre arose. The greater the intensity on neighbouring receptors the greater the inhibition they exerted on the test receptor, and the greater the number of the

neighbouring receptors illuminated, the greater the inhibition. Furthermore, it was found that: 1) the threshold of inhibitory action increased with the increasing distance between the units involved, and 2) the coefficient of inhibitory action decreased with the increasing distance.

Figure 1:13 shows the experimental results of Ratliff and Hartline(1959); the pattern of illumination is shown on the top right of the figure. It was focussed on the eye of Limulus. A mask with a very small aperture, much smaller than the aperture of a single receptor unit, was used in order that no inhibitory influences should be exerted on it by the neighbours. The response is shown by the upper curve. When the mask was removed, the response of the same receptor unit which was now inhibited by the neighbours is represented by the lower curve.

Ratliff, Hartline and Miller (1963) suggested that the activity of each element was the resultant of the excitatory stimulus of that receptor unit and the inhibitory influences exerted back upon it by the others. This inhibitory network was called recurrent or Renshaw inhibition. In the recurrent system influences were not only exerted on neighbours, but also indirectly on others by way of those affected directly.

In 1957, Barlow, Fitzhugh and Kuffer suggested that the effect of lateral inhibition was highly reduced

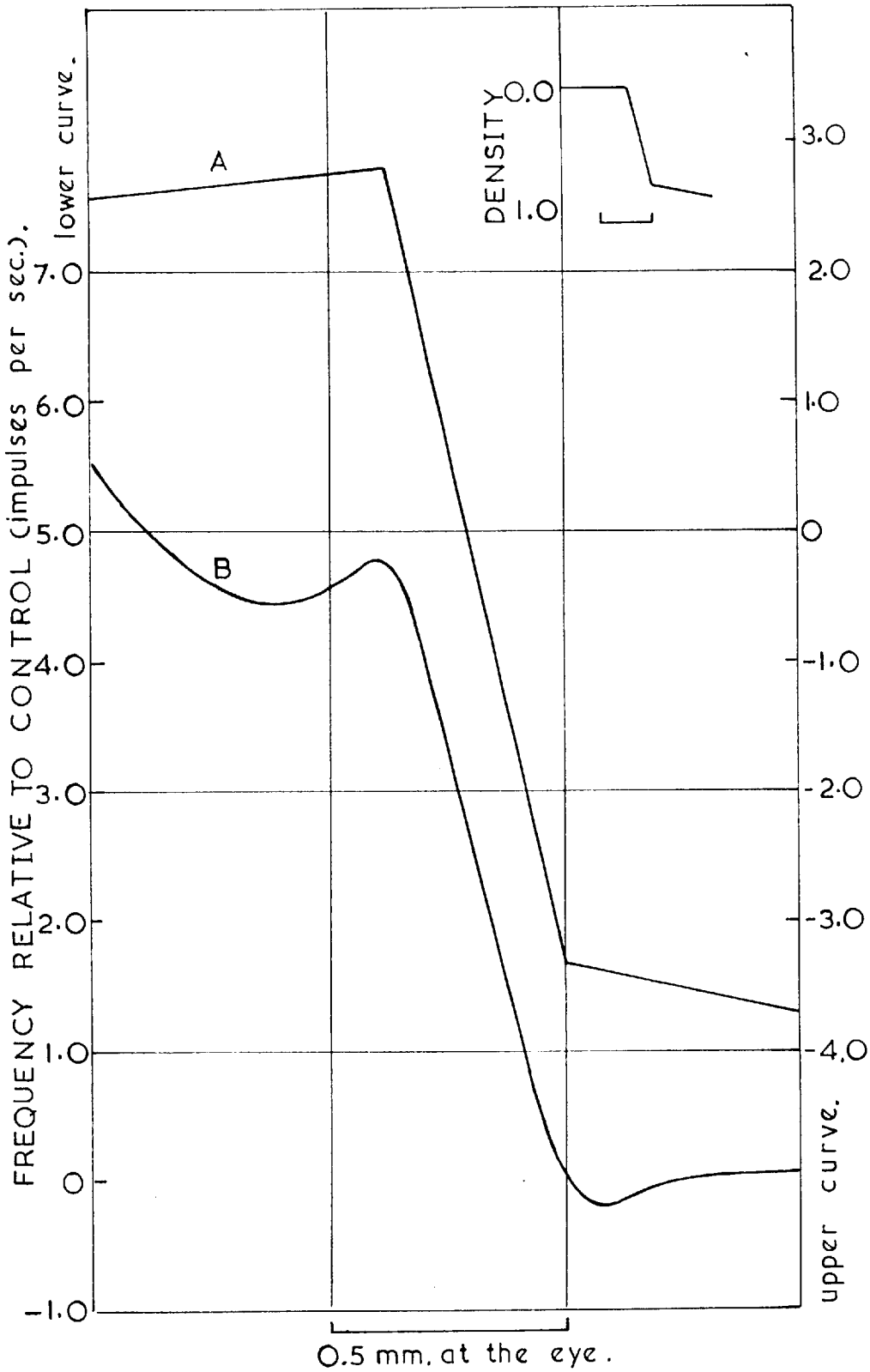



Fig.1:13. A—Response without inhibition from neighbour, B—Response with inhibition from neighbour. (Hartline and Ratliff 1959).

when short observation times were used. This could be because the inhibitory mechanism took a longer time to build up its full activity than the excitatory mechanism.

Ercoles and Fiorentini, in 1959, concluded from their experimental results that at low luminance levels the mechanism responsible for the perception of the subjective contours became less sensitive and a higher value of $\frac{E - \bar{E}}{E}$ mentioned by Green, was required in order that the contours could be perceived. Different mechanisms were responsible for the dark and the bright bands since the dark band was perceived at level lower than the minimum level at which the bright band was visible.

Békésy(1959, 1960) also considered the mechanism as a lateral neural interaction. The assumption was that every stimulus produced an area of inhibition around the area of sensation as illustrated by figure 1:14a. For simplicity in calculation the inhibitory regions were assumed to be uniform throughout as shown in figure 1:14b. The area of inhibition was called a refractory area ; the whole combination of the sensation and the refractory areas was a neural unit. The inhibition covered a larger area than the sensation and spread out to a certain distance with the same effectiveness; beyond this distance inhibition was no longer present. At a certain value of the

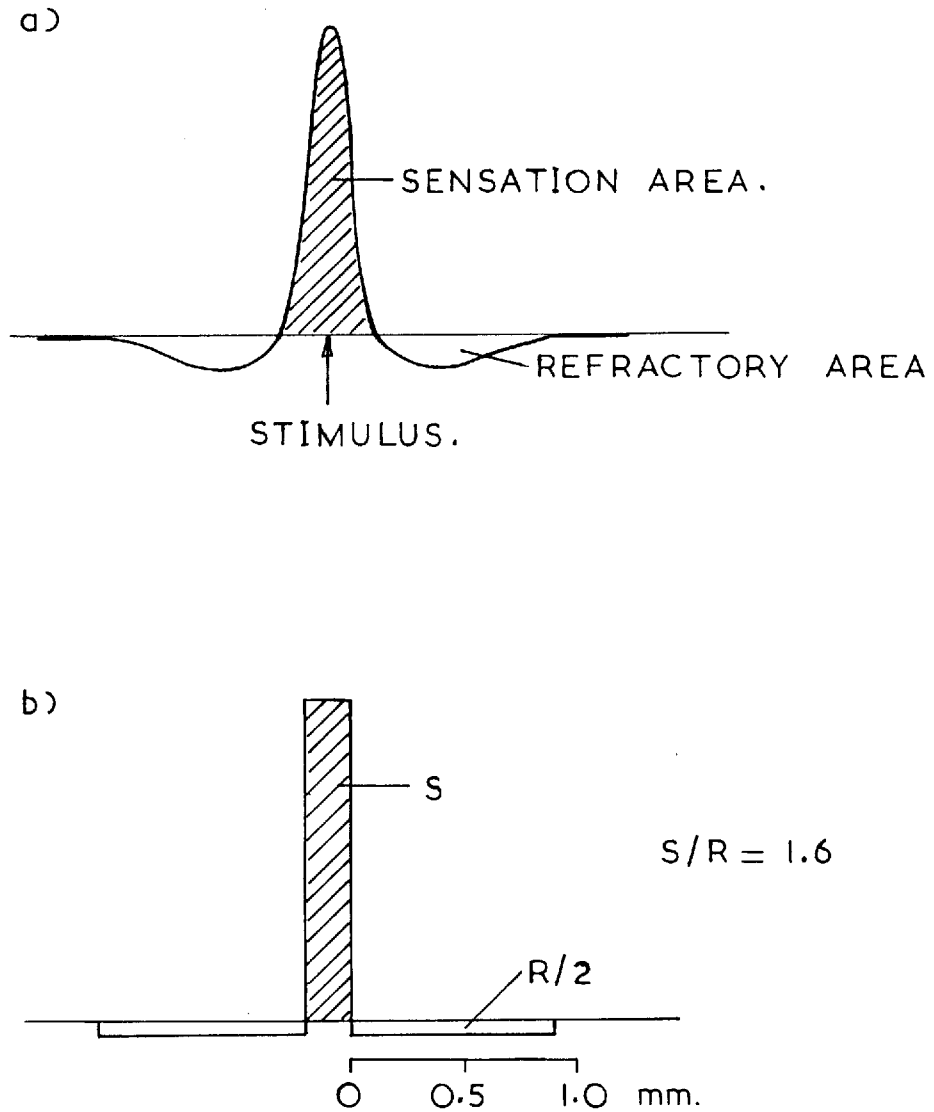



Fig. 1:14. Békésy's neural unit.

intensity(100 milli-lamberts), the width of the refractory area or R/2 in figure 1:14b equals 0.9 millimetre in object space for an object seen at a distance 25 cms. away, S/R equals 1.6 .

R and S/R would change with the change of intensity of illumination. Furthermore, the sensation area had positive value while the refractory area had negative value. The width of the band seen in the sensation pattern would depend on the width of the inhibitory region.

1:5 Predictions on the Locations of Mach Bands.

Equations 1:1 and 1:3, which were set up by Mach, imply that the second derivative term of the illumination with respect to the distance along the retina has a significant influence on the sensation of brightness. The bands will be perceived where the second derivatives are maximal or minimal. The bright band occurs at the position of the maximum negative value while the dark band occurs at the maximum of the positive value of the second derivative curve.

There are a number of observers whose works agree with Mach's conclusion. For example, Ludvigh(1953), on studying the location of the bands, considered the spherical and the chromatic aberrations of the eye as the chief causes of image blurring. With an artificial pupil

of 1 millimetre diameter and a source of 5600 to 5850 $^{o}$A in wavelength, he looked at the visual bands on a rotating freshly cut white paper disc placed against a black background. He found that the energy increment $\Delta E$ on the retina had little effect upon the appearance of an edge, and the rate of change of illumination with respect to retinal distance was an unimportant factor for the formation of a contour. The lowest derivative which was implicated in the perception of bands was the second. The results are shown in figure 1:15. Each curve represents a different energy distribution on the retina; the squares represent observed points. Curves 1 and 2 present only three contours while four contours can be seen on curves 3 and 4. At B and B', the second derivatives of the retinal stimulus with respect to the distance along the retina are maximal and minimal respectively. Contours $E_1$ and $E_2$ are symmetrically distributed as a doublet about B; contours $E_3$ and $E_4$ are symmetrically distributed as a doublet about B'. The brightness of the region between $E_2$ and $E_3$ will be between the brightest and the darkest regions. On curve 2, C indicates the point at which (dE/dx)/E is maximal; no contour edge or apparent discontinuity in the figure occurs at C. Therefore, $\frac{dE/dx}{E}$ is not a substantial factor in determining the perception of the band. The separation of the contours, i.e; the width

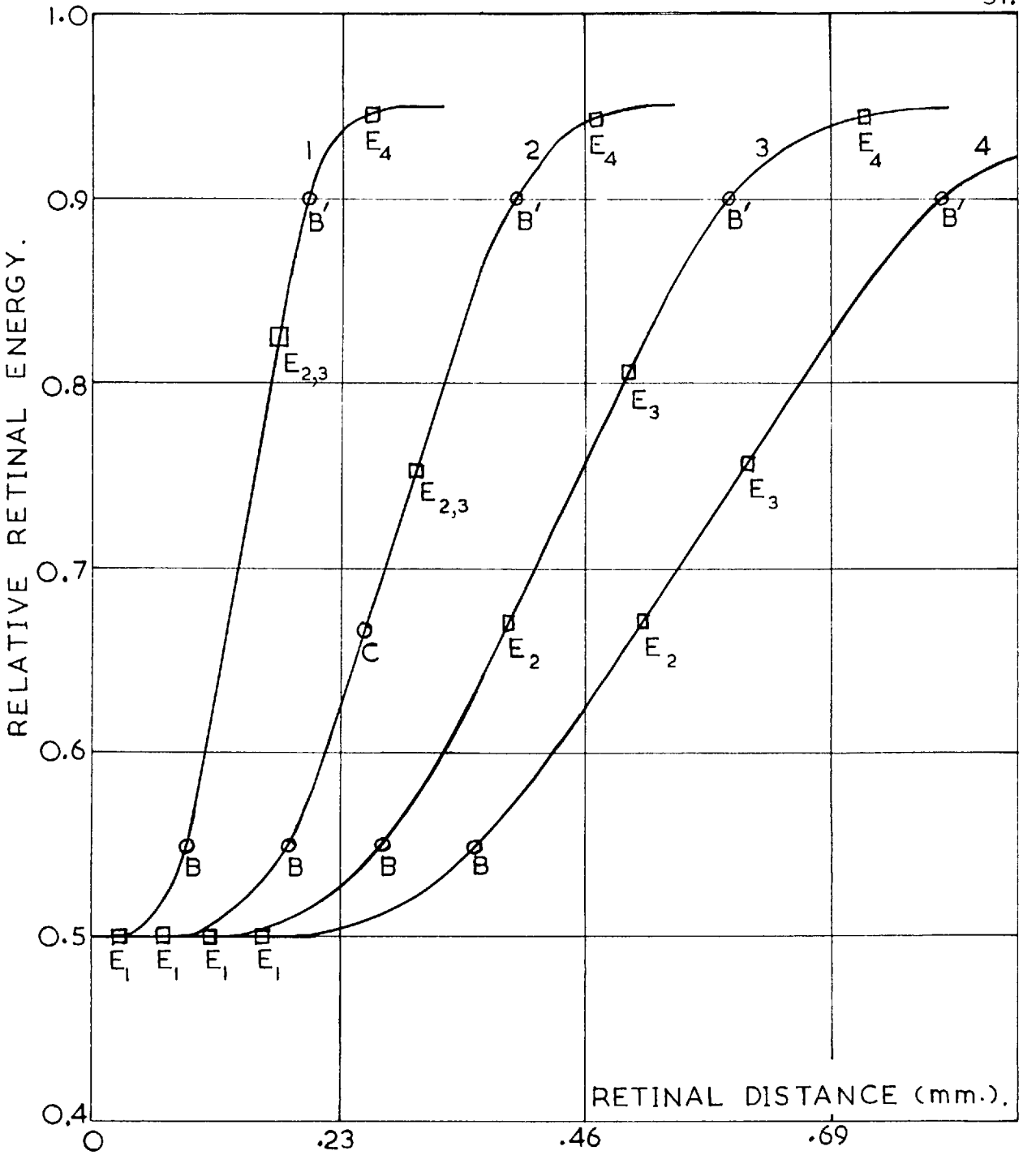



Fig.1:15. Contours seen on various energy distributions. B and B′ are maxima and minima of second derivatives. $E_1$, $E_2$, $E_3$ and $E_4$ are points where contours are seen.

(Ludvigh 1953).

of the bright or dark bands perceived depends on the fourth derivative. The greater the fourth derivative the smaller their separation. Finally, he concluded that the maximum perception of a line depended upon the magnitudes of $E$, $d^2E/dx^2$ and $d^4E/dx^4$. If $d^4E/dx^4$ was greatly increased the line might be made too "small" to be seen; if $d^2E/dx^2$ was greatly decreased the line would have too little "contrast" and would not be seen; and if E was greatly reduced, all derivatives would decrease and the line would become too "dim" to be seen easily.

Figure 1:16 was obtained by Charman and Watrasiewicz (1964) on measurement of the bands seen through a microscope. They were the first to use a microscope in studying the characteristics of the Mach effect. $A_1$, $A_2$, $A_3$, and $A_4$ in the figure indicate the points of maximum values of second derivatives; $B_1$, $B_2$, and $B_3$ are the points of minimum of second derivatives. It can be seen that the positions of the observed bands are in good agreement with the positions of the maximum and the minimum of the second derivatives of the luminance with respect to the distance along the retina.

The equations given by Hartline and Ratliff and by Fry, do not have the second derivative term explicitly in them, but the computation work shows that the bright

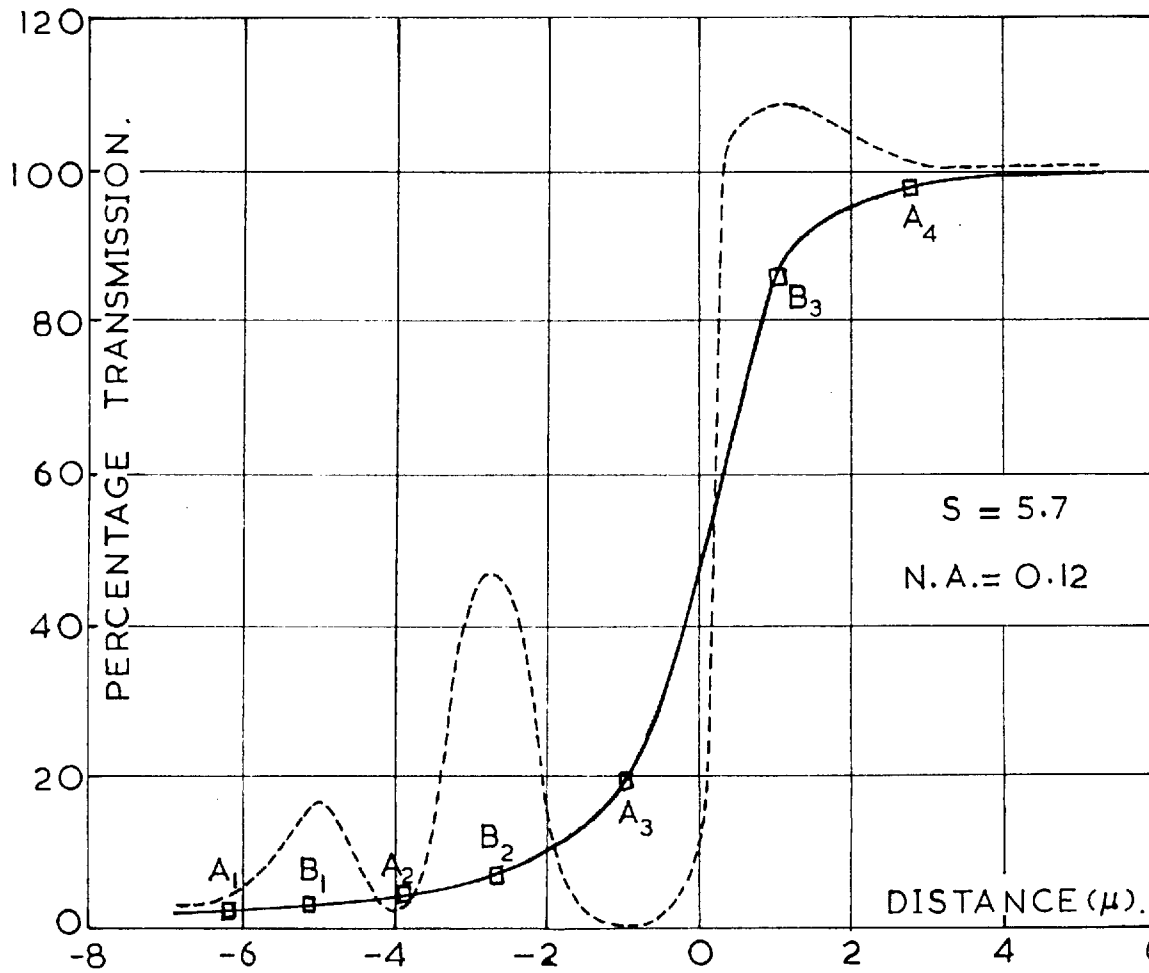



Fig. 1:16. Visual Mach bands and their predicted positions. (Charman and Watrasiewicz 1964).

band occurs approximately at the position of the maximum of the second derivatives. And sometimes, the dark band occurs at the minimum of the second derivative. This will be discussed in Chapters III and IV.

However, most of the observers report that the bright band is more prominent and more nearly centred on its corresponding inflection in the light curve than is the dark band.

# CHAPTER II

## MATHEMATICAL MODELS OF THE MACH EFFECT

### 2:1 Introduction.

Many attempts have been made to obtain mathematical expressions describing the visual phenomenon since Mach's time. Various theories which have been proposed have some basic ideas in common, such as, the use of the retinal illumination instead of the actual luminance distribution of the object, the inhibitory action among neighbouring elements in the retinal network and the diminishing of its influence with the distance between them. Mach considered the diminishing of inhibition as an exponential function, decreasing rapidly at first and then more slowly, as illustrated in figure 1:11. Békésy and Taylor, for simplicity in calculation, assumed that the inhibitory zone was uniform throughout a certain area. However, the form of inhibition in each model is not identical. Some consider inhibition as being stimulus-dependent but others take it as response-dependent.

Furthermore, there are many bases on which the assumptions depend. Some, for example, are based on physiological observations in which the excitatory and inhibitory influences seem to be the fundamental mechanisms in the

retina. Others are based on the supposition that the human visual system operates under steady-state conditions, although as a matter of fact, the eyes of the observers are always in continual motion even during a supposedly steady fixation. Moreover, some are based on psychophysical experiments where the entire visual system is practically involved, making it difficult to identify the various processes which have been taking place in the retina.

The relations between the subjective and objective distributions of intensity are expressed variously in terms of linear equations, non-linear equations and simultaneous quasi-linear equations. In a linear system, inhibitory actions are additive and their sum is subtracted directly from the excitation to determine the response. The influence of a constant term, then, will have a constant effect on the response. Therefore, the equation will yield the same magnitudes for the dark and the bright bands. The inhibitory effects in a non-linear system, however, are also additive, but the excitatory influences are divided by the sum of the inhibitory influences. Thus, a constant inhibitory influence exerted by an element in this system may produce different inhibitory effects, depending upon whether it acts alone or in conjunction with others.

The observations so far support the view that

the amount by which the bright bands are brighter than the surroundings exceeds the amount by which the dark bands are darker than the surroundings for incoherent illumination, that is, the overshoot of the subjective distribution curve is greater than the undershoot. This seems to suggest that the system is non-linear. In 1963, Marimont drew attention to this point. The curves shown in figure 2:1 were the ones she used to demonstrate the non-linearity of the human visual system with regard to the Mach phenomena. $O_1(x)$ and $O_2(x)$ are object functions. $I_1(x)$ and $I_2(x)$ are corresponding image functions. It is obvious that the sum of $O_{1+2}(x)$ is equal to a constant which will give a constant subjective reponse, that is, $I_{1+2}(x)$ is constant. One necessary condition for linearity is

$$I_{1+2}(x) = I_1(x) + I_2(x).$$

If we consider the left half of the figure, at the point where the luminance of the object start to change its slope, we have

$$I_1(x) + I_2(x) = I_{1r} + I_{1o} + I_{2r} + I_{2u} .$$

But , at the far left end of the figure $I_1(x)$ and $I_2(x)$ are constant and

$$I_1(x) + I_2(x) = I_{1r} + I_{2r} .$$

If this system is linear, these last two equations must be equal, that is, $I_{1o} = I_{2u}$ . Since $O_1(x)$ and $O_2(x)$ are

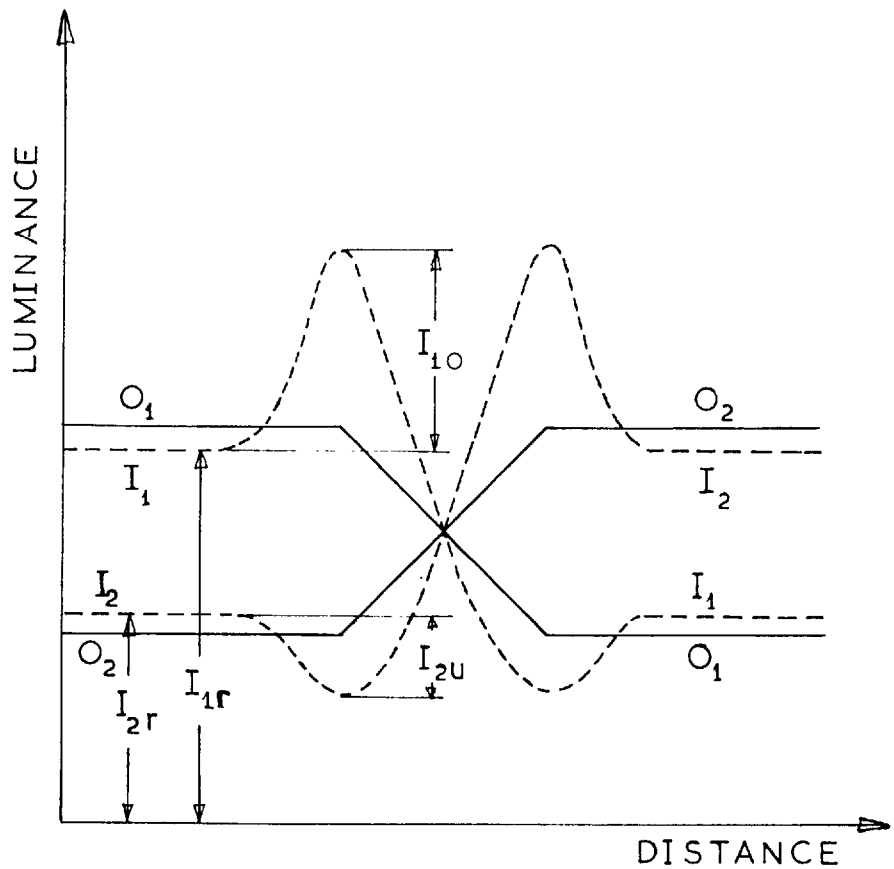



Fig. 2:1. The non-linearity of Mach phenomena (Marimont 1963).

mirror objects, $I_1(x)$ and $I_2(x)$ will also be mirror images. So we can write, $I_{1u} = I_{2u}$. Therefore, $I_{1o} = I_{1u}$. But, in the experimental work the overshoot($I_{1o}$) is always greater than the undershoot($I_{1u}$). Thus, Marimont concluded that the visual system was non-linear. This was contrary to the assumption of Lowry and De Palma in 1961 where the eye was presumed to behave linearly when the transfer function of the eye was evaluated. However, their experimental data showed the non-linear characteristics of the system (the bright and the dark bands in the subjective images were not symmetrical in their forms).

Moreover, it has been observed that the border between the dark and the bright bands does not occur at the geometrical position of the edge. This border gets displaced to one or the other side of the edge, the displacement depending on many factors. The right mathematical model, therefore, should contain a parameter which could influence the position of this border relative to the geometrical edge. Observers who are not used to the effect may be led to believe that the dark band occurring near the edge is the border between two areas. This consideration would give a great error in small particle sizing.

## 2:2 Mach's Model.

In the year 1868, Ernst Mach, starting from psychophysical experiments, set up a non-linear equation to represent the reciprocal inhibition in the retina in the effect which he called the 'contrast-phenomenon'.

Let the distribution of the illumination, i.e; lumens per unit area, at a point p on the retina be described by $I = I_p = I(x,y)$; when a nearby retinal point which participates in a reciprocal action with the first point is considered, then the reciprocal relation between these two points depends on a function of their separation r, say, $\phi(r)$. The response F at p when several neighbouring points come into play is then given according to Mach by

$$F_p = I_p \cdot \frac{I_p \sum_j \phi(r_{jp}) \Delta a_j}{\sum_j I_j \phi(r_{jp}) \Delta a_j}, \qquad \ldots\ldots\ldots\ldots\ldots (2:1)$$

where $I_j$ is the illumination at another retinal region of area $\Delta a_j$. $I_j$ can be written according to the Taylor expansion,

$$I_j = I(x+h, y+k)$$

$$= I(x,y) + \frac{\partial I(x,y).h}{\partial x} + \frac{\partial I(x,y).k}{\partial y} + \frac{1}{2!}\left[\frac{\partial^2 I(x,y).h^2}{\partial x^2} + \frac{2.\partial^2 I(x,y).hk}{\partial x\, \partial y} + \frac{\partial^2 I(x,y).k^2}{\partial y^2}\right] + \ldots \qquad \ldots (2:2)$$

The factor $I_p\sum_j \phi(r_{jp})\Delta a_j$ in equation 2:1 is supposed to be the excitatory influence. If $\phi$ is the same function everywhere in the network and $\Delta a$ is the same for all elements, $\sum_j \phi(r_{jp})\Delta a_j$ can be expressed as a single number. The whole factor then can be replaced by $I_pK$. The denominator, $\sum_j I_j \phi(r_{jp})\Delta a_j$, is the inhibitory influence in the network. Since $I_j$ may be different for each element, the factor can be expressed as $\sum_j I_j k_{jp}$. Hence, the formula can be modified to ;

$$F_p = I_p \frac{I_p \cdot K}{\sum_j I_j k_{jp}} .$$

That is, the neural network in the retina as described by Mach consists of elemental networks, in each of which there is a central excitatory component surrounded by an inhibitory component that diminishes with distance. The individual inhibitory influences exerted on any particular element are additive.

From equation 2:1, it can also be seen that when the intensity distribution across the retina is uniform the intensity at any observed point p will be the same as at a surrounding point j. Therefore, $I_p\sum_j \phi(r_{jp})\Delta a_j$ equals $\sum_j I_j \phi(r_{jp})\Delta a_j$. The sensation then is determined solely by $I_p$ and is the same for every observed point. Furthermore, when the intensity at point p is greater than the intensities at the other points in the neighbourhood, the value of the

fraction $\dfrac{I_p \sum_j \phi(r_{jp}) \triangle a_j}{\sum_j I_j \phi(r_{jp}) \triangle a_j}$ is greater than 1, and

then the sensation also will be correspondingly greater. On the other hand, if the intensity at the observed point is decreased, $I_j$ becomes greater than $I_p$ and the value of the above fraction becomes less than 1. The observed point will appear darker than if it were in the uniform intensity area.

There is one case for which the formula fails to give a satisfactory explanation. That is, when only the point p is illuminated, the value of $I_j$ is zero and, therefore, the value of the fraction approaches infinity. The response will become infinitely large. This can, however, be avoided by supposing that the group of elements j includes the element p. The value of the fraction then cannot increase beyond a certain finite value as $I_p$ appears in the numerator as well as in the denominator.

Let us consider four typical points surrounding the point of illumination I, that is, the points I (x+h,y+k), I(x+h,y-k), I(x-h,y+k) and I(x-h,y-k) : these points have illuminations given by

$$I(x+h,y+k) = I + \left[\frac{\partial I}{\partial x}h + \frac{\partial I}{\partial y}k\right] + \frac{1}{2!}\left[\frac{\partial^2 I}{\partial x^2}h^2 + 2\frac{\partial^2 I}{\partial x \partial y}hk + \frac{\partial^2 I}{\partial y^2}k^2\right],$$

$$I(x+h,y-k) = I + \left[\frac{\partial I}{\partial x}h - \frac{\partial I}{\partial y}k\right] + \frac{1}{2!}\left[\frac{\partial^2 I}{\partial x^2}h^2 - 2\frac{\partial^2 I}{\partial x \partial y}hk + \frac{\partial^2 I}{\partial y^2}k^2\right],$$

$$I(x-h,y+k) = I + \left[ -\frac{\partial I}{\partial x}h + \frac{\partial I}{\partial y}k \right] + \frac{1}{2!}\left[ \frac{\partial^2 I}{\partial x^2}h^2 - \frac{2\partial^2 I}{\partial x \partial y}hk + \frac{\partial^2 I}{\partial y^2}k^2 \right],$$

$$I(x-h,y-k) = I + \left[ -\frac{\partial I}{\partial x}h + \frac{\partial I}{\partial y}k \right] + \frac{1}{2!}\left[ \frac{\partial^2 I}{\partial x^2}h^2 + \frac{2\partial^2 I}{\partial x \partial y}hk + \frac{\partial^2 I}{\partial y^2}k^2 \right].$$

$\phi(r)$ can be written in the form $\phi(\sqrt{h^2+k^2})$ and the area $\triangle a_j$ will be dhdk, then we have, writing the summations as integrals over the positive quadrant,

$$\Sigma_j \phi(r)\triangle a_j = 4\iint \phi(\sqrt{h^2+k^2})\,dhdk.$$

$$\Sigma_j I_j \phi(r)\triangle a_j = \iint I(x+h,y+k)\,\phi(\sqrt{h^2+k^2})\,dhdk$$
$$+ \iint I(x+h,y-k)\,\phi(\sqrt{h^2+k^2})\,dhdk$$
$$+ \iint I(x-h,y+k)\,\phi(\sqrt{h^2+k^2})\,dhdk$$
$$+ \iint I(x-h,y-k)\,\phi(\sqrt{h^2+k^2})\,dhdk,$$
$$= 4I\iint \phi(\sqrt{h^2+k^2})\,dhdk + 2\frac{\partial^2 I}{\partial x^2}\iint \phi(\sqrt{h^2+k^2})h^2\,dhdk$$
$$+2\frac{\partial^2 I}{\partial y^2}\iint \phi(\sqrt{h^2+k^2})k^2\,dhdk.$$

Therefore,

$$F = I - \frac{I.\ 4\iint \phi(\sqrt{h^2+k^2})\,dhdk}{4I\iint \phi(\sqrt{h^2+k^2})\,dhdk + 2\frac{\partial^2 I}{\partial x^2}\iint \phi(\sqrt{h^2+k^2})h^2\,dhdk + 2\frac{\partial^2 I}{\partial y^2}\iint \phi(\sqrt{h^2+k^2})k^2\,dhdk}.$$

.....(2:4)

Since $\phi(\sqrt{h^2 + k^2})$ must vanish for large values of h and k, we can simply carry out the integral from 0 to $\infty$, putting

$$\int_0^\infty\int \phi(\sqrt{h^2 + k^2})\,dh\,dk = m \,.$$

$$\int_0^\infty\int \phi(\sqrt{h^2 + k^2})\,h^2 \,.\, dh\,dk = \int_0^\infty\int \phi(\sqrt{h^2 + k^2})\,k^2 dh\,dk = n \,.$$

We then obtain:

$$F = I.\frac{4mI}{4mI + 2n\left[\frac{\partial^2 I}{\partial x^2} + \frac{\partial^2 I}{\partial y^2}\right]} \,,$$

$$= I.\frac{I}{I + \frac{k}{2}\left[\frac{\partial^2 I}{\partial x^2} + \frac{\partial^2 I}{\partial y^2}\right]} \,; \quad \ldots\ldots\ldots (2{:}5)$$

where $k/2 = 2n/4m$ .

When a luminance distribution as shown in figure 2:2 (full line) is observed the predicted bands from this luminance distribution can be evaluated by using equation 2:5 . The luminance distribution is constant along the y-axis and varies along a perpendicular direction, the x-axis. Therefore the equation becomes

$$F = I.\frac{I}{I + \frac{k}{2}.\frac{\partial^2 I}{\partial x^2}} \,.$$

The second derivative values of the objective luminance distribution are obtained from a formula which will be derived in section 4:3 . Using k = 0.12, the predicted luminance distribution is shown by the dotted line in the

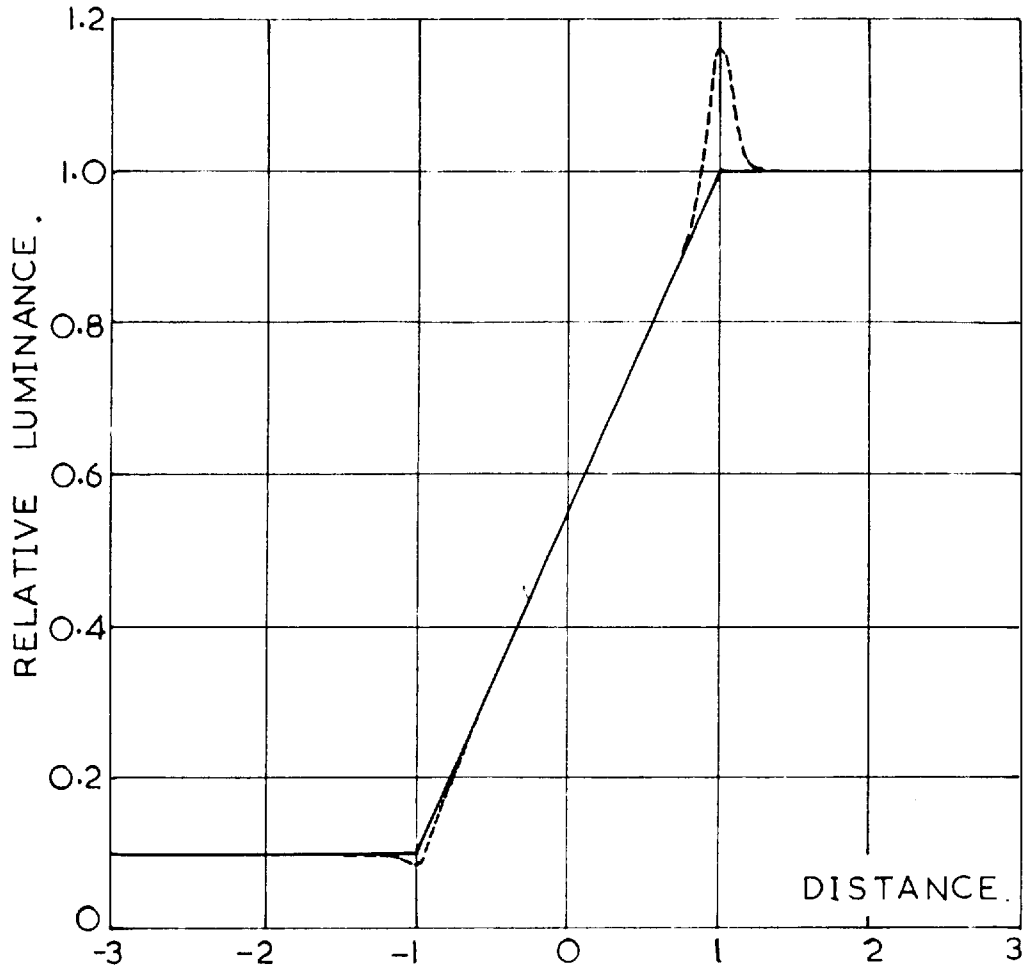



Fig. 2:2. Subjective luminance distribution (dotted line) of a graded luminance distribution (full line) calculated from Mach model (eq. 2:5).

same figure. The fact that the bright band is more pronounced than the dark band, clearly shows the non-linearity of the model. However, the widths of the bands are smaller than the ones actually obtained from observation.

2:3 Fry's Model.

The mathematical model due to Fry (1948) is the first which is based on direct electrophysiological observation. It was developed on the hypothesis that stimulation at any given point on the retina sets up an electrical field in which the potential difference at another point at a certain distance away is some function of that distance. The magnitude of the potential difference is proportional to the magnitude of the stimulus generating it.

In figure 2:3, Q is a given point of area dA on the retina which is stimulated by retinal illumination I. Stimulation at point Q will set up an electric field at point P which is at a distance r from Q . The potential difference(dE) at point P can be expressed in some such form as

$$dE = kI.\exp\left(-\frac{r^2}{2\sigma^2}\right).dA \quad . \qquad \ldots\ldots\ldots\ldots (2:6)$$

where k and $\sigma$ are constants.

The total potential difference (E) produced by all the elements of surrounding area then can be written in

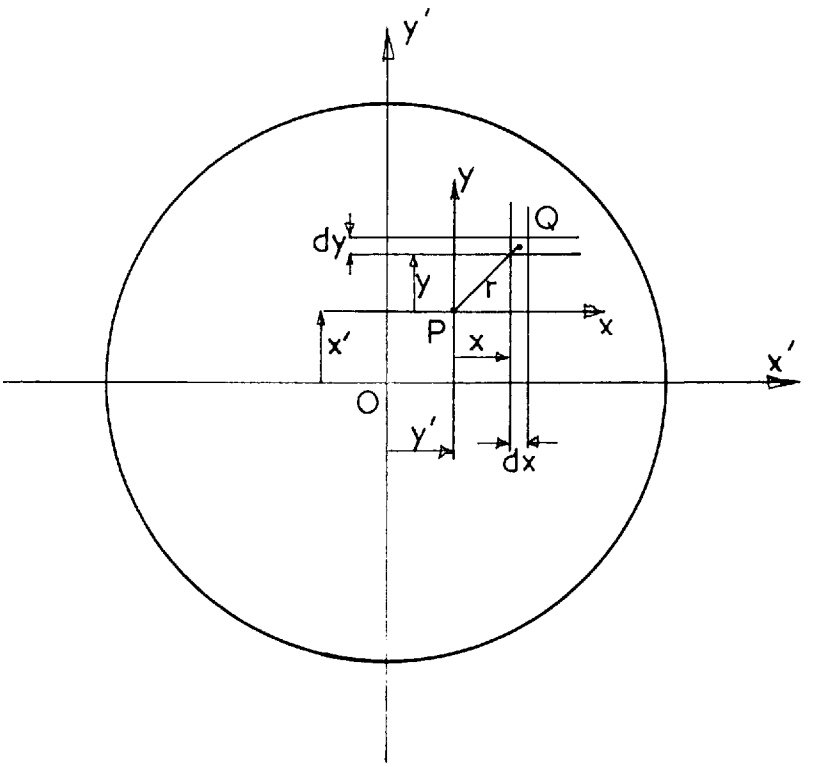



Fig. 2:3. Analysis of inhibition in the retina.

the form

$$E = k_1 \int_{-\infty}^{+\infty} I(r).\exp(-r^2/2\sigma^2).dA, \quad \ldots\ldots\ldots(2:7)$$

or,

$$E = k_1 \iint I(x,y).\exp\left(\frac{-x^2 - y^2}{2\sigma^2}\right).dxdy, \quad \ldots\ldots(2:8)$$

in cartesian coordinates. The constant, $\sigma$, will express the extent of the region which contributes to E.

This total potential difference will reduce the frequency of impulses transmitted through the retina at point Q. The inhibition is greatest where the potential difference is greatest.

This inhibiting potential affects the frequency of impulses in a bipolar cell according to the following relation:

$$F = F' + k_2 \log Q, \quad \ldots\ldots\ldots(2:9)$$

where F represents the frequency of impulses after inhibition by potential E, F' is the frequency that occurs in the absence of inhibiting potential; k is a constant, and Q is a function of E.

It is assumed that the relation between Q and E is of the form,

$$Q = 1/(1 + k_3 E) . \quad \ldots\ldots\ldots\ldots(2:10)$$

It is experimentally found that the frequency F' is related to the luminance(R) of the surface seen by the eye by the following equation,

$$F' = k_2 \log R + k_4 , \quad \ldots\ldots\ldots\ldots(2:11)$$

where $k_4$ is a constant.

For a given pupil size, the retinal illumination (I) is directly proportional to the luminance R, i.e ;

$$R = k_5 I \text{ .} \qquad \text{.....(2:12)}$$

Therefore,

$$F' = k_2 \log(k_5 I) + k_4 \text{ ,}$$

$$= k_2(\log k_5 + \log I) + k_4 \text{ .}$$

At any point P(x,y),

$$F = k_2(\log k_5 + \log I_p) + k_4 + k_2 \log\left(\frac{1}{1 + k_3 E}\right) \text{ ,}$$

$$= k_2 \log \frac{I_p}{1 + k_3 E} + (k_2 \log k_5 + k_4) \text{ ,}$$

$$= k_2 \log \frac{I(x,y)}{1 + k_7 \int_{-\infty}^{+\infty} \int I(x,y).\exp\left(-\frac{x^2 + y^2}{2\sigma^2}\right).dxdy} + k_6 \text{.}$$

.....(2:13)

In figure 2:4, the edge is shown in full line; the model predicts only two peaks, a maximum and a minimum, which resemble Mach bands reasonably well, occurring nearly at the extreme values of the rate of change of gradient of luminance distribution. Figure 2:5 shows the dark and the bright bands ( dotted line ) when the inflections of the intensity distribution curve (full line) of the object are significant. Both were calculated by Fry in 1948.

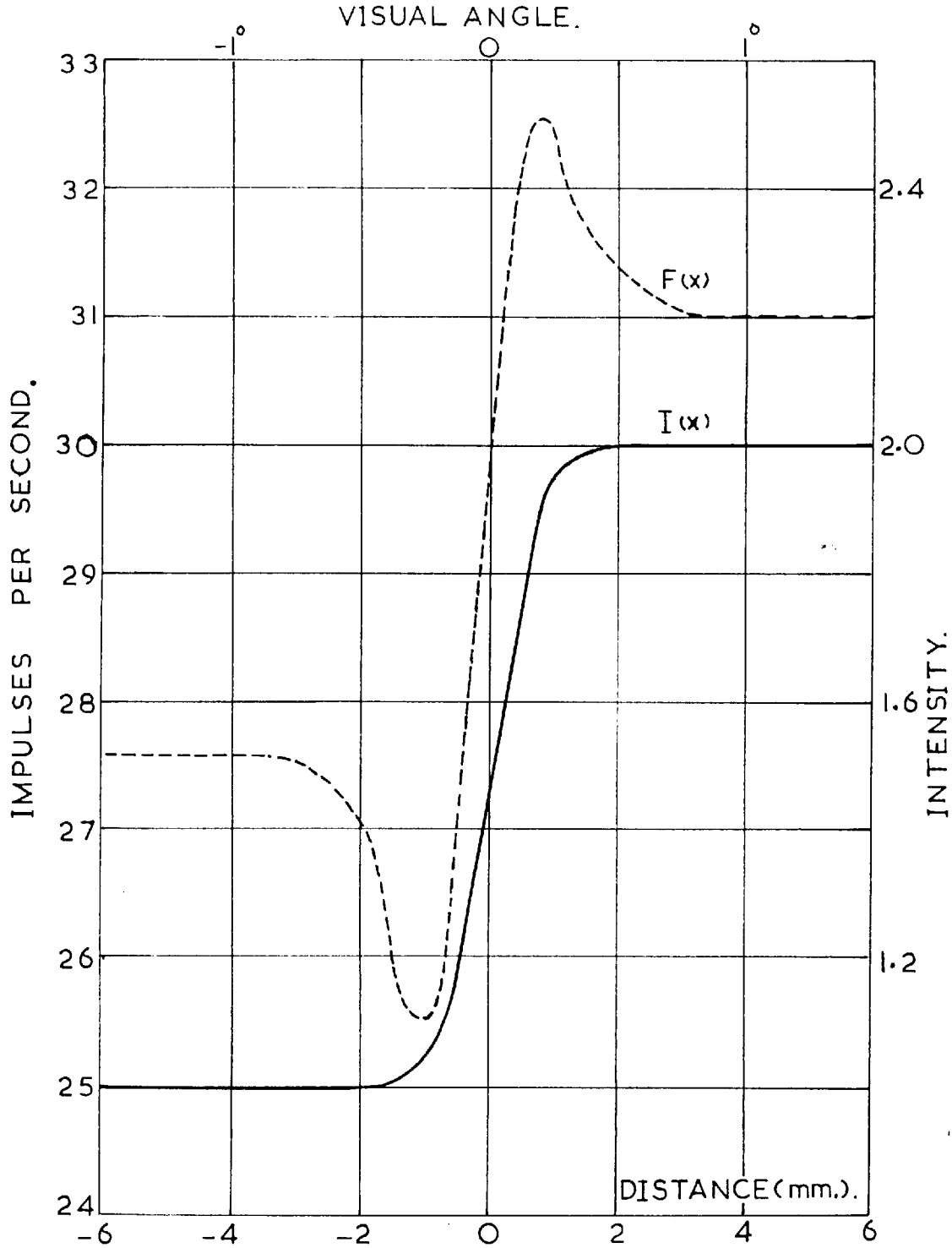



Fig. 2:4. Calculated subjective luminance distribution (F(x)) of a blurred edge (I(x)). (Fry 1948).

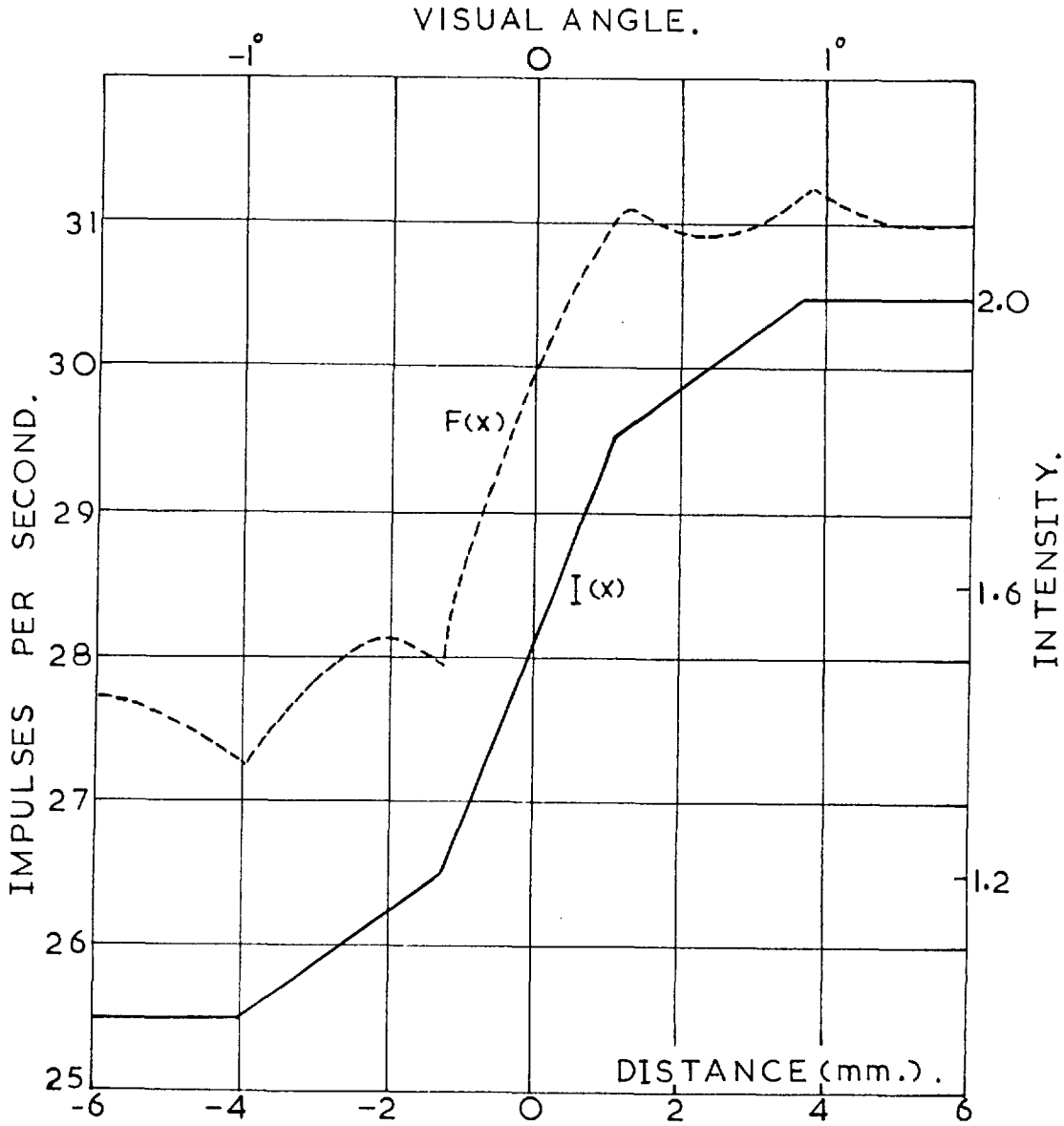



Fig. 2:5. Calculated subjective distribution (dotted line) of sharp edges (full line).
(Fry 1948).

## 2:4 The Model of Hartline and Ratliff.

Hartline and Ratliff (1957,1958) proposed a model based on electro-physiological observations of the inhibitory network in the compound eye of horseshoe crab, Limulus. They postulated that there are mutual inhibitory influences among the receptors in the eye so that each inhibits, and is inhibited by, its near neighbours. The strength of the mutual inhibitory influence is determined by the degree of activity of each of these receptor units and also depends on the number and location of units interacting.

Consider two receptors, A and B ; when they are stimulated they inhibit each other mutually. Responses to steady illumination may be described quantitatively by two simultaneous quasi-linear equations,

$$f_A = e_A - K_{AB}(f_B - f^{o}_{AB}), \text{ for receptor A ;} \quad \ldots\ldots(2:14)$$

$$f_B = e_B - K_{BA}(f_A - f^{o}_{BA}), \text{ for receptor B ,} \quad \ldots\ldots(2:15)$$

where f is the response, measured by the frequency of discharge of impulses in its optic nerve fibre; e is the excitation of the receptor; $f^{o}$ is the threshold frequency which must be exceeded before a receptor can exert any inhibition on a particular neighbouring unit. Therefore, $f^{o}_{AB}$ is the frequency of the receptor B at which it begins

to inhibit receptor A ; $f^{o}_{BA}$ is the reverse. K is the inhibitory coefficient, $K_{AB}$ is the coefficient of the inhibitory action of receptor B on receptor A ; $K_{BA}$ is the reverse.

When the inhibitory term $K(f - f^{o})$ is greater than e, the corresponding response f must be set equal to zero because negative frequencies have no meaning. Furthermore, if $(f - f^{o})$ is negative the inhibitory term must be omitted.

However, these equations are so far only for the interactions of two elements. If there are n interacting receptor units in the network, the equations become a set of simultaneous quasi-linear equations, each with $(n - 1)$ inhibitory terms, that is,

$$f_i = e_i - \sum_{\substack{j=1 \\ \neq i}}^{n} K_{ij}(f_j - f^{o}_{ij}) \; . \qquad \ldots\ldots\ldots\ldots (2{:}16)$$

where $i = 1,2,3, \ldots\ldots\ldots, n$ . Negative frequencies cannot occur since all the solutions of the equation must be positive, therefore, the set must fulfil the following conditions;

$$\left.\begin{array}{l} \text{if, } \quad e_i < \sum_{\substack{j=1 \\ \neq i}}^{n} K_{ij}\,(f_j - f^{o}_{ij}) \text{ , then } f_i = 0 \; ; \\ \text{if, } \quad f^{o}_{ij} > f_j \text{ , then } f_i = e_i \; . \end{array}\right\} \qquad \ldots\ldots (2{:}17)$$

The numerical work must be carried out step by

step. Suppose i represents any particular element out of n elements in the network and let j represent all the others.

The first step in the iterations is,

$$f_i^{(1)} = e_i \ , \qquad \ldots\ldots\ldots\ldots\ldots\ldots\ldots\ldots (2:18)$$

which gives the uninhibited response of any particular element in the network.

The first approximation to the inhibited response or the second step in the iteration is to use these uninhibited responses to determine the inhibition on any particular element,

$$f_i^{(2)} = e_i - \sum_{\substack{j=1 \\ \neq i}}^{n} K_{ij}(f_j^{(1)} - f_{ij}^{o}) . \qquad \ldots\ldots\ldots (2:19)$$

Similarly, using the inhibited responses determined in the second step in the iteration to determine the responses in the third step , we obtain,

$$f_i^{(3)} = e_i - \sum_{\substack{j=1 \\ \neq i}}^{n} K_{ij}( f_j^{(2)} - f_{ij}^{o} ) , \qquad \ldots\ldots\ldots (2:20)$$

and so on to the $s^{th}$ step in the iteration,

$$f_i^{(s)} = e_i - \sum_{\substack{j=1 \\ \neq i}}^{n} K_{ij}( f_j^{(s-1)} - f_{ij}^{o} ) . \qquad \ldots\ldots (2:21)$$

Generally,if the inhibitory coefficients are small, convergence is rapid; if they are large, convergence is slow and the system may even be unstable.

In 1959, Ratliff and Hartline found that the threshold of inhibitory action $f^o$ increased with increasing distance between the receptors, and the coefficient of inhibitory action K decreased with increasing distance.

Using equation 2:16, Watrasiewicz(1964) assumed that the inhibitory coefficient K varied inversely as the separation between the receptors, and the threshold of inhibition $f^o$ varied directly as the distance, i.e;

$$\left.\begin{aligned} K_{ij} &= B/(i - j)^2 , \\ \text{and,} \quad f^o_{ij} &= C(i - j)^2 . \end{aligned}\right\} \qquad \ldots\ldots\ldots\ldots\ldots\ldots (2:22)$$

The results obtained are shown in figures 2:6 and 2:7 . The multiple Mach bands are clearly visible in figure 2:7, a consequence of the two dimensional model.

## 2:5 Taylor's Model.

Taylor(1956) also proposed a model based on electro-physiological experiments, in this case on the ganglion cells in the cat's retina. He found that the area of the receptor mosaic which was illuminated to cause a discharge of impulses had a sensitive central excitatory region surrounded by a less sensitive inhibitory region. The interaction was specified by two parameters, the avarage magnitudes and the spread of interaction. The relation between the logarithm of light intensity and the frequency

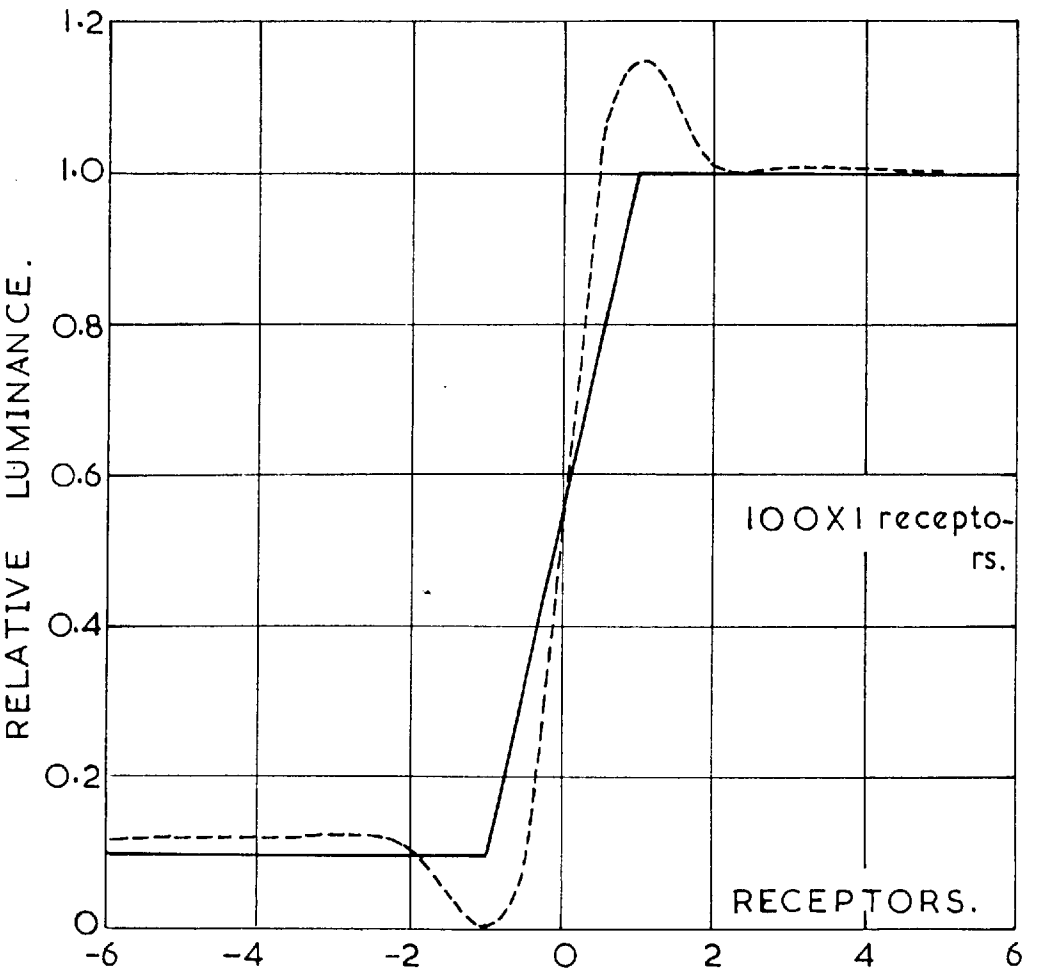



Fig. 2:6. One-dimensional model of Hartline and Ratliff calculated by Watrasiewicz (1964).

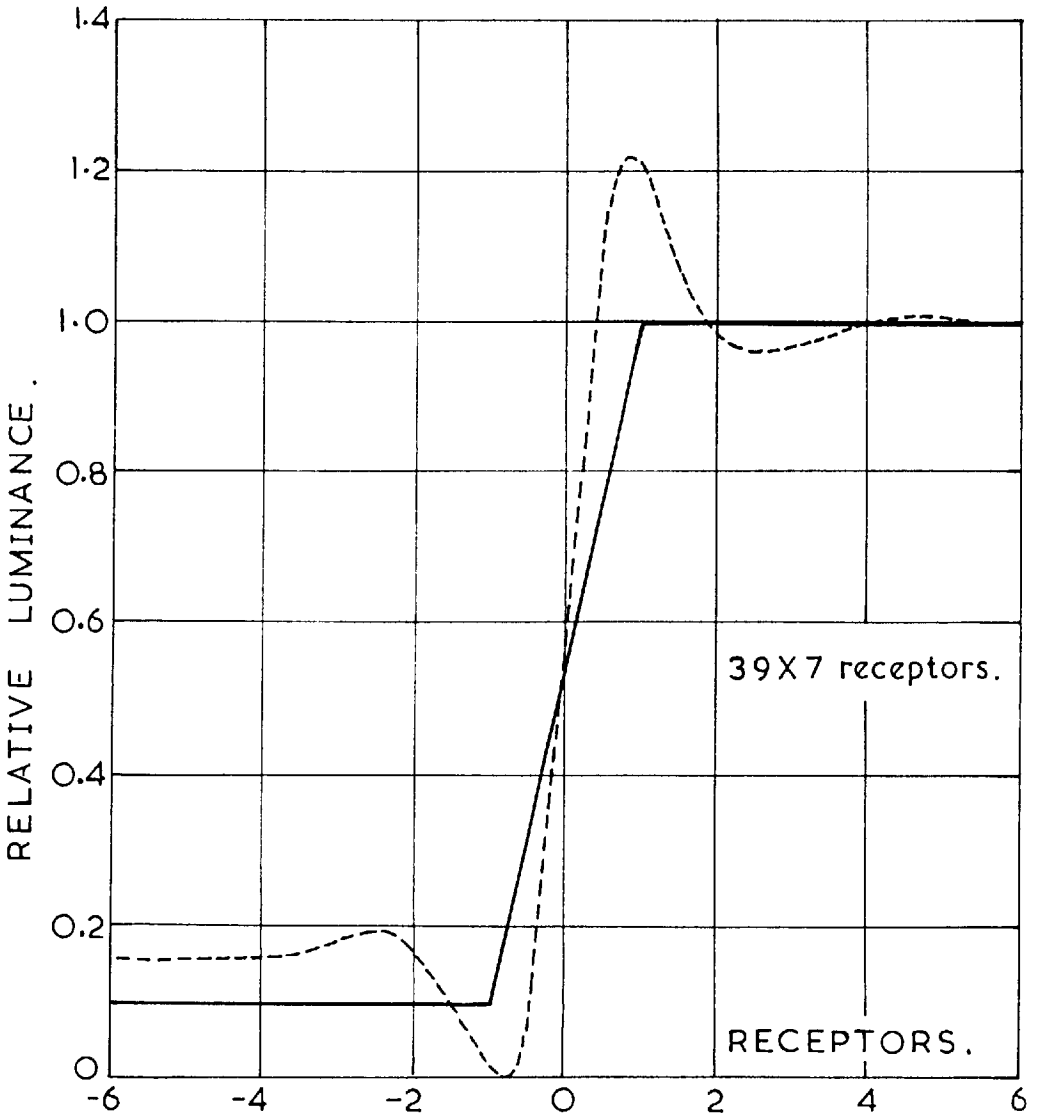



Fig. 2:7. Two-dimensional model of Hartline and Ratliff calculated by Watrasiewicz (1964).

of response was again assumed to be approximately linear, as in the eye of Limulus.

The basic properties of this mathematical model are similar to those of the others; central excitatory influences are opposed by the surrounding inhibitory influences; these inhibitory influences are additive and they diminish with increasing distance. But, in agreement with the model of Hartline and Ratliff, Taylor's assumption differs from the others in that the inhibitory influence exerted by any element is response-dependent or recurrent rather than stimulus-dependent. The interaction is expressed by the equation

$$f_i = e_i + K \sum_{p-s}^{p+s} f_j \ , \qquad \text{.....(2:22)}$$

where f and e are respectively the response and the average frequency of the ganglion cell discharged at a given point. The spread of the inhibitory influence is governed by the choice of s. K is the average magnitude of interaction . When K = 0, the response will equal the excitation at the point resulting from the illumination on the receptor. The sign of the coefficient of interaction may be changed with the intensity; at low intensity K can be positive and thus lead to additive excitatory effects; at higher intensity K will become zero, and at a still higher intensity it will

be negative so that inhibition would result. This changing of sign is unique to this particular model.

For a two dimensional model the equation becomes,

$$f_{(i,j)} = e_{(i,j)} + K^2 \sum_{A} f_{(p,q)} , \qquad \text{.....(2:23)}$$

where A is the area over which the summation is taken. The calculation must be carried out step by step as in the model of Hartline and Ratliff.

Figures 2:8 and 2:9 show the light distribution calculated from both equations by Watrasiewicz(1964) by assuming the inhibitory constant, K, = $b.\exp(-a|i-j|)$ where a and b are constants. If in the one dimensional equation the integration was carried over a range, say, h, the integration for the two dimensional equation would be taken over an area of $4h^2$. With the two dimensional model the multiple Mach bands are obtained (figure 2:9). Using Fourier analysis, Watrasiewicz demonstrated that the inhibitory term of the two dimensional model was much more complicated than that of the one dimensional model. The two dimensional inhibitory function consisted of terms which would give sharp variations in luminance distribution. This might lead to a multiple band structure of the Mach effect.

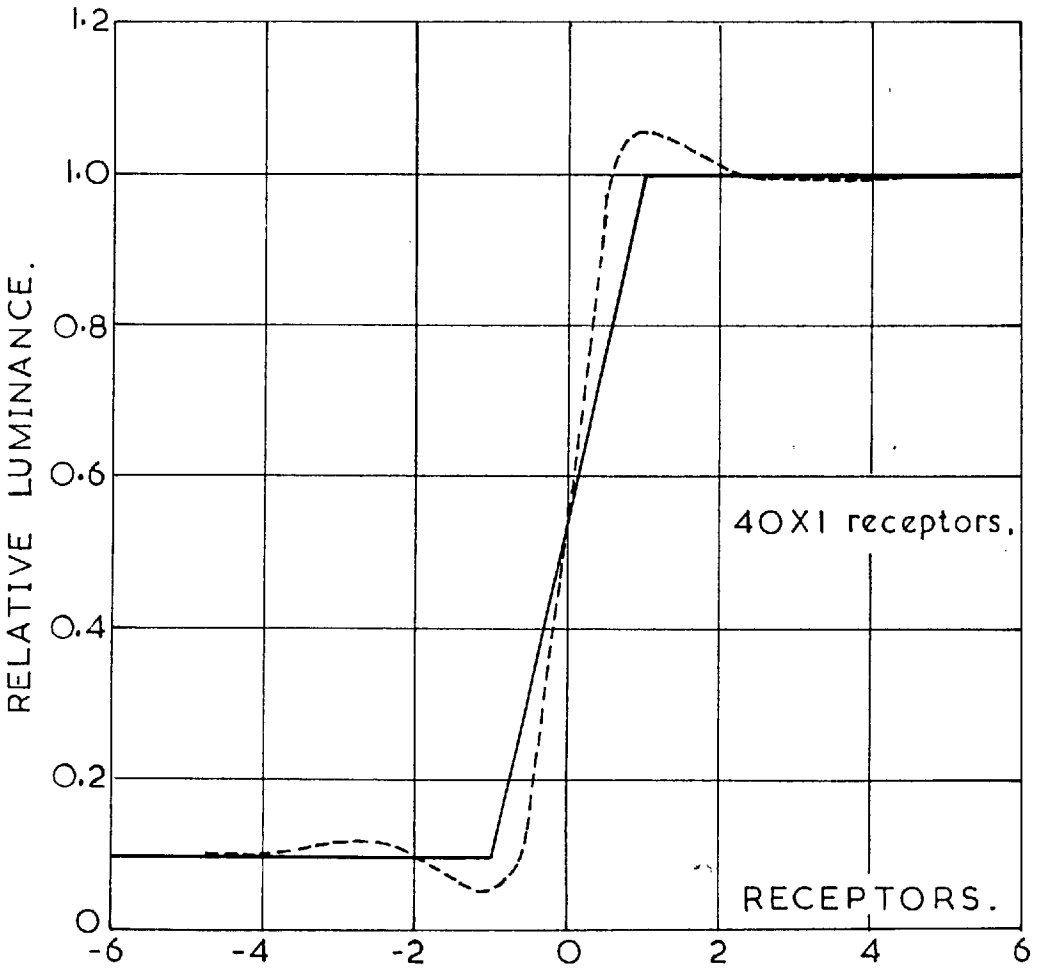



Fig. 2:8. One-dimensional model of Taylor calculated by Watrasiewicz (1964).

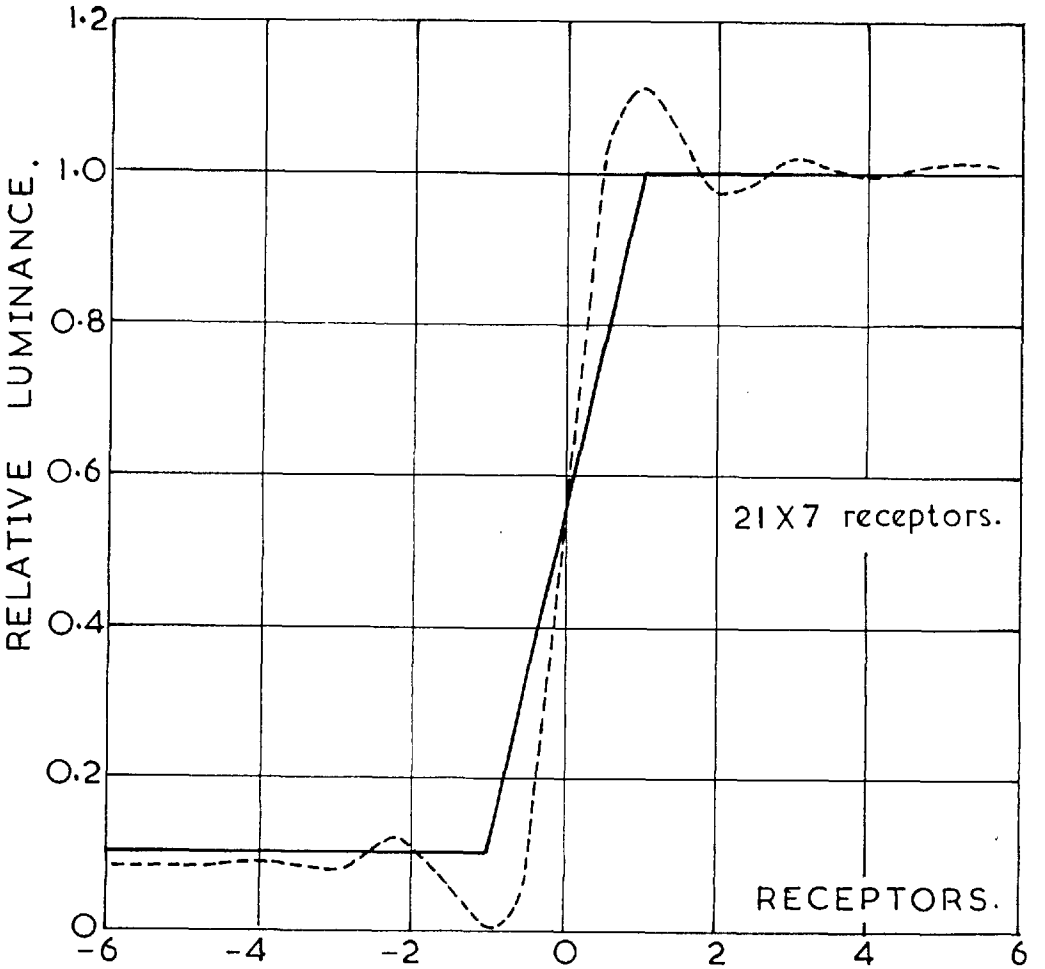



Fig. 2:9. Two-dimensional model of Taylor calculated by Watrasiewicz (1964).

## 2:6 O'Brien's Model

O'Brien (1958) used an apparatus similar to that of Mach, the subjective intensity distributions being observed on a rotating disc in order to confirm her assumption about the contour perception mechanism of the eye. Her model is also based on Mach's model. She started from Mach's model, equation 2:5, where the response(F) is given by,

$$F = I \cdot \frac{I}{I + \frac{k}{2}\left( \frac{\partial^2 I}{\partial x^2} + \frac{\partial^2 I}{\partial y^2} \right)} .$$

This equation can be written in the approximate form,

$$F = I - \frac{k}{2}\left( \frac{\partial^2 I}{\partial x^2} + \frac{\partial^2 I}{\partial y^2} \right) , \qquad \text{.....(2:24)}$$

if k is small. From this equation it would follow that the second partial derivatives of the luminance distribution on the retina act as a determining factor for the occurrence of the bands. O'Brien suggested that since the retinal mosaic has a finite spacing it would be better to consider finite differences instead of the above partial derivatives. Therefore, the above equation can be written in one dimension as,

$$F(x) = I(x) - \frac{k}{2} \cdot \frac{\delta^2 I(x)}{(\delta x)^2}$$

$$= I(x) - \frac{m}{2} \cdot \delta^2 I(x) , \qquad \text{.....(2:25)}$$

where, $\delta^2 I(x) = I(x + \delta x) - 2I(x) + I(x - \delta x)$, .....(2:26)
and, $I(x)$ is the retinal illumination.

The luminance distribution of the image on the retina is considered by assuming the eye to be a Gaussian filter, i.e; owing to the aberrations and diffraction of the eye the luminance of the image on the retina will have the form,

$$I(x) = a \int_{-\infty}^{+\infty} \exp\left( - \frac{(x' - x)^2}{2\sigma^2} \right) . \, i(x')dx,$$

where, $i(x')$ is the luminance distribution of the object (i.e; external stimulus), a and $\sigma$ are constants. $\sigma$ varies approximately inversely as the diameter of the eye pupil.

From equation 2:25 we can see that the subjective bands are visible whenever the second difference corrections are high enough. O'Brien inferred that when one observed through small apertures(i.e; $\sigma$ is big), the retinal image would have a greater broadening and correspondingly there would be smaller second difference corrections. Therefore, the contours got softened and disappeared. Her experiment also showed that with a normal pupil the bands of an external stimulus could be clearly seen, but when an artificial pupil of 0.2 mm in diameter was used those bands disappeared. This is contradictory to Watrasiewicz's (1964) results, by whom the multiple Mach bands were seen under a microscope with

an eye pupil of 0.23 millimetre diameter. However, O'Brien did not give enough experimental details to make a careful comparison. The disappearance of the bands could have been caused by using too low retinal illumination since the small pupil was introduced into the system.

O'Brien also claimed that in her experiments the variations with absolute intensity level were practically negligible; placing the light source at varying distances giving factors of illumination up to 16:1 on the object had little influence on the subjective impression until glare interfered. This also seems to contradict reports by many observers, such as, McCollough (1955) and Ercoles and Fiorentini (1959) whose results show changes in the Mach bands with changes in the luminance levels.

The intensities of the subjective bands in O'Brien's model depend on the value of $\delta x'$, and their positions depend on the value of $\sigma \cdot \delta x'$ must have a sufficiently high value to produce the subjective bands; beyond such a value the intensities of the bands increase with the increase of $\delta x'$. When $\delta x'$ exceeds a certain value the dark band shows a negative intensity. This influence of $\delta x'$ is shown in figure 2:10. Keeping $\sigma$ constant ($\sigma = 9$), the curves calculated by using O'Brien's model with $\delta x' = 9, 12$ and 15 are shown. When $\delta x' = 15$ the negative

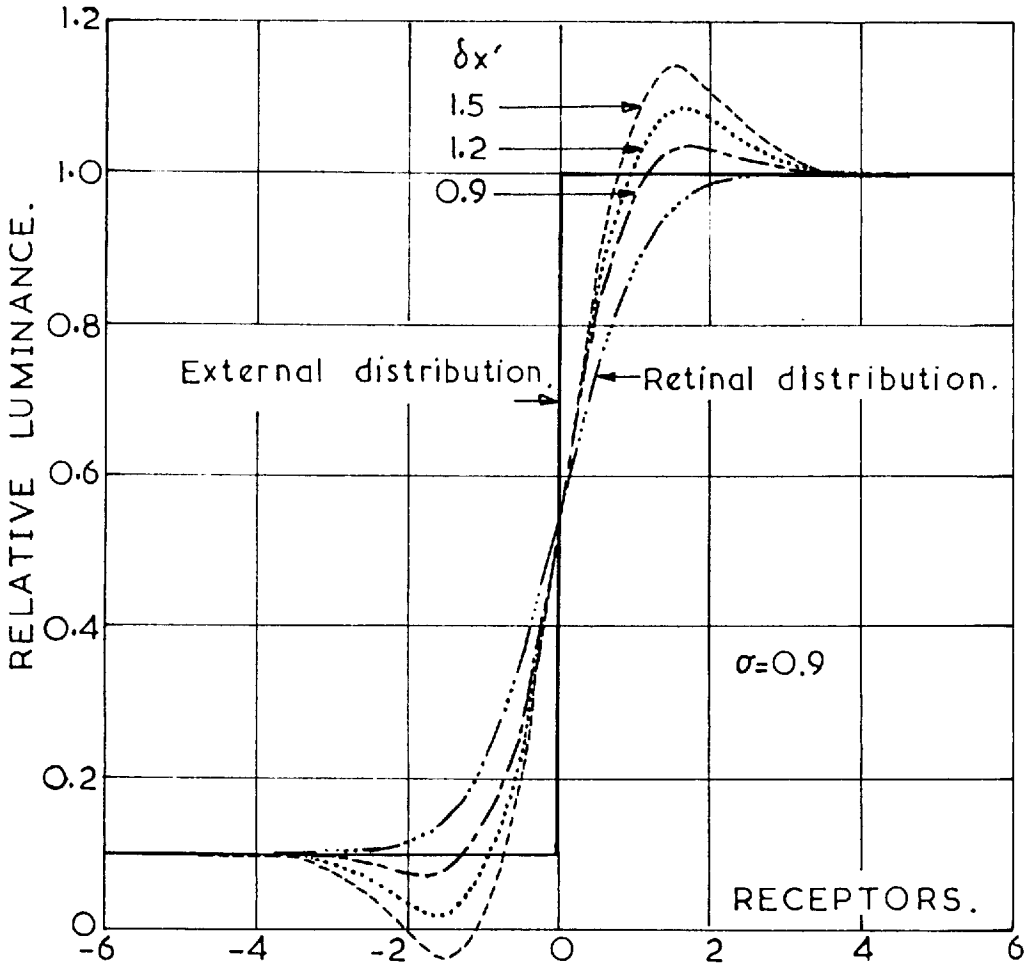



Fig. 2:10. Influence of $\delta x'$ in O'Brien's model.

value of intensity of the dark band is obtained. This must be avoided and will be further discussed in Chapter VI.

When the value of $\sigma$ is varied, the change in the positions of the bands will be as shown in figure 2:11 where the values of $\delta x'$ are chosen to give positive values of intensities of the dark bands.

## 2:7 Békésy's Model.

Békésy (1960) proposed a model in which the inhibition covers a larger area than the sensation and, as for the other models, the inhibition generally decreases with the increasing distance from the point of stimulation. However, for simplicity, the inhibition is assumed to spread out around the area of sensation to a certain distance with equal effectiveness. Beyond this distance no inhibition occurs. The width of the sensation area is very small compared to that of the inhibitory area. The area of inhibition is called the refractory area. The combination of the sensation area and the refractory area is termed a neural

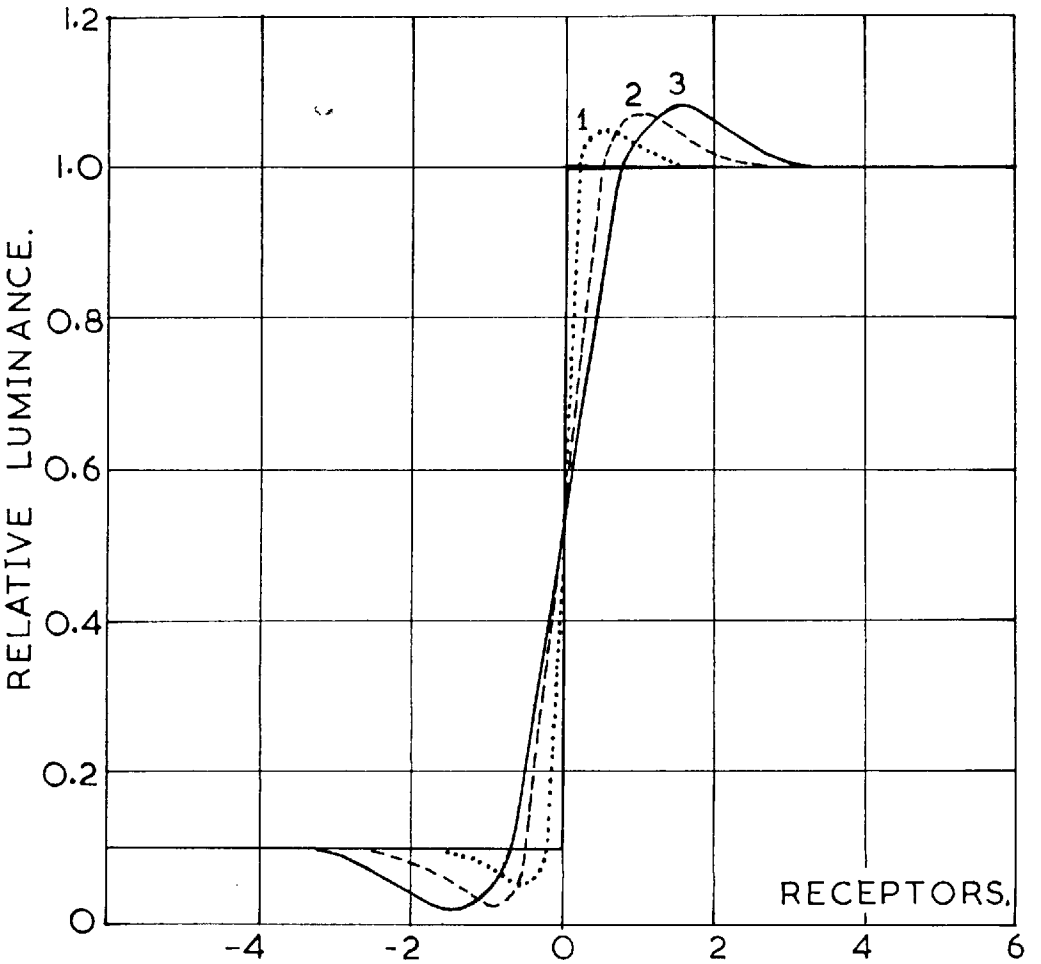



Fig. 2:11. Influence of $\sigma$ in O'Brien's model,

1) $\sigma = .3$, $\delta x' = .45$;

2) $\sigma = .6$, $\delta x' = .60$;

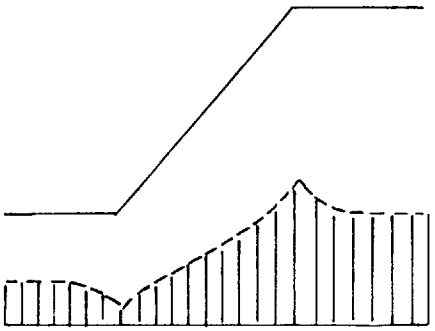
3) $\sigma = .9$, $\delta x' = 1.2$.

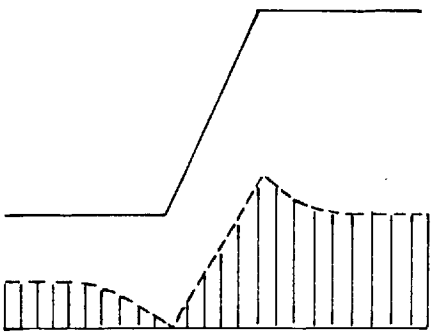
unit (see figure 1:14). By applying neural units of various widths of sensation areas to a stimulus curve, Békésy demonstrated that the width of the sensation area was not important in the formation of Mach bands, provided the width of the refractory area was much larger than that of the sensation area and the ratio of the sensation area to the refractory area stayed the same(1.6).

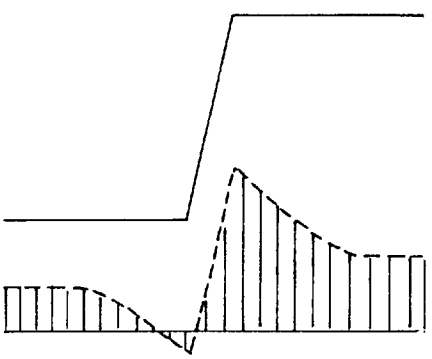
In order to transform the stimulus pattern into a sensation pattern, two assumptions are made: 1) Every narrow vertical section of stimulus has to produce a neural unit whose height is adjusted to be the same as that of the stimulus at any given point; 2) the threshold sensation magnitude at any given point is the arithmetic sum of all magnitudes of the neighbouring neural units.

With his neural unit and these two assumptions, Békésy obtained, by geometrical drawings, many results as shown in figures 2:12 and 2:13 where the influences of luminance gradient and the radii of inflection points of the intensity distribution of the object on visual bands are shown (the dotted lines are the subjective impressions). Furthermore, he noted that the width of the refractory area does not change the sensation distribution, provided the ratio of the sensation and refractory areas of the neural unit stays the same.

An equation giving the sensation magnitude







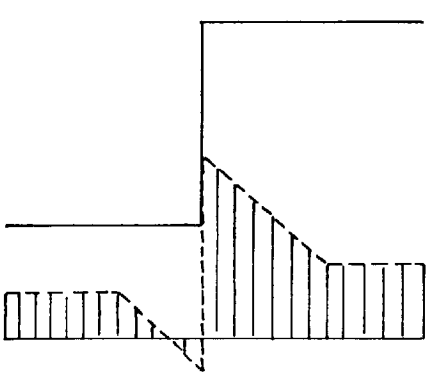
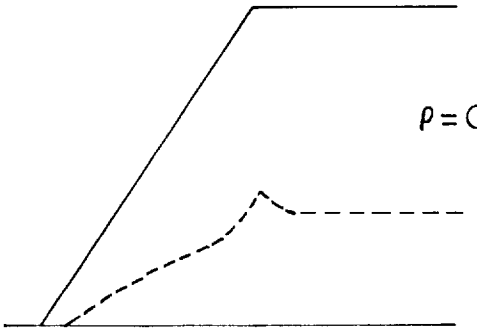
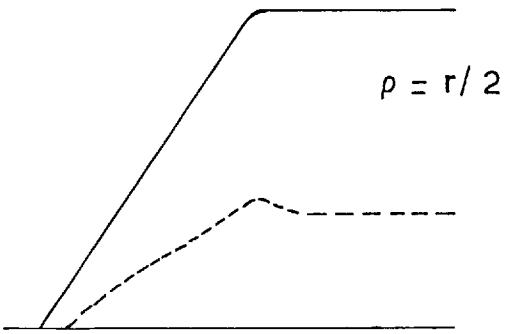
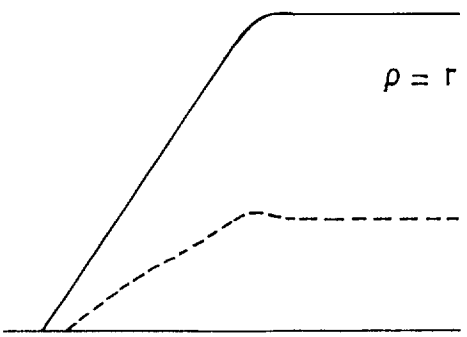


Fig. 2:12. Influence of luminance gradient on Mach bands (Békésy 1960).



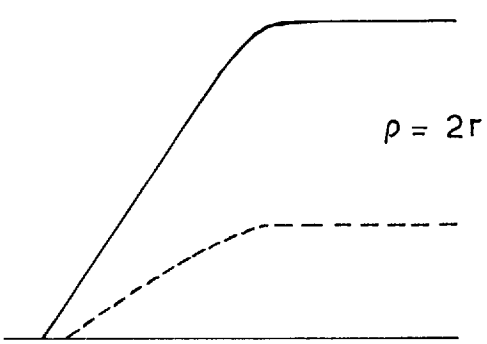




Fig. 2:13. Influence of radius of curvature of inflection on Mach bands (Békésy 1960).

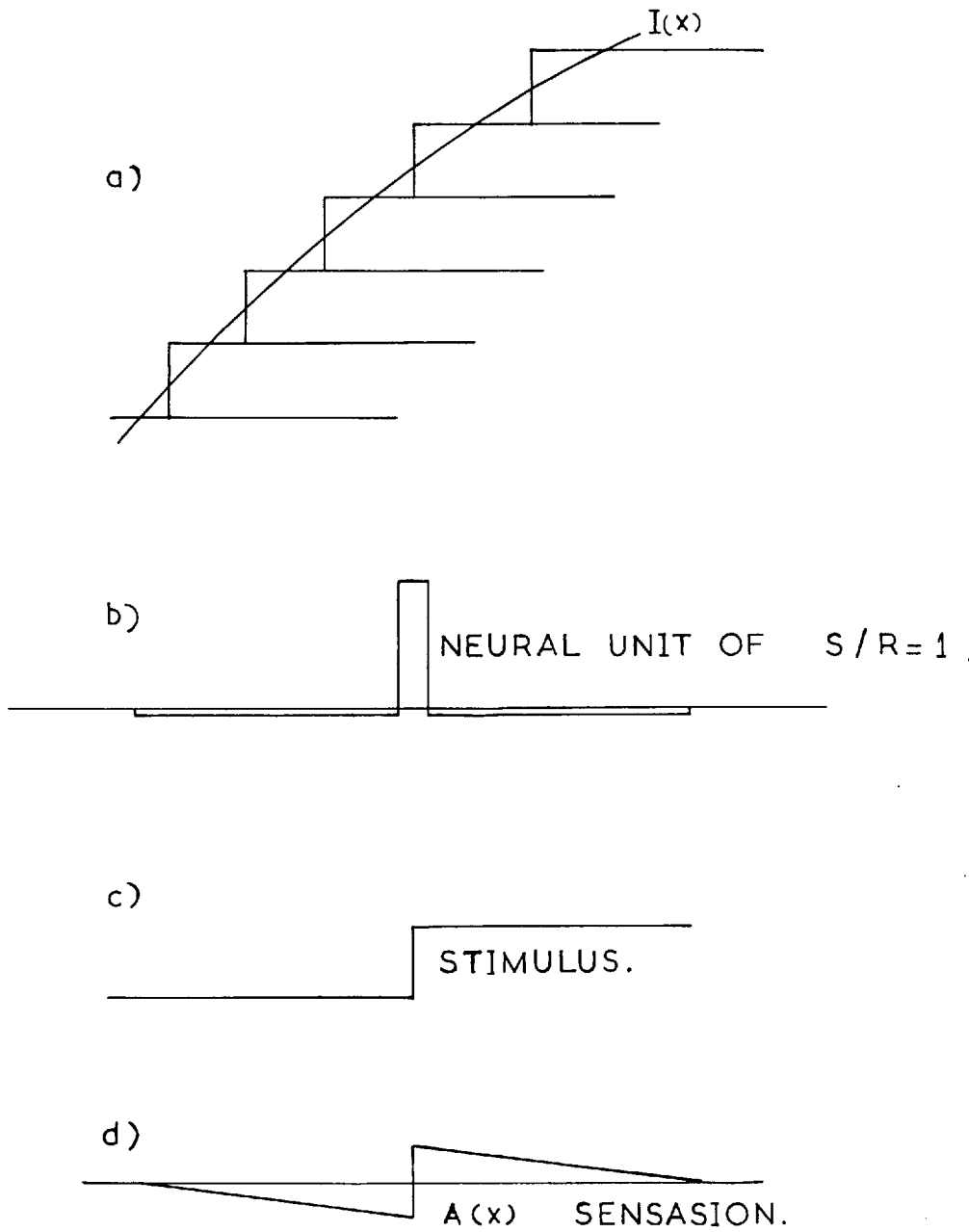



Fig. 2:14. Development of Békésy's model.

produced by any given stimulus distribution was proposed by Békésy. From figure 2:14 where any stimulus distribution I(x) is divided into a series of equal steps, the equivalent sensation distribution for each step can be drawn by application to a neural unit. For simplicity, a neural unit of S/R = 1 is used so that the sensation distribution produced by each step is the same and the magnitude is stimulus-independent. The result of applying each step (figure 2:14c) on the neural unit (figure 2:14b) is a sensation distribution (figure 2:14d) with equal areas of positive and negative magnitude, A(x). The sum of these sensation steps along the x-axis gives the sensation magnitude corresponding to the stimulus distribution, I(x). As the step becomes smaller and smaller, an integral is approached. From figure 2:14d, the areas above and below the zero line are equal, that is, a sensation distribution can be represented by any straight line $\sum A(x) = 0$ . Therefore, only a curvature of the stimulus function I(x) can produce a sensation magnitude which is negative for a stimulus distribution convex towards the axis of abscissa and positive for a concave distribution.

The sensation magnitude for a neural unit of S/R = 1 is given by,

$$E_o = \int_{-\infty}^{+\infty} A(x - \lambda).I'(\lambda).d\lambda , \quad .....(2:27)$$

where $I'(\lambda)$ is the derivative of $I(\lambda)$.

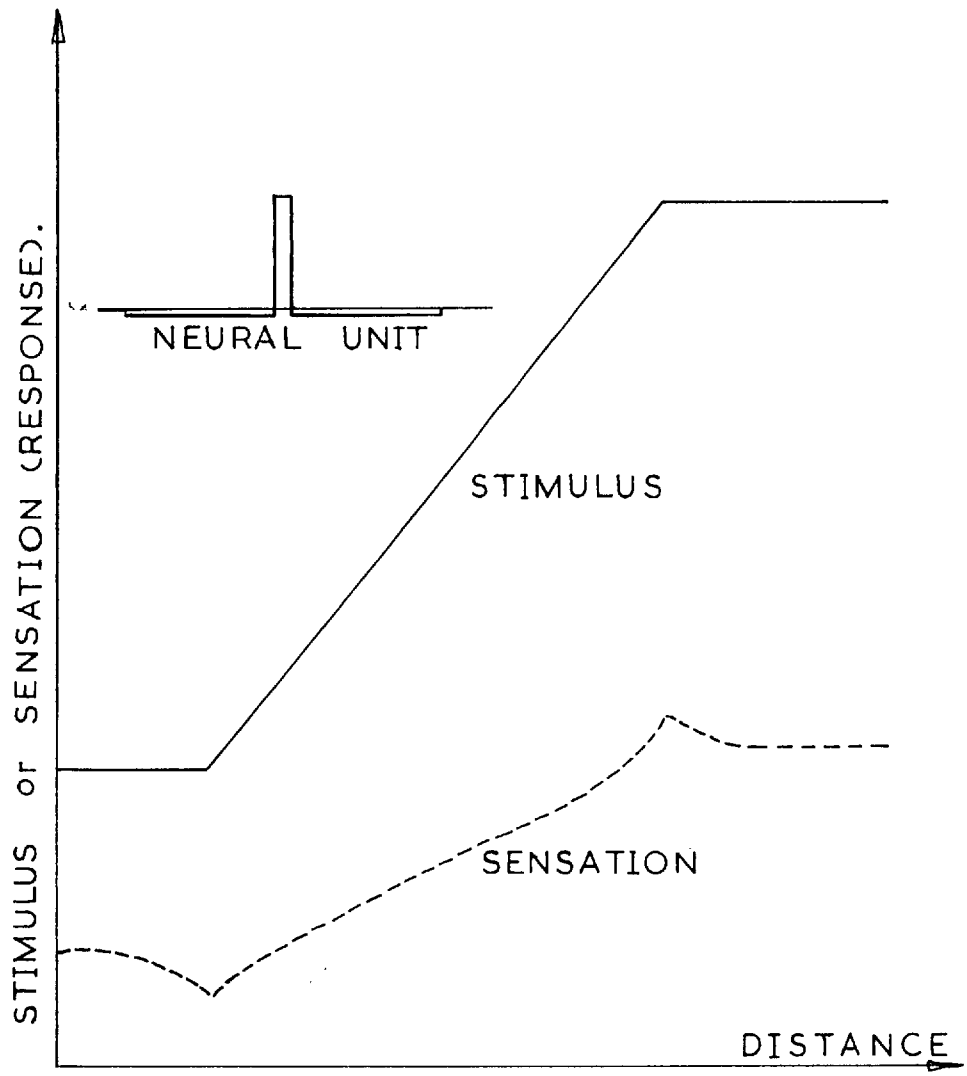



Fig. 2:15. A calculated subjective luminance distribution ( Békésy 1960 )

Then adding to it at every point a sensation magnitude corresponding to the excess, $S - S_o$ ,

$$E = (S - S_o).I(x) + E_o \quad . \qquad \ldots\ldots\ldots\ldots (2:28)$$

Figure 2:15 shows the result calculated by these mathematical expressions. However, Békésy noted that the widths of the calculated Mach bands were equal to the full width of the inhibitory zone, and because the widths of the bands depended upon the intensity levels of illumination and other factors, the widths of the inhibitory zone might not be constant.

Békésy's and O'Brien's models are linear, as is shown by the fact that for an antisymmetrical distribution the subjective bright and dark bands obtained will be symmetrical about the origin. This does not seem to fit the observed results where the bright band is always more pronounced than the dark band.

## 2:8 Discussion.

If we return to figure 2:4 in which the subjective impression calculated by Fry is shown, it will be seen that the magnitude of the overshoot of the distribution is less than that of the undershoot. In fact, the response in Fry's equation is expressed in terms of the frequency of impulses of the receptors while the input is in terms of the intensity stimulating the retina. Using the assumption

that the frequency of the output is proportional to the logarithm of the stimulus, as in the eye of Limulus, one can write Fry's equation in terms of the subjective brightness, that is,

$$\log B = k.\log \frac{I(x,y)}{1 + A\int_{-\infty}^{+\infty}\int I(x,y).\exp\left(-\frac{x^2+y^2}{2\sigma^2}\right).dxdy} + k_6 ,$$

or,

$$B = K\left[\frac{I(x,y)}{1 + A\int_{-\infty}^{+\infty}\int I(x,y).\exp\left(-\frac{x^2+y^2}{2\sigma^2}\right).dxdy}\right]^k , \qquad \ldots\ldots(2:29)$$

where B is the output in terms of brightness; K,k and A are constants.

Calculations were carried out with this equation and with equation 2:13 for a gradient edge which is shown in figure 2:16. The result obtained from equation 2:29 is shown by curve 1, the bright band is more prominent than the dark band, which is in better agreement with the experiment than the results from Fry's original equation (equation 2:13), shown by curve 2, where the undershoot is greater than the overshoot.

The theories behind these mathematical models are based only on psycho-physiological experiments. The physical mechanism of the eye in the perception of light

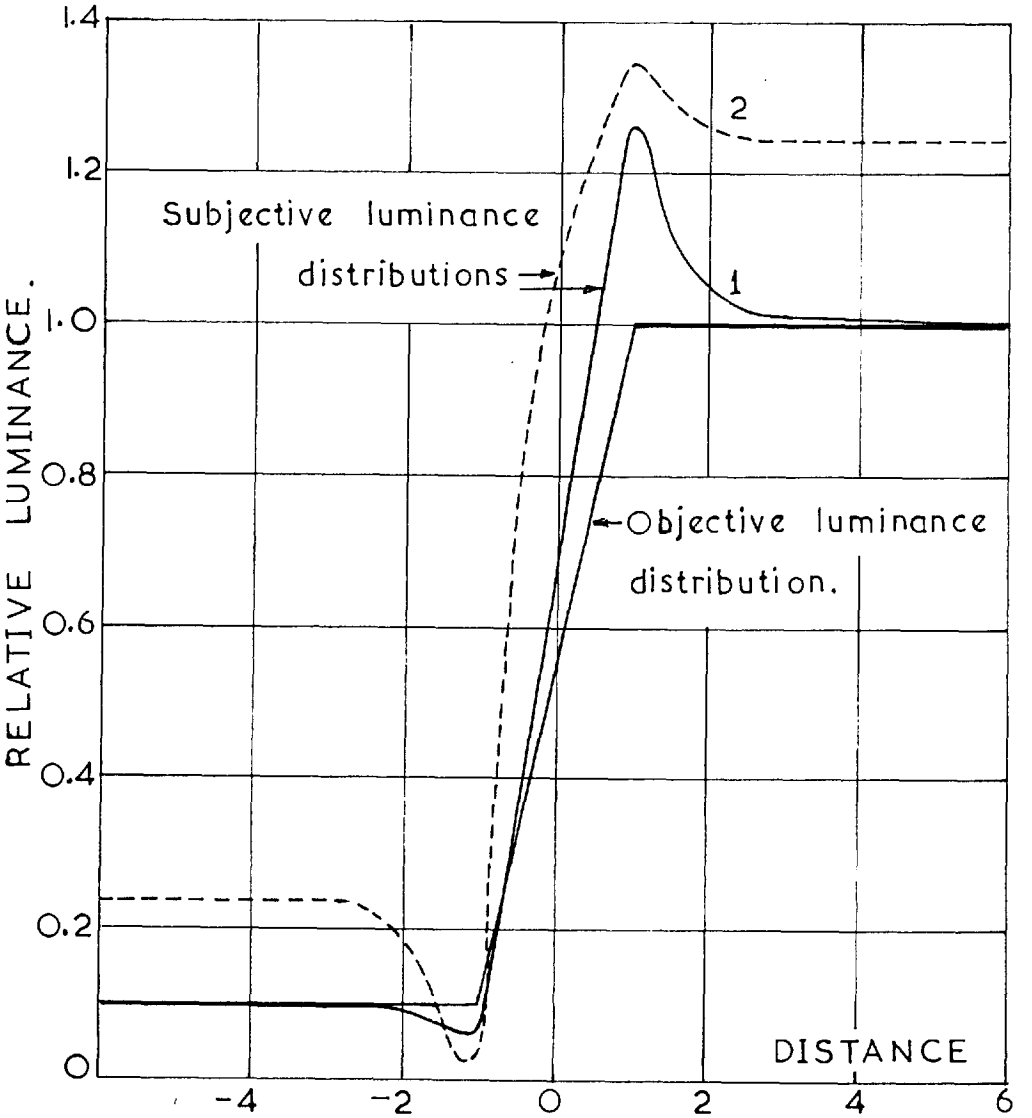



Fig. 2:16. Predicted luminance distributions calculated from,

1) Fry's modified model (eq. 2:29),

2) Fry's original model (eq. 2:13).

has never been determined. It is thus worth seeing whether the transformation from the physical image to the visual image can be modelled mathematically without appeal to the details of the physiological mechanisms.

We start from fact that the inhibitory action exerted on neighbouring receptors when the light stimulates any point $P_o$ on the retina increases at first rather rapidly and then decreases slowly with increasing distance from that point. A simple mathematical expression for this action contains an exponential, that is, the influence of distance between two given points on the inhibitory action will depend on $\left[x^2 . \exp(-Bx^2)\right]$, where B is a constant and x is the retinal distance. With $x^2$ the function will give a symmetrical distribution about the origin, as required.

However, the strength of the inhibitory action does not depend only on the distance between receptors, but also on the level of illumination. Suppose element P of an area dxdy is stimulated by illumination of an amount $I(x,y)$. P will exert an inhibitory action on $P_o$; the inhibition could then be dependent on the expression, now written two-dimensionally,

$$I(x,y)\left[(x-x_o)^2+(y-y_o)^2\right].\exp\left[-\frac{1}{2\sigma^2}\left\{(x-x_o)^2+(y-y_o)^2\right\}\right]\,dxdy,$$

where $\sigma$ is a constant.

In order to get the overall inhibition, an integration over the whole area must be carried out with respect to distances x and y along the retina. The response then appears as,

$$F(x_o,y_o)=\frac{I(x_o,y_o)}{1+A\int_{-\infty}^{+\infty}\int I(x,y)\left\{(x-x_o)^2+(y-y_o)^2\right\}\exp\left\{-\frac{(x-x_o)^2+(y-y_o)^2}{2\sigma^2}\right\}.dxdy} \quad \ldots\ldots\ldots\ldots(2:30)$$

where A is a constant. The denominator of the equation is put in such a way that a large value of the inhibition will affect $I(x_o, y_o)$ while a small value will not.

Figures 2:17 and 2:18 show respectively the one dimensional and two dimensional subjective luminance distributions calculated from this equation; the non-linearity is obtained.

If now the inhibitory action in equation 2:30 is normalized so that the whole function does not change when the overall light level in the physical image is altered, we have,

$$F(x_o,y_o)=\frac{I(x_o,y_o)}{1+\dfrac{A\int_{-\infty}^{+\infty}\int I(x,y)\left\{(x-x_o)^2+(y-y_o)^2\right\}\exp\left\{-\frac{(x-x_o)^2+(y-y_o)^2}{2\sigma^2}\right\}dxdy}{\int_{-\infty}^{+\infty}\int I(x,y).\exp\left\{-\frac{(x-x_o)^2+(y-y_o)^2}{2\sigma^2}\right\}dxdy}} \quad \ldots\ldots\ldots(2:31)$$

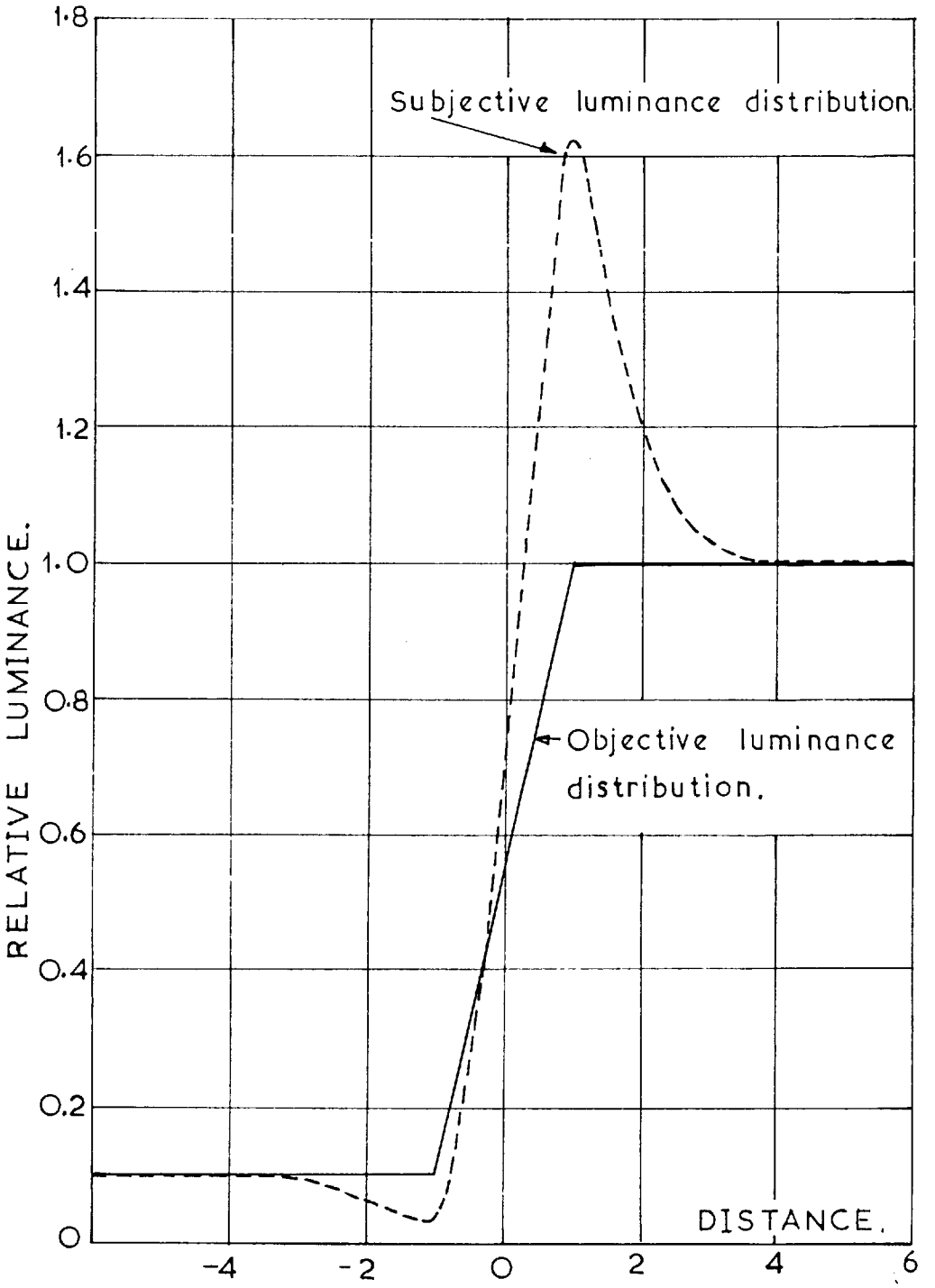



Fig. 2:17. Newly proposed one-dimensional model (eq. 2:30).

$A = 0.0017$, $\sigma = 0.9$.

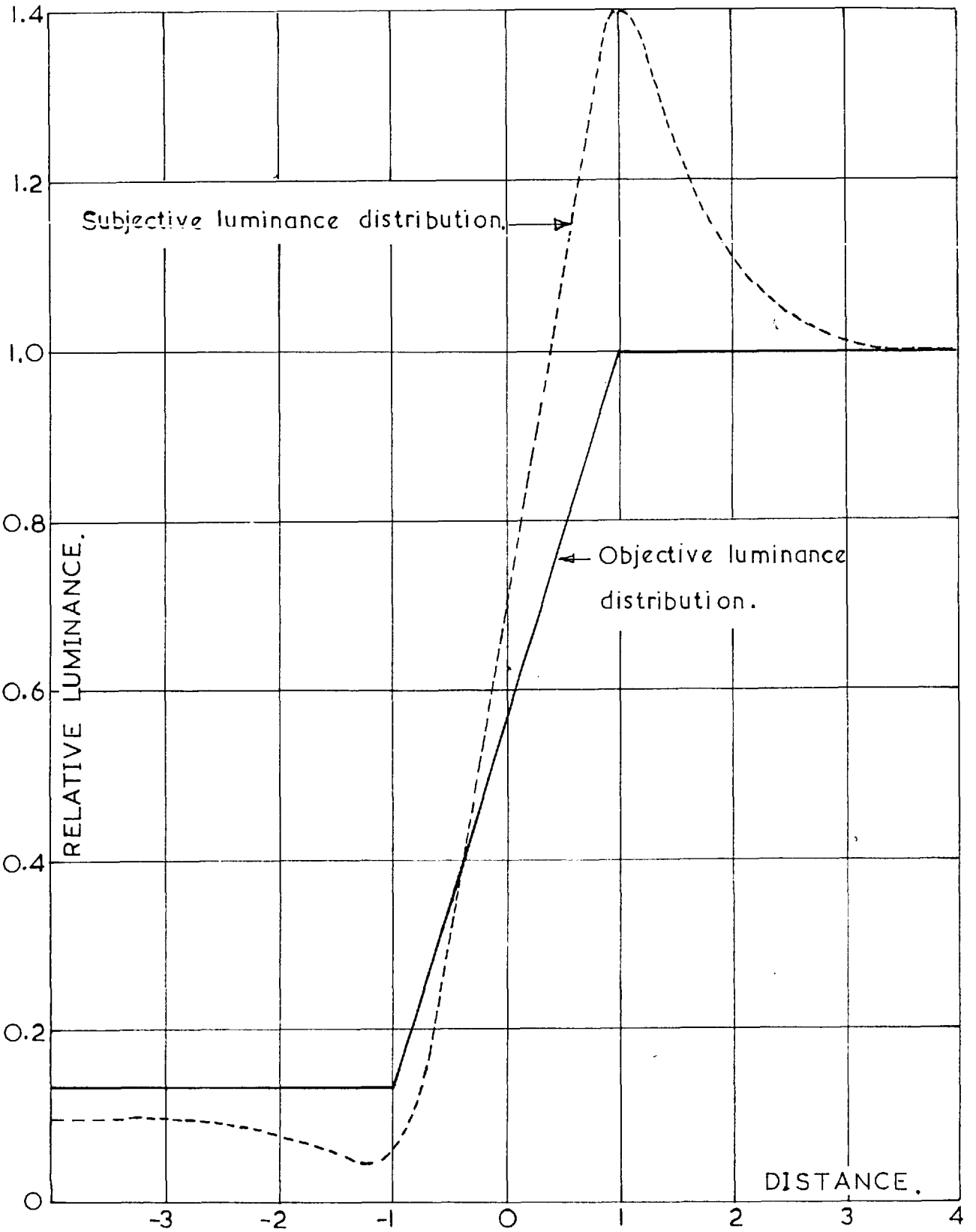



Fig. 2:18. Newly proposed two-dimensional model (eq. 2:30).

The results are shown in figures 2:19 and 2:20 for the one dimensional and two dimensional models respectively.

Let us now consider in more detail the inhibitory action which is as above only a function of the distance along the retina from a given point of stimulus. In this new model, the inhibition has the form,

$$f(x) = x^2 . \exp(- x^2/2\sigma^2) .$$

The graph of this function is shown in figure 2:21. Two factors are found to depend on $\sigma$ ; the extent of the inhibitory field involved and the positions of the maxima of the inhibitory action.

If we return to Fry's model(equation 2:13) or to the modified model of Fry (equation 2:29), the inhibition is described by,

$$f(x) = \exp(- x^2/2\sigma^2) .$$

The results of the calculation for various values of $\sigma$ are shown in figure 2:22. $\sigma$ only influences the extent of the inhibitory field around the stimulated point .Thus the new model may provide more flexibility in fitting to experimental results.

Another way of studying the neural mechanism in the human retina is by Fourier analysis calculations, although experimental observations on these lines are not yet possible. Since the object distribution and the spread

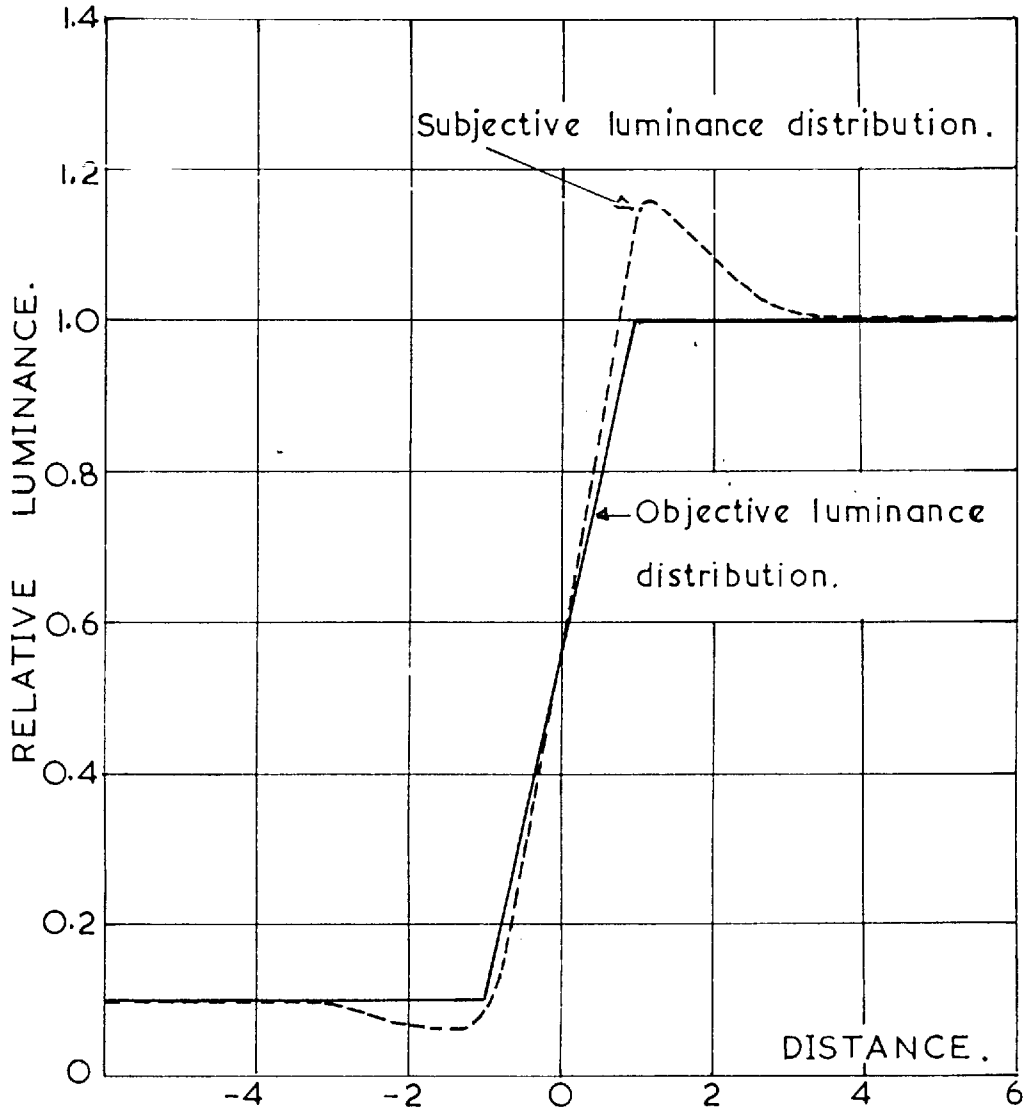



Fig. 2:19. Newly proposed one-dimensional model (eq. 2:31).

$A = 0.04$ , $\sigma = 0.9$ .

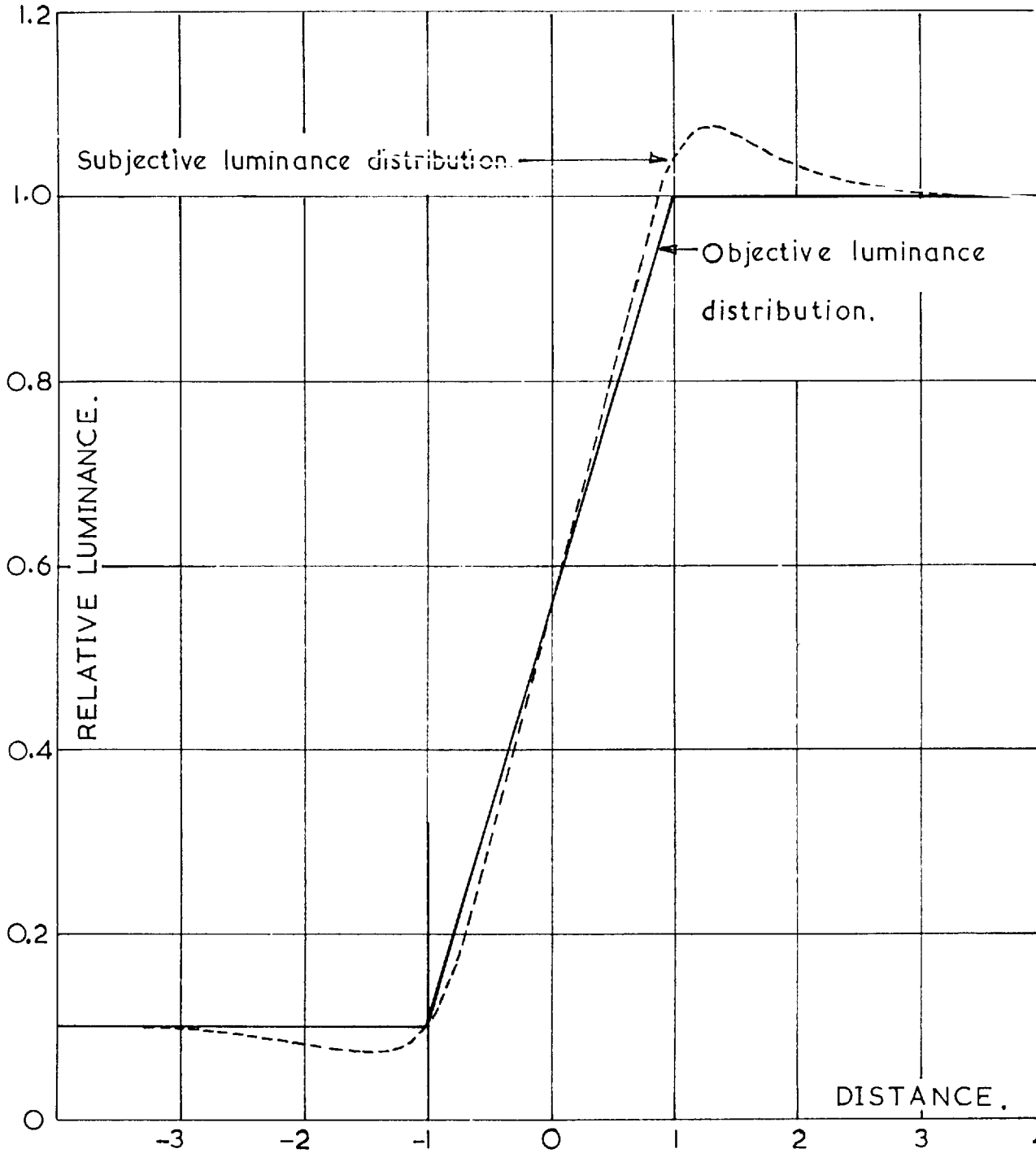



Fig. 2:20. Newly proposed two-dimensional model (eq. 2:31).

$$f(x) = x^2 . e^{-x^2/2\sigma^2}$$

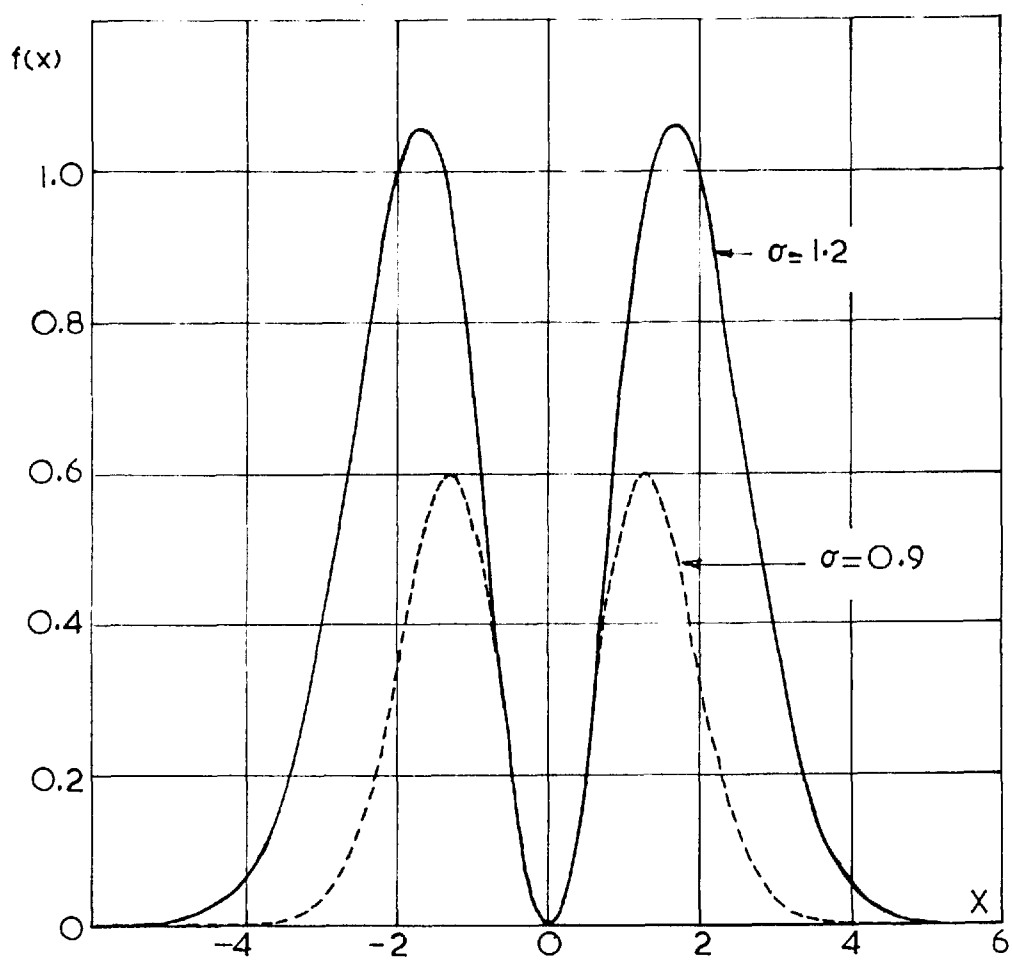



Fig. 2:21. Inhibition as a function of retinal distance (x) in the proposed new model.

function of the optical elements of the eye may be measured independently, the image form by an eye can be determined by making a Fourier analysis of the spatial frequencies which make up the object pattern, multiplying these by the optical transfer function of the eye, and then summing the results to obtain the image distribution.

However, to evaluate accurately the transfer function for the optical media of the human eye, especially for the higher spatial frequencies, is very difficult. In 1959, Menzel evaluated the composite transfer function for the human eye by measuring the relative visibility of several sinusoidal distributions of illumination with different spatial frequencies. The average result obtained by five observers is shown in figure 2:23 where the function increases rapidly at low frequencies, remains constant for a while, and then decreases with increasing frequency. When the subjective distribution was calculated, a fair approximation to the observed one was obtained. The Mach bands were seen as expected but the calculated bands were symmetrical while the observed ones were not, and the calculated widths of the bands were larger than those observed.

In 1961, the average composite transfer function for the whole visual system was calculated by Lowry and DePalma . They approached the problem by making measurements

$$f(x) = e^{x^2/2\sigma^2}$$

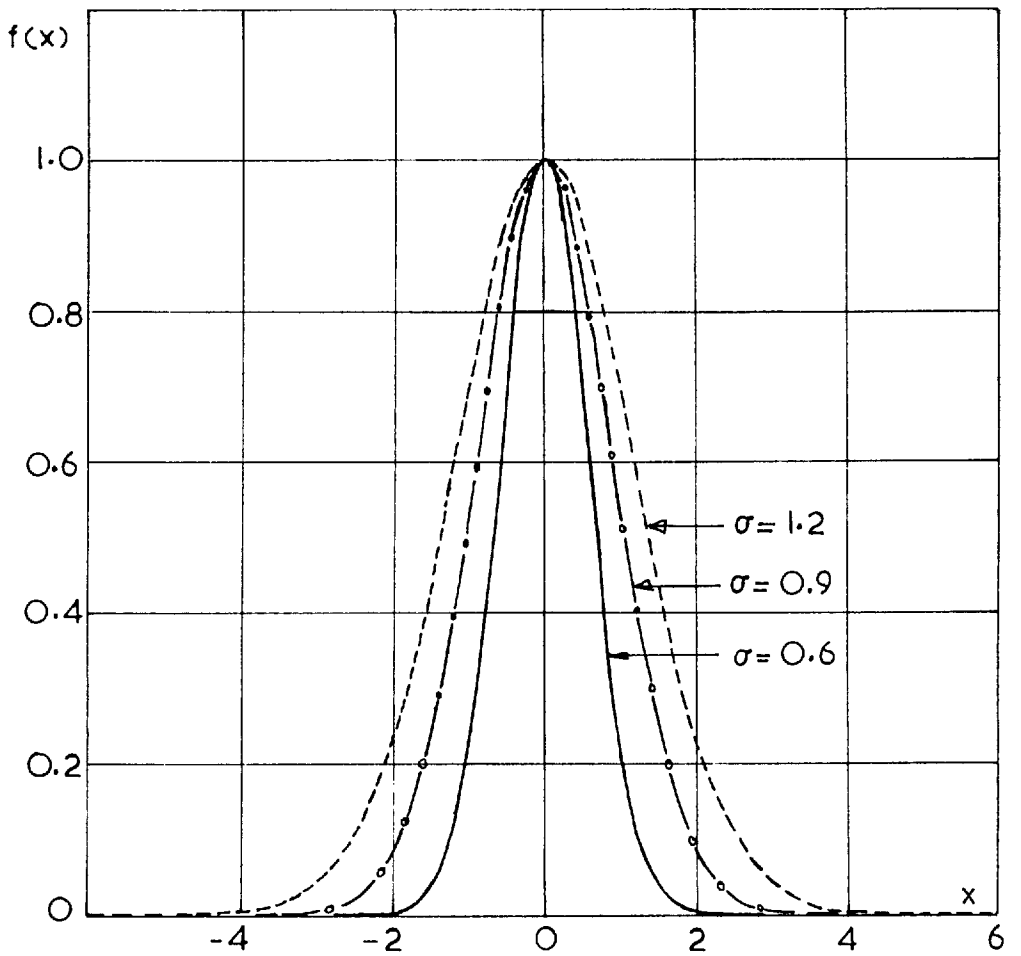



Fig.2:22. Inhibition as a function of distance in Fry's model.

COMPOSITE TRANSFER FUNCTION OF THE VISUAL SYSTEM

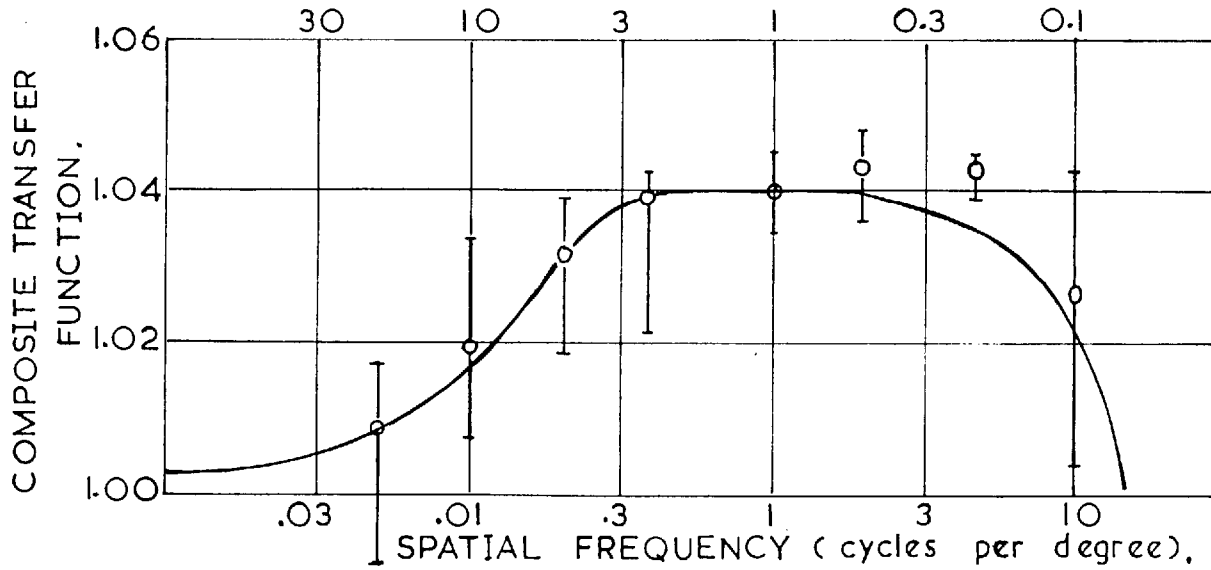



Fig. 2:23. After Menzel (1959).

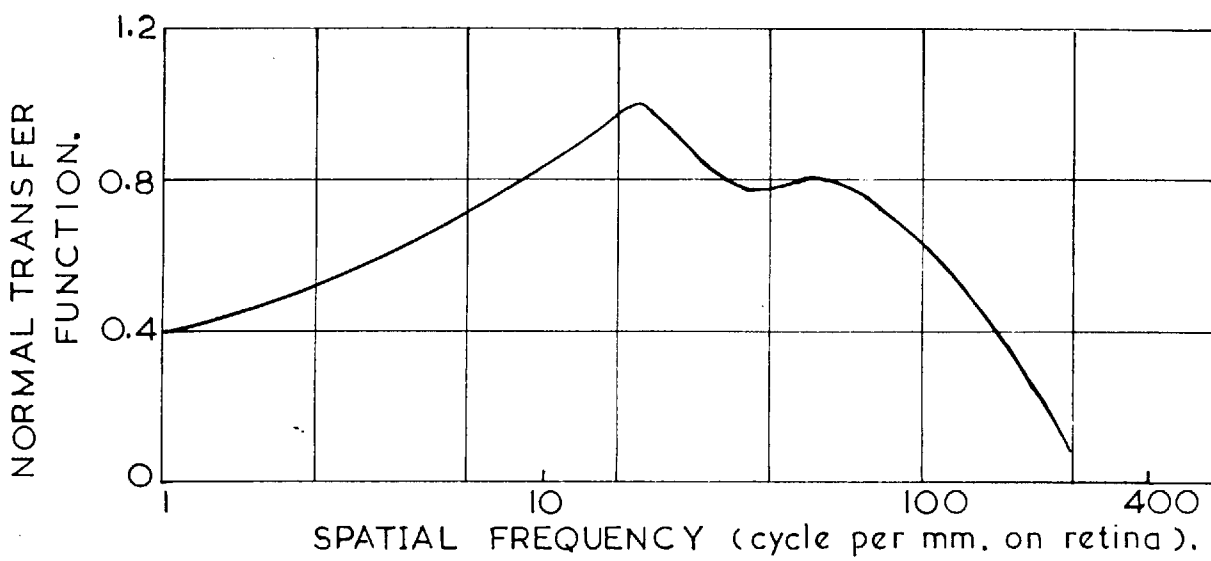



Fig. 2:24. After Lowry and De Palma (1961).

on the objective luminance distribution pattern and the corresponding subjective distribution seen by the observer; then the spatial frequencies contained in these two distributions were analysed. The calculated composite transfer function obtained for the whole visual system is shown in figure 2:24.

However, in these frequency response methods linearity of the system is assumed. This is contrary to the results observed by many workers and to the proof which was given by Marimont in 1963 (already discussed in section 2:1) where non-linearity in the visual system was demonstrated.

# CHAPTER III

## THE MACH EFFECT AT AN ABRUPT EDGE.

### 3:1 Introduction.

A sharp transition edge presents another problem which has been discussed by many observers. For example, Fiorentini and Radici (1958) claimed that Mach bands would not be seen on an abrupt step function object. Lowry and DePalma (1963) suggested that for a given luminance distribution, the width of the bright and dark bands became less, the steeper the gradient. As the width of the edge approached zero the widths of the bright and dark bands also approached zero. For a really sharp edge the eye might be unable to distinguish any bands differing in apparent luminance from those luminances which formed the edge itself. On the contrary, Charman and Watrasiewicz (1964), observing through a microscope, were able to see multiple Mach bands on aluminized straight edges. In 1966, Matthews showed that a bright band on a straight edge could be observed by the great majority of subjects.

If the luminance distribution of a step function object is considered, the distribution as a function of distance(x) is defined by,

$$f(x) = 0, \quad \text{when } x = 0,$$
$$= 1, \quad \text{when } x > 0.$$

This type of function is also called a Heaviside unit function. The function and its derivatives are shown in figure 3:1. The first derivative is only a line (actually a delta function ). The minimum and maximum of the second derivative curve for this case appear at the same position as shown in figure 3:1c .

In fact, the luminance distribution in the image of a step function on the retina is not a sharp transition distribution. The diffraction and aberrations of the eye cause blurring of the retinal image. The blurring which is due to the chromatic aberration depends on the wavelength of light used, and will be minimized when the eye is presented with the monochromatic light. Figure 3:2 shows the results of the mean chromatic aberration of the human eye reported by Ivanoff (1953) and Wald and Griffin (1947), compared with the calculated values (Ivanoff 1953). From this graph, the dioptric power of the refracting system of the eye varies from -0.62 dioptre at $\lambda$ = 0.750 micron to +2.63 dioptres at $\lambda$ = 0.365 micron. These values are referred to $\lambda$ =0.578 micron as origin, where the chromatic aberration is taken as zero and the power of the refracting system of the eye is 60 dioptres.

Blurring produced by monochromatic aberrations and diffraction of the eye depends very much on the pupil

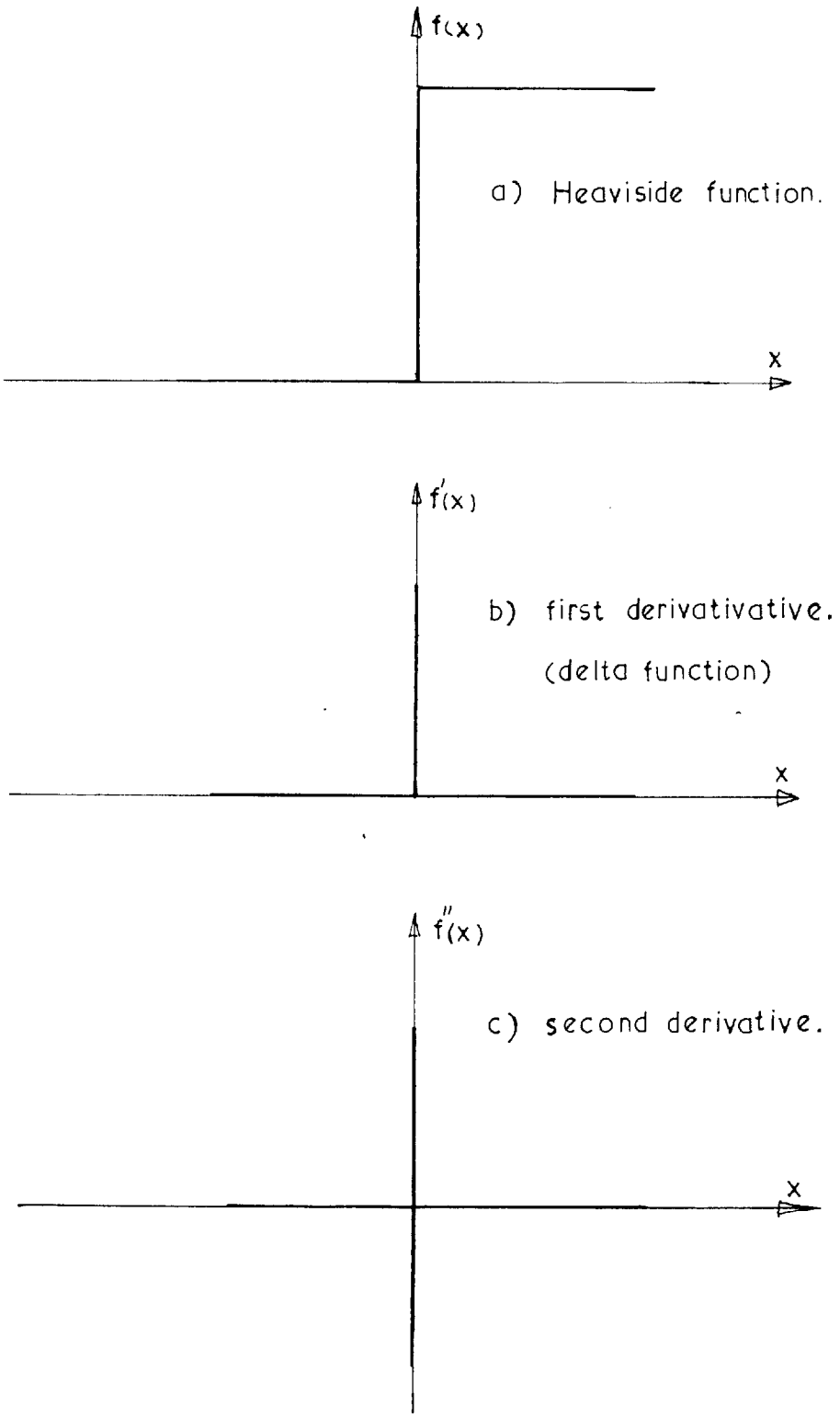



Fig. 3:1. The light distribution of an abrupt edge and its derivatives.

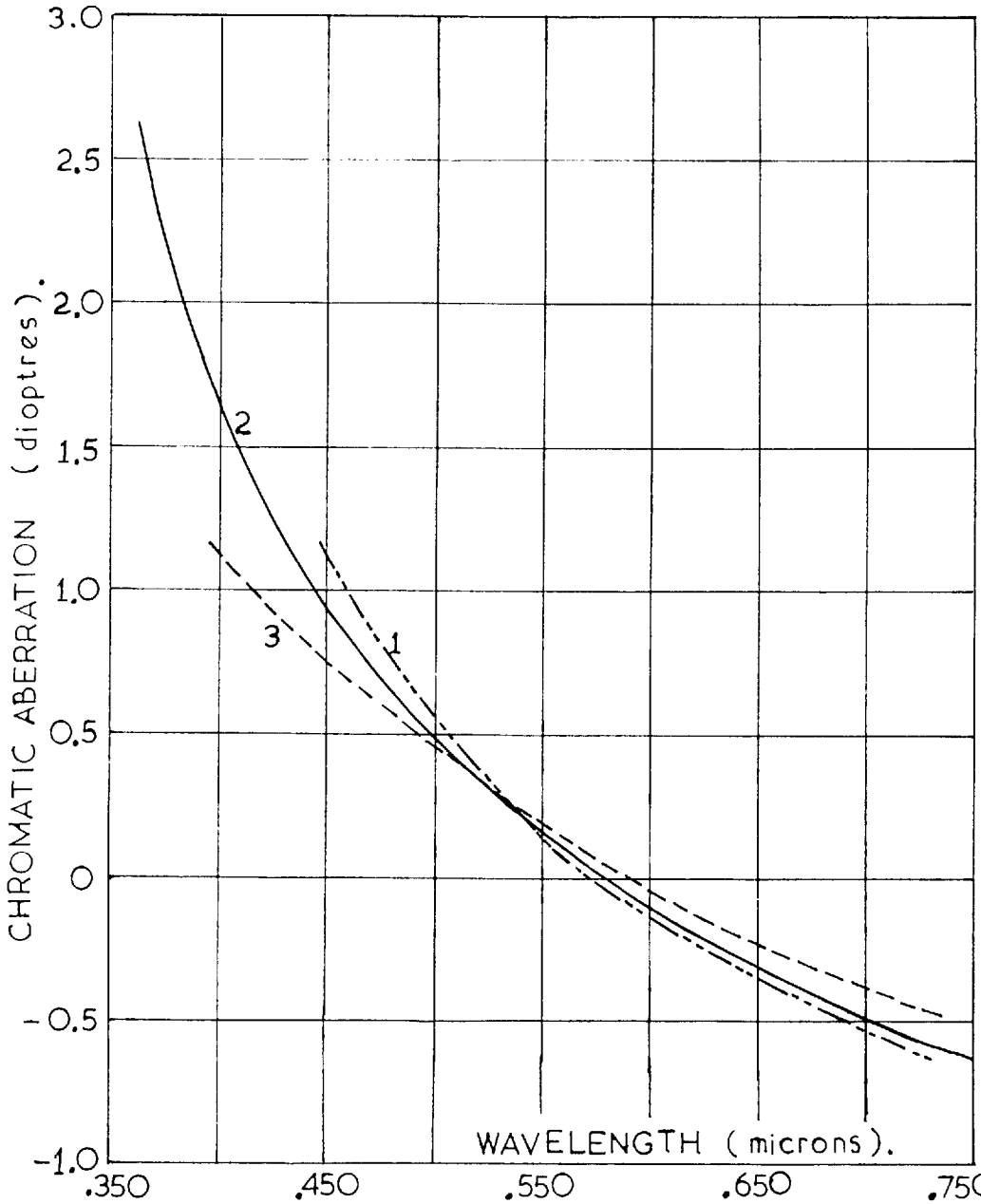



Fig. 3:2. The chromatic aberration of the eye,

1) Ivanoff (11 observers) 1953,

2) Wald and Griffin (14 observers) 1947,

3) The calculated values (Ivanoff 1953).

size. The major monochromatic aberration of the eye in the forveal region is spherical aberration. The presence of spherical aberration in the human eye appears to have been recognized in 1801 by Thomas Young. Koomen, Tousey and Scolnik (1949) showed that positive (under-corrected) spherical aberration is present in the non-accommodated eye; this aberration is reduced when the eye is accommodated. They suggested that when the effect of spherical aberration on vision was considered the aberration had to be measured for the individual under observed conditions. Figure 3:3 shows the mean spherical aberration of 10 observers reported by Ivanoff (1956); the spherical aberration varies from under-correction to over-correction as accommodation changes.

The luminance distribution in an image of an abrupt edge in incoherent illumination is known in terms of the Struve function and from this the second derivative curve can be derived. A number of inflections on the luminance distribution curve which are not actually maxima or minima are found. Even though these inflections are very small they still give extreme values in the second derivative curve, and they are amplified by the visual mechanism into bright and dark bands when viewed under proper conditions. The exact positions where the second derivative has maximum and minimum values are determined by the vanishing

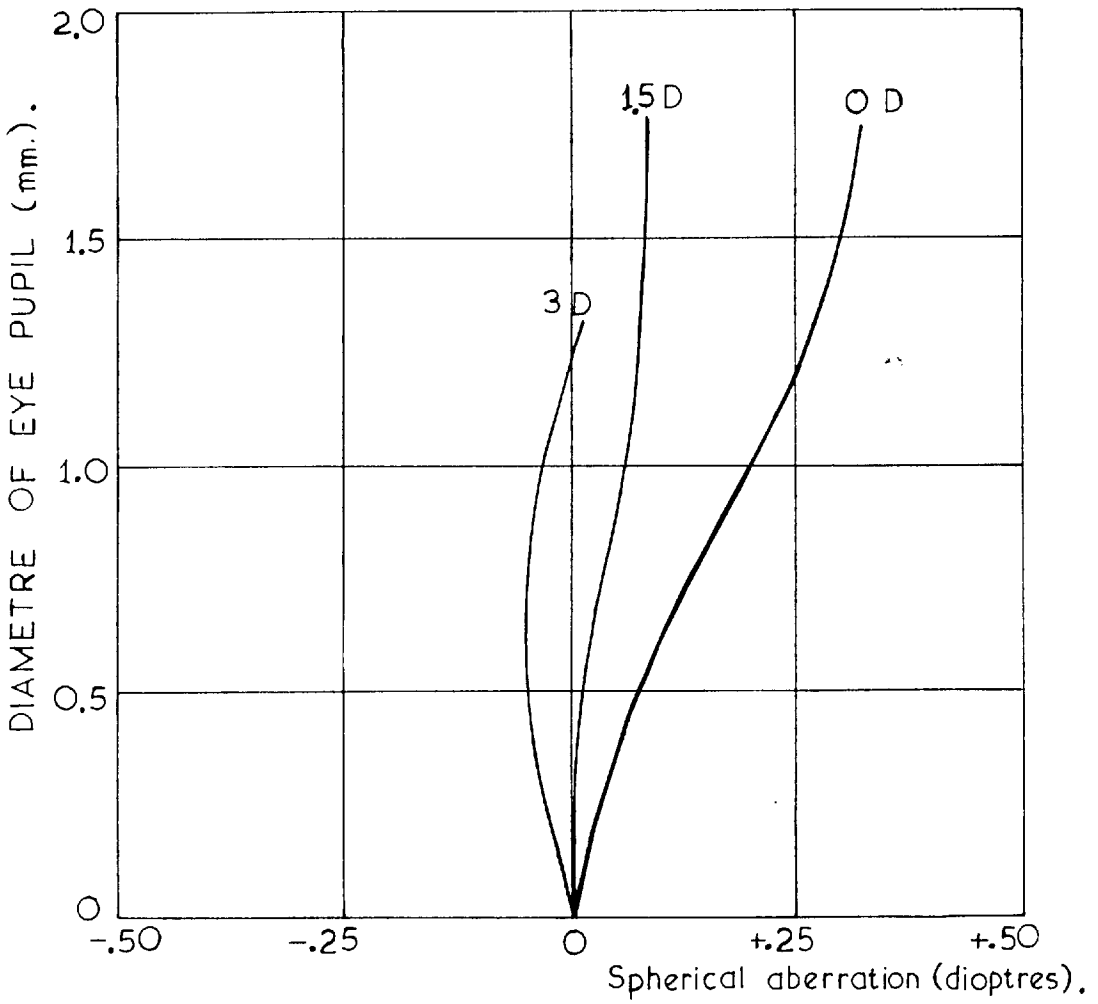



Fig. 3:3. Mean spherical aberration at various accommodation levels. (IVANOFF 1956)

of the third derivative. Again, referring back to the second derivative theory of Mach phenomena, a few bands could be seen at those points where the third derivative vanishes or the second derivative has the extreme value.

Ludvigh (1953) mentioned that in a family of retinal energy distributions, the widths of the bands were reduced when the magnitudes of the fourth derivative of the energy with respect to the distance along the retina were increased. The formula for the fourth derivative of the image distribution of an abrupt edge and the numerical calculations from it will also be given. The computations of the edge intensity distribution and its derivatives were carried out on a National Elliot 803A computer.

An optical system was set up for measuring the positions of the Mach bands at an incoherently illuminated edge, in order to see how the second derivative theory and other mathematical models fit the experimental results.

The results are given in terms of the diffraction units as well as in units of minutes of arc subtended from the eye. The distance Z in diffraction units is defined by,

$$Z = \frac{2\pi(N.A)}{\lambda}\eta \,, \qquad \text{.....(3:1)}$$

where $\lambda$ is the wavelength of light used, $\eta$ is the object size, and (N.A) is the numerical aperture in the object

space of the optical system. The numerical aperture in the object space of a lens is $n.\sin\alpha$, where n is the refractive index of the medium in which the object exists, and $\alpha$ is half the angle subtended by the aperture of the lens. The Abbe sine condition gives the generalised form of Lagrange's relation as follows:

$\eta.(N.A)$ in object space = $\eta'.(N.A)$ in image space,

or, $$\eta.n.\sin\alpha = \eta'.n'\sin\alpha' . \quad .....(3:2)$$

Thus, we can write,

$$Z = (2\pi/\lambda).n.\sin\alpha.\eta \quad , \quad \text{in object space,}$$

and, $$Z = (2\pi/\lambda).n'\sin\alpha'.\eta' \quad , \quad \text{in image space.}$$

In this way the geometrical optics sizes of object and image are equal in Z units. Suppose the size measured in the object space is $\eta$ millimetres, the distance from the object to the eye is D millimetres, and the eye pupil diameter is d millimetres, then the object size in diffraction units will be,

$$Z = (2\pi/\lambda).n.(d/2D).\eta . \quad .....(3:4)$$

The same result will be obtained if we considered it in the image space. The table of optical properties of the eye which was prepared by Stenström (1964) gives the object focal length as 17.055 millimetres, the image focal length as 22.785 millimetres, and the refractive index of the aqueous humour and of the vitreous body as

1.336. Then,

$$\eta' = \eta \frac{17.055}{D} \quad \text{mm.} ,$$

and,

$$Z = \frac{2\pi}{\lambda}.(1.336).\frac{d}{2(22.785)}.\eta\frac{17.055}{D} ,$$

$$= \frac{2\pi}{\lambda}.\frac{d}{2D}.\eta . \qquad \ldots\ldots\ldots(3:5)$$

3:2 The Physical Distribution of Illumination in an Edge Image and Its Derivatives.

The image of an incoherently illuminated edge was computed by Struve in 1882. The well-known formula giving the intensity of the normalized retinal image at distance z from the geometrical image is of the form,

$$I(z) = \frac{4}{\pi}\int_{z}^{\infty}\frac{H_1(2z)}{(2z)^2}.dz , \qquad \ldots\ldots\ldots\ldots\ldots(3:6)$$

where $H_1$ is the Struve function of the first order.

The Struve function of order $\nu$ (see Abramowitz and Stegun 1965) is defined by,

$$H_\nu(2z) = \frac{2(z)^\nu}{\Gamma(\nu+1/2)\Gamma(1/2)}\int_0^{\pi/2}\sin(2z.\cos\theta).\sin^{2\nu}(\theta).d\theta, \ldots(3:7)$$

or,

$$H_\nu(2z) = \sum_{m=0}^{\infty}\frac{(-1)^m.(z)^{\nu+2m+1}}{\Gamma(m+3/2)\Gamma(\nu+m+3/2)}. \qquad \ldots\ldots\ldots(3:8)$$

The first derivative of the expression 3:6, then, will be,

$$I'(z) = \frac{4}{\pi} \cdot \frac{H_1(2z)}{(2z)^2} ; \qquad \text{.....(3:9)}$$

and the second derivative is,

$$I''(z) = \frac{H_0(2z)}{\pi z^2} - \frac{3}{\pi z^3} . H_1(2z). \qquad \text{.....(3:10)}$$

Also the third derivative is,

$$I'''(z) = \frac{8}{\pi^2 z^2} - \frac{10}{\pi z^3} . H_0(2z) + \left( \frac{12}{\pi z^4} - \frac{4}{\pi z^2} \right) . H_1(2z); \qquad \text{..(3:11)}$$

and the fourth derivative is,

$$I^{IV}(z) = - \frac{56}{\pi^2 z^3} - \frac{2}{\pi} \left( \frac{4}{z^2} - \frac{27}{z^4} \right) . H_0(2z) + \frac{4}{\pi} \left( \frac{8}{z^3} - \frac{15}{z^5} \right) . H_1(2z).$$

$$\text{.....(3:12)}$$

The recurrence relations for the Struve functions (see Abramowitz and Stegun 1965 ) were used to put these formulae in terms of $H_0$ and $H_1$, which are tabulated by Jahnke and Emde (1945) where the symbols $S_0$ and $S_1$ have been used instead of $H_0$ and $H_1$.

The equations mentioned above become indeterminate at the origin; it is necessary to obtain a direct power series expansion.

From equation 3:8 we get,

$$H_1(2z) = \frac{2(2z)^2}{3.\pi} - \frac{2(2z)^4}{3^2.5.\pi} + \frac{2(2z)^6}{3^2.5^2.7.\pi} , \qquad \text{.....(3:13)}$$

and from equation 3:6 we can write,

$$I(z) = \frac{4}{\pi}\left[\int_0^{\infty} \frac{H_1(2z).dz}{(2z)^2} - \int_0^{z} \frac{H_1(2z).dz}{(2z)^2}\right] . \qquad \ldots\ldots(3:14)$$

Substituting equation 3:13 in equation 3:14, we obtain,

$$I(z) = \frac{1}{2} - \frac{4}{\pi^2}\left[\frac{2z}{1^2.3} - \frac{(2z)^3}{1^2.3^2.3.5} + \frac{(2z)^5}{1^2.3^2.5^2.5.7} - \ldots\ldots\right] \ldots.(3:15)$$

The derivatives, then, are obtained;

$$I'(z) = -\frac{8}{\pi^2}\left[\frac{1}{1^2.3} - \frac{(2z)^2}{1^2.3^2.5} + \frac{(2z)^4}{1^2.3^2.5^2.7} - \ldots\ldots\right], \ldots.(3:16)$$

$$I''(z) = \frac{32}{\pi^2}\left[\frac{(2z)}{1^2.3^2.5} - \frac{2(2z)^3}{1^2.3^2.5^2.7} + \frac{3(2z)^5}{1^2.3^2.5^2.7^2.9} - \ldots\right], \ldots(3:17)$$

$$I'''(z) = \frac{64}{\pi^2}\left[\frac{1.1}{1^2.3^2.5} - \frac{2.3.(2z)^2}{1^2.3^2.5^2.7} + \frac{3.5.(2z)^4}{1^2.3^2.5^2.7^2.9} - \ldots\right], \ldots(3:18)$$

and,

$$I^{IV}(z) = -\frac{256}{\pi^2}\left[\frac{1.2.3(2z)}{1^2.3^2.5^2.7} - \frac{2.3.5(2z)^3}{1^2.3^2.5^2.7^2.9} + \frac{3.4.7(2z)^5}{1^2.3^2.5^2.7^2.9^2.11} - \ldots\right]$$

$$\ldots\ldots\ldots\ldots(3:19)$$

Therefore, at the origin,

$$I(z) = 1/2 ,$$

$$I'(z) = -\frac{8}{3\pi^2} ,$$

$$I''(z) = 0 ,$$

$$I'''(z) = \frac{64}{45\pi^2} ,$$

$$I^{IV}(z) = 0.$$

An asymptotic expansion can be obtained for large values of z; we have,

$$H_\nu(2z) = N_\nu(2z) + \frac{z^\nu - 1}{\sqrt{\pi}(\nu - 0.5)!}\left[1 + \frac{0.5}{(\nu+0.5)z^2} + \frac{0.5 \cdot 1.5}{(\nu+0.5)(\nu+1.5)z^4} + \ldots\right], \quad \ldots\ldots(3:20)$$

( see Jahnke and Emde, 1945, page 211)

where,

$$N_\nu(x)\sqrt{\frac{\pi x}{2}} = P_\nu(x).\sin\left\{x - (\nu+0.5)\frac{\pi}{2}\right\} + Q_\nu(x).\cos\left\{x - (\nu+0.5)\frac{\pi}{2}\right\}, \quad \ldots\ldots(3:21)$$

(Jahnke and Emde, 1945, page 138 )

$$P_\nu(x) = 1 - \frac{(4\nu^2-1)(4\nu^2-9)}{2!\,(8x)^2} + \frac{(4\nu^2-1)(4\nu^2-9)(4\nu^2-25)(4\nu^2-49)}{4!\,(8x)^4} \ldots \quad \ldots\ldots\ldots(3:22)$$

$$Q_\nu(x) = \frac{4\nu^2-1}{8x} - \frac{(4\nu^2-1)(4\nu^2-9)(4\nu^2-25)}{3!\,(8x)^3} + \ldots\ldots, \quad (3:23)$$

( Jahnke and Emde, 1945, page 137 ).

Therefore,

$$H_o(2z) = N_o(2z) + \frac{1}{\sqrt{\pi}\,(-0.5)!z}\left(1 + \frac{1}{z^2} + \frac{1}{z^4} + \ldots\right),$$

$$= \frac{1}{\sqrt{\pi}\, z}\left(1 - \frac{9}{512z^2}\right)\sin\left(2z - \frac{\pi}{4}\right) - \frac{1}{16z}\cdot\frac{1}{\sqrt{\pi}\, z}\cdot\cos\left(2z - \frac{\pi}{4}\right)$$

$$- \frac{1}{2\pi}\left(1 + \frac{1}{z^2} + \frac{1}{z^4}\right), \qquad \text{.....(3:24)}$$

and,

$$H_1(2z) = N_1(2z) + \frac{1}{\sqrt{\pi}\,(0.5)!}\left[1 + \frac{1}{3z^2} + \frac{1}{5z^4} + \ldots\right],$$

$$= \frac{1}{\sqrt{\pi}\, z}\left(1 + \frac{15}{512z^2}\right).\sin\left(2z - \frac{3\pi}{4}\right) + \frac{1}{\sqrt{\pi}\, z}\cdot\frac{3}{16z}\cdot\cos\left(2z - \frac{3\pi}{4}\right)$$

$$+ \frac{2}{\pi}\left(1 + \frac{1}{3z^2} + \frac{1}{5z^4}\right). \qquad \text{.....(3:25)}$$

The luminance distribution and its derivatives, omitting higher power term, are obtained;

$$I(z) = \frac{2}{\pi^2}\left(\frac{1}{z} + \frac{1}{12z^2}\right) - \frac{1}{2\pi^{3/2}}\cdot\frac{\cos(2z + \pi/4)}{z^{5/2}}, \qquad \text{.....(3:26)}$$

$$I'(z) = \frac{2}{\pi^2}\left(\frac{1}{z^2} + \frac{1}{3z^4}\right) + \frac{1}{\pi^{3/2}}\cdot\frac{1}{z^{5/2}}\cdot\sin(2z - 3\pi/4)$$

$$+ \frac{3}{16\,\pi^{3/2}\, z^{7/2}}\cdot\cos(2z - 3\pi/4), \qquad \text{..(3:27)}$$

$$I''(z) = -\frac{4}{\pi^2}\left(\frac{1}{z^3} + \frac{2}{3z^5}\right) - \frac{1}{\pi^{3/2}}\cdot\frac{23}{8z^{7/2}}\cdot\sin(2z - 3\pi/4)$$

$$+ \frac{1}{\pi^{3/2}}\,\frac{2}{z^{5/2}}\cdot\cos(2z - 3\pi/4), \qquad \text{.....(3:28)}$$

$$I^{III}(z) = \frac{4}{\pi^2}\left(\frac{3}{z^4} + \frac{10}{3z^6}\right) - \frac{1}{\pi^{3/2}}\cdot\frac{4}{z^{5/2}}\cdot \mathrm{Sin}\left(2z - \frac{3\pi}{4}\right) -$$

$$\frac{1}{\pi^{3/2}}\cdot\frac{43}{4z^{7/2}}\cdot \mathrm{Cos}\left(2z - \frac{3\pi}{4}\right), \qquad \text{.....(3:29)}$$

$$I^{IV}(z) = -\frac{48}{\pi^2}\left(\frac{1}{z^5} + \frac{5}{3z^7}\right) + \frac{1}{\pi^{3/2}}\cdot\frac{63}{2z^{7/2}}\cdot\mathrm{Sin}\left(2z - \frac{3\pi}{4}\right)$$

$$-\frac{1}{\pi^{3/2}}\cdot\frac{8}{z^{5/2}}\cdot\mathrm{Cos}\left(2z - \frac{3\pi}{4}\right). \qquad \text{.....(3:30)}$$

When the illumination at the object plane is extended from $-\infty$ to $+\infty$ we have,

$$I(+z) + I(-z) = 1. \qquad \text{.....(3:31)}$$

That is, the luminance distribution of the incoherently illuminated edge image is antisymmetrical about the origin, or, the intensities at two points equally distant from the geometrical edge but on opposite sides of it, are together equal to the full intensity.

Using the equations given above, the intensity distribution of an incoherently illuminated edge image and its derivatives were calculated. They are tabulated in Appendix A. Equations 3:9 to 3:12 were used for small values of z(from 0 to 8.0); $H_0$ and $H_1$ from the tables of Jahnke and Emde(1945) were used. For large values of z(from 6.2 to 15.0) the asymptotic equations(equations 3:26 to 3:30) were

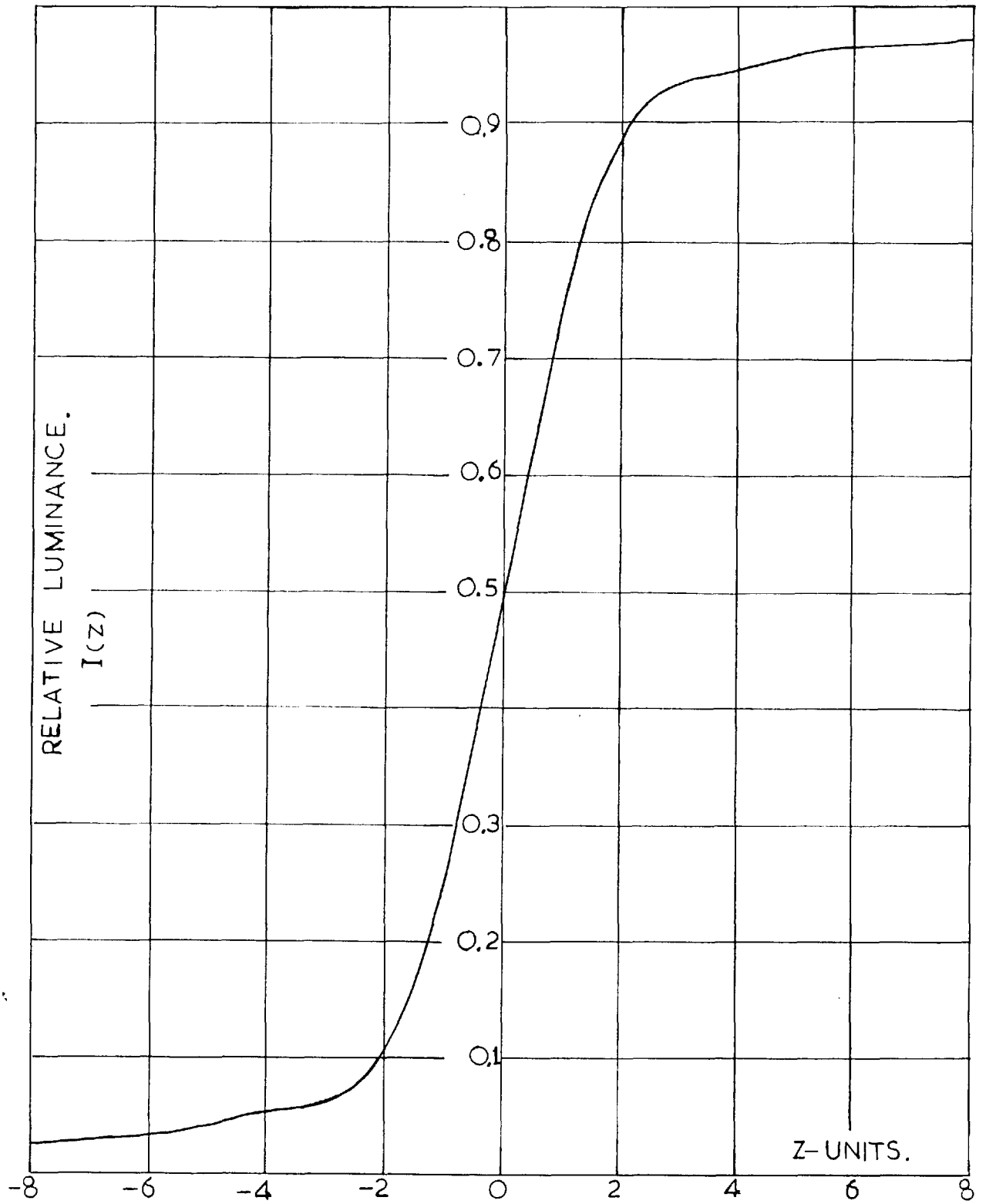



Fig. 3.4. The light distribution in the retinal image of an incoherently illuminated abrupt edge.

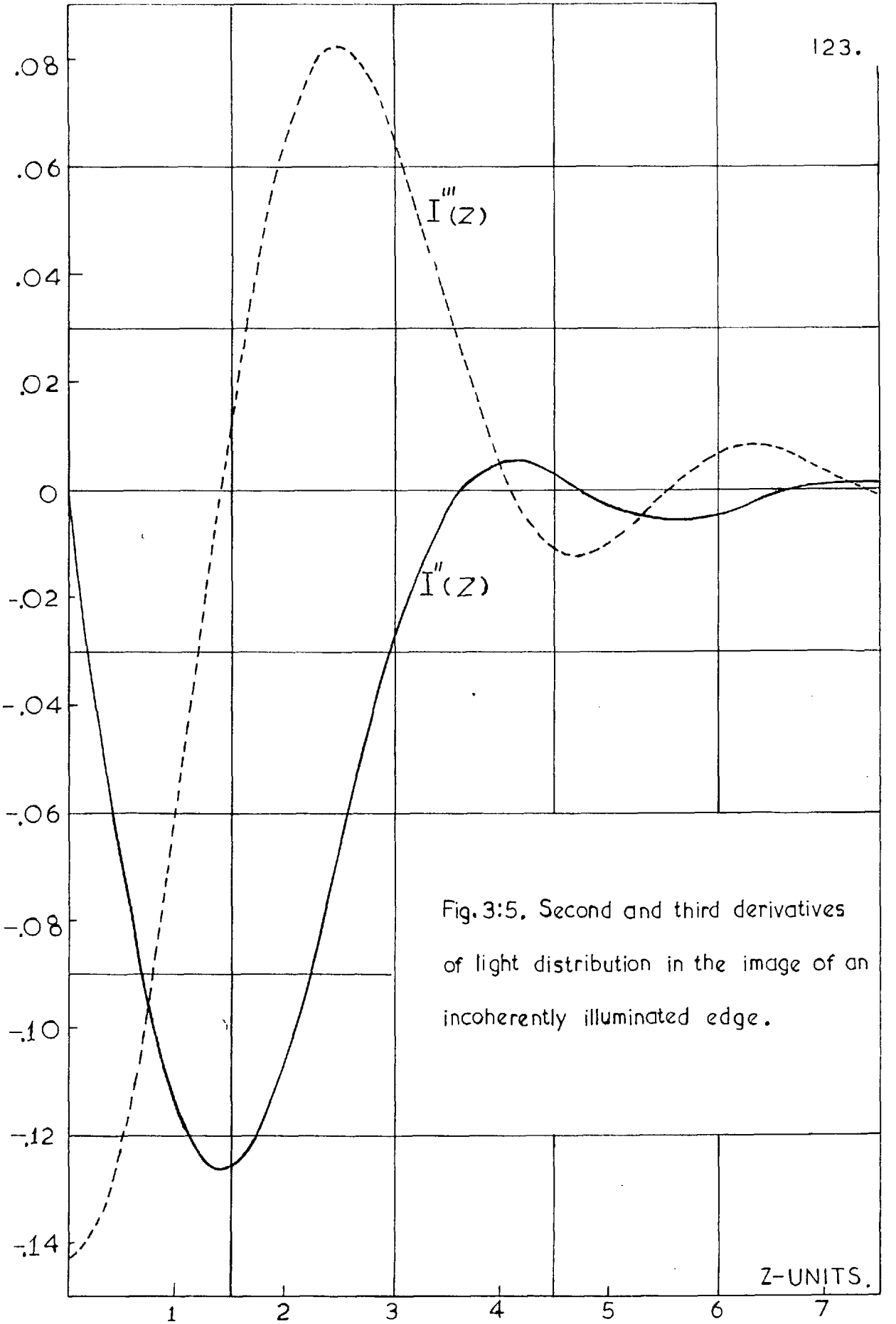



Fig. 3:5. Second and third derivatives of light distribution in the image of an incoherently illuminated edge.

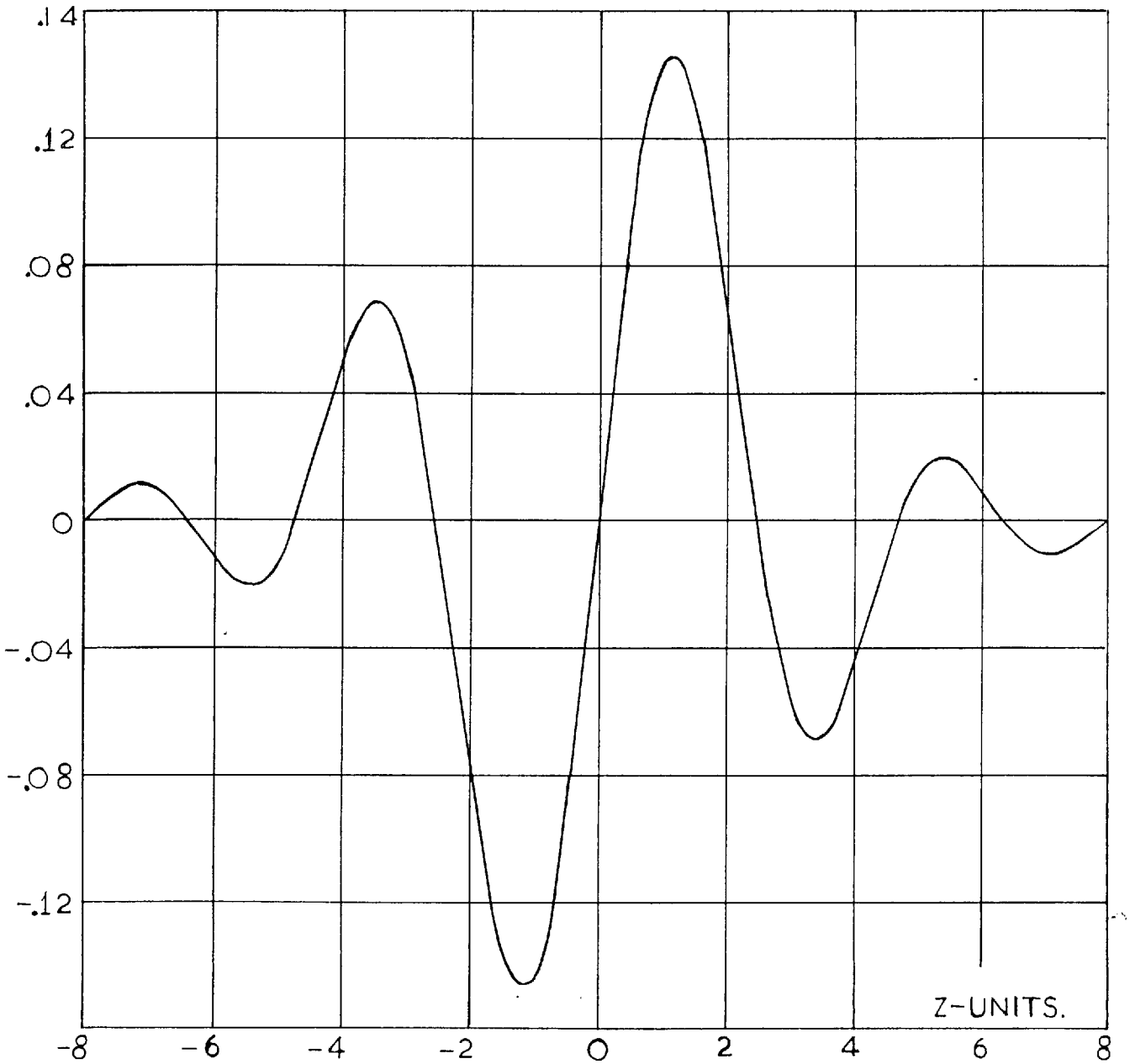



Fig. 3:6. The fourth derivative curve of the edge image.

used. The results are shown in figures 3:4 to 3:6 where the asymptotic formulae are used when z is greater than 6.8. The inflections of the luminance distribution of the retinal image, which is shown in figure 3:4, correspond to the maxima and minima of the second derivative values, shown in figure 3:5, in which the extreme values can be determined by the vanishing of the third derivative. The fourth derivative curve is shown in figure 3:6.

## 3:3 The Visual Mach Bands.

An arrangement must be devised in order to observe directly the phenomena occurring on the edge without intervention from the optics. Clearly, visual photometric matching is the only way to measure the intensities of the subjective bands. Therefore, an optical system as shown in figure 3:7 was set up for the study of widths, positions and brightnesses of the bands produced by an edge. Two channels were used to produce respectively the edge image and a photometric comparison beam.

The system on the left of the figure produces a comparison beam for photometric matching. The source(A) is an Osram mercury vapour lamp. The light from the lamp passes through a condenser (B) and focusses on a rectangular slit (D). With a green filter (C) of wavelength 0.55 micron,

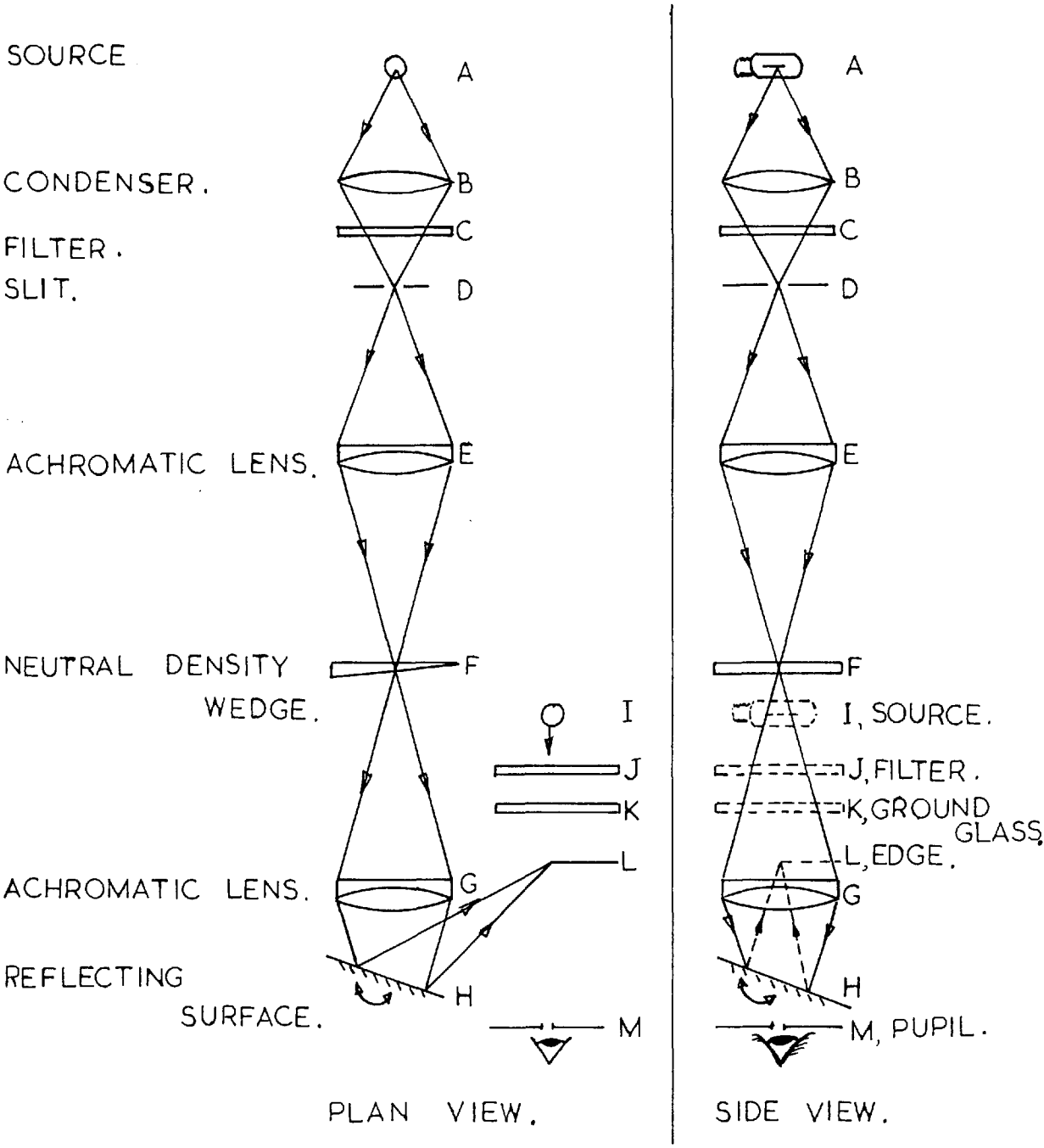



Fig. 3:7. Apparatus for measuring visual Mach bands at a straight edge.

the monochromatic light from slit D forms an image on a neutral density wedge (F) after passing through an achromatic lens (E). The final image is formed by another achromatic lens (G) in the same plane as the edge (L), this being viewed by means of the system on the right. The final image in plane L could be shifted across by means of a rotating front aluminized surface (H), which is placed between the achromatic lens E and the final image in plane L, so that the comparison field could be brought in line with the band being observed.

The lamp A is a high pressure mercury lamp (250 Watt., ME/D), situated in a lamp house with circular glass window of 4.5 cms. diameter, as shown in figure 3:8 a. The lamp runs from the mains (240 V) through a choke which limits the current to a correct value. The starting current for the lamp is 4 - 5 amperes and then the operating current is 3.7 to 4.6 amperes. The maximum arc brightness is stated by the maker to be approximately 20,000 stilbs ( $2.10^8$ candelas per square metre). The spectrum is the line spectrum of mercury at high pressure which gives the principal wavelengths at 3650°A (ultraviolet), 4046°A (violet), 4358°A (blue), 5460°A (green) and 5790°A (yellow). The ripple due to the lamp is about 100 cycles per second. Thus, the visual measurements will not be affected since the critical fusion

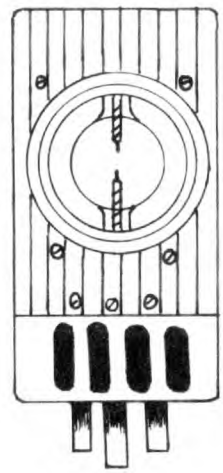


Fig. 3:8a. Vapour mercury lamp.

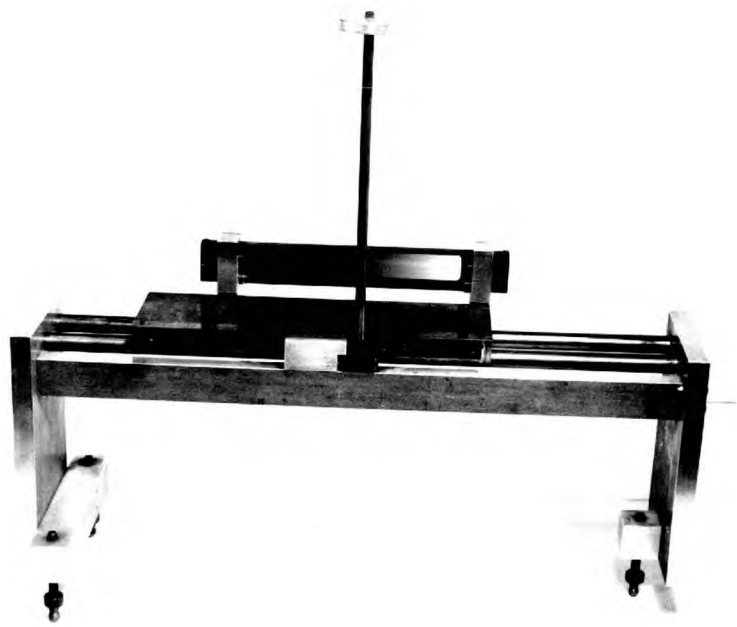


Fig. 3:8b. Neutral density wedge.

frequency of the eye is about 15 cycles per second.

The neutral density wedge is made by Ilford Ltd. It is about 15 cms. long and the nominal diffuse density gradient is 0.10 density unit per cm. . It is mounted on a carrier which can move the wedge perpendicular to the optical axis (see figure 3:8b). The position of the wedge is noted from a vernier scale on the carrier. The calibration for transmission was done by directing the beam onto a pinhole in front of a photomultiplier and noting the output signal at various positions of the wedge. Figure 3:9a shows the transmission curve of the wedge while figure 3:9b shows the optical density curve calculated from, density $d = - \log T$, where T is the transmittance. The density gradient obtained from figure 3:9b is 0.21 density unit per cm.

In the right hand system of figure 3:7, the sharp transition edge (L) is viewed directly, 25 cms. away, through an artificial pupil (M) of 0.64 mm. diameter. The edge is incoherently illuminated from behind by a diffusing source provided by putting a ground glass screen (K) in front of another high pressure mercury lamp (I) with a green filter (J). The widths and positions of the bands were measured directly with a very fine wire, placed at the same plane as the edge, moving across the length of the edge. The position of the pointer (i.e; fine wire) could

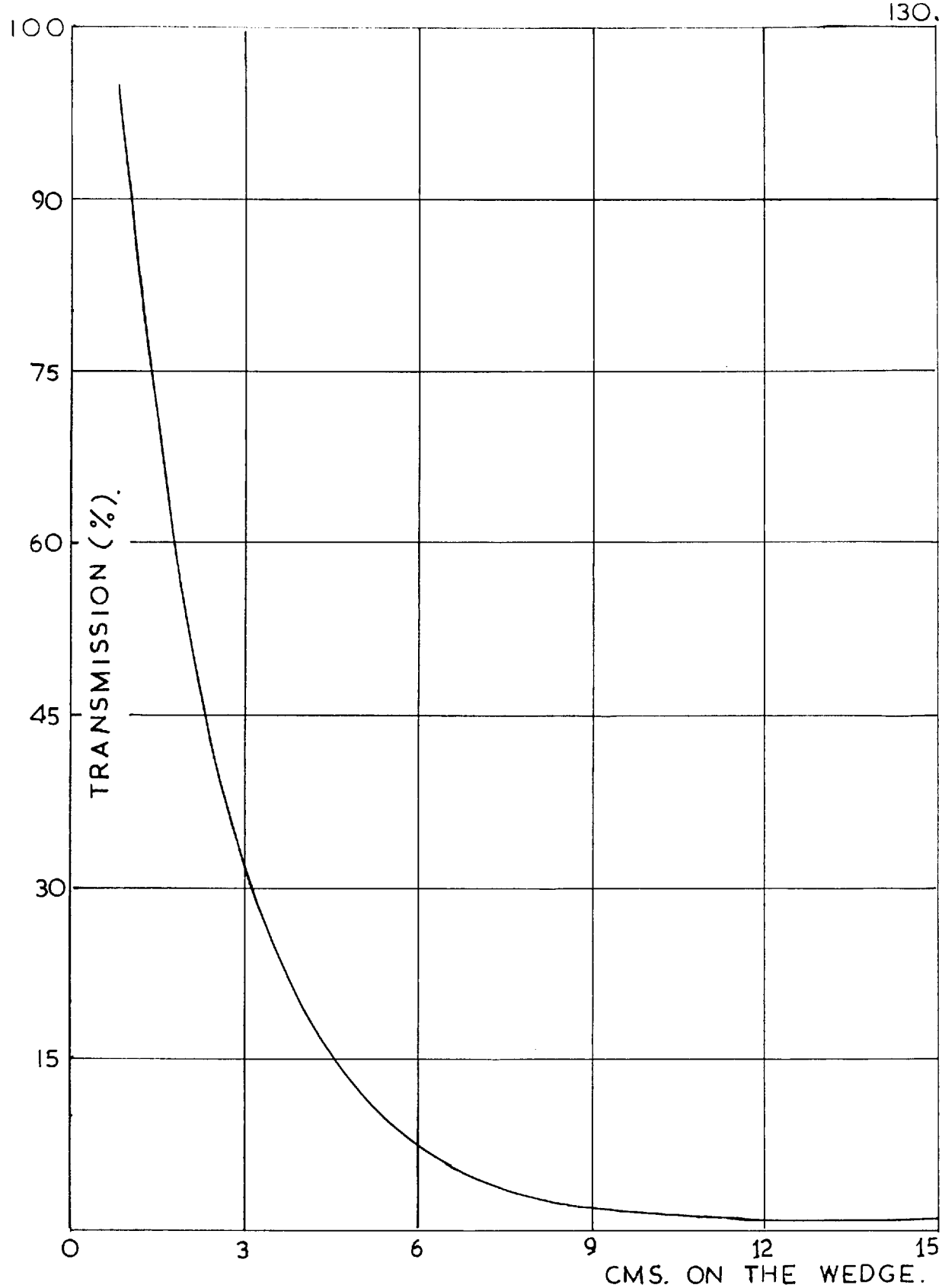



Fig. 3:9a. A wedge calibration.

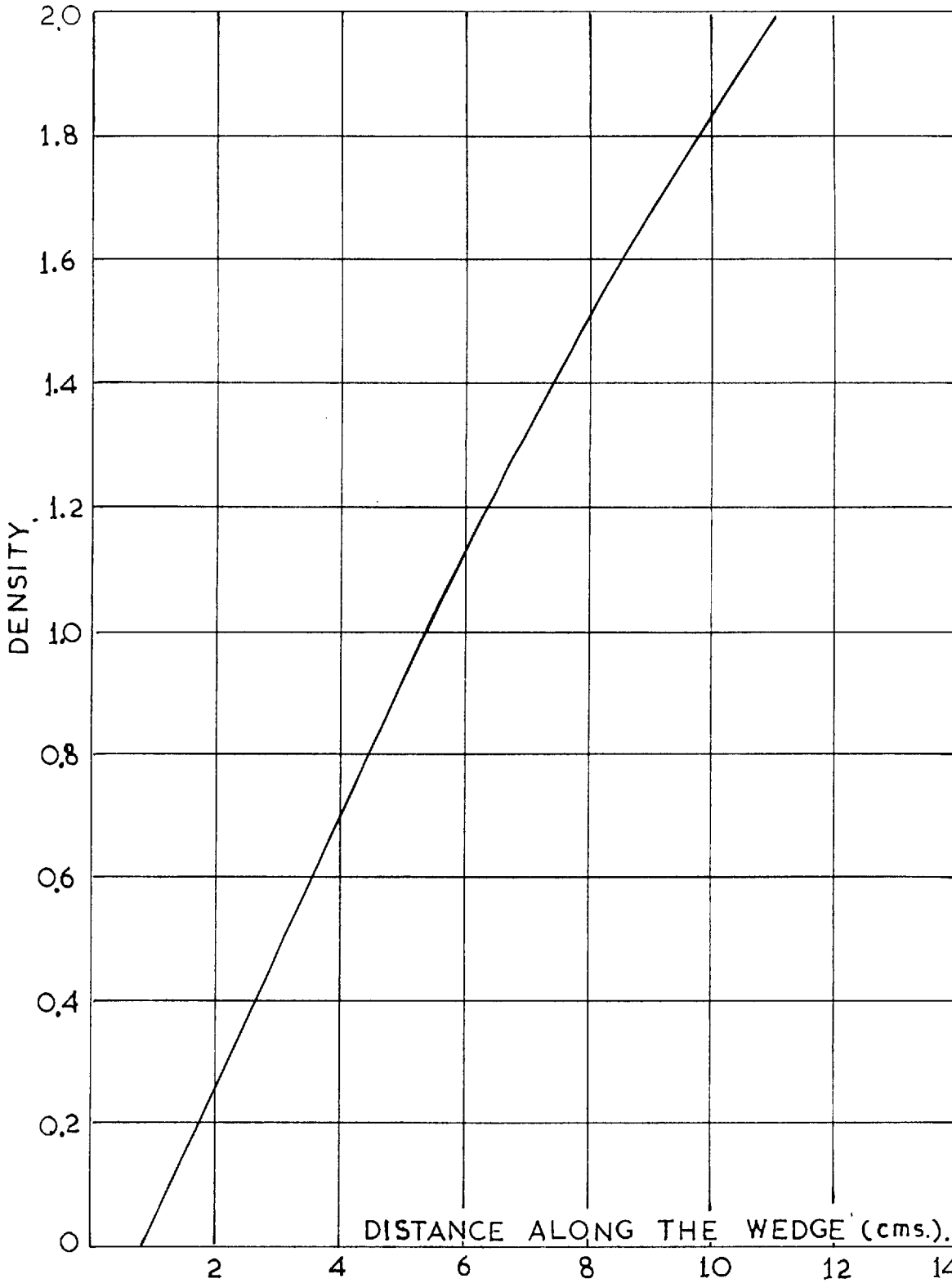



Fig. 3.9b. Density along the wedge.

be noted by a vernier scale to which the pointer is fixed.

There was no perceptible stray light in the system, so that the pointer could not be seen when it was on the dark side of the edge. Thus instead of an opaque knife edge, a glass plate with a sharp transition border between a clear part and an aluminized part was used. The aluminizing covered one half of the plate, and the film had a transmission of about 7%. The microphotometer trace for the transmission of the plate gave a graded zone between two uniform areas; no physical band was obtained. The graded zone occupied a distance of 0.05 mm. on the plate. When the plate was viewed at a distance 25 cms. away, with an eye pupil of 0.64 mm. in diameter, the graded zone corresponded to about 1/2 Z-unit which was negligible and the plate could be said to have an abrupt luminance distribution. With this plate, under the conditions used, it was found that the pointer could just be seen when it was moved into the dark region. The transmission of this aluminized area is another factor which must be selected carefully; if the transmission is too high, the contrast between the bright and the dark areas (as measured by the ratio between the difference of the intensities of the two areas and the sum of these two intensities) will be very low, causing difficulty in perceiving the bands, and if the transmission is too low, the pointer cannot be seen in the dark area.

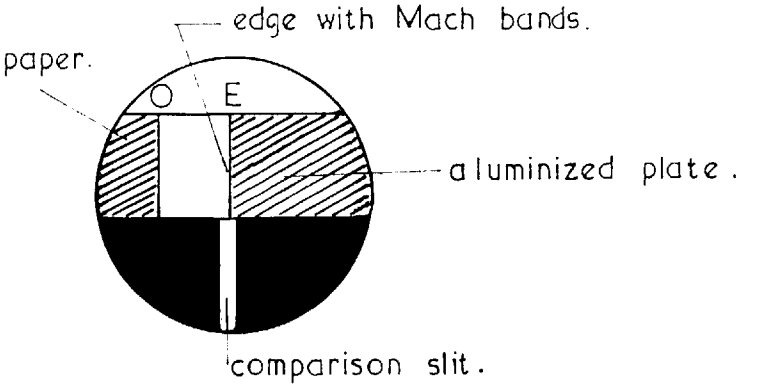
As has been mentioned, the retinal illumination is defined by the product of the luminance of the object in candelas per square metre and the area of the eye pupil in square millimetres. The luminance of the clear area of the plate, in this case, is determined by the luminance of the object. It was measured by an S.E.I photometer while the plate was in the system. With this photometer, the luminance can be noted directly in candelas per square metre when the brightness of the measured field is matched to that of the field produced by the instrument. The luminance of the bright region of the area being observed, measured with this instrument, was 3,430 candelas per square metre. With an artificial pupil, the size of the eye pupil was restricted to 0.64 millimetre in diameter in order that the multiple Mach bands could be seen. Both, the eye pupil and the luminance of the object were kept constant during the observations. Therefore, a retinal illumination of about 1100 trolands ( which is in photopic region) was obtained throughout the work.

Under the observed conditions of 90% contrast object, 1100 trolands retinal illumination and an eye pupil of 0.64 millimetre diameter, three bands were seen; one bright band in the bright region, and, one dark and one bright band in the dark region.

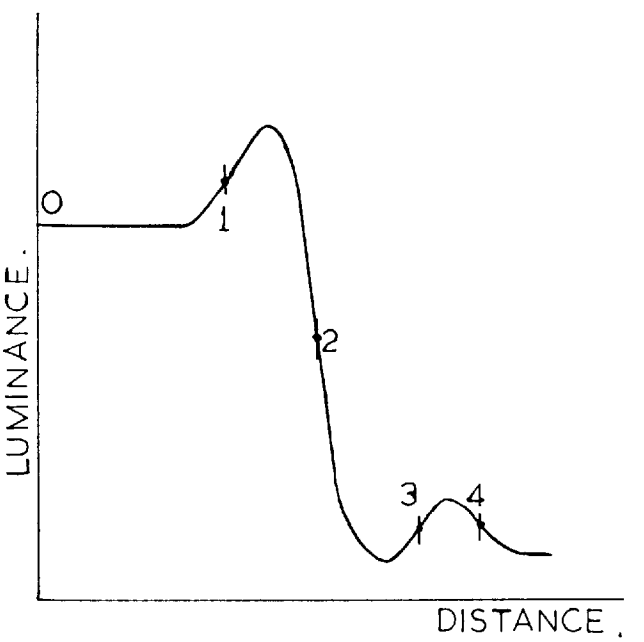
It is necessary to know the pointer reading

corresponding to the geometrical edge position; this was found as follows. During the measurements, a part of the clear field of the aluminized plate was covered with a piece of paper having a straight edge which was placed parallel to the aluminized edge (see figure 3:10a). The distance between these two edges (i.e; distance OE in figure 3:10a) was measured by a travelling microscope. Then the plate was put in the system. With a large viewing aperture, about 4 mms. in diameter, and frontal illumination from an ordinary reading lamp, the light from behind having been shielded, the pointer was brought to the border between the paper and the clear field. The reading for the position of the pointer was noted. Then the large aperture was replaced by an aperture of 0.64 mm. and the reading lamp and the light shield were taken away. In this way the geometrical edge position was found.

In order to measure the positions of the bands the pointer was made to coincide successively with 1) the first margin of the first bright band (in the bright field), 2) the border between the first bright band and the dark band, 3) the border between the dark band and the second bright band ( in the dark field), and, finally with, 4) the margin of the second bright band remote from the edge ( see figure 3:10b). In this way, the widths and the positions




a) Field of view.




b) Measurement.

Fig. 3:10.

of the bands were obtained.

Brightness matchings were made only for the two uniform fields and the two bright bands. The intensity of light produced by the wedge could not be made low enough for comparison with the intensity of the dark band and hence the latter was assumed to be zero.

Five different subjects have made the above-mentioned observations under similar conditions and using the same edge. These five observers were chosen from eight people; two of these eight could not see the second bright band(the bright band in the dark region) and one could see one extra dark and one extra bright band in the bright and dark regions respectively away from those shown in figure 3:11 ; unfortunately, this observer gave up the measurements as they were very tiring for the eye. The subject had to have a few minutes rest after taking a set of readings.The results obtained from these five subjects are shown in figure 3:11 . Each of the curves was obtained from ten sets of readings.On the top of the figure, the second derivative curve of the incoherently illuminated edge image is shown.

## 3:4 The Mach Bands Predicted By Mathematical Models.

Numerical work was carried out on a National Elliot 803 A computer and an IBM 7090 computer for all the mathematical models described in Chapter II. Taking the

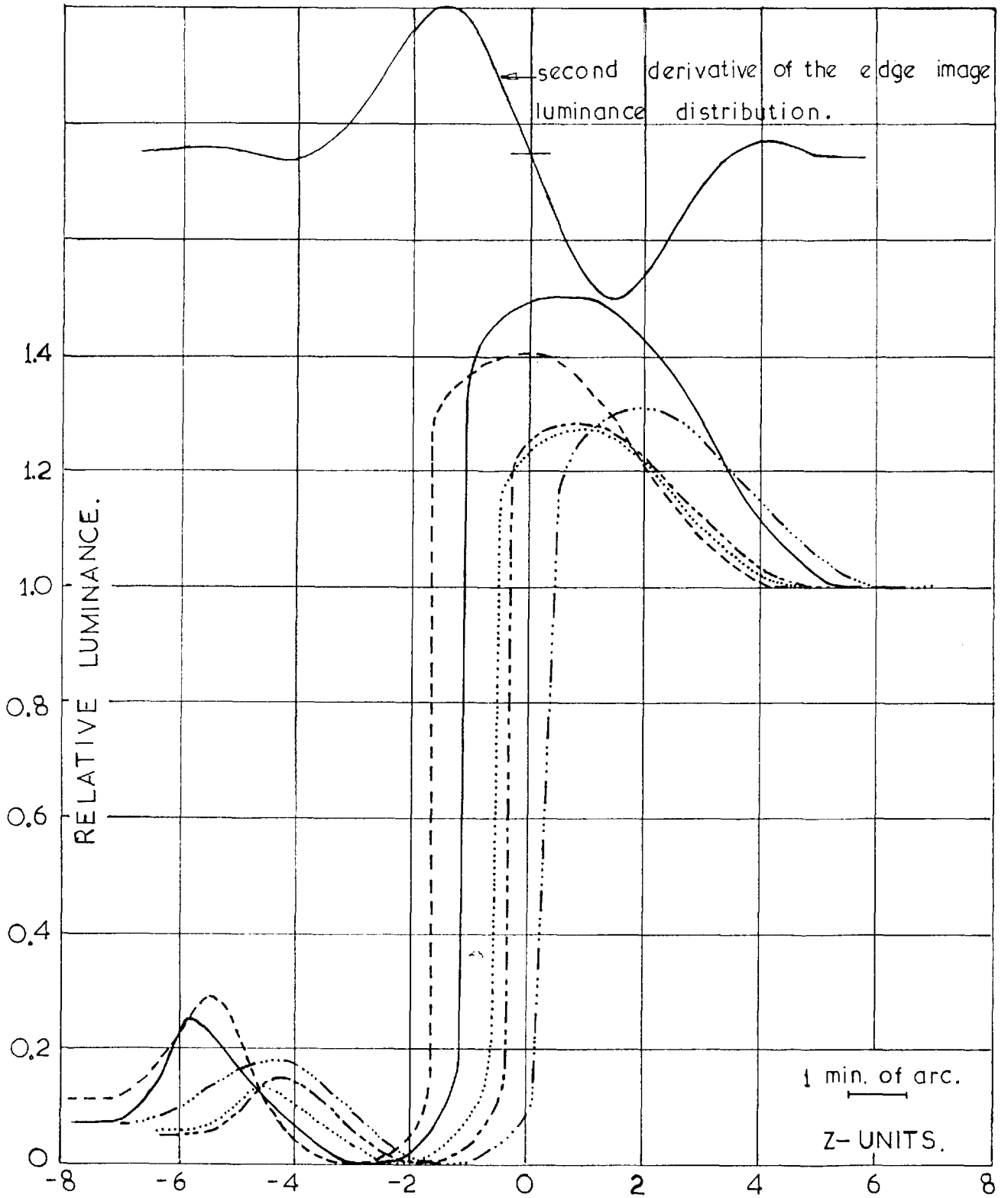



Fig. 3:11. Visual Mach bands seen at an incoherently illuminated abrupt edge by five observers.

distribution of the retinal image of a sharp edge (calculated in section 3:2), as the stimulus for each model, the subjective impression was worked out and compared with the second derivative of the luminance distribution of the retinal image which has already been calculated and shown in figure 3:5. The best value of each parameter in each model was chosen in order to bring the maxima and minima of the predicted subjective curve as close as possible to the visual bands obtained by five observers, as shown in figure 3:11. For further discussion on the computations see Appendix B where the details of the programming and the values of constants are given.

Figure 3:12 shows Mach's model on the retinal image distribution calculated from equation 2:5. The second derivative curve of the stimulus is shown at the top of the figure.

The modified model of Fry in which the response was expressed in subjective brightness (equation 2:29) was also applied to this distribution; the result is shown in figure 3:13. It yields the same positions of the bands as those from Mach model ; but the bright band in the Mach model is somewhat narrower than the one in the modified model of Fry, and the dark band of the former model is broader than that of the latter.

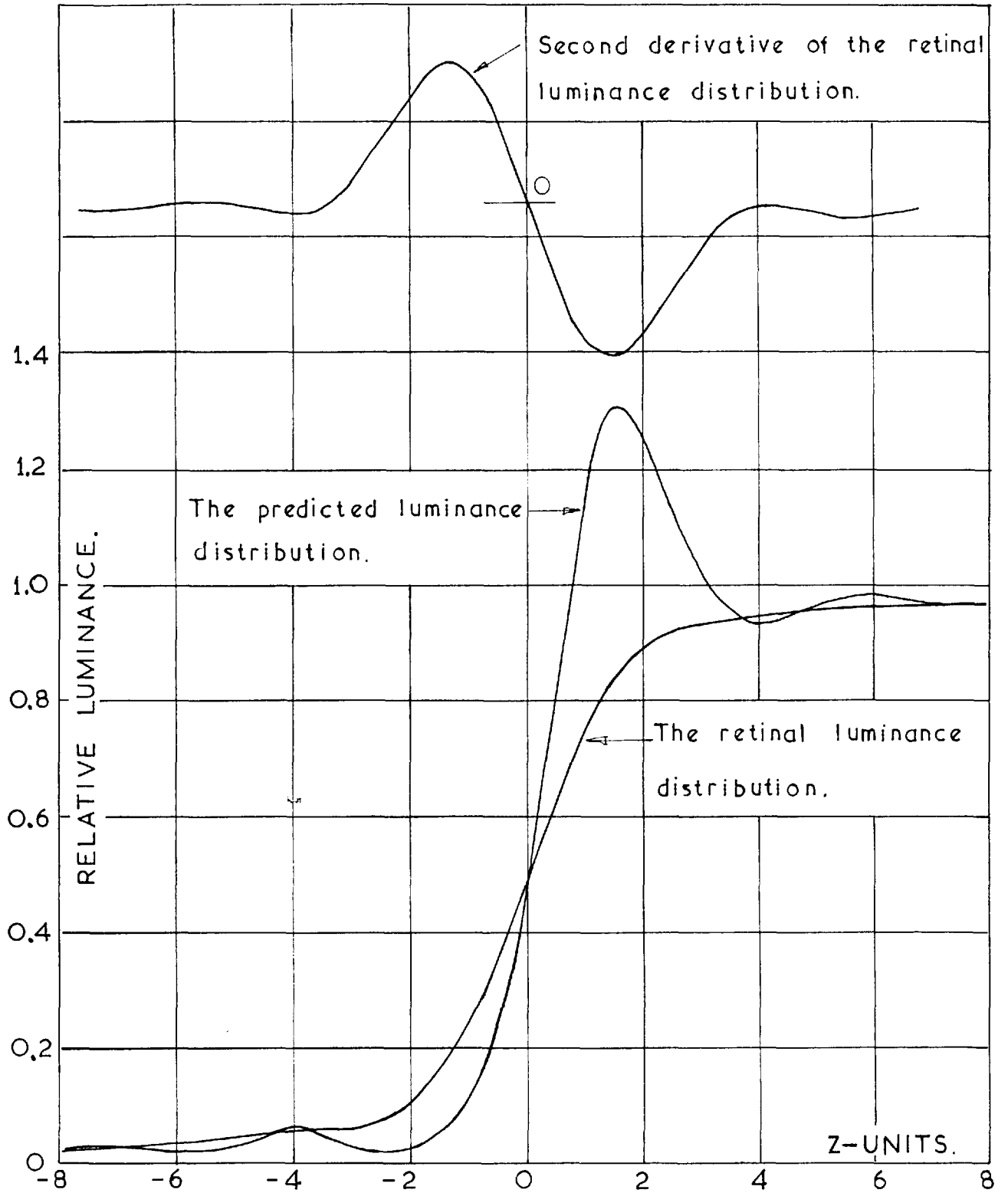



Fig. 3:12. Mach's model for an edge image.

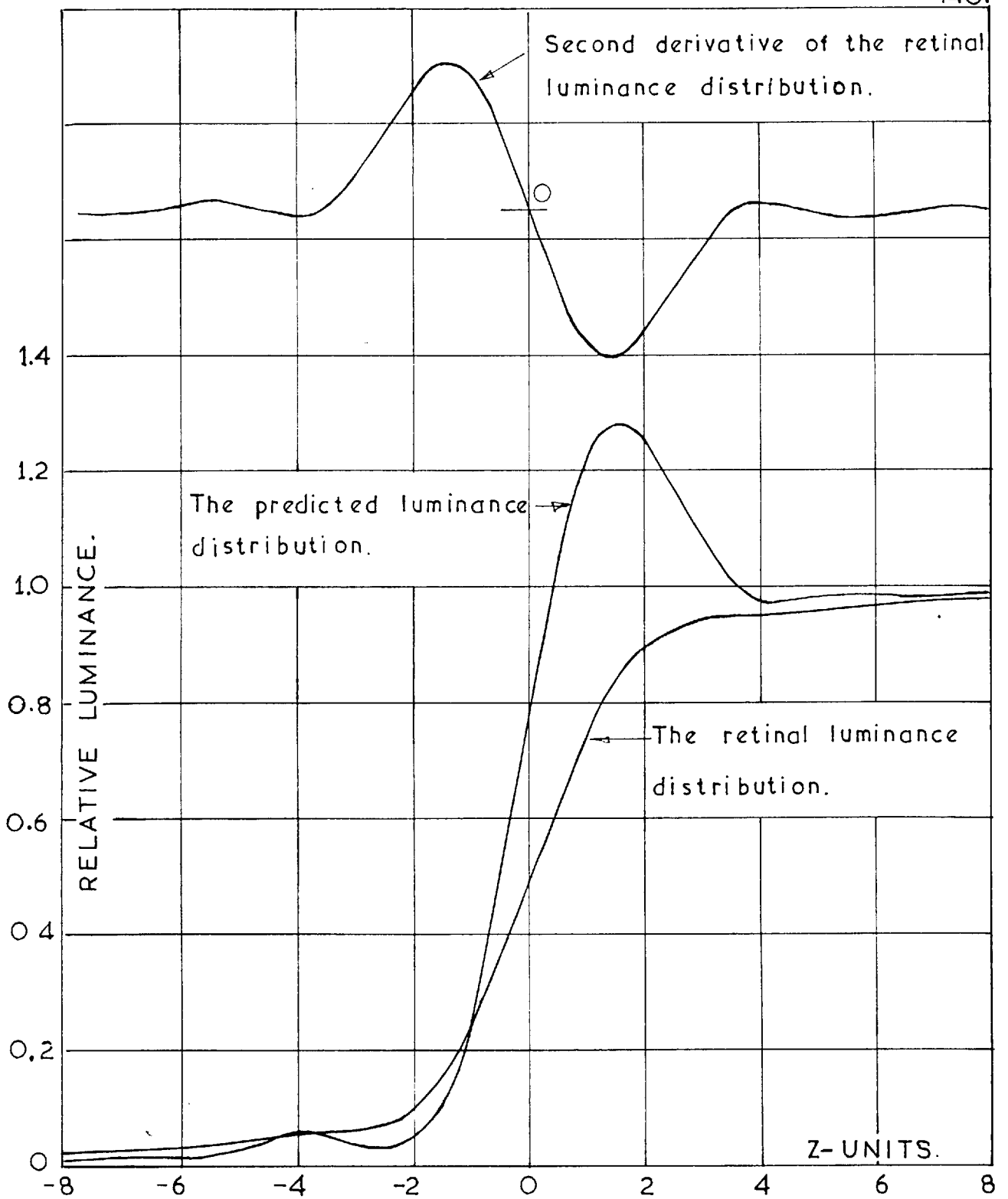



Fig. 3:13. The modified model of Fry for an edge image.

The Hartline and Ratliff model, which made good predictions in the case of the luminance distribution with sharp inflections, as shown in figures 2:6 and 2:7, seems to fail when applied to the distribution of the retinal image mentioned above where the great rounded curvatures are present. The subjective distribution gives only the bright band near the edge as shown in figure 3:14, no band in the dark area is obtained.

Figure 3:15 shows Taylor's linear model which gives the same magnitudes of bright and dark bands. The bands are at equal distance from the edge but on the opposides of it. The second dark and the second bright bands can just be seen next to the first bright and the first dark bands (which are near the edge ) respectively.

Other linear distributions, from the models of O'Brien and Békésy, are shown in figure 3:16. Both of them give negative intensities for the dark bands when the bright bands are brought above the relative luminance of 100%.

The results of the proposed new model, equations 2:30 and 2:31, are shown in figures 3:17 and 3:18 respectively. Figure 3:17 and figure 3:13 (modified model of Fry) give almost the same results. In figure 3:18, the dark band cannot be seen; various parameters were tried, but no good results were obtained. This model suffers from the same

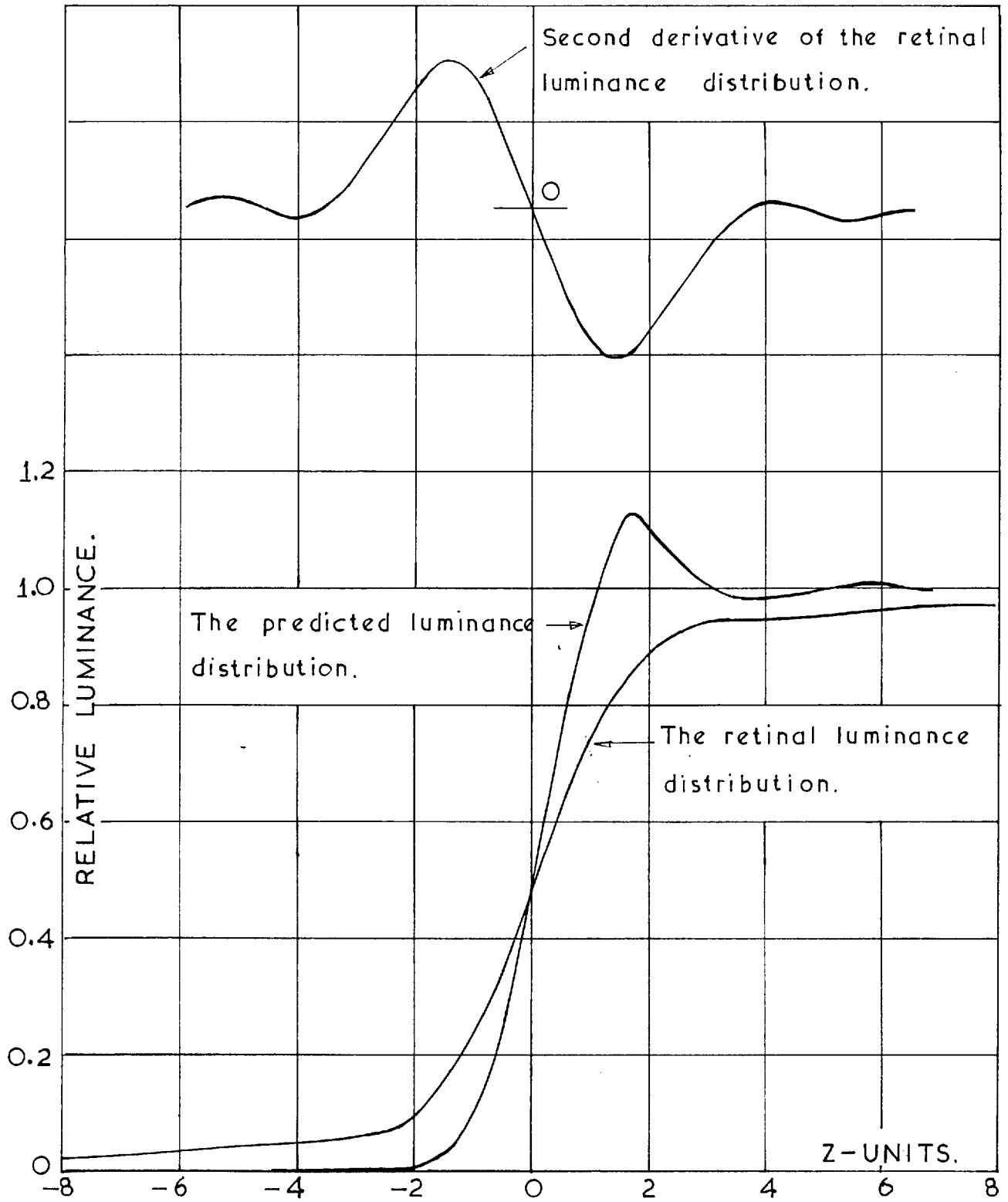



Fig. 3:14. Model of Hartline and Ratliff for an edge image.

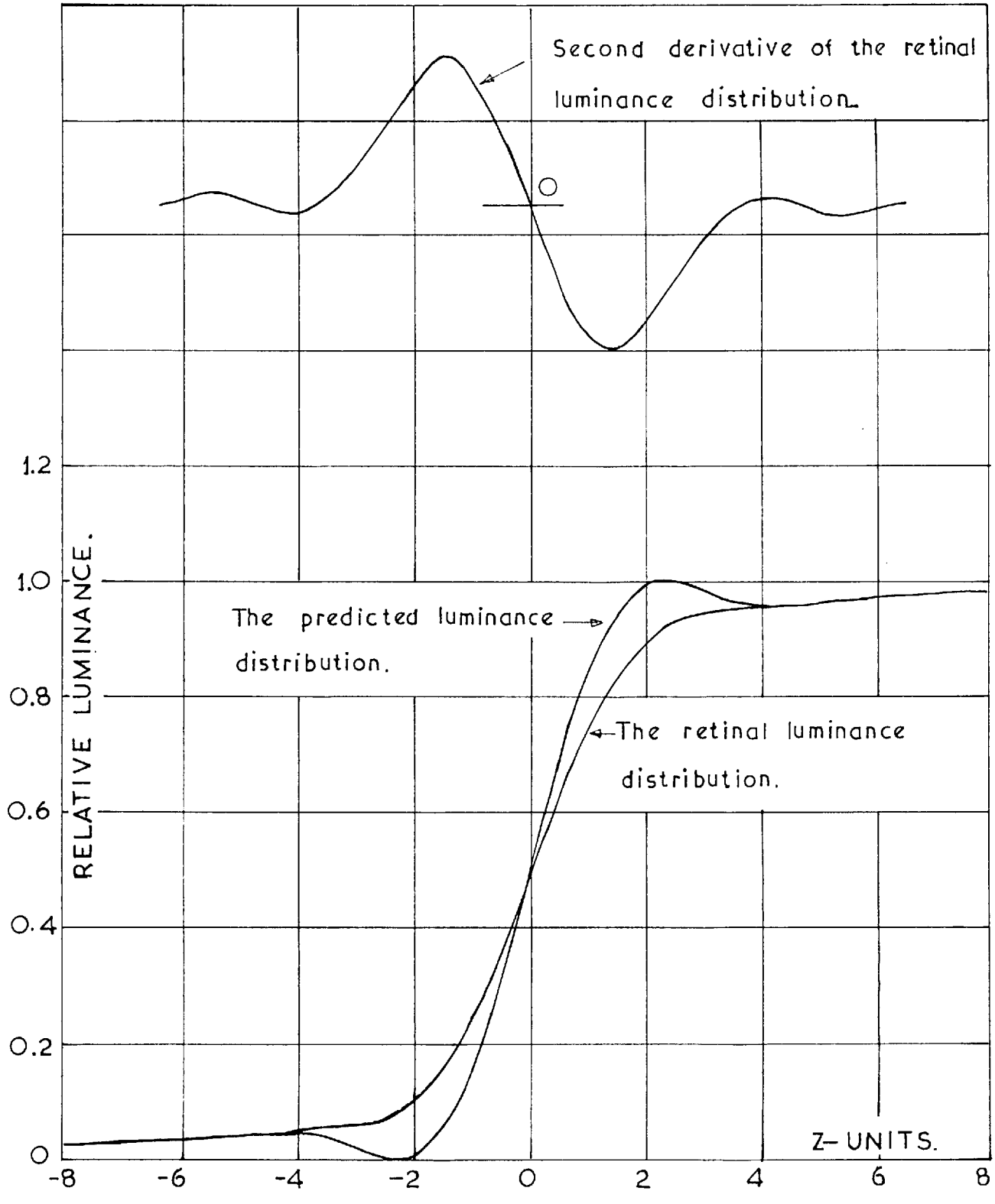



Fig. 3:15. The Taylor's model for an edge image.

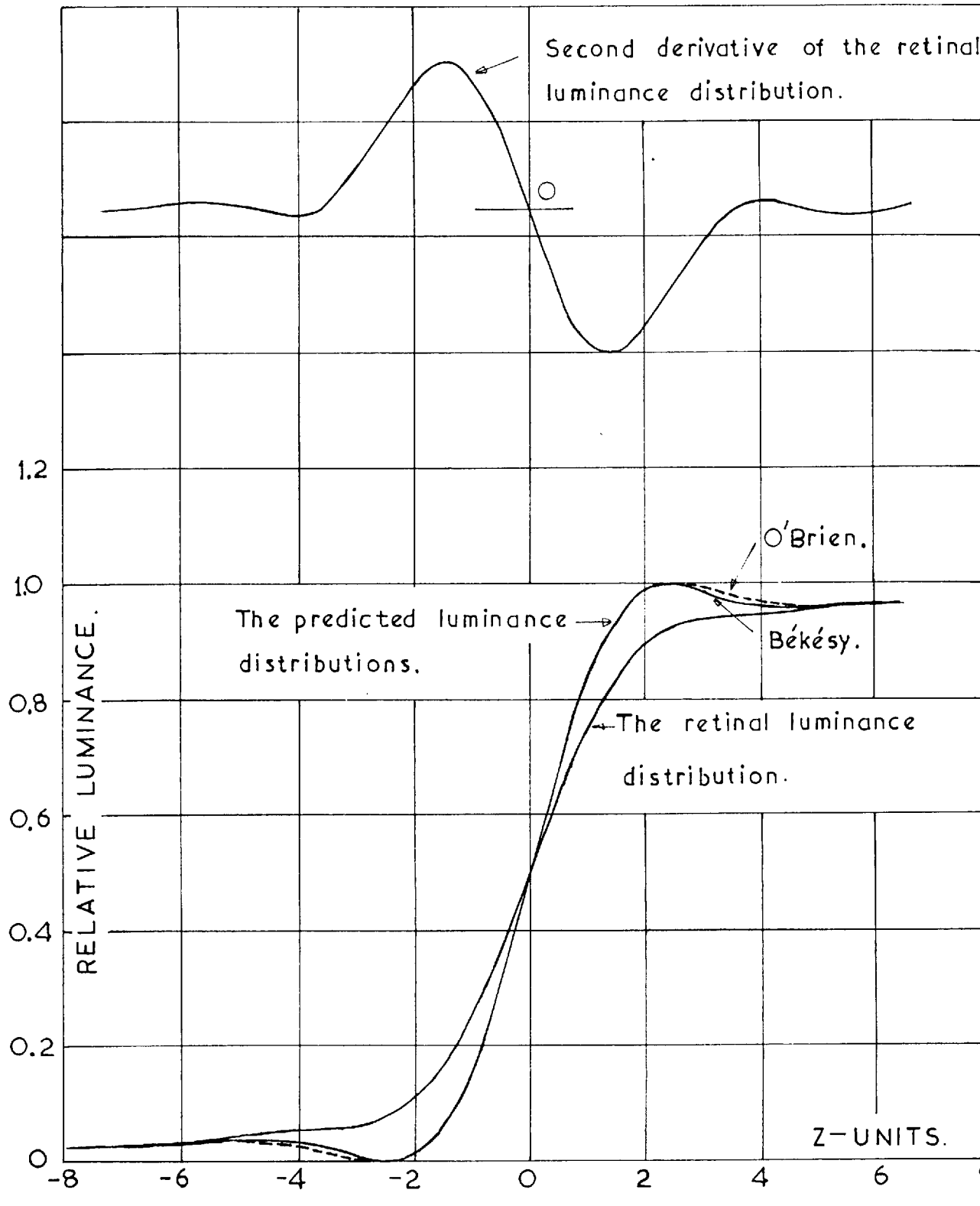



Fig. 3:16. The O'Brien and the Békésy models for an edge image.

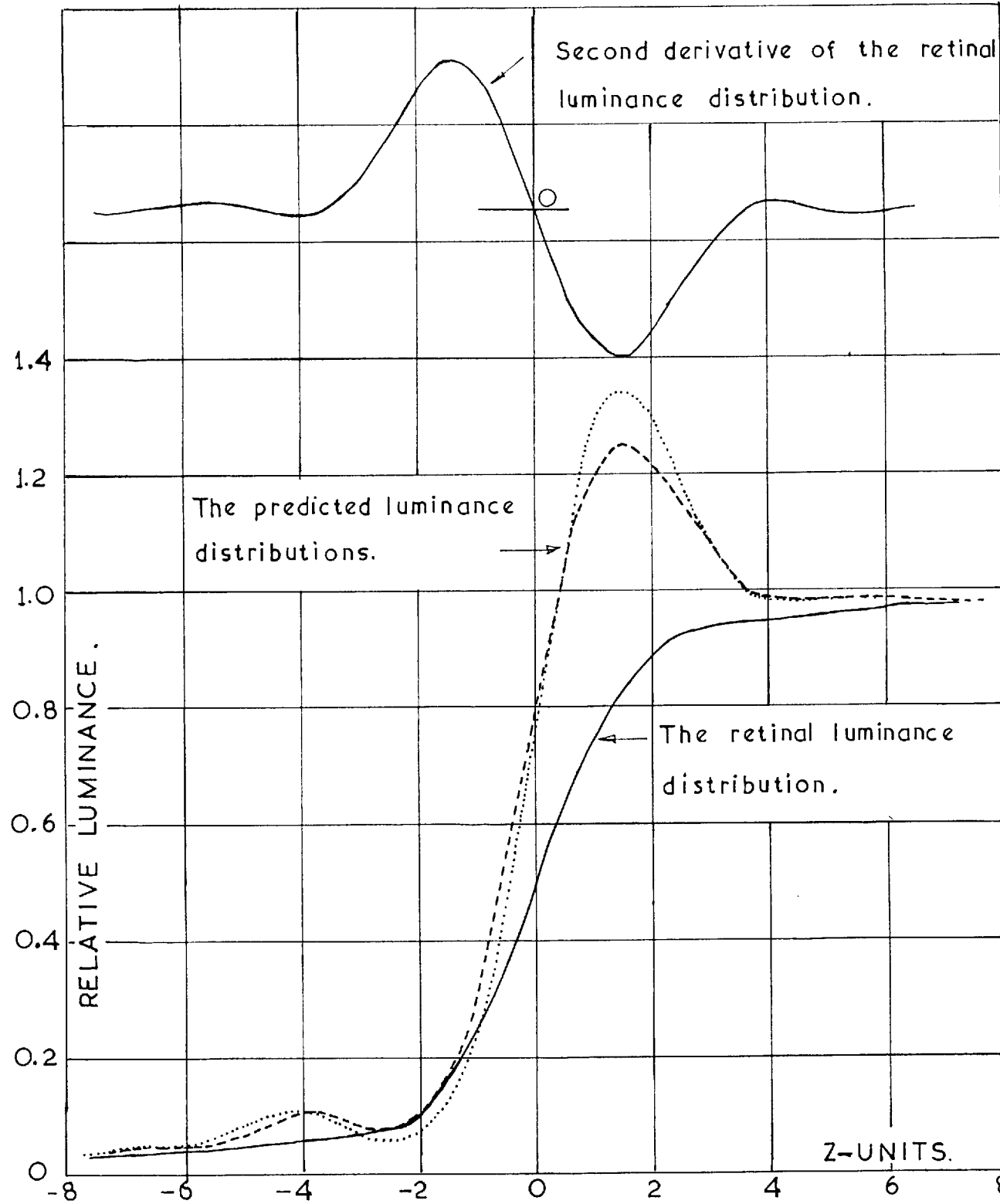



Fig. 3:17. The proposed new models (eq.2:30) for an edge image,

.....one-dimensional model,

----- two-dimensional model.

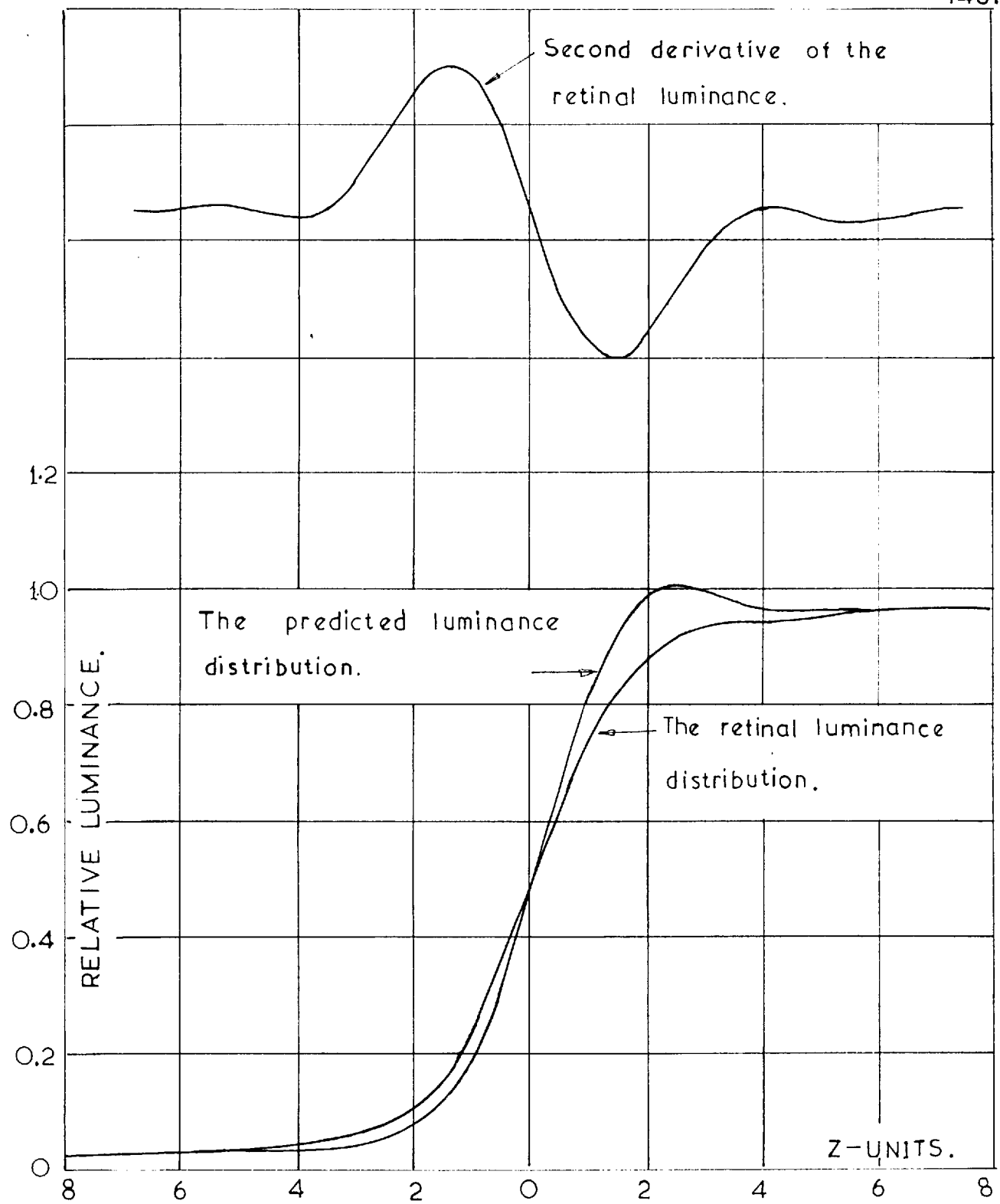



Fig. 3:18. The proposed new model (eq. 2:31).

drawbacks as the Hartline and Ratliff model. Both of them show no dark band at low intensity with flexions of big values of radius of curvature. But they would give good agreement with observations where the luminance level is high enough.

3:5 Discussion.

The result obtained by Charman and Watrasiewicz (1964) in observing an edge under a microscope is put together in figure 3:19 (the ordinate represents, on a logarithmic scale, the relative luminance) with those obtained by five observers on macroscopical visual Mach bands so that comparison can be easily made. The conditions for the observations were not exactly the same; the edge was illuminated with S=5.7 in the case of Charman and Watrasiewicz, and incoherently illuminated in the present five-observer experiment. In microscopy, however, an illumination of S=5.7 yields approximate incoherence. Furthermore, the contrast between the bright and the dark areas in the former case was 100% while in the other 90% contrast was used. The retinal illumination is another factor; it was approximately $10^4$ trolands in the Charman and Watrasiewicz experiment and only 1100 trolands in the present case.

The dependence of the characteristics of the effect on the individual observer are clearly seen in the

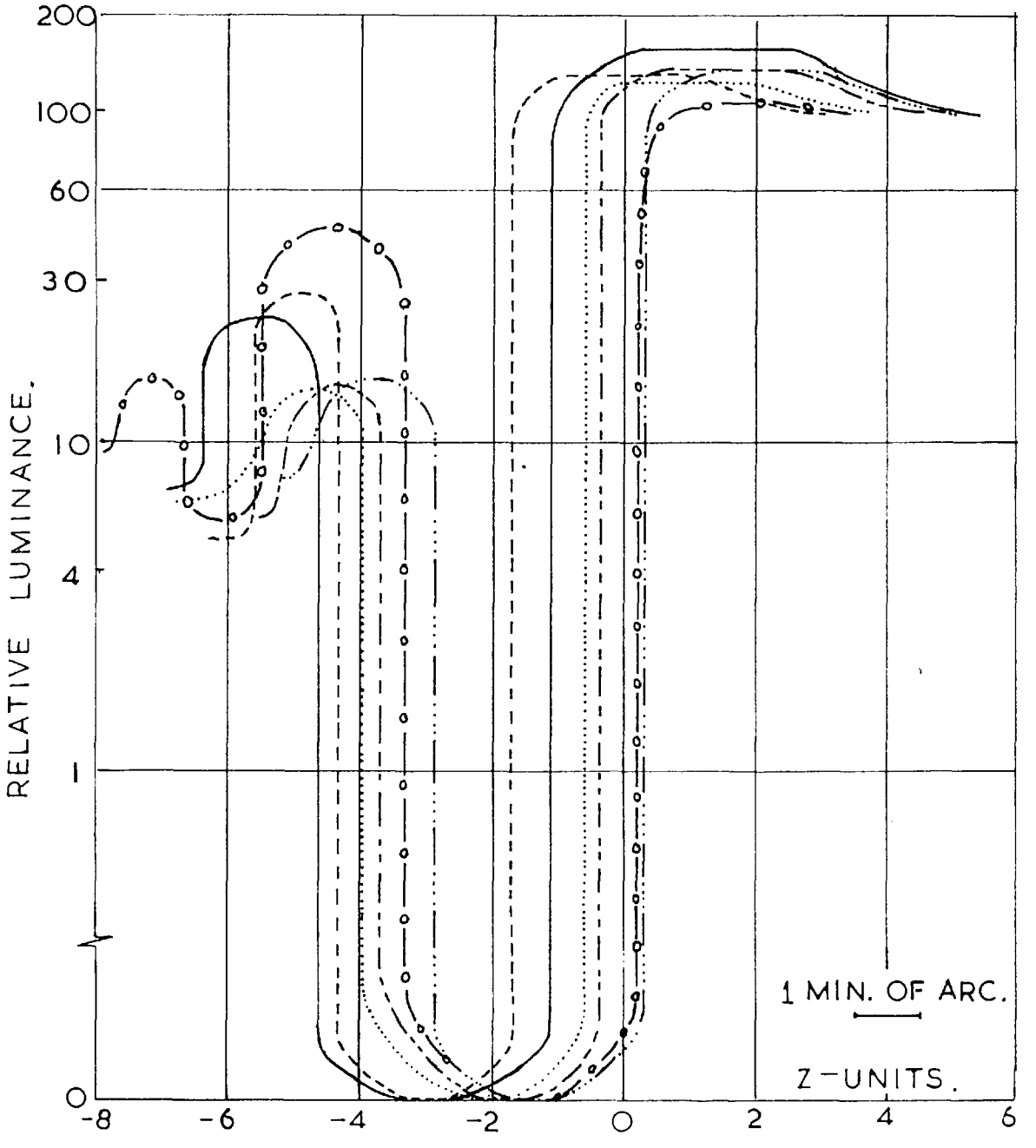



Fig. 3:19. The measured luminance distributions seen at an incoherently illuminated abrupt edge by various observers with 0.64 mm. eye pupil compared with Watrasiewicz's results (—o——o——).

visual results obtained (see figure 3:19). The variations are about the same as those reported by Rowe (1966) microscopically observed by ten observers in partially coherent light (S=0.22), as shown in figure 3:20.

The second derivative of the luminance distribution of the retinal image was drawn at the top of each figure of the mathematical model. It is obvious that there are partial agreements between the non-linear models and the second derivative curve. For example, in Mach model (figure 3:12), the modified model of Fry (figure 3:13) and the new model (figure 3:17), the bright bands predicted by the models occur exactly at the minima of the second derivative curve shown on the top of the figure. But the dark bands are slightly shifted with respect to the maxima of the second derivative curve. Furthermore, in each non-linear model, a greater magnitude of intensity of the bright band than that of the dark band is obtained.

In the linear models of Taylor (figure 3:15), O'Brien, and Békésy (figure 3:16), the positions of the bands differ from those of the maxima and minima of the second derivative. The magnitude of the intensity of the bright band obtained is equal to that of the dark band, which contradicts the effect visually observed where the first bright band is always more pronounced than the dark band. Moreover, when the overshoots of the predicted curves are brought over 100%

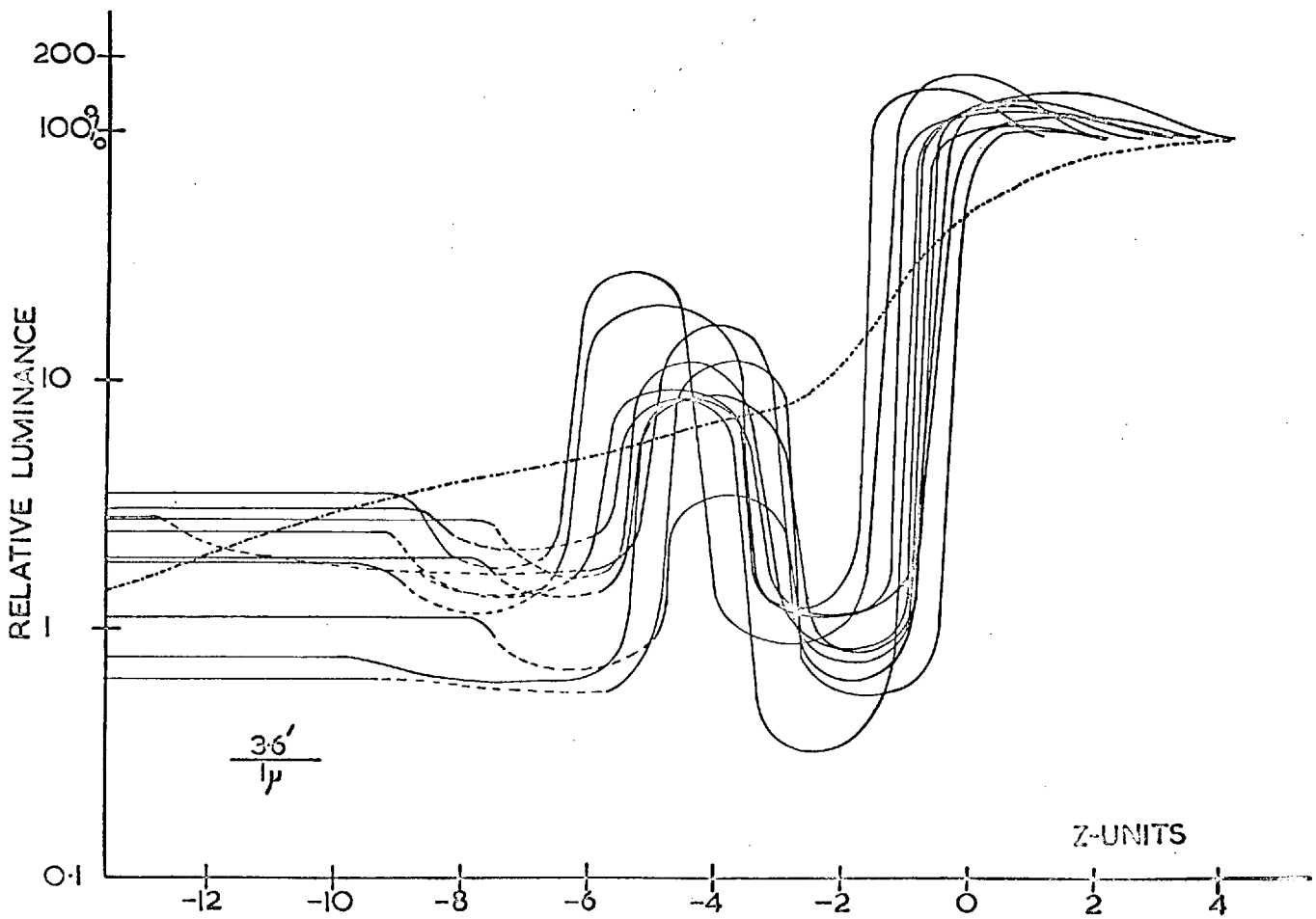



Fig. 3:20. The measured luminance distributions seen at a straight edge, when S=2.2, by ten observers. (Rowe 1966).

of the relative luminance, the undershoots acquire negative values, which is practically impossible.

The structure seen by each observer as shown in figure 3:11 is non-linear. But, it is hard to draw any conclusion as to which model fits the experimental results, since the individual variations are great, not only in the band widths but also in the positions.

# CHAPTER IV

# CALCULATIONS OF THE VISUAL IMAGES OF EXPERIMENTALLY PRODUCED GRADIENTS.

## 4:1 General.

In the last chapter the phenomena occurring with an object having a sharp transition of luminance from bright to dark were considered: owing to diffraction and aberrations in the eye, the luminance distribution in the image on the retina differs from that of the object in object space. Since the Mach phenomena can occur on an object with a graded luminance distribution as well, the mathematical models of the effect can also be studied by using this type of object.

There are many methods by which edges with a finite luminance gradient can be produced. For example, one can use a rotating disc with black and white sectors, as used by Mach (1865), Sherrington (1897), McDougall(1903), and Ludvigh (1953). Alternatively one can use optical systems such as the one used by Fiorentini, Jeanne and Toraldo di Francia in 1955, and that used by Thomas in 1965.

Figure 4:1a shows the sketch of the apparatus used by Fiorentini, Jeanne and Toraldo di Francia. Source S

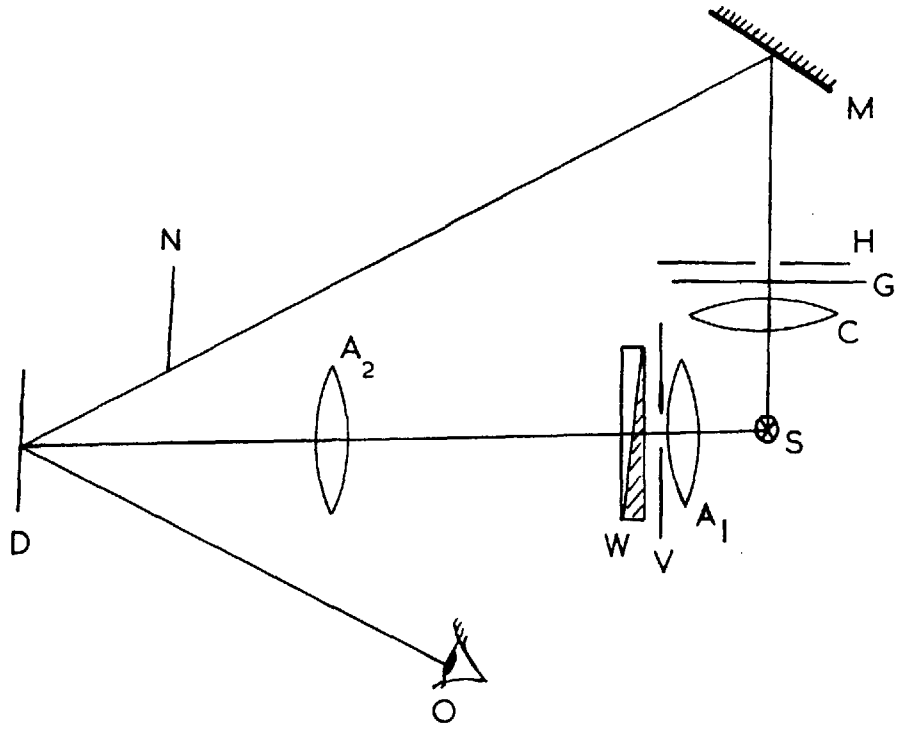



Fig. 4:1a. The apparatus used by Fiorentini, Jeanne and Toraldo di Francia.

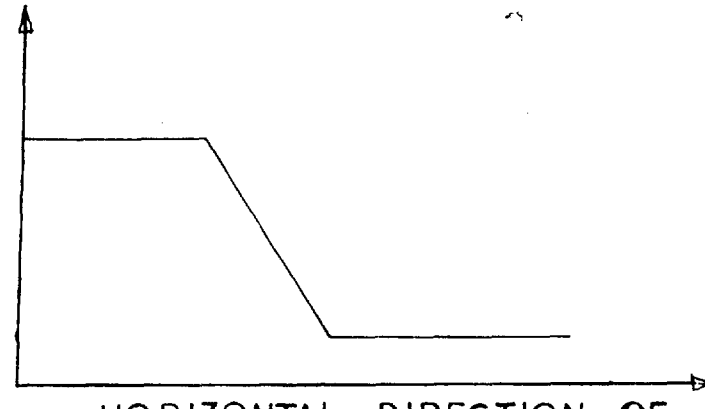
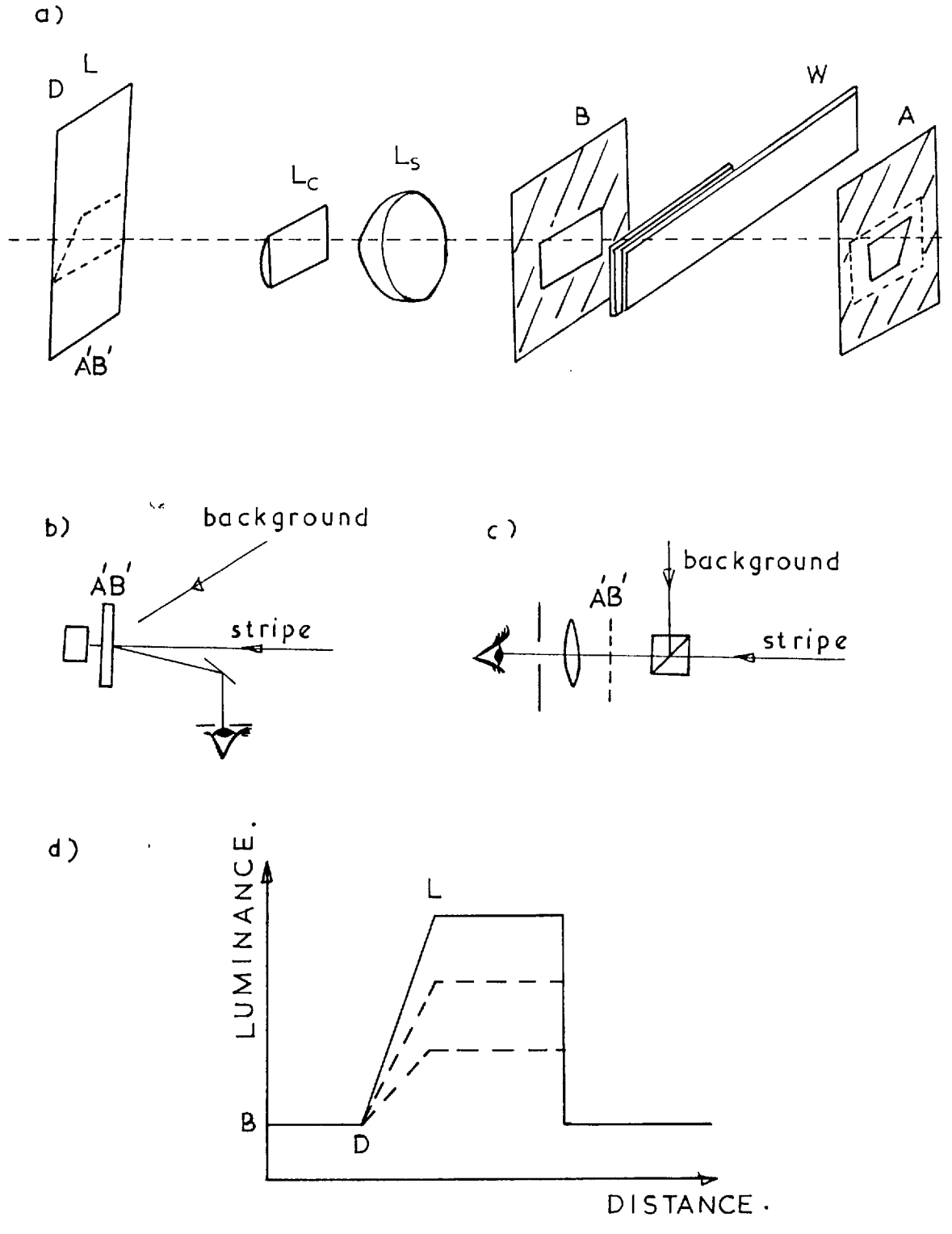



Fig. 4:1b. Luminance distribution obtained with the above apparatus.

is a 100 watt filament lamp. Light passes through a field lens(C) and uniformly illuminates the ground glass screen (G). H is a black diaphragm with a square aperture and is placed in contact with the ground glass (G). Light is then reflected by a mirror (M) and falls upon a diffusing surface (D) which is a magnesium carbonate plate. N is a screen with a straight vertical edge parallel to one side of diaphragm G. The screen (N) will produce a shadow on the surface D. The light distribution on D is as shown in figure 4:1b. The illuminated area was 8 cm. by 10 cm. The Mach bands were seen at the inflection points. Their brightnesses were measured by using photometric matching method. The comparison field was produced from the following system. A lens $A_1$ focusses the image of the source S on lens $A_2$. A diaphragm (V) having five small holes aligned in the vertical direction is in contact with the lens $A_1$ and the holes are imaged on D by lens $A_2$. The images of these holes can be horizontally displaced across D by moving $A_2$ along a direction perpendicular to its optical axis by means of a micrometer screw.The luminance of these five hole images can be varied by means of a wedge W. The observations were performed in a dark room. The observer (O) had been dark adapted for ten minutes before taking the measurements.

Figure 4:2a shows the optical system used by

Fig. 4:2. Apparatus used by Thomas (1965)



Thomas for projecting luminance stripes. An incandescent ribbon filament is imaged (dotted line) on an aperture (A). Each point in the aperture A radiates equally towards every point in another aperture (B). A spherical lens ($L_s$) forms an image of A in plane A'B (dotted figure). A cylinderical lens ($L_c$) increases the power along the vertical axis and at the same time it focusses the aperture B in the plane A'B'. The result is the stripe shown by the solid line. The luminance along any vertical line of the stripe is uniform from top to bottom and is proportional to the height, at the same vertical, of the image of aperture A formed by the spherical lens ($L_s$) alone. The variation of luminance along any horizontal axis is shown in figure 4:2d. The dotted lines in the figure show the effect of filtering when the wedge W in figure 4:2a is in place. Different luminance distributions can be obtained by placing different shapes of apertures at A. The aim of Thomas's experiments was to find the threshold for the Mach bands by filtering the discontinuous luminance gradients until the bands disappeared. Therefore, the subjective brightness measurement was not needed. Thomas showed two ways of viewing arrangements as shown in figures 4:2b and 4:2c. The background illumination is provided by a tungsten lamp and a collimating lens. In figure 4:2d, B is the luminance level of the background. In

figure 4:2b, a rotating white disc is placed at A'B'. An artificial pupil of 2.8 millimetres diameter was used in both figures (4:2b and 4:2c). The luminance stimuli were calibrated with a photometer.

For the work described in this chapter an optical system was constructed which produced a number of photographic plates of various density distributions; each had a transmission graded between uniform bright and dark areas. The physical luminance distributions produced by incoherently illuminating the plates could be directly recorded with a microphotometer. Then the theoretical distribution curve from each mathematical model mentioned before could be evaluated.

In preparing these plates precautions must be taken to avoid various effects which could occur, for example, the border effect and the fringe effect, since these photographic effects might lead the observer to confuse them with the Mach effect.

The edge effect, or the Mackie line, is a general term used for various effects which occur at the boundary between areas of different intensities in the developed image. During development, the developer in a heavily exposed area becomes rapidly exhausted and the rate of development decreases. In the less exposed area which is

adjacent to the heavily exposed one, however, the developer remains comparatively active. A more active developer will diffuse laterally across the boundary between two areas and make a small increase in the rate of development in the region just inside the boundary of the heavily exposed area. This narrow strip develops to a higher density. The increase in density at this heavily exposed area is sometimes called the ' border effect'. Similarly, the exhausted developer on the heavily exposed side diffuses across the boundary into the less exposed area and lowers the activity of the solution at this point. Thus, a line of lower density is to be found just inside the edge of the low density area. The decrease in density at this less exposed area is called the ' fringe effect'. These effects may be minimized by using fresh developer and providing sufficient agitation while developing.

In working with photographic plates which were exposed to light through circular openings in contact with the plates, Eberhard noticed that they did not have uniform densities on the developed areas. The openings were ranged from 0.3 to 3.0 millimetres in diameter; he found that the smaller images were denser than the larger ones, as if the smallest had received from one and a half times to twice as much exposure as the largest. The effect increases with increasing thickness of the emulsion. This is called the

'Eberhard effect'. It rises to a maximum for moderate degrees of developement, then decreases as development is continued. (For details of these photographic effects see Mees 1954).

However, these photographic effects are objective and with a suitable physical light detector, it is easy to determine whether they are actually on the plates or not.

The plates used in the present work were Ilford HP3. (HP stands for Hypersensitive Panchromatic). Response curves obtained by plotting density against log(exposure) (known as characteristic curves or H and D curves, see the Ilford Manual of Photography 1958) of an Ilford HP3 plate are shown in figure4:3a. They indicate the effect on the emulsion, of every degree of exposure, from under-exposure to over-exposure, for development times of 4,8 and 16 minutes, using an ID-2 developer. The HP3 plate is a fast panchromatic plate, sensitive to all colours. The wedge spectrogram, which indicates the relative sensitivity of the emulsion at different wavelengths through the spectrm, is shown in figure 4:3b.

The plates were measured on a Hilger and Watts recording microphotometer (see figure 4:4). In this micro-photometer light from a 6 Volt 8 Watt line filament lamp(M), passes through a cylinderical lens(L) and is reflected upwards by a right-angled prism(H) through a 25 millimetre

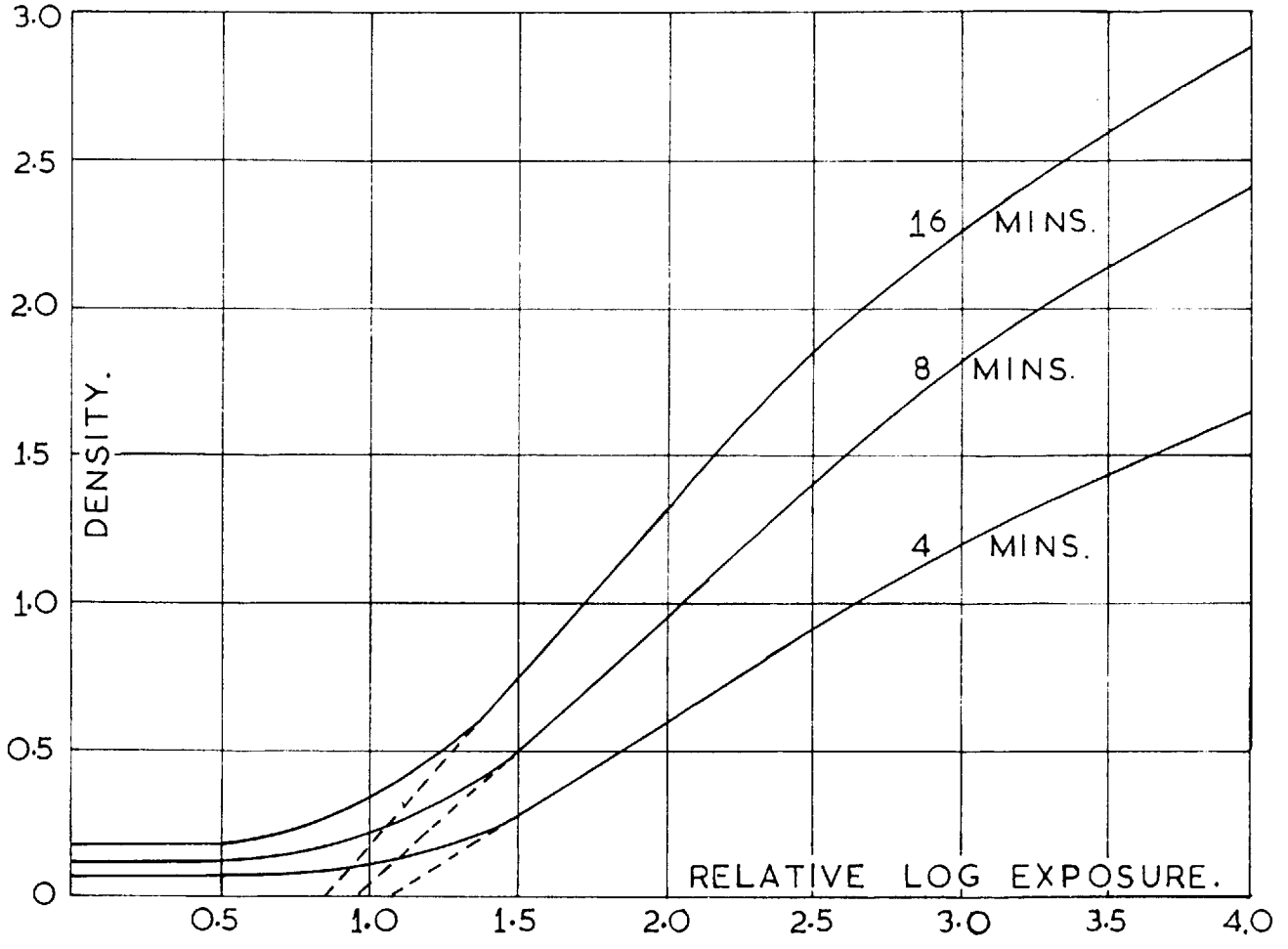



Fig. 4:3a. H and D curves, The plate was developed in ID 2 (1+5) at 68°F with intermittent agitation.

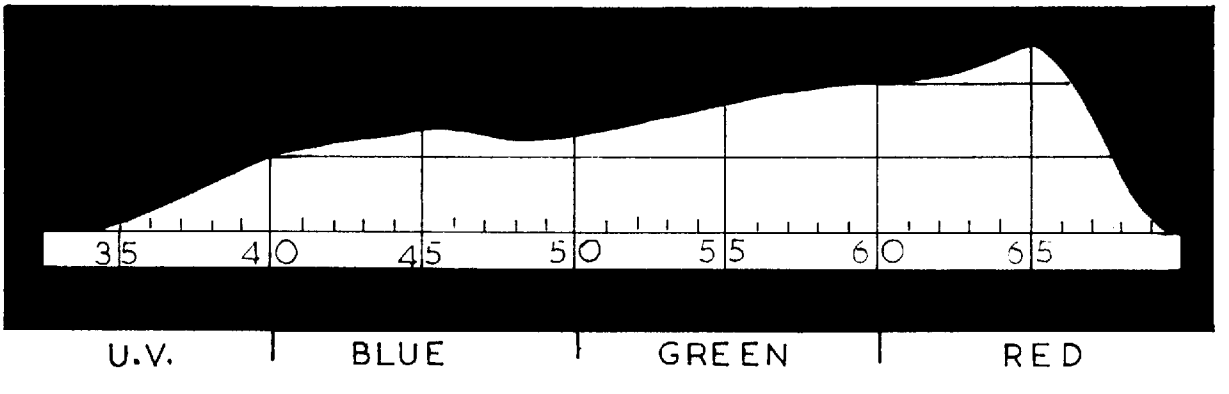



Fig. 4:3b. Wedge spectrogram for tungsten light (2850°K).

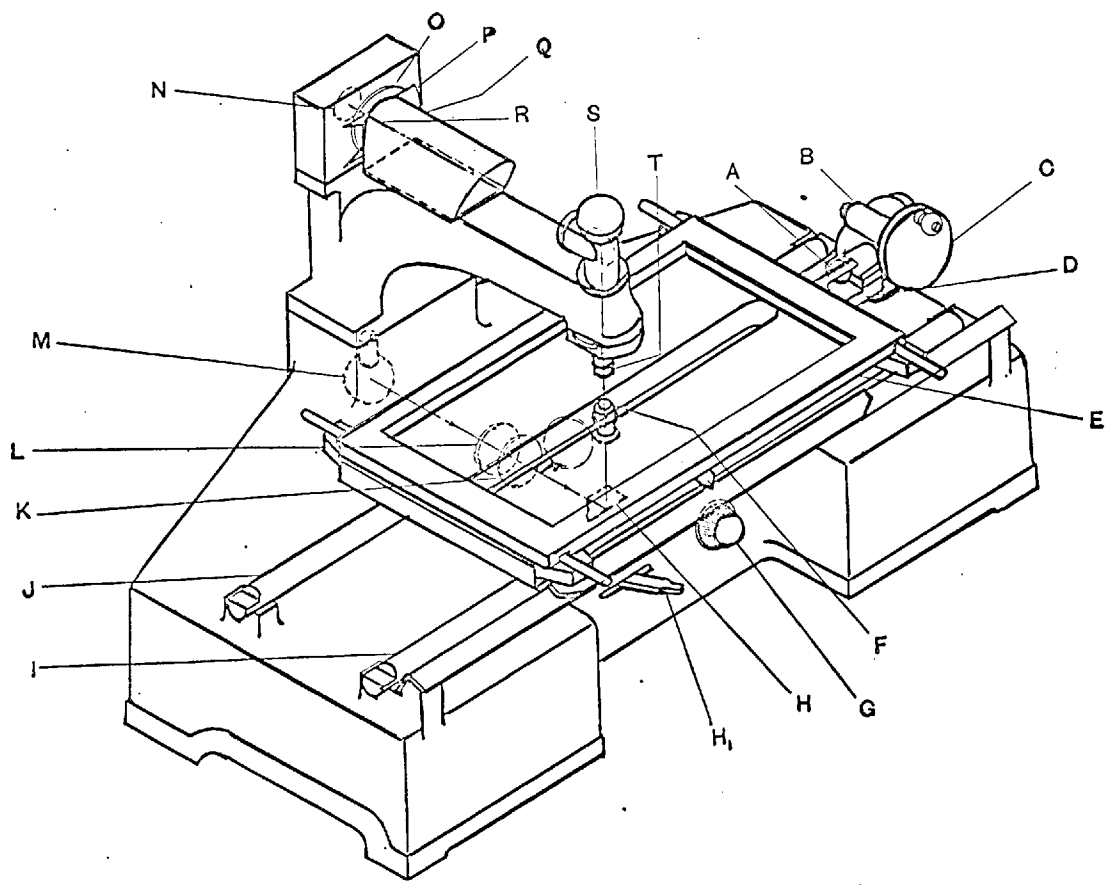



Fig. 4:4. Hilger and Watts microphotometer.

microscope objective(F) onto the plate, which is held on a plate-carrier (E). The movement of this plate-carrier is controlled by an electric motor. The width of the image on the plate is one-tenth of the width of the filament and its length is two millimetres. The beam then passes through the plate and through an upper objective (T) and forms an image of the plate on a symmetrical slit (O) of which the length and width are adjustable. The magnification of this system is 10. Behind the slit, a photomultiplier (N) is mounted and the light flux is registered with a pen recorder of which the full scale deflection is about 10 mV.K is a spherocylindrical lens. It can be introduced into the beam as required; and is known as a viewing lens.

The resolving power of the 25 millimetre objective, or the smallest distance between two points which the lens will render as separate images, is about 2 microns. This distance is defined as the radius of the first dark ring of the Airy disc given by the lens. Therefore, it can be written as,

$$h = \frac{0.61\,\lambda}{(N.A)},$$

where $\lambda$ is the wavelength of light used in the system, and (N,A) is the numerical aperture of the lens.

Knowing the numerical aperture of the lens, which is 0.20 for a 25 millimetre objective (Martin and Johnson

1958), the resolving power can then be calculated. This is then found to be very much smaller than the smallest detail which can be resolved on the plate under the conditions of use to be described.

4:2 The Production of Graded Luminance Distributions.

The apparatus shown in figure 4:5 was set up on an optical bench. The light source A is an Osram sodium lamp. The condenser B focussed the light source A onto a wide slit C. Two cylinderical lenses (D and E) were used to form an image of the slit on a ground glass screen F which could be replaced by a photographic plate. The first cylinderical lens D produced a uniform distribution of light from the slit on the screen. With the aid of a low power eyepiece, the exact position of the screen could be obtained. The second lens E which was placed with its axis perpendicular to that of the first lens, produced on the same screen(F) a variation of light intensity along one direction caused by a mask M placed just behind the first lens. Thus, in the image plane, a rectangular patch of light with constant luminance distribution along one direction and varying along a perpendicular direction would be obtained.

The sodium lamp (A) which operates at 20 V,1.3 A, needs a resistor in series to drop the voltage as it works off the 220 V mains supply. The lamp emits about 99% of its

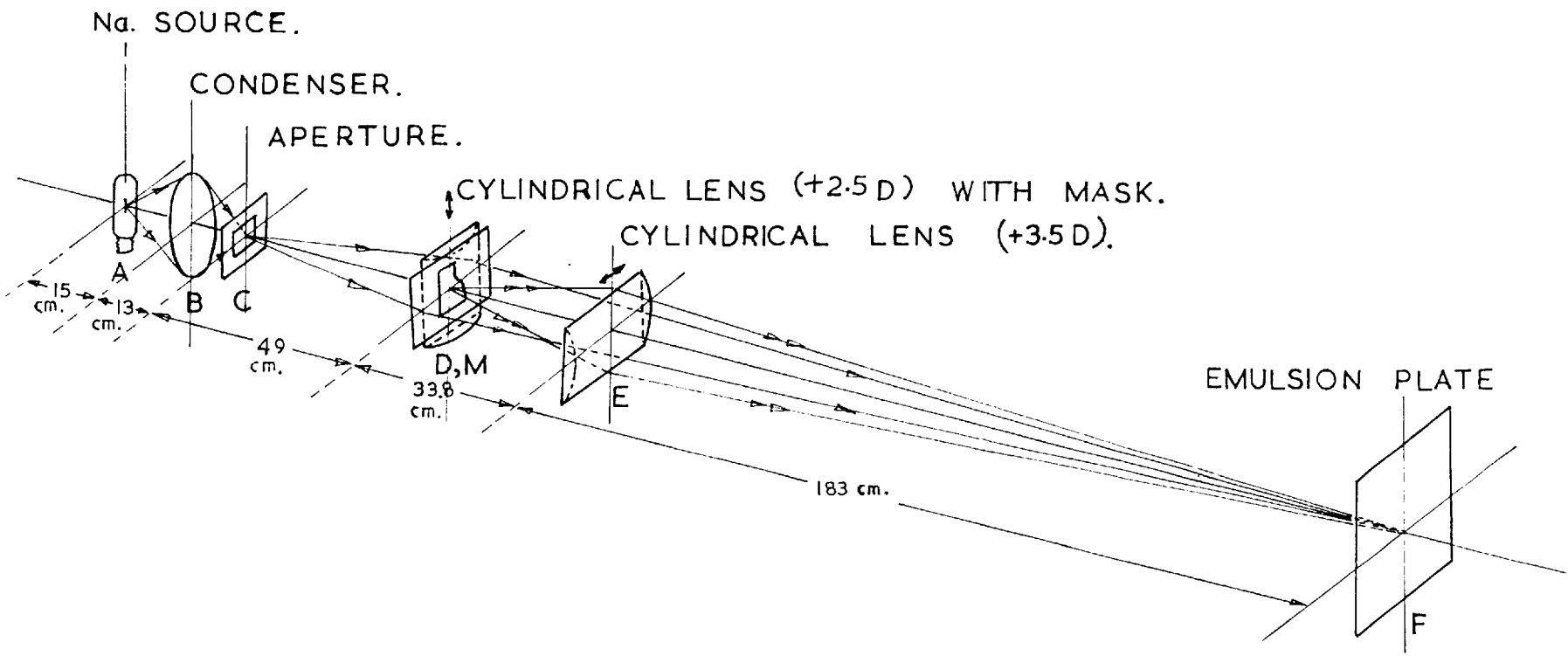



Fig. 4:5. Apparatus for producing graded luminance profiles on photographic plates.

visible radiation at wavelengths of 5890 and 5896 °A. The brightness is about 7 candelas per square cm. The area of uniform brightness inside the lamp is 2 x 1 square cms.

The focal length of the lens B is 7 cms. and the distance between the lamp A and the lens B is 15 cms. The lens focusses the image of source A onto slit C which is 13 cms. away Thus, an image of the area of uniform brightness on plane C will be 1.74 x 0.87 sq.cms. This will cover the whole slit C of which the size is 0.4 x 0.6 sq. cm.

The axes of the cylindrical lenses used in the system are indicated by the lines with arrows above the lenses, which were plano-convex. Figure4:6 shows refraction by a cylindrical lens; it behaves like a plane parallel plate for the dimension of the object parallel to its length and as a convex lens for the dimension perpendicular to its length. Light from a luminous point B on the optical axis of the thin cylindrical lens continues unchanged in divergence in the axis plane after leaving the lens. In another plane, the light is refracted by an amount depending on the power of the lens in that plane. In the figure, the light in the plane at right angles to the axis is shown converging to B'. The refraction in oblique sections is such that all the light from the object point on leaving the lens will pass through the focal plane at B'. The position of this

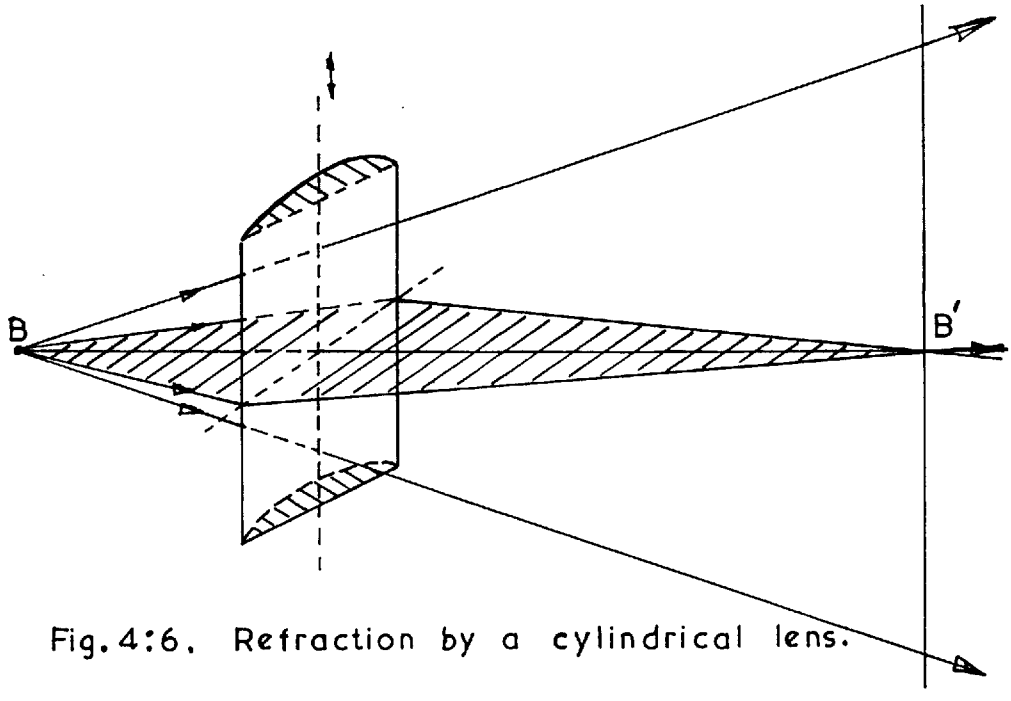



Fig. 4:6. Refraction by a cylindrical lens.

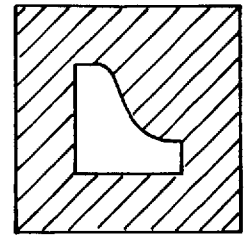


Fig. 4:7. Metal mask.

line focus can be found from the usual formula for conjugate foci; its direction is parallel to the cylindrical axis.

Each metal mask M which was put after the first cylindrical lens D (see figure 4:5) had three straight sides and one side having a profile like that shown in figure 4:7 with a flat top and bottom. Different light distributions could be obtained by changing the shape of the curved side.

The screen F was then replaced by a photographic plate. An exposure was taken with each mask so that the required luminance distributions would be obtained. The exposure time was 4 seconds. The development was carried out with ID-11 which is a fine grain developer. The time needed for development was 7 minutes in a dish with continuous agitation at $68^{\circ}$ F (i.e; $20^{\circ}$ C). The unwanted silver halide was then removed by Ilford Hypam fixer which is a rapid fixer. The fixing time was 1 to 2 minutes. In order to avoid photographic effects mentioned in section 4:1, the development was carried out as suggested by Ilford (the Ilford Manual of Photography, 1958). Fresh developer was used. The plate was lying flat in the dish, emulsion side upwards. The surface of the plate had to be wetted quickly and evenly, otherwise developing marks would result. During development, the dish was rocked continuously to provide agitation. The

rocking should not be too rapid and had to be varied at intervals (e.g; first to and fro, then from side to side) to avoid patterns of uneven density caused by regular waves.

It was found that in order to get a smooth distribution of density, without any objective bands, care had to be taken over the following points :

1). The rectangular slit C(see figure 4:5) should be sufficiently large (this was to avoid diffraction bands).

2). The vertical edges of the slit C had to be parallel to the axis of the cylindrical lens D, otherwise sharp images of the edges would not be obtained.

3). The edges of the metal mask M had to be filed smooth, and cleared from dust in order not to get any physical bands on the photographic plates.

4). All angles of the rectangular patch of light would not be $90^{\circ}$ unless the axes of the two cylindrical lenses ( D and E) were exactly perpendicular to each other.

Figure 4:8 shows the negative photograph of the patch of light on one of the plates produced by this process. The size of the photograph is the same as in the original.

The developed photographic plates were then scanned with Hilger and Watts recording microphotometer. The recorder of the microphotometer was adjusted to maximum deflection when the image of the light source was focussed

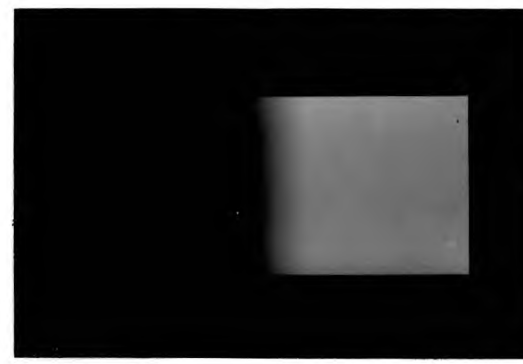


Fig. 4:8 A luminance gradient experimentally produced on a photographic plate.

on the uniform bright area of the photographic plate, and to give zero deflection when there was no light on the photocell. In this way, relative transmissions were directly recorded.

The transmission distributions of two sets of plates, prepared as described above, are shown in figures 4:9 and 4:10. In the first set (A), figure 4:9, a variety of luminance gradients was obtained while the higher and lower luminance levels remained constant. In the second set(B), figure 4:10, the lower luminance was altered to give various luminance contrasts between the bright and the dark regions while the higher level remained constant. These

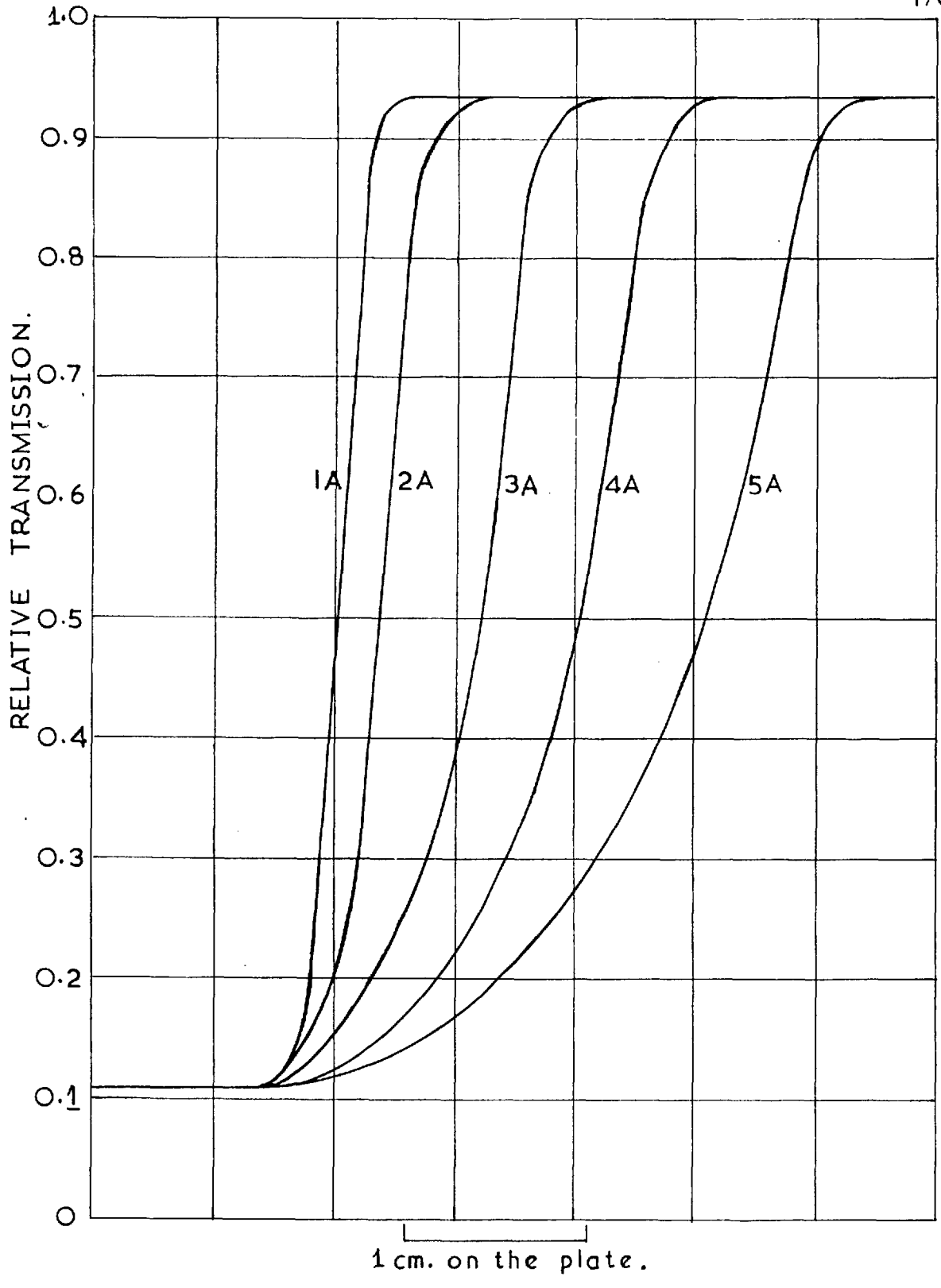



Fig. 4:9. The transmissions of the first set (A) of photographic plates.

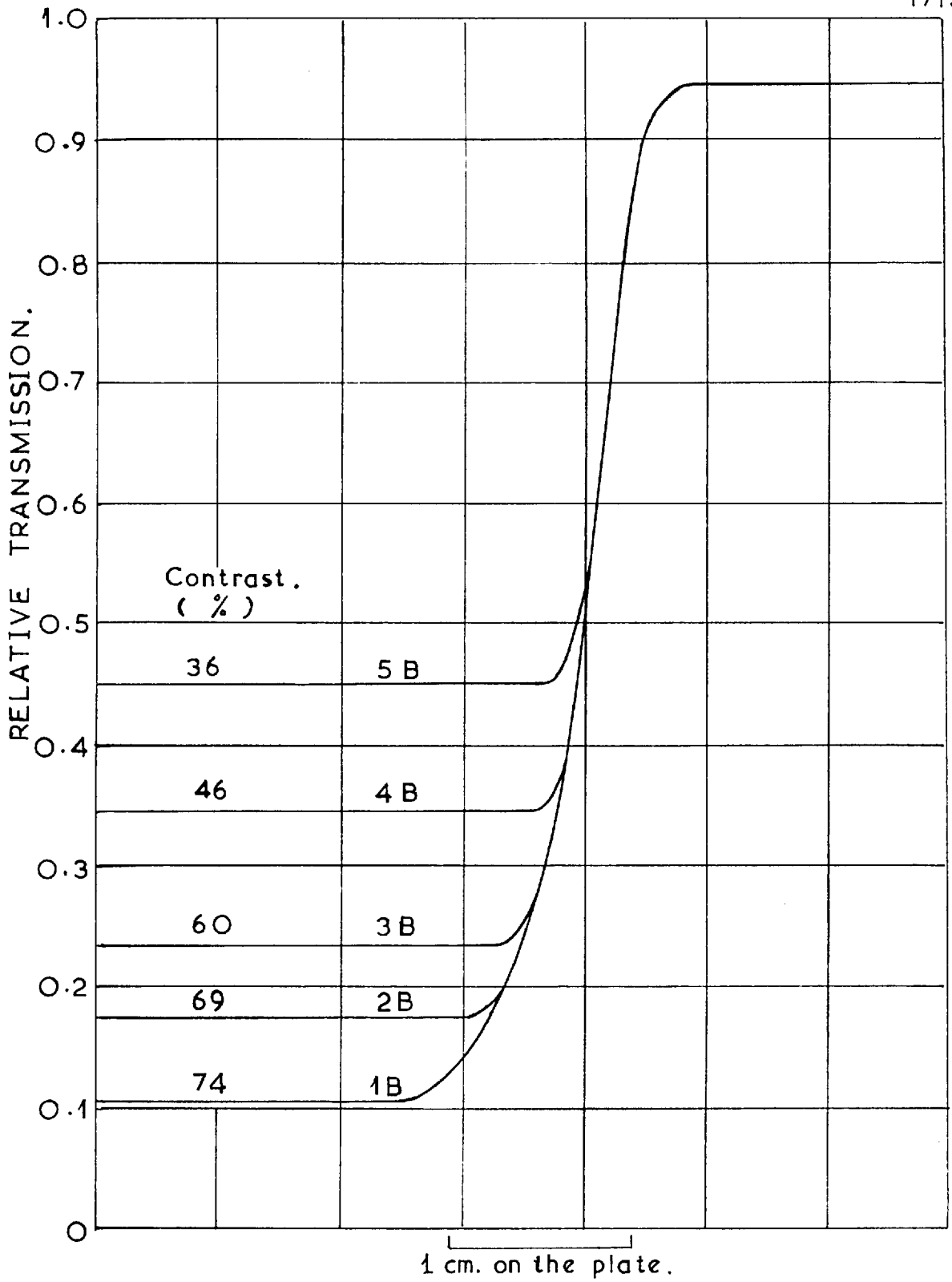



Fig. 4:10. The transmissions of the second set (B) photographic plates.

ten plates were used as the objects for the observations to be considered in the next chapter.

## 4:3 The Retinal Image Distribution and Its Derivatives.

One way of obtaining the distribution of the image of an incoherently illuminated object is to take the convolution of the intensity distribution in the object with the spread function of the optical system forming that image. When the eye is considered as the optical system, the spread function of the eye has also to be determined.

Westheimer and Campbell(1962) and Krauskopf (1962), have independently obtained estimates of the spread function of a bright vertical thin line-object on a uniform background for an eye in best focus, with various pupil diameters. An image of a line was formed on the retina and then the light was reflected out of the eye along the path by which it entered, forming an image outside the eye. The light distribution of this aerial image was measured by photoelectric scanning. In this way the spread function was obtained for a series of pupil diameters. The results obtained by Krauskopf are shown in figure 4:11, where the distributions of the retinal images with eye pupil diameters 3, 4,5,6,7, and 8 millimetres are shown. With the same techniques, Campbell and Gubisch (1966) measured the line spread functions of the eye at eight pupil sizes (see figure 4:12).

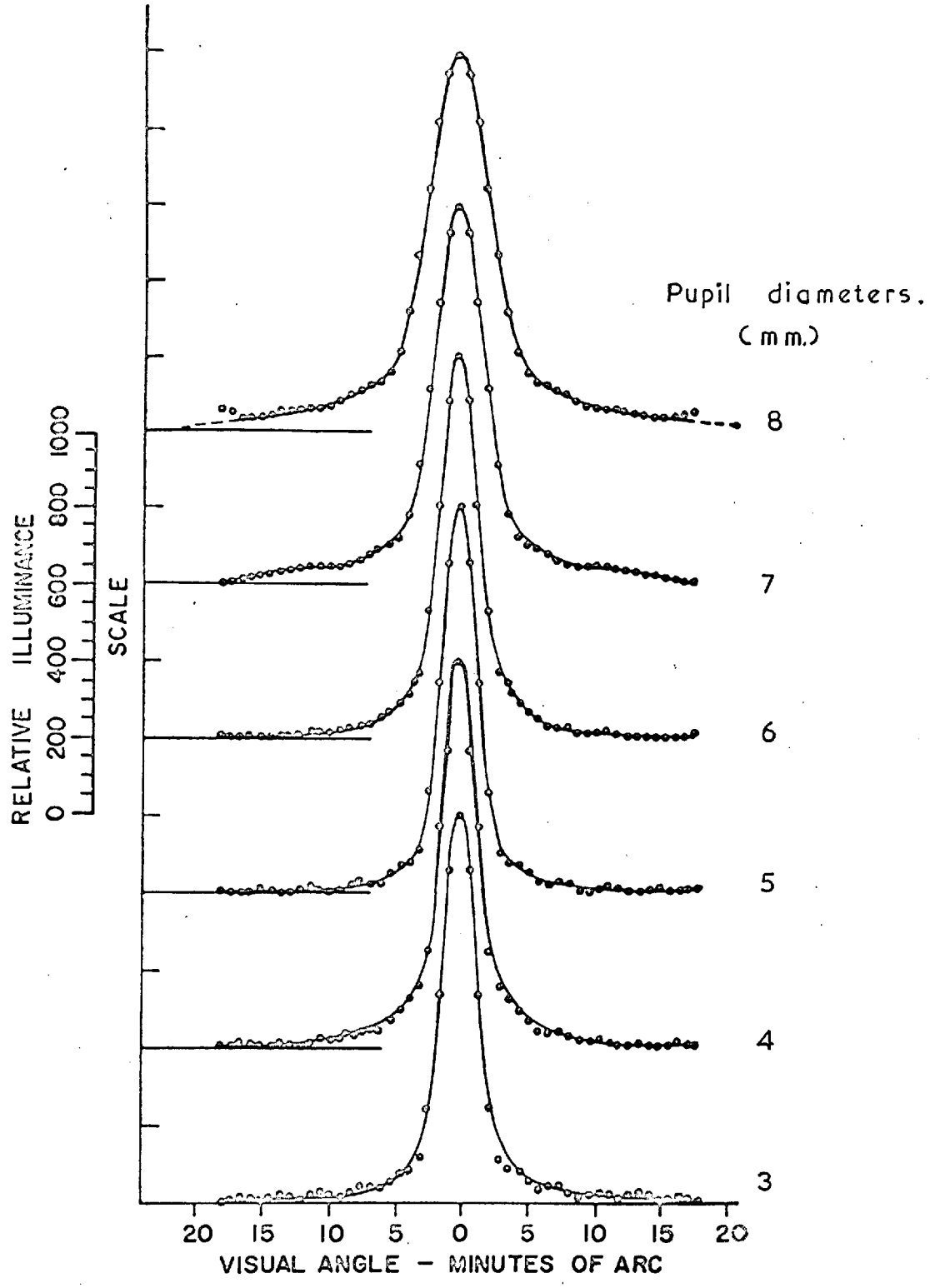



Fig.4:11. Reconstructed retinal images of bright vertical line target (1.6 second wide) for various pupil diameters (Krauskopf 1962).

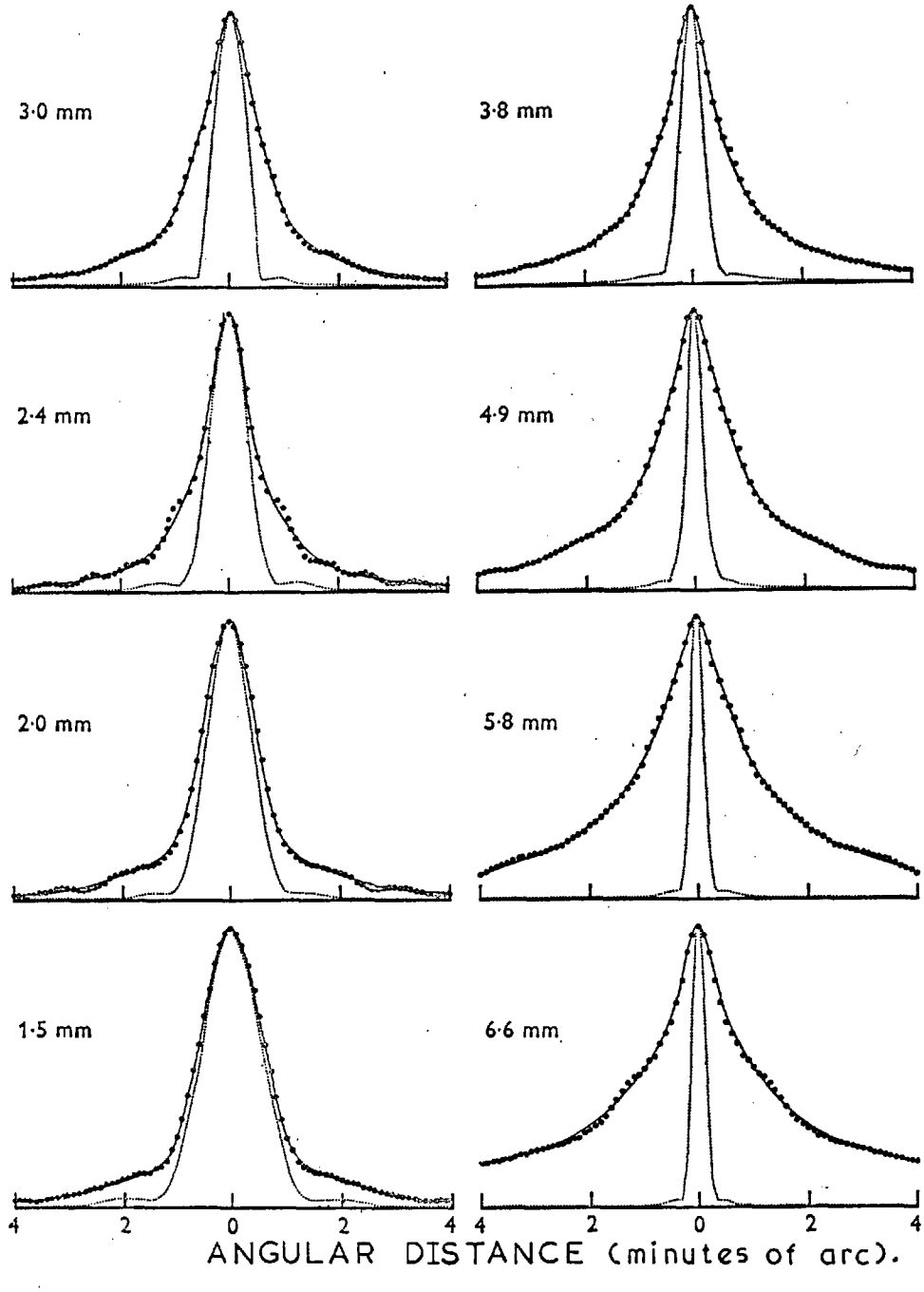



Fig. 4:12. Retinal images of a bright vertical line for various pupil sizes (Campbell and Gubisch 1966).

They obtained broadly similar results to those shown by Krauskopf but the spread of the light distributions are narrower than Krauskopf's. In each case the same assumptions were made in order to obtain the retinal image from the luminance distribution of the aerial image traced by photo-electric scanning. The basic assumption in the treatment was that the optics of the eye form a reversible optical system. Since the aerial image was formed from a double passage, the response for a single passage was computed for each spatial frequency by taking the square root of the response for the double passage. The luminance distribution of the retinal image was then deduced by multiplying the Fourier transform of the object by the appropriate responses and computing the inverse transform.

In the previous chapter it was noted that the intensity in the image of an incoherently illuminated edge is given by

$$I(z) = \frac{4}{\pi} \int \frac{H_1(2z)}{(2z)^2} . dz. \qquad \ldots\ldots\ldots (4:1)$$

Hence, the intensity of a line image, i.e; a line spread function can be written as,

$$W(z) = \frac{4}{\pi} . \frac{H_1(2z)}{(2z)^2},$$

$$= \frac{H_1(2z)}{\pi z^2} . \qquad \ldots\ldots\ldots\ldots (4:2)$$

The value of W(z) can also be determined from (as shown in the last chapter),

$$I(z) = \frac{1}{2} - \frac{4}{\pi}\left[\frac{2z}{1^2.3} - \frac{(2z)^3}{1^2.3^2.3.5} + \frac{(2z)^5}{1^2.3^2.5^2.5.7} - \ldots\ldots\right],$$

which will give,

$$W(z) = \frac{4}{\pi^2}.\ 2\left[\frac{1}{1^2.3} - \frac{(2z)^2}{1^2.3^2.5} + \frac{(2z)^4}{1^2.3^2.5^2.7} - \ldots\ldots\ldots\right]. \quad \ldots(4:3)$$

Therefore, at the origin where z = 0,

$$W(z) = 8/3\pi^2 \ . \qquad \ldots\ldots\ldots\ldots\ldots\ldots(4:4)$$

Figure 4:13 shows the line spread function calculated from equation 4:2. There are no completely dark minima separating the maxima of intensity as in the point spread function.

If we look closely at figure 4:11 and figure 4:12, some minute inflections on the sides of the distribution curves will be seen. When the size of the eye pupil is decreased, the inflections become more pronounced. For a 3.0 mm. diameter eye pupil, the first dark ring appears at about 5 minutes of arc from the centre in figure 4:11 and at about 1.5 minutes of arc in figure 4:12. These correspond to distances 0.032 and 0.010 mm. respectively on the retina. Campbell and Gubisch claimed that there were many improvements in accuracy in their measurements so that narrower responses were obtained (figure 4:12). From figure

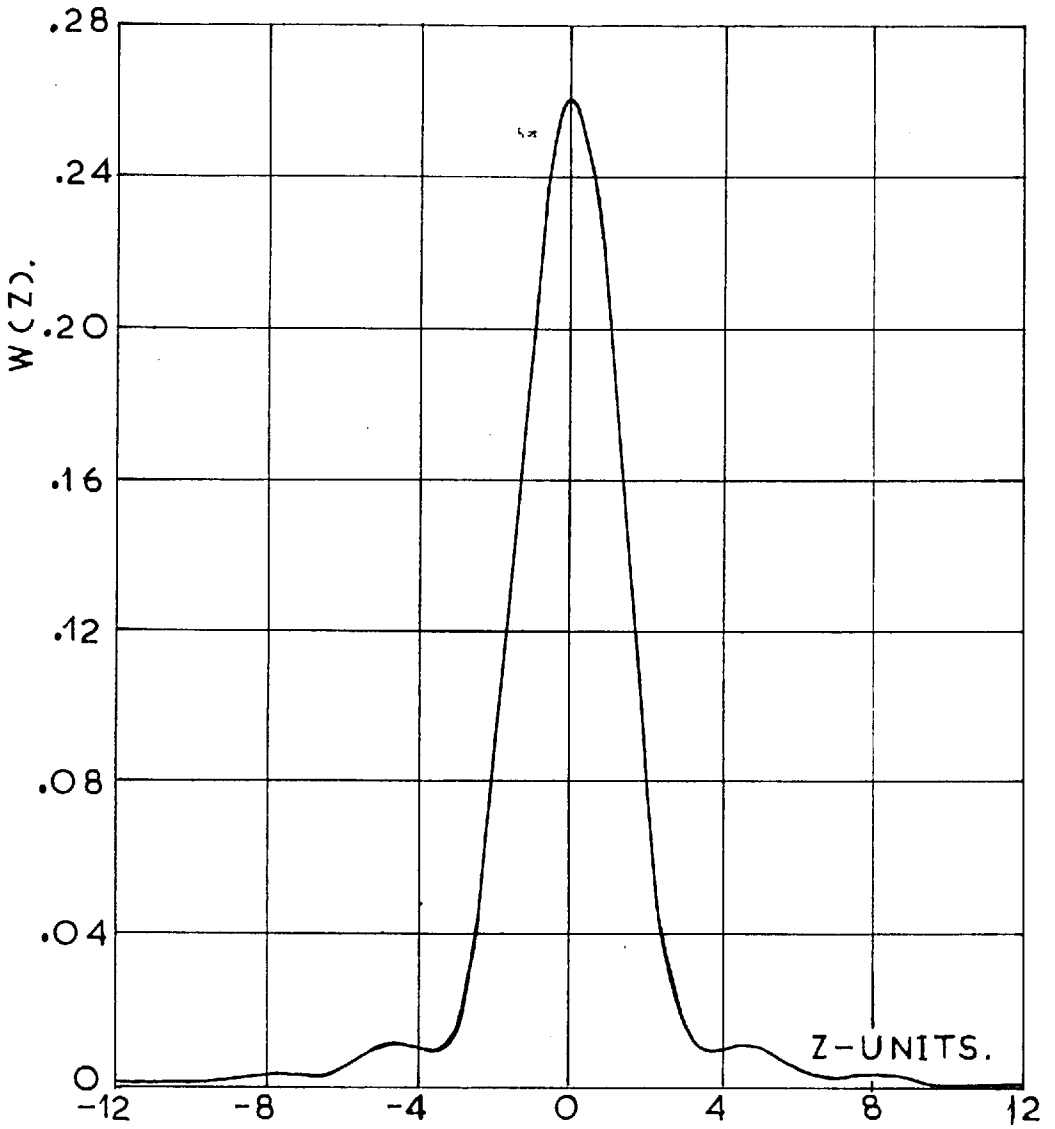



Fig. 4:13. A line spread function calculated from equation 4:2.

4:13, the line spread function is obtained theoretically; the first dark ring appears at about 3.7 Z-units which is equivalent to a distance 0.004 mm. on the retina. In the experimental results, however, one would expect a broader spread of the light distribution due to scattered light entering the eye and the aberrations of the eye while in the theoretical work perfect imagery is assumed.

The intensity distributions obtained from the microphotometer traces in the last section are the object luminance distributions. The distribution in the image space, when the object is incoherently illuminated, can be determined by the convolution of the line spread function of the system with the luminance distribution of the object, that is,

$$E(z') = \int_{-\infty}^{+\infty} F(z).W(z'-z).dz \ , \qquad \ldots\ldots\ldots\ldots (4:5)$$

where $E(z')$ is the luminance distribution of the image, $F(z)$ is that of the object, $z$ and $z'$ are spatial coordinates of object and image spaces, and $W(z)$ denotes the line spread function.

Since the experimental line spread function is not yet known with confidence, we decided to use the theoretical line spread function in the calculations. The convolution integration was carried out numerically for the

luminance gradient plate 1A which was the one with the steepest gradient among the produced plates;taking the eye pupil of 3 mm. in diameter and the distance between the plate and the observer 5420 mms. The dimension of the exposed area on the plate was 25 x 50 square mms.(the luminance varied along the side of 50 mm. length). The distance along the x-axis of the line spread function(figure 4:12) was converted from Z-units into mm.-units (one Z-unit = 0.34 mm. in object space). The result of the convolution of the luminance distribution of plate 1A with the line spread function is shown in figure 4:14.The image distribution curve (dotted line) does not differ much from the object one (full line). The second derivative curve of the luminance distribution of the object gives the stationary values nearly in the same places as those given by the intensity distribution of the image. When the slope of the luminance gradient is less steep, as shown by the full line in figure 4:15, the blurring of the image obtained by the convolution of the luminance distribution of the object with the line spread function will be much less, as shown by the dotted line in the same figure. In this case, the difference between the luminance distribution of the object and that of the image is insignificant. A considerably blurred image is yielded only when the line spread function is applied to a luminance distribution with a fairly abrupt step.

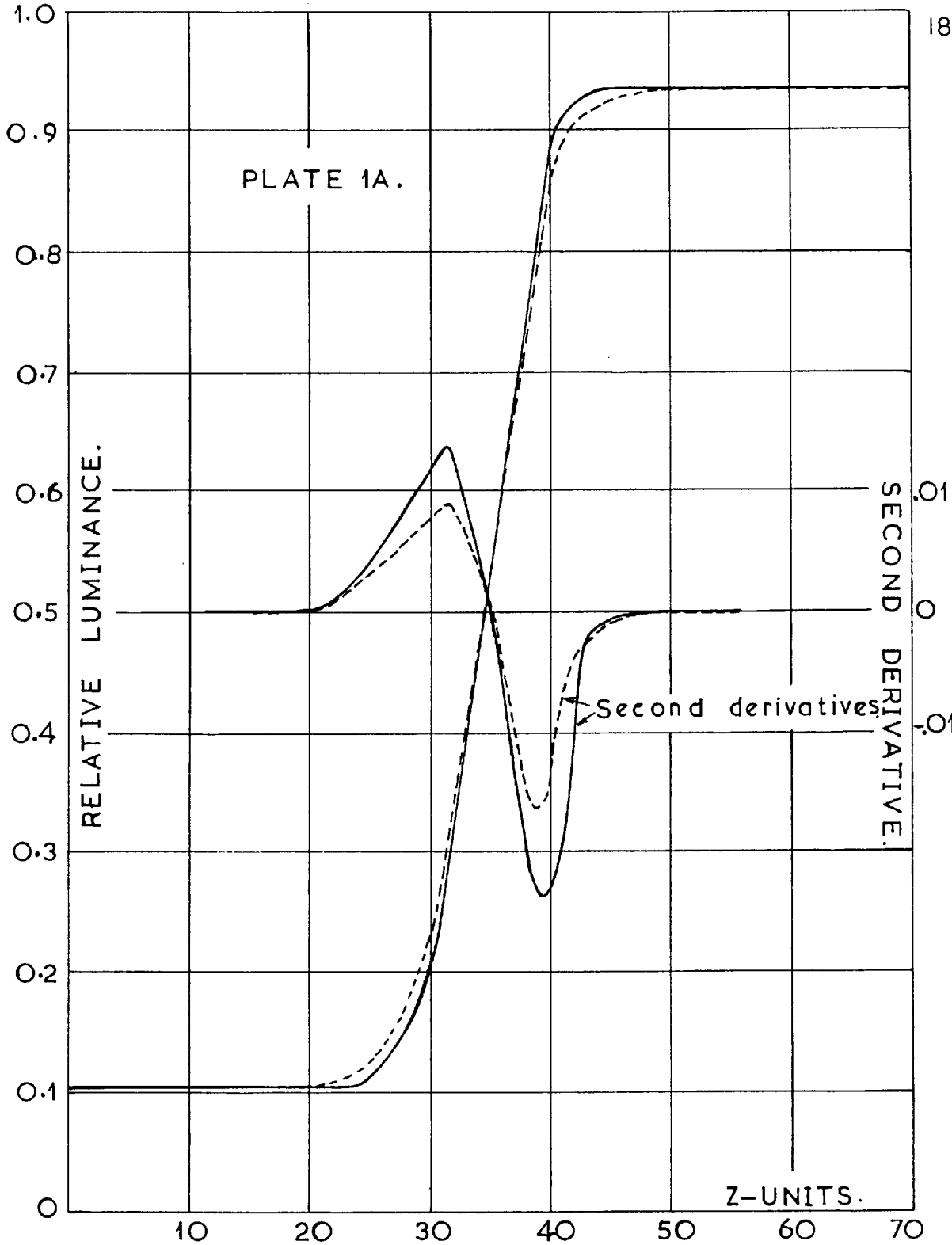



Fig. 4:14. The object luminance distribution (full line) and the retinal luminance distribution (dotted line), obtained from the convolution of the object luminance distribution with the line spread function, and their corresponding second derivatives.

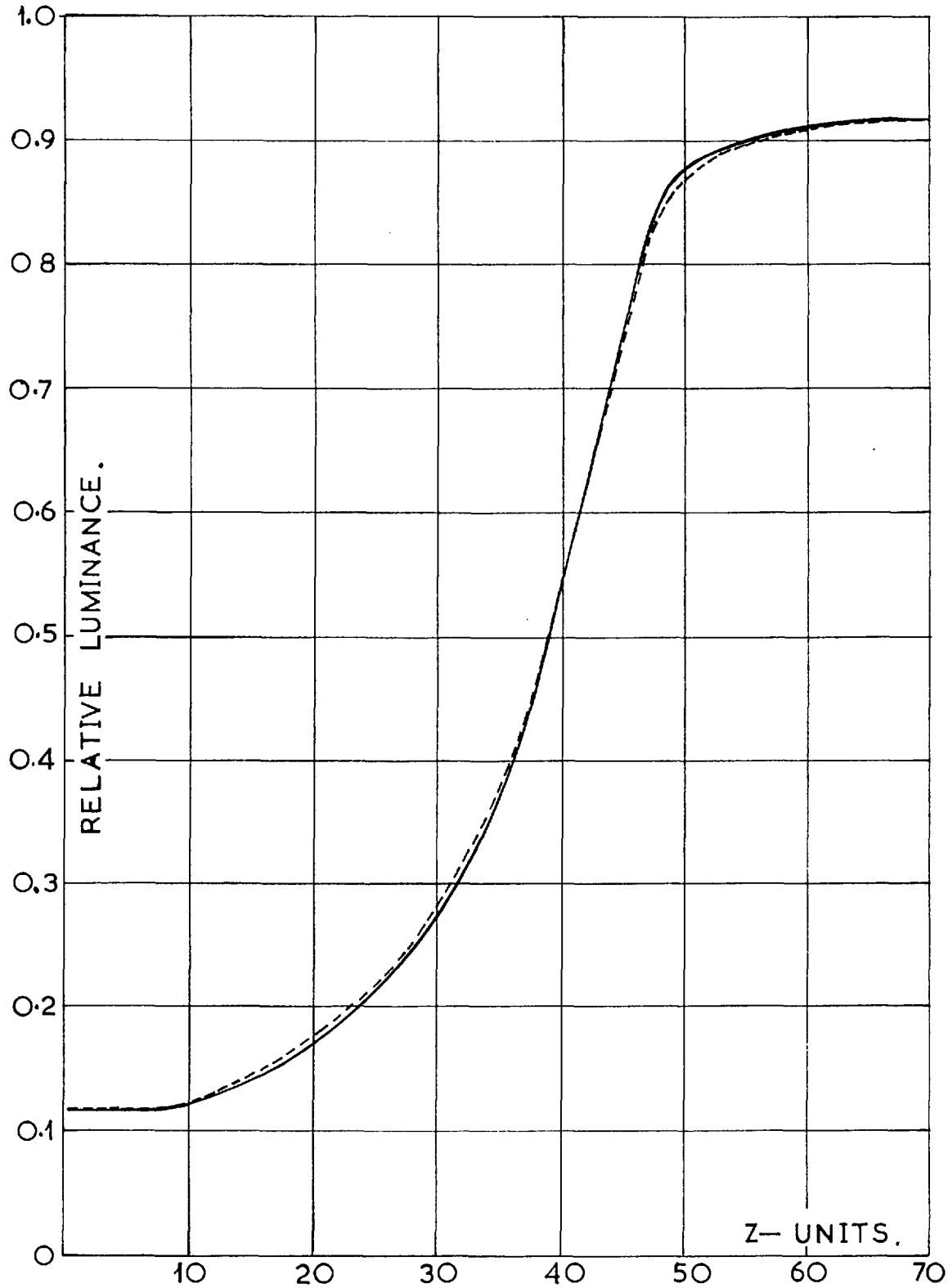



Fig. 4:15. The object luminance distribution (full line) and the retinal luminance distribution (dotted line), obtained from the convolution of the object luminance distribution with the line spread function.

Since plate 1A had the steepest gradient in this work but gave rise to very little blurring, the blurrings produced by all the other plates were expected to be negligible. Therefore, the distributions of the objects themselves were considered as the distributions of the retinal images in doing the calculations on the various models.

Let us now consider how a second derivative of any curve, when its equation is not known, can be obtained (see Hartree 1952).

If the values of a function f(x) at various points along the x-axis are tabulated and $\delta x$ is a small interval along x-axis, as shown in figure 4:16, then, at any point

$$f(x+\delta x) = f(x) + (\delta x)\frac{d}{dx}f(x) + \frac{(\delta x)^2}{2!}\frac{d^2f(x)}{dx^2} + \frac{(\delta x)^3}{3!}\frac{d^3f(x)}{dx^3} + \ldots\ldots\ldots\ldots$$

If D is the differential operator, $D \equiv d/dx$, Taylor's expansion can be written as,

$$f(x+\delta x) = f(x) + \frac{(\delta x)Df(x)}{1!} + \frac{(\delta x)^2D^2f(x)}{2!} + \frac{(\delta x)^3D^3f(x)}{3!} + \ldots\ldots\ldots\ldots$$

$$= \exp((\delta x)D).f(x) = E.f(x), \qquad \ldots\ldots(4:6)$$

where $E = \exp((\delta x)D)$.

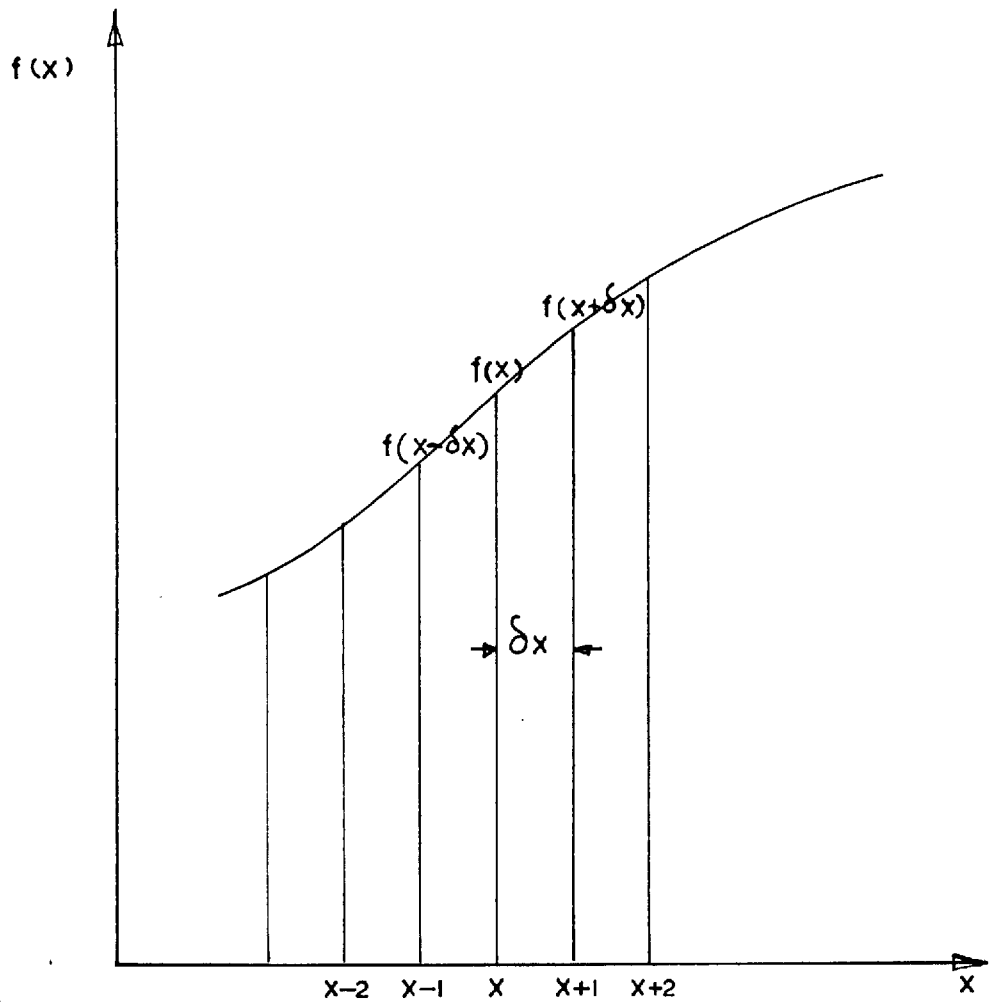



Fig. 4:16. The determination of the derivatives of any function where its equation is not known.

A difference can be expressed in terms of the function values, that is,

$$\delta f(x) = f(x+ 1/2) - f(x - 1/2),$$

$$= E^{1/2}f(x) - E^{-1/2}f(x),$$

or,
$$\delta = E^{1/2} - E^{-1/2}, \qquad \ldots\ldots\ldots\ldots (4:7)$$

$$= \exp(\frac{1}{2}(\delta x)D) - \exp(-\frac{1}{2}(\delta x)D),$$

$$= 2.\mathrm{Sinh}(\frac{1}{2}(\delta x)D). \qquad \ldots\ldots\ldots (4:8)$$

Suppose $\mu$ is an averaging operator, we can write,

$$\mu f(x) = \frac{1}{2}( f(x+1/2) + f(x-1/2) ),$$

$$= \frac{1}{2}( E^{1/2}f(x) + E^{-1/2}f(x) ),$$

or,
$$\mu = \frac{1}{2}( E^{1/2} + E^{-1/2}), \qquad \ldots\ldots\ldots (4:9)$$

$$= \frac{1}{2}(\exp(\frac{1}{2}(\delta x)D) + \exp(-\frac{1}{2}(\delta x)D) ),$$

$$= \mathrm{Cosh}(\frac{1}{2}(\delta x)D ). \qquad \ldots\ldots\ldots\ldots (4:10)$$

From equations 4:7 and 4:9 we obtain,

$$\mu^2 = 1 + \tfrac{1}{4}\delta^2 . \qquad \ldots\ldots\ldots\ldots (4:11)$$

And from equation 4:8 we can write,

$$U = \frac{\mathrm{Sinh}^{-1}(\frac{1}{2}\delta x)}{\frac{1}{2}\delta} \cdot \delta . \qquad \ldots\ldots\ldots\ldots\ldots\ldots (4:12)$$

Taking the nth power of both sides,

$$U^n = \left[\frac{\mathrm{Sinh}^{-1}(\frac{1}{2}\delta)}{\frac{1}{2}\delta}\right]^n . \delta^n . \qquad \ldots\ldots\ldots\ldots\ldots\ldots (4:13)$$

Since $\mathrm{Sinh}^{-1}z/z$ is an even function of z, this expresses $U^n = (\delta x)^n . D^n$ in even powers of $\delta$ if n is even, and in odd powers of $\delta$ if n is odd. The available central differences $\delta^n f_j$ of even-order have integral values of j whereas those of odd-order have (integer $+\frac{1}{2}$) values of j. Hence equation 4:13 can be used to obtain expressions for even-order derivatives at tabular values, or odd-order derivatives half-way between tabular values.

The useful formula for odd-order derivatives at tabular values can be determined from

$$U^n = \left[\frac{1}{\mu}\left\{\frac{\mathrm{Sinh}^{-1}(\frac{1}{2}\delta)}{\frac{1}{2}\delta}\right\}^n\right] . \mu\delta^n . \qquad \ldots\ldots (4:14)$$

Bickley (1948) has given the expansion for $(U/\delta)^n$ as follows:-

$$(U/\delta)^n = 1 - \frac{n\delta^2}{24} + \frac{5n^2 + 22n}{5760} . \delta^4 - \frac{35n^3 + 462n^2 + 1528n}{2903040} . \delta^6 +$$

$$\frac{175n^4+4620n^3+40724n^2+119856n}{1393,459,200}.\ \delta^8 + O(\delta x)^{10} \quad \ldots\ldots(4:15)$$

Therefore, for n=2, it gives,

$$(U/\delta)^2 = \left[1 - \frac{1}{12}\delta^2 + \frac{1}{90}.\delta^4 - \frac{1}{560}.\delta^6\right] + O(\delta x)^8,$$

$$\text{or,}\quad (\delta x)^2\frac{df_o}{dx} = \left[\delta^2 f_o - \frac{1}{12}\delta^4 f_o + \frac{1}{90}\delta^6 f_o - \frac{1}{560}\delta^8 f_o\right] + O(\delta x)^{10}. \quad \ldots\ldots\ldots(4:16)$$

When $n = 4$,

$$(U/\delta)^4 = \left[1 - \frac{1}{6}.\delta^2 + \frac{7}{240}.\delta^4\right] + O(\delta x)^6,$$

$$\text{or,}\quad (\delta x)^4\frac{df_o}{dx} = \left[\delta^4 f_o - \frac{1}{6}\delta^6 f_o + \frac{7}{240}.\delta^8 f_o\right] + O(\delta x)^{10}. \quad \ldots\ldots\ldots(4:17)$$

For $n = 1$, we obtain,

$$(U/\delta) = \left[1 - \frac{1}{24}\delta^2 + \frac{3}{680}.\delta^4 - \frac{5}{7168}.\delta^6 + \frac{35}{294912}.\delta^8\right] + O(\delta x)^{10}.$$

But the first order derivative at the tabular values can be obtained from $U/\mu\delta$ as has been mentioned before. Therefore,

$$U/\mu\delta = \left[\left\{1 - \frac{1}{24}\delta^2 + \frac{3}{680}\delta^4 - \frac{5}{7168}.\delta^6 + \frac{35}{294912}.\delta^8\right\} + O(\delta x)^{10}\right] \cdot \left[1 + \tfrac{1}{4}\delta^2\right]^{-1/2},$$

$$= \left[\left\{1 - \frac{1}{24}\delta^2 + \frac{3}{680}.\delta^4 - \frac{5}{7168}.\delta^6 + \frac{35}{294912}.\delta^8\right\} + O(\delta x)^{10}\right]$$

$$\cdot\left[1 - \frac{1}{8}.\delta^2 + \frac{3}{128}.\delta^4 - \ldots\right],$$

$$= \left[1 - \frac{1}{6}.\delta^2 + \frac{1}{30}.\delta^4 - \frac{1}{140}.\delta^6 + \frac{1}{630}.\delta^8\right] + O(\delta x)^{10},$$

$$\text{or,}\quad (\delta x)\frac{df_o}{dx} = \left[\mu\delta f_o - \frac{1}{6}\mu\delta^3 f_o + \frac{1}{30}\mu\delta^5 f_o - \frac{1}{140}\mu\delta^7 f_o + \frac{1}{630}\mu\delta^9 f_o\right] + O(\delta x)^{11},$$

$$= \tfrac{1}{2}\left[(\delta f_{\frac{1}{2}} + \delta f_{-\frac{1}{2}}) - \frac{1}{6}(\delta^3 f_{\frac{1}{2}} + \delta^3 f_{-\frac{1}{2}}) + \frac{1}{30}(\delta^5 f_{\frac{1}{2}} + \delta^5 f_{-\frac{1}{2}}) - \frac{1}{140}(\delta^7 f_{\frac{1}{2}} + \delta^7 f_{-\frac{1}{2}}) + \frac{1}{630}(\delta^9 f_{\frac{1}{2}} + \delta^9 f_{-\frac{1}{2}})\right] + O(\delta x)^{11},$$

$$= \tfrac{1}{2}\left[(f_1 - f_{-1}) - \frac{1}{6}(\delta^2 f_1 - \delta^2 f_{-1}) + \frac{1}{30}(\delta^4 f_1 - \delta^4 f_{-1}) - \frac{1}{140}(\delta^6 f_1 - \delta^6 f_{-1}) + \frac{1}{630}(\delta^8 f_1 - \delta^8 f_{-1})\right] + O(\delta x)^{10} \quad \ldots(4{:}18)$$

It is sometimes convenient to have differences expressed in terms of the function values from which they

are derived,

$$\delta^2 f_n = f_{n+1} - 2f_n + f_{n-1} ,$$

$$\delta^4 f_n = f_{n+2} - 4f_{n+1} + 6f_n - 4f_{n-1} + f_{n-2} ,$$

$$\delta^6 f_n = f_{n+3} - 6f_{n+2} + 15f_{n+1} - 20f_n + 15f_{n-1} - 6f_{n-2} + f_{n-3},$$

$$\delta^8 f_n = f_{n+4} - 8f_{n+3} + 28f_{n+2} - 56f_{n+1} + 70f_n - 56f_{n-1}$$
$$+ 28f_{n-2} - 8f_{n-3} + f_{n-4} .$$

From equations 4:16, 4:13, and 4:14, by substituting the above values of differences, using formulae for the first, second, and 4th derivatives are obtained, as given below:-

$$f'_o = \frac{1}{\delta x}(0.0035f_{-4} - 0.038f_{-3} + 0.200f_{-2} - 0.800f_{-1}$$
$$+ 0.800f_1 - 0.200f_2 + 0.038f_3 - 0.0035f_4). \quad (4:19)$$

$$f''_o = \frac{1}{(\delta x)^2}(0.011f_{-3} - 0.150f_{-2} + 1.500f_{-1} - 2.722f_o$$
$$+ 1.500f_1 - 0.150f_2 + 0.011f_3). \quad .....(4:20)$$

$$f^{IV}_o = \frac{1}{(\delta x)^4}(0.029f_{-4} - 0.400f_{-3} + 2.817f_{-2} - 8.133f_{-1}$$
$$+ 11.375f_o - 8.133f_1 + 2.817f_2 - 0.400f_3$$
$$+ 0.029f_4). \quad .....(4:21)$$

The derivatives can thus be obtained directly from a tabulation of the ordinates of the curve.

But it is advisable that for better results in obtaining the higher-order derivatives of a curve, the calculation should be carried out step by step. For example, if a second derivative is wanted, the first derivative is first determined; its values then are smoothed. Once again, the formula for the first derivative is applied to the smoothed values. This will give better approximated values of second derivatives than can be obtained directly from the equation for the second derivative (equation 4:20).

## 4:4 Theoretical Subjective Luminance Distributions.

In order to be able to predict the luminance distribution seen on each photographic plate, various mathematical models were applied to the physical luminance distribution on the plate, as recorded by the microphotometer. With the same computer programmes used in chapter III (see also Appendix B) the predicted luminance distributions were calculated. The results are shown in figures 4:17 to 4:26. The second derivative of the luminance distribution of the object with respect to distance, as calculated from the method mentioned in the last section, using the National Elliot 803A computer, is also shown on each figure.

The model of Hartline and Ratliff (eqn. 2:16) is an interesting one in that it is response-dependent and does not give a dark band on the distribution due to an

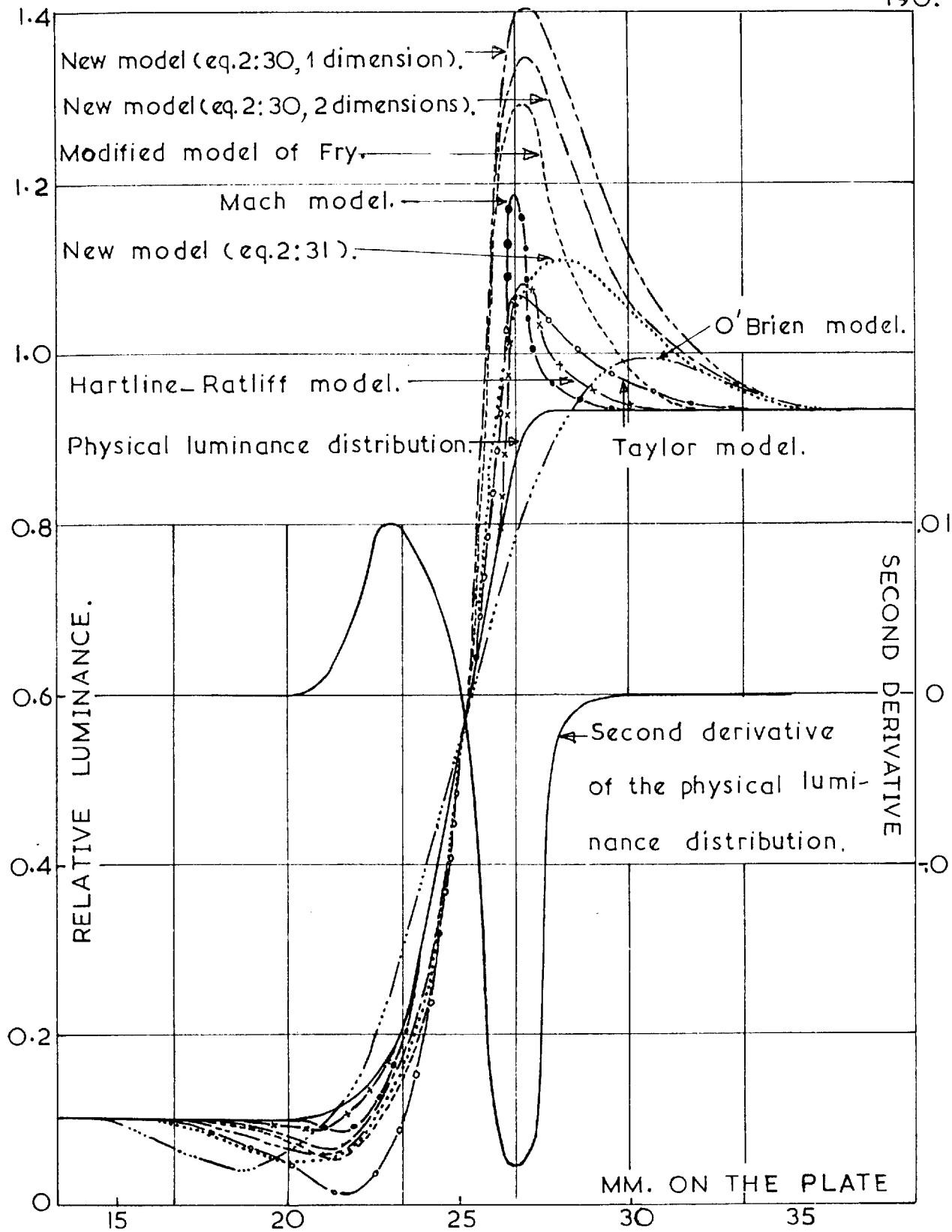



Fig. 4:17. Predicted luminance distributions on plate IA.

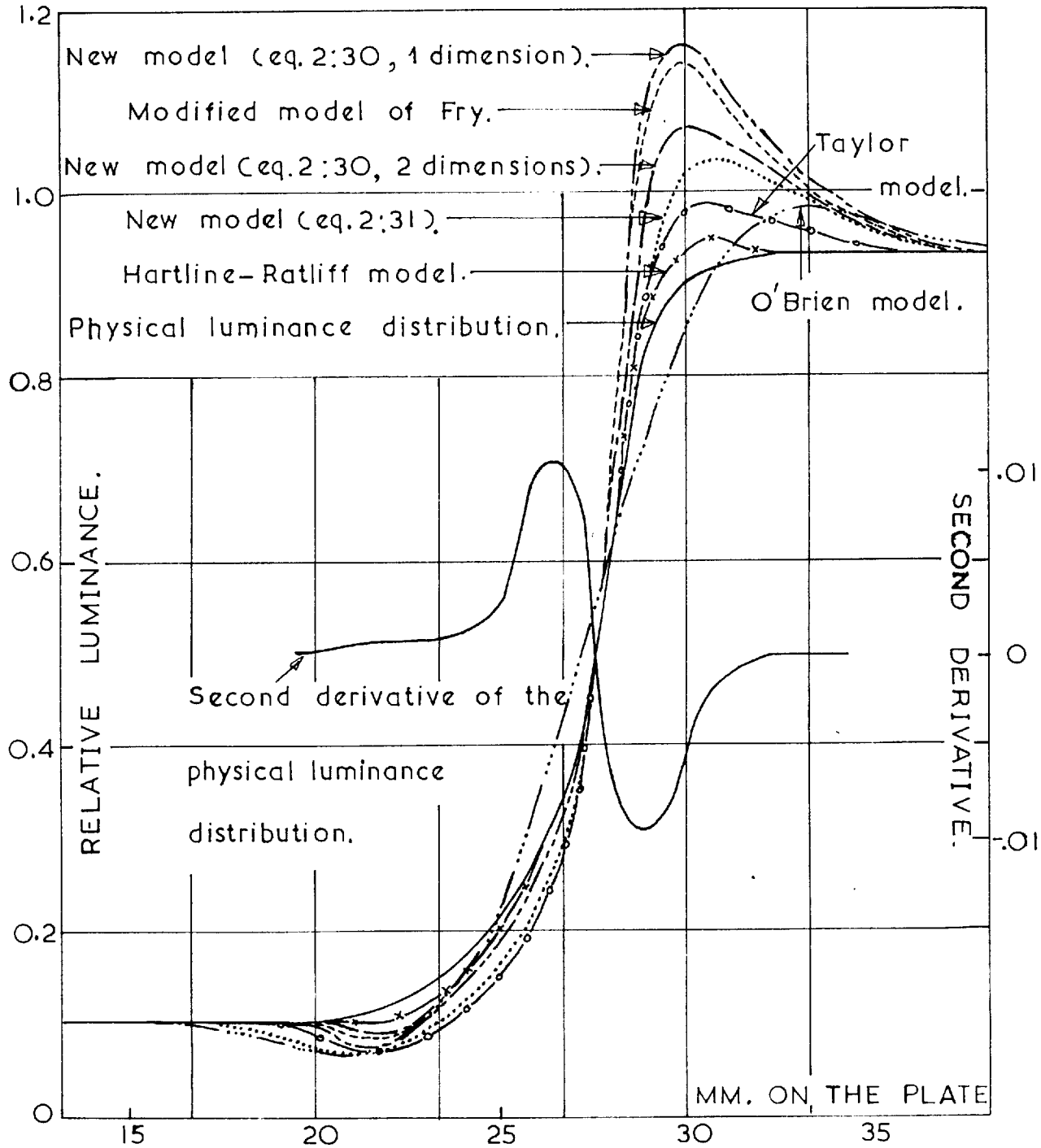



Fig. 4:18. Predicted luminance distributions on plate 2A.

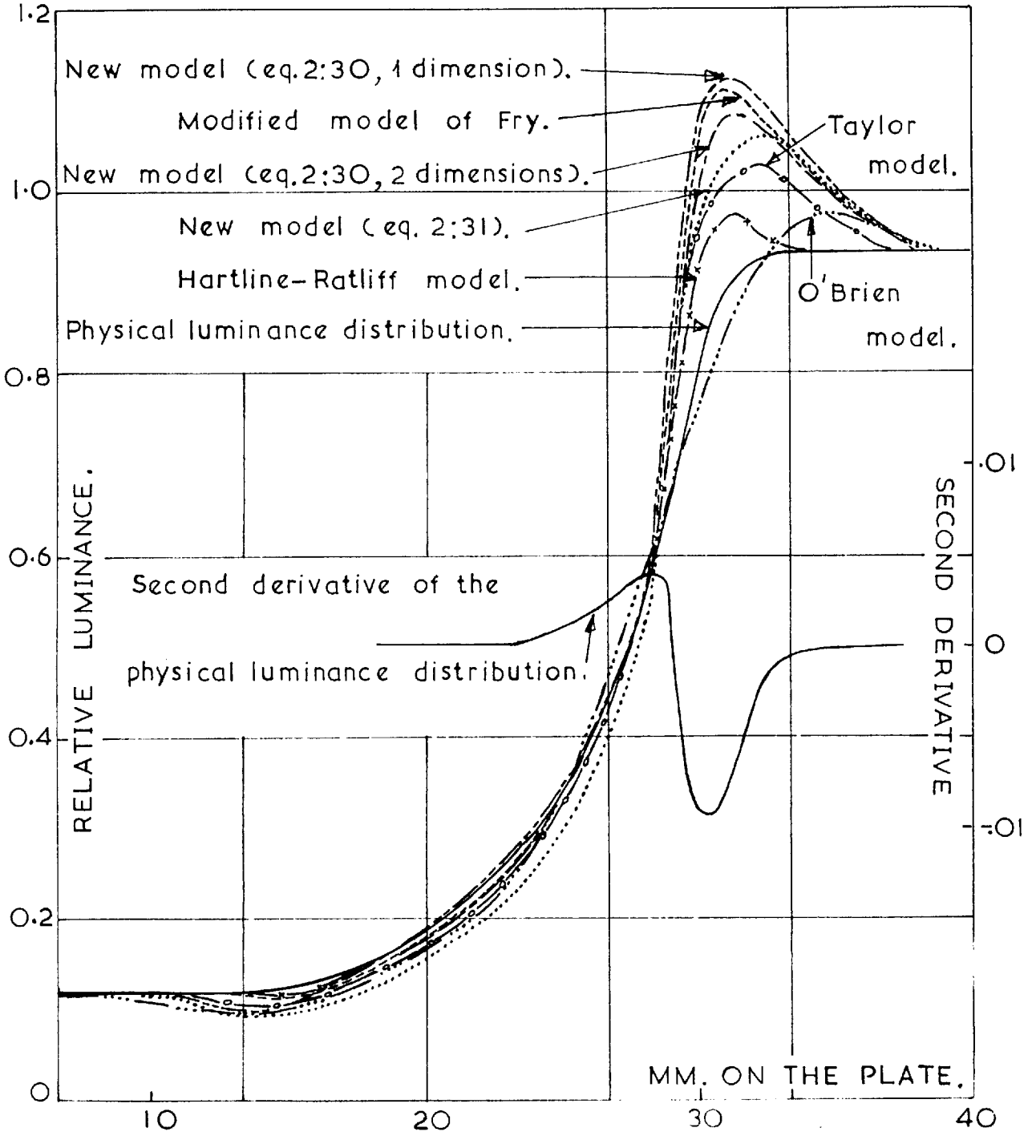



Fig. 4:19. Predicted luminance distributions on plate 3A.

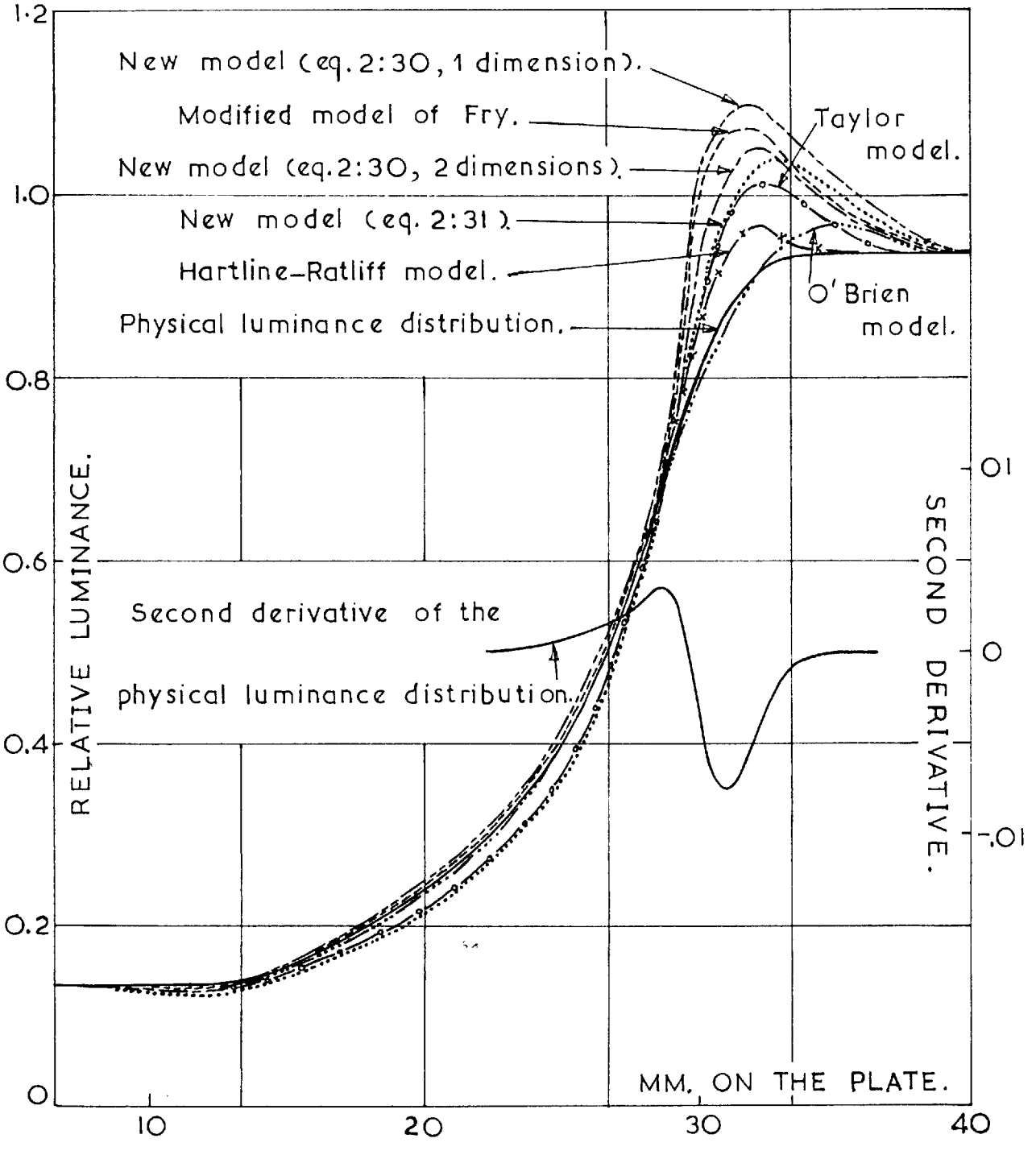



Fig. 4:20. Predicted luminance distributions on plate 4A.

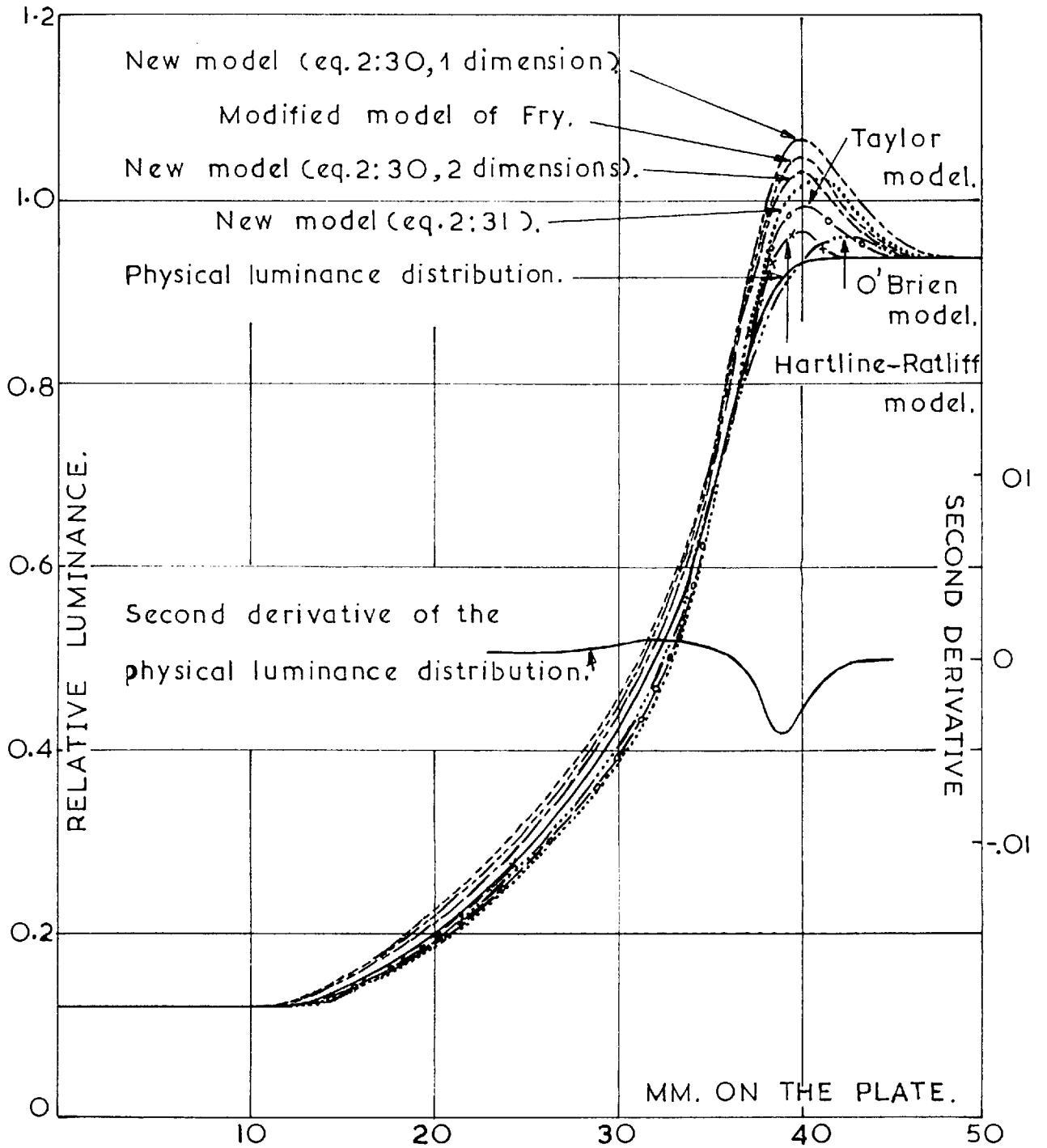



Fig. 4:21. Predicted luminance distributions on plate 5A.

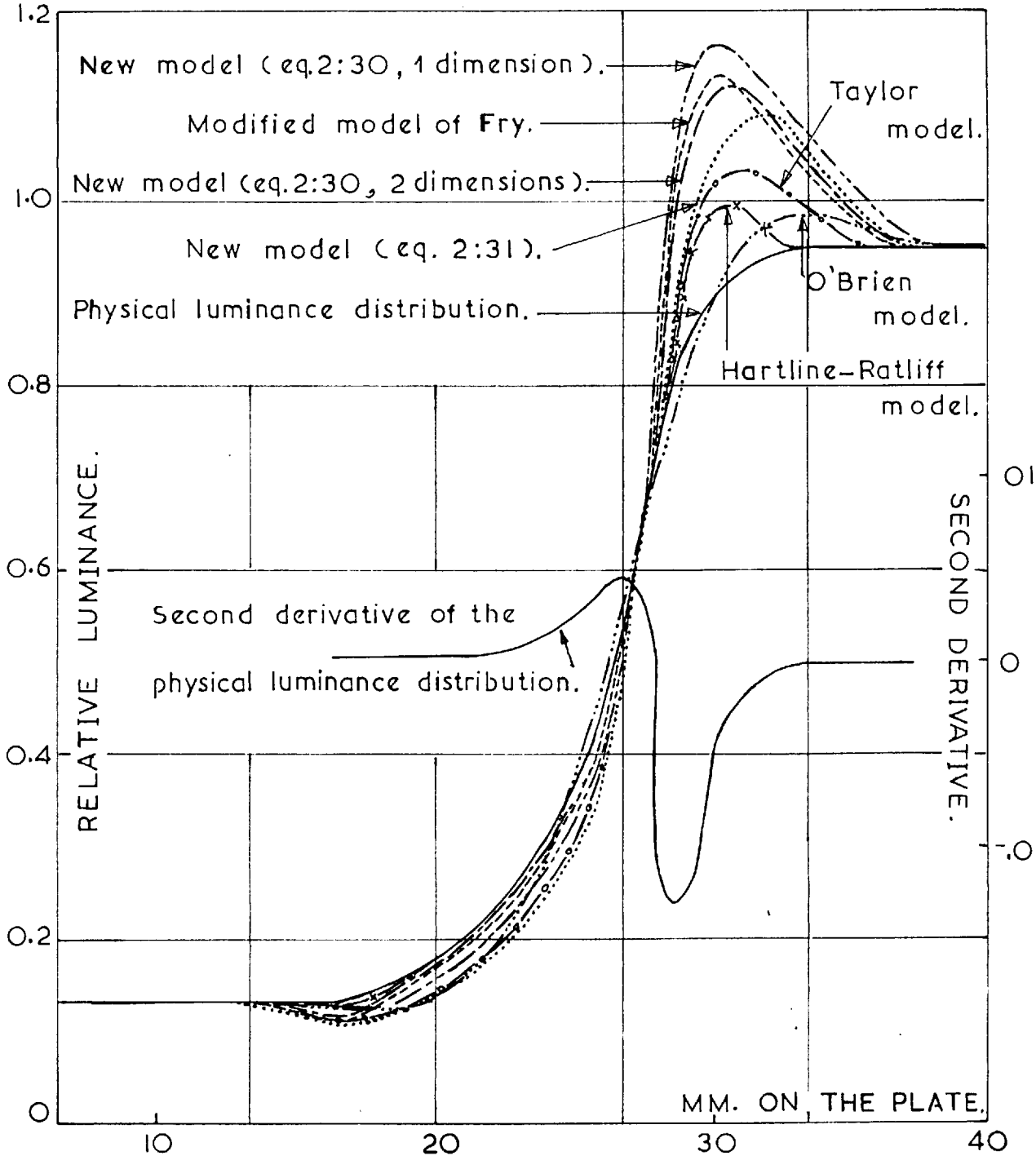



Fig. 4:22. Predicted luminance distributions on plate 1B.

(74 % contrast).

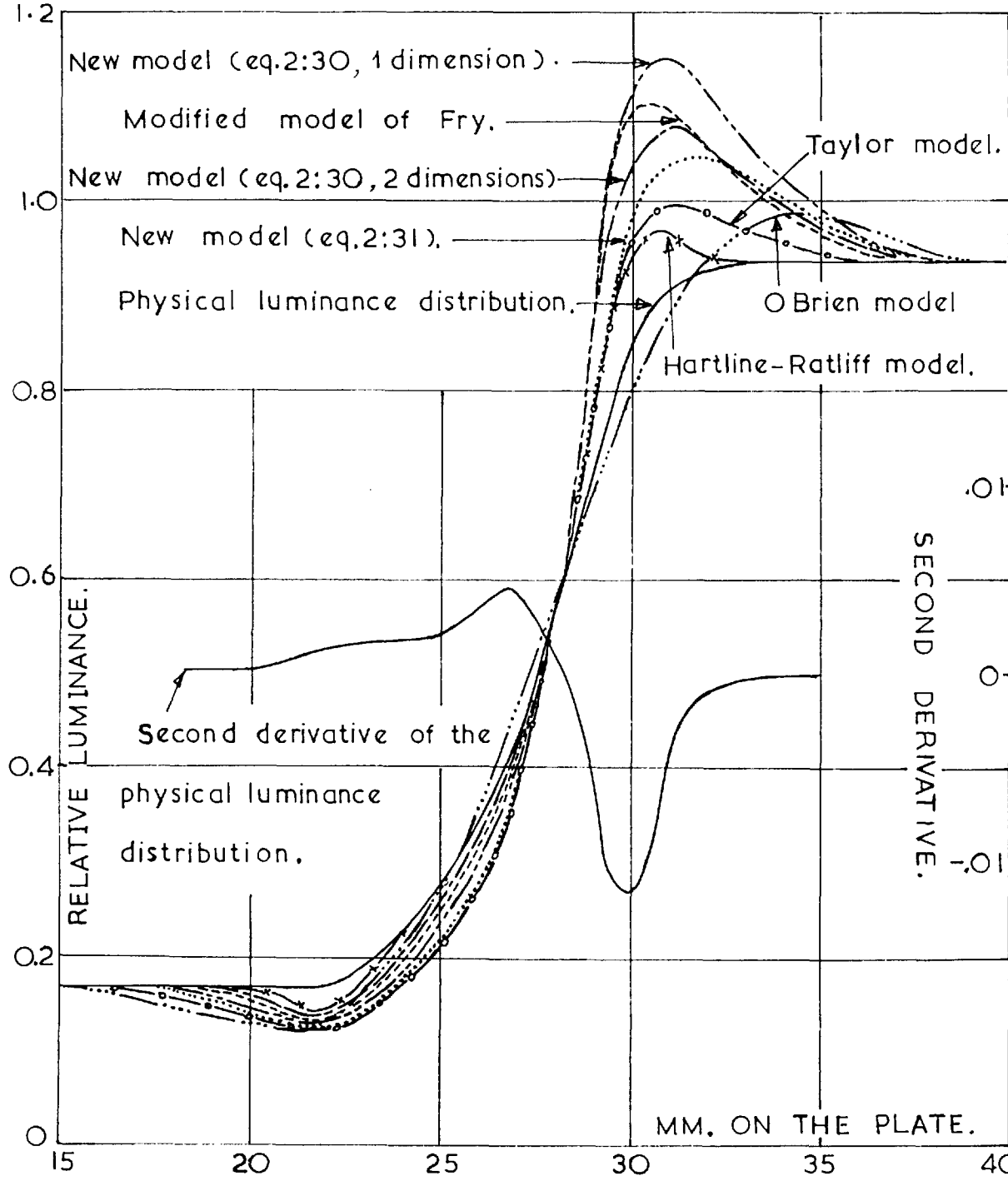



Fig. 4:23. Predicted subjective luminance distributions on plate 2B (69 % contrast).

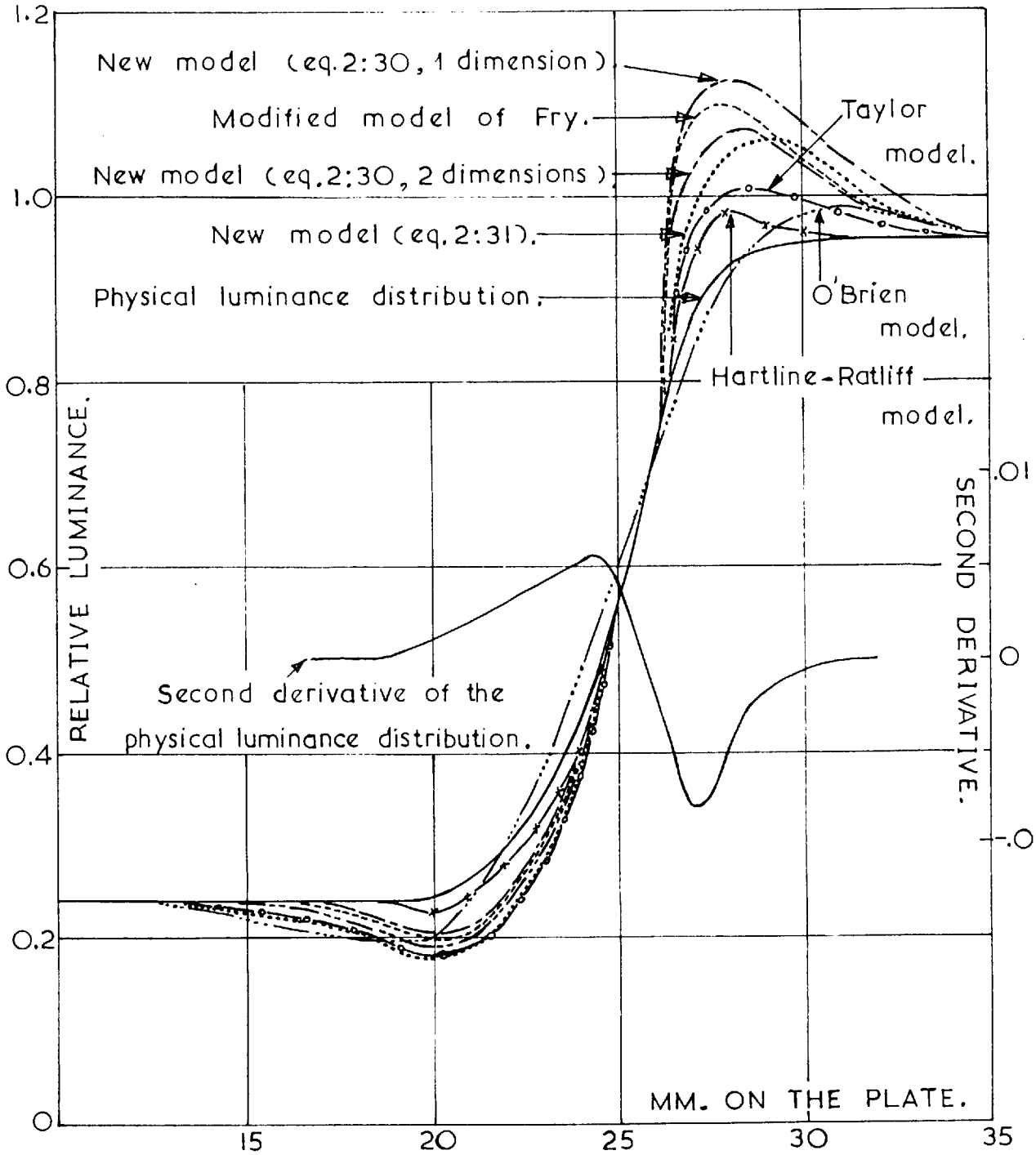



Fig. 4:24. Predicted subjective luminance distributions on plate 3B (60 % contrast).

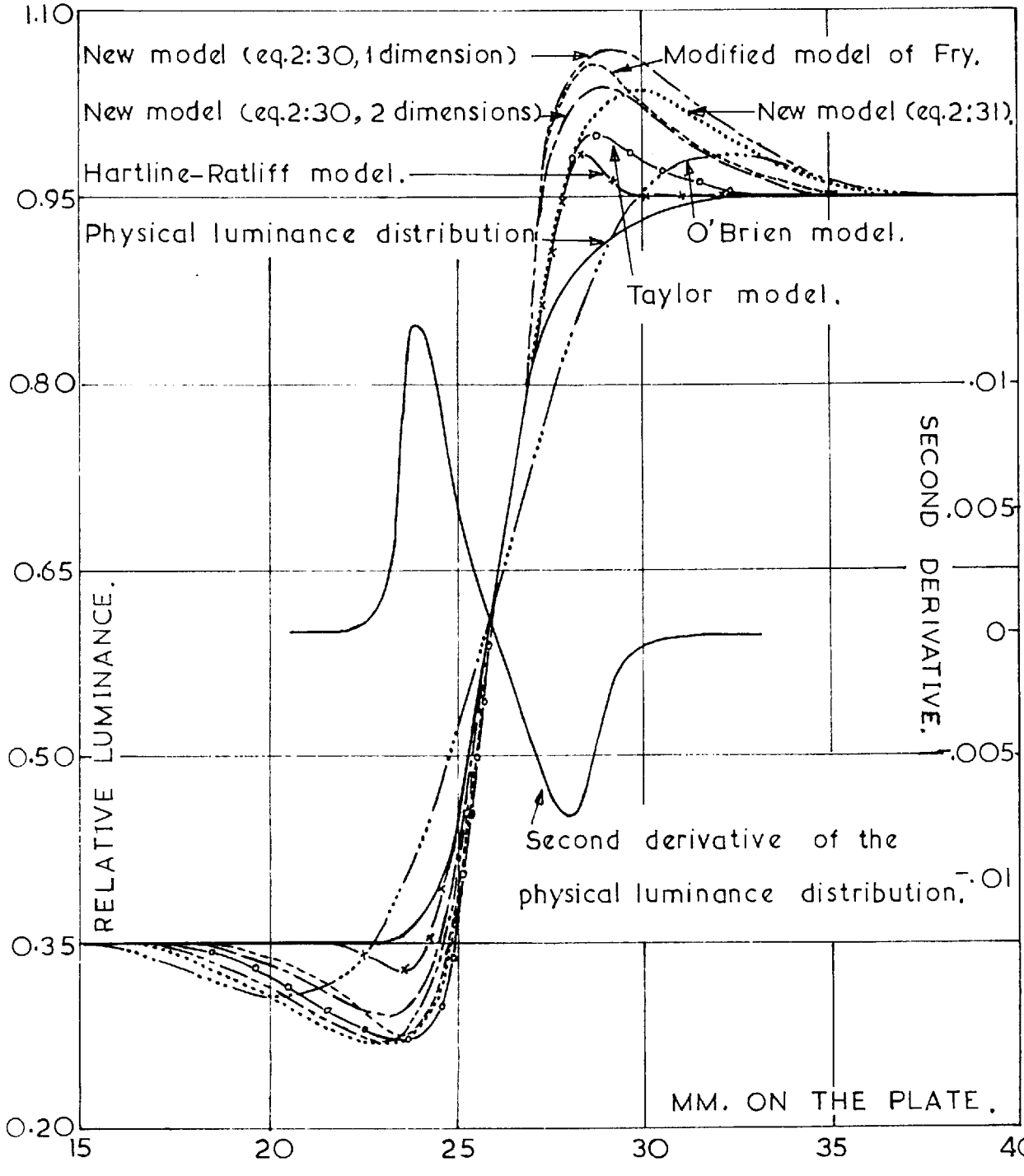



Fig. 4:25. Predicted subjective luminance distribution on plate 4B (46 % contrast).

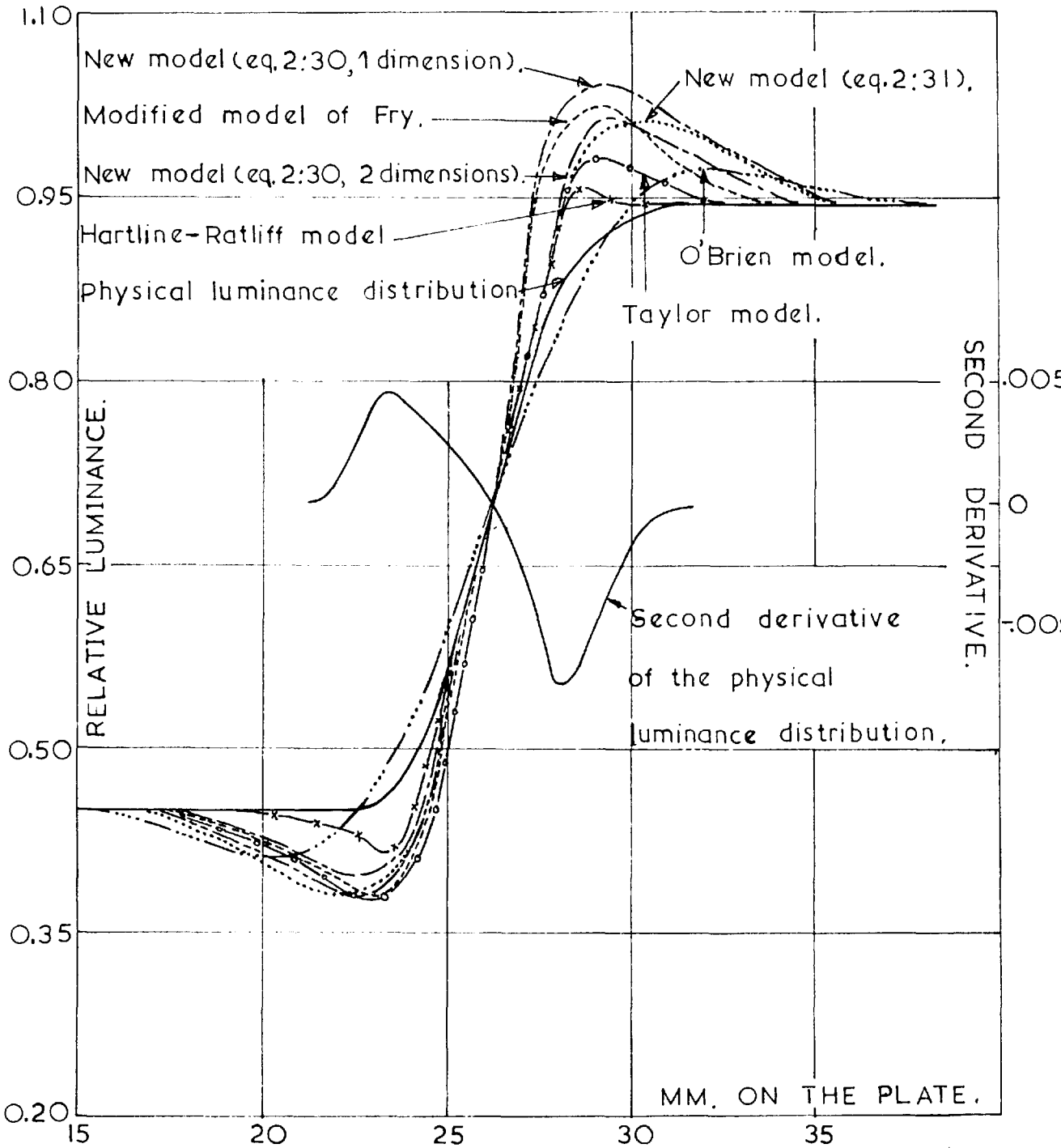



Fig. 4:26. Predicted subjective luminance distribution on plate 5B (36 % contrast).

image of an abrupt edge on the retina (see figure 3:14) even though many different values of the parameters were employed. However, with the luminance distribution on these plates, a dark band was obtained when the slope of the luminance gradient was sufficiently steep. On plate 4A, the dark band predicted by this model is very small and it disappeared completely in plate 5A where the slope becomes shallower. The proposed new model with the normalized function (eqn. 2:31) is another model which fails to show dark band when it is applied to the luminance distribution of the image of a sharp transition edge (see figure 3:18). It seems to give some evidence of the dark bands when employed with the luminance distributions on the plates depicted in figures 4:17 to 4:26. The reasons for obtaining the dark bands from these two models on these luminance distributions possibly are that, 1) the lower luminance levels of the plates were higher than that belonging to the edge image, and, 2) the flexions on their luminance distribution curves had smaller radii of curvature than those of the image of a sharp edge.

From figures4:17 to 4:26, as far as the non-linear models are concerned, the following conclusions can be made:- 1) The luminance distribution with a steep gradient (plates 1A, 4B and 5B) gives the maximum and the minimum of the second derivatives at the same positions as the predicted

dark and bright bands respectively.

2) The bright bands given by most of the models on the luminance distribution with a shallower gradient occur approximately at the minimum of the second derivative of the object luminance distribution, but the dark bands are slightly displaced into the dark area with respect to the maximum of the second derivative.

3) Most of the models predict the occurrence of the bands at about the same positions.

4) The luminance distributions predicted by the model of Hartline and Ratliff and Mach's model give very narrow Mach bands when compared to the others.

5) From the first set of the plates(figs.4:17 to 4:21),the brightness of the predicted band becomes smaller when the radius of curvature of the flexion on the luminance distribution increases. No dark band has been predicted on plate 5A.

6) The second set of the plates (figures 4:22 to 4:26), of which the contrast has been decreased by increasing the lower luminance level of the pattern, shows a small increase in the amplitude of the dark band when the contrast decreases from 74% to 64% ; when the contrast decreases from 46% to 36% the amplitude of the dark band tends to be constant.

The linear models all predict different positions and widths for the Mach bands, and these are also different from those given by the non-linear models.

# CHAPTER V

## AN EXPERIMENTAL STUDY OF GRADED LUMINANCE PROFILES.

### 5:1 Introduction.

Using the photographic plates with known density distributions, prepared as described in chapter IV, the characteristics of the bands occurring on graded luminance objects can be observed. The purpose of the work described in this chapter was to observe the effect on the Mach bands when varying, 1) the luminance gradient, 2) the luminance level, 3)the contrast, and, 4) the size of the illuminated area on the retina. The influences of some of these factors on the Mach phenomena have been discussed by other workers in different connections, but the numerical data are not accurate and detailed enough for the present purpose, i.e; studying mathematical models of the Mach effect. The visibility of the Mach bands was studied by Ercoles and Fiorentini (1959) as a function of luminance; only the luminance thresholds for dark and bright bands were measured. McCollough (1955) measured the width of the bright band as a function of the luminance of the observed field, but the brightness of the band was not included. The experimental results showed by Lowry and De Palma (1961) were quite extensive, but some details, such as the diameter of the eye pupil and the distance between the object and the observer, were not

given. The effects of luminance level and contrast on the Mach effect were also studied by Ronchi, Bittini and Adachi (1963). The luminance and the contrast thresholds of the sharpness of the contour border were measured. The border between two different zones of luminances was said to be sharp when two thin Mach bands were seen to delimit the graded zone.

In the present experiments the physical luminance distributions in the objects were obtained from microphotometer traces to determine transmissions and S.E.I. photometer readings to determine the absolute luminance levels. Together with the geometrical conditions of measurement, this makes it possible to calculate the illumination distribution on the retina. The observed visual distribution then can be compared with the calculated physical one.

The apparatus for observing the effect on photographic plates must be arranged such that the luminance on the photographic plate and the angle subtended by the plate on the eye can be easily varied. Visual photometric matching is needed for measuring the brightness of a band. The system which was used to produce the comparison slit as described in chapter III was found to be usable with modifications for the present work. A telescope of unit magnification was used in the viewing system. The angular magnification M of a telescope may be defined as,

M= Angle subtended by the image as seen through the instrument
Angle subtended by the object as seen by unaided eye

Therefore, when a telescope of unit magnification is used to view an object of dimension $\eta$ at a distance D from the observer, the object subtends an angle of $\sin^{-1}(\eta/D)$ (where $\eta$ and D are in the same units), or $\eta/D$ radians when the angle is small. That is the size of the retinal image is

$$\eta' = \frac{\eta}{(n' D)} . f ,$$

where n' is the refractive index of the aqueous and f is the front focal length of the eye. When the same object is viewed from various distances, the size of the retinal image will change, i.e ; the number of receptor units involved in the mechanism of perception is changed.

The entrance pupil of a telescope is determined by the aperture of the telescope. Knowing that the exit pupil is the image of the objective formed by the eyepiece, the size and the plane of the exit pupil can be evaluated. For a unit magnification telescope, the exit pupil will be found outside the telescope at some distance away from the principal plane of the eyepiece.This distance equals the distance between the objective (i.e: entrance pupil plane) and the principal plane of the eyepiece. The diameter of the exit pupil will then equal that of the entrance pupil.

5:2 The Apparatus.

Figures 5:1a and b show the arrangement which was set up for measuring the widths, positions and brightnesses of the bands seen on incoherently illuminated gradient edges. The photographic plate M which served as the object was incoherently illuminated with an illuminating system from behind. Light, which passed through the plate M, an objective lens N and a glass block unit O, formed an image coplanar with a pointer at P, which was used for taking measurements. The lower half of the field of view in that plane was covered with black paper, in the centre of which a narrow vertical strip of white paper was fixed. Looking through an eyepiece Q an image was seen of the same size as the object.

The viewing system was in fact a telescope of unit magnification built up from 3 thin lenses, one for the objective(N) and two for the eyepiece(Q). The diameter of each lens was 3.4 cms. The magnification of a telescope may be defined as,

$$M = \frac{\text{focal length of objective } (f_{OG})}{\text{focal length of eyepiece } (f_{EP})}.$$

The power of the objective lens in the present work was +5 dioptres (or 20 cms. focal length). In order to get a unit magnification telescope, the focal length of the eyepiece

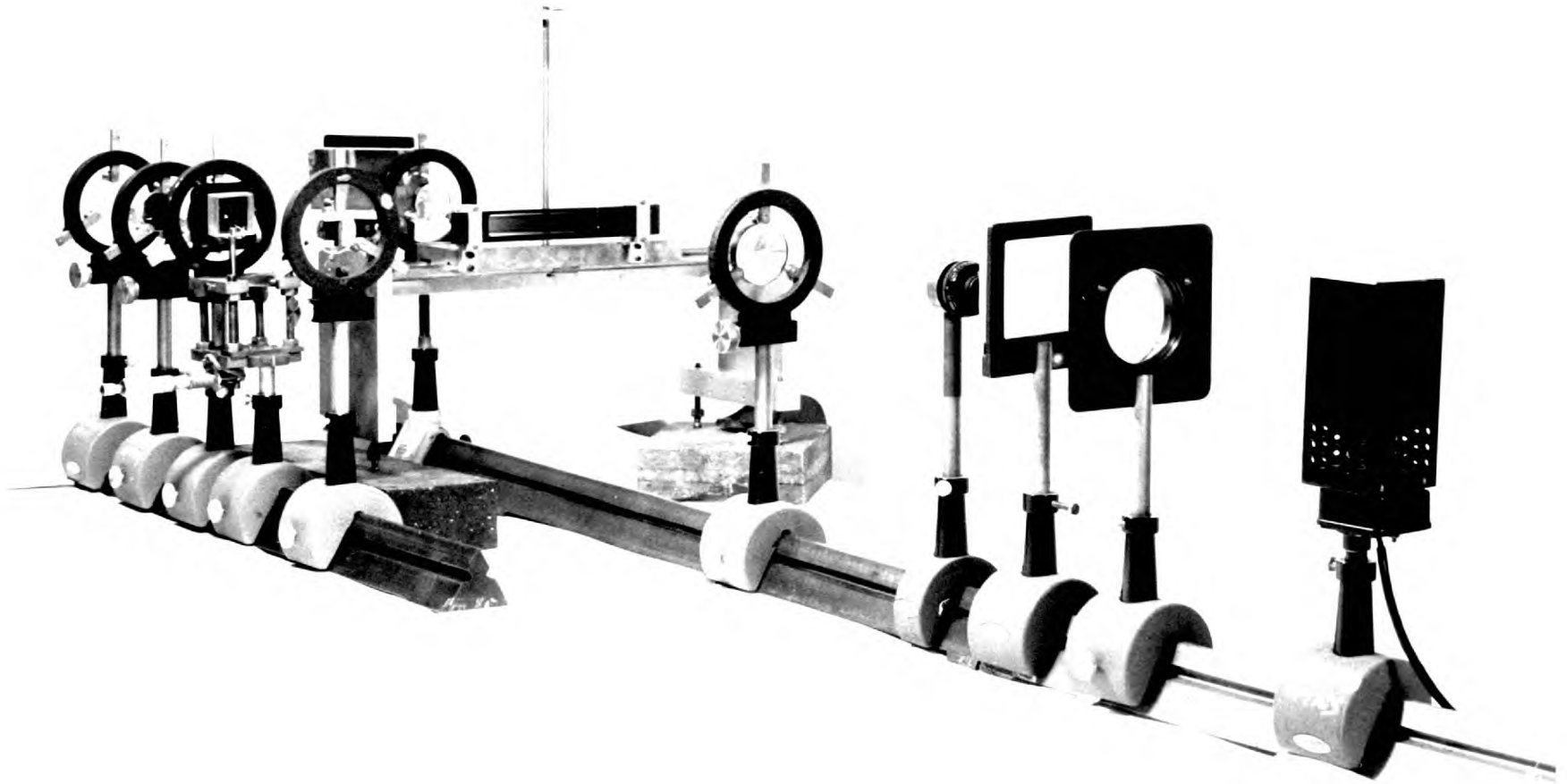


Fig. 5:1a. Apparatus for measuring visual Mach bands on graded luminance profiles.

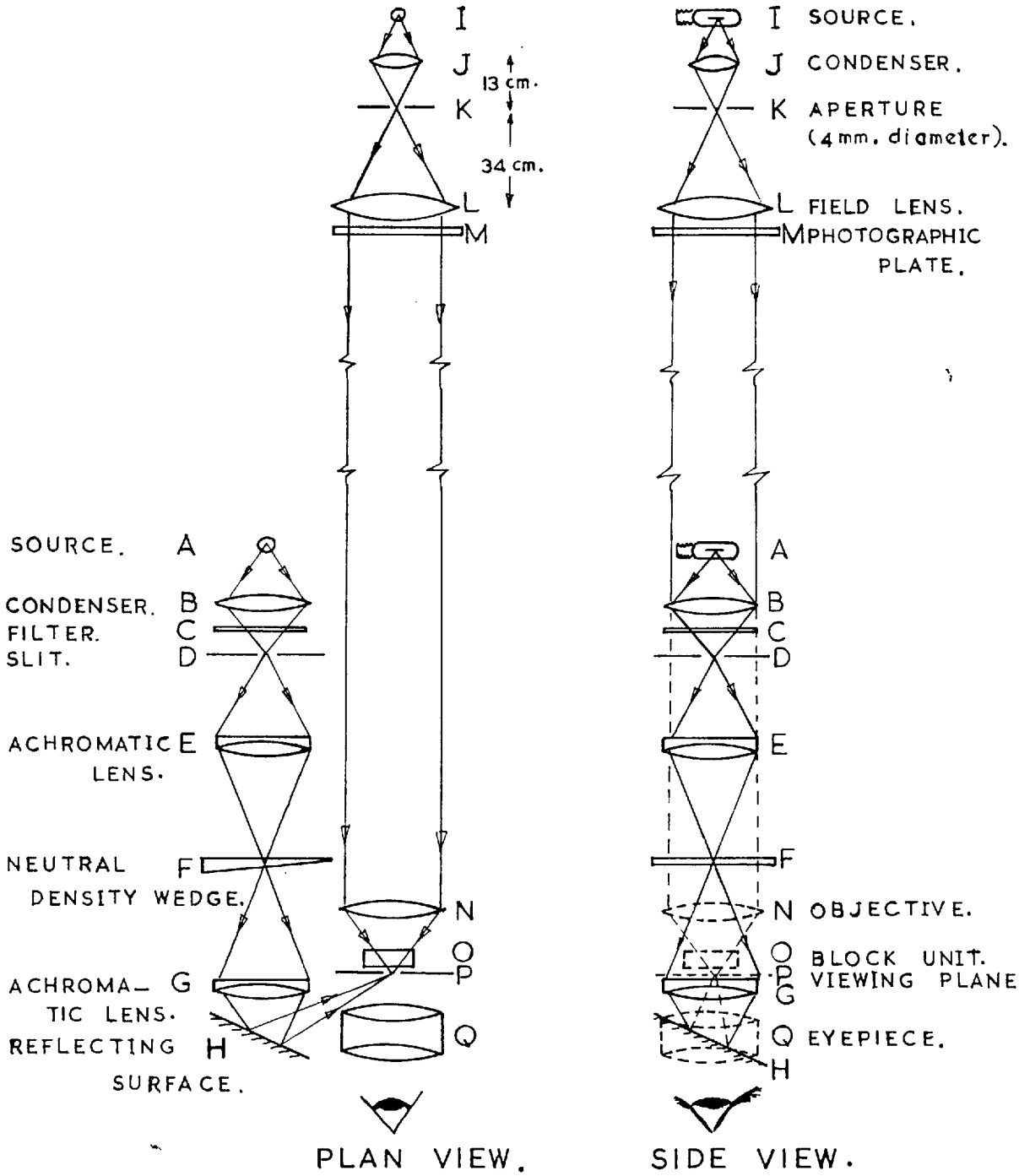



Fig. 5:1b. Apparatus for measuring visual Mach bands on graded luminance profiles.

had also to be 20 cms. The eyepiece was built up from two thin lenses, each of power +3 dioptres. The formulae for two thin lenses separated by a distance d (see figure 5:2) are as follows:-

The equivalent focal length, $f_E = \frac{f_1 \times f_2}{f_1 + f_2 - d}$, ...(5:1)

The back focal length, $f_B = \frac{f_2(f_1 - d)}{f_2 + f_1 - d}$, .....(5:2)

where $f_1$ and $f_2$ are the focal lengths of the lenses. From equation 5:1, in order to obtain an equivalent lens of power +5 dioptres from two thin lenses of powers +3 dioptres each, the separation (d) between the two lenses must be 11.1 cms. And from equation 5:2, the distance $f_B$ will be 13.3 cms. Therefore, a telescope was built as shown in figure 5:3. The magnification of the telescope was checked by a direct observation method, i.e ; one eye looked through the telescope and at the same time the other eye looked directly onto a scale which was about 10 yards away, the sizes were then compared, and found to ~~be~~ equal. Thus, the magnification of the telescope was unity.

The block unit(O) which was placed between the objective and the first image plane of the telescope (see figure 5:1) was used for shifting the image across a horizontal plane perpendicular to the line of sight so that the

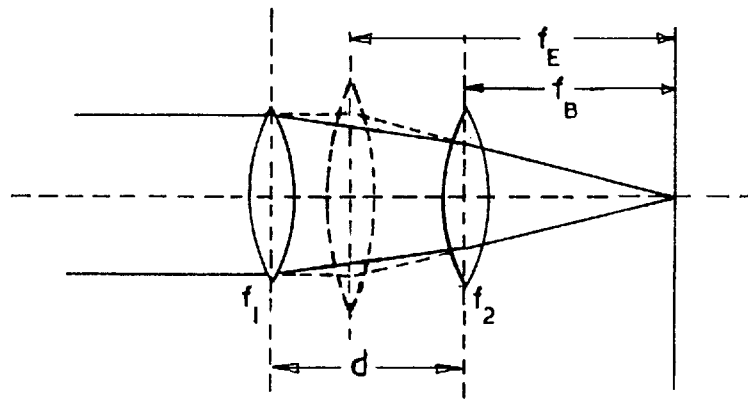



Fig. 5:2. Two separate thin lenses.

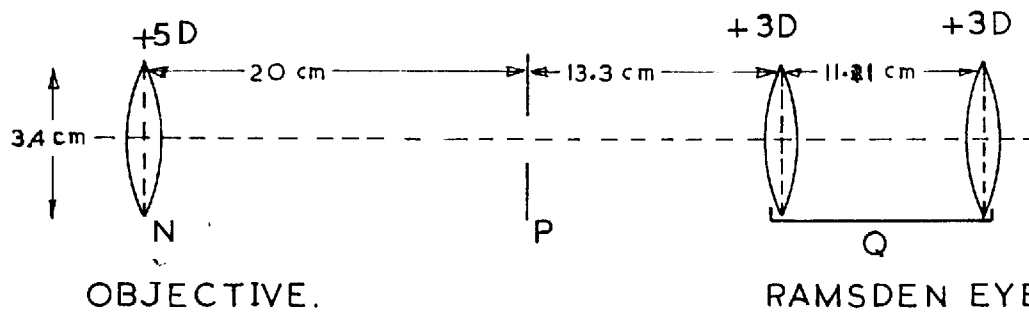



Fig. 5:3. Telescope used in figure 5:1.

widths and positions of the bands could be measured and the photometric matchings could be easily done. The rotating of the block was controlled through a lever by a micrometer head. Good linearity of the image displacement with respect to the rotation of the micrometer was desirable. The two faces of the block which were perpendicular to the optical axis were required to be adequately flat and parallel and the material of the block was to be homogeneous. These factors are important because they can cause errors in the displacement of the image. This block unit was the one used by Charman in 1961. He had tested the homogeneity of the glass and the optical flatness of the faces with a Twyman and Green interferometer and the parallelism of the faces was verified with an autocollimator.It was found that the opposite faces were parallel to within 0.2 second of arc and the optical thickness of the block was constant to within $\lambda/4$ over the full area of the faces. Thus, the aberrations introduced by the insertation of the micrometer block unit into the system was within the Rayleigh tolerance , i.e ; the aberrated wavefront after passing through the objective and the block unit departed by much less than $\lambda/4$ from a reference sphere centred at the Gaussian image point.

Figure 5:4 shows the calibration of the displacement in the final image plane with respect to the rotation

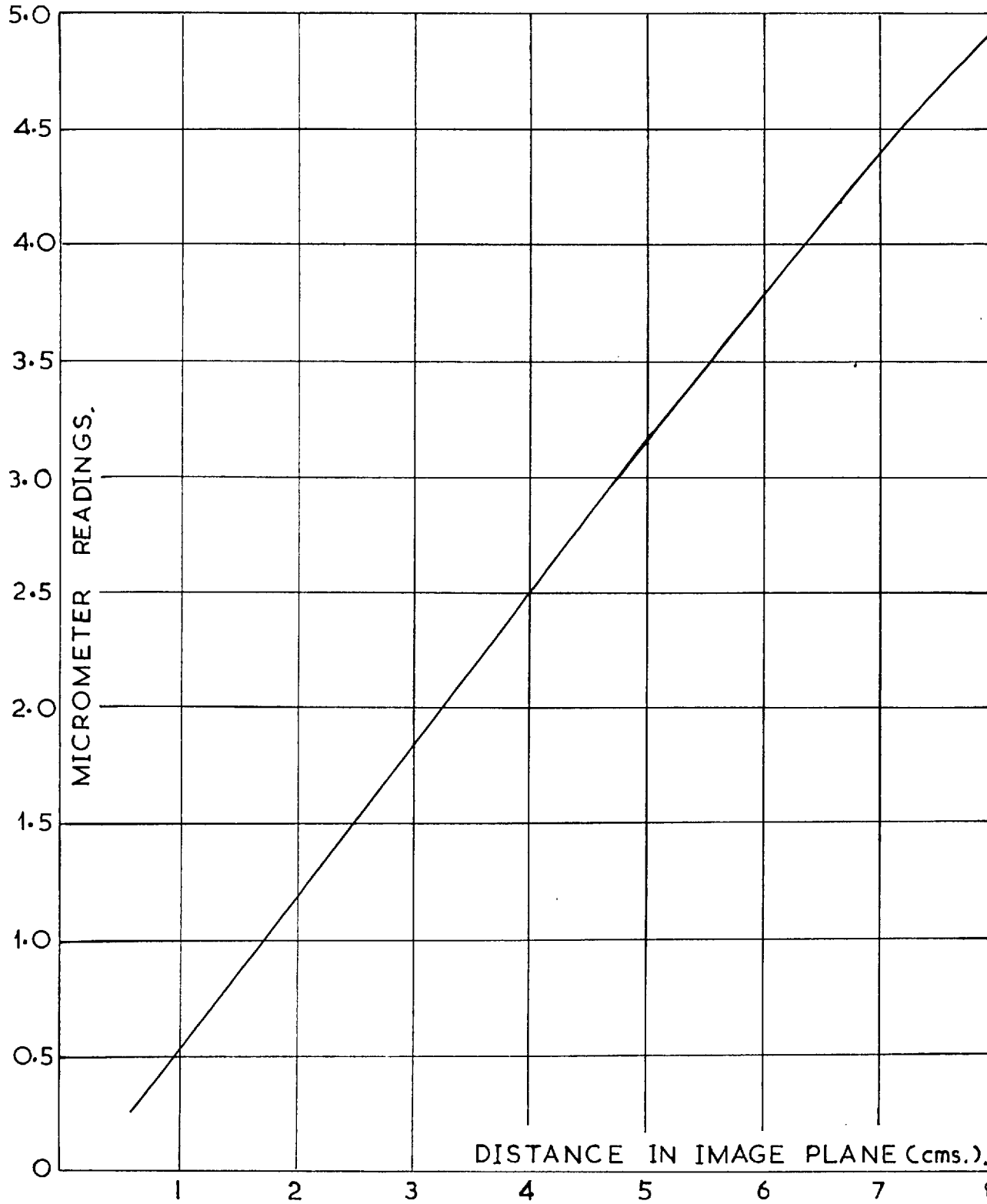



Fig. 5:4. The block unit calibration ( distance between the final image and the observer = 522 cms.).

of the block unit. The measurements were made when the image was 5.22 metres away from the observer. A linear increase was obtained within a certain range (about 0 to 3 units on the micrometer scale). All the measurements in this chapter, therefore,were carried out using this range of the micrometer scale.

In the illuminating system of figure 5:1 a high pressure mercury lamp (I) was used as a light source. A condenser (J) focussed light on an aperture K of which the diameter was about 4 millimetres. Light passing through the aperture K filled the whole aperture of a field lens L which was 34 cms. away. The photographic plate M was put after lens L.

We now examine the question of the extent to which the illumination of the plate can be assumed to be incoherent. In the first chapter it was noted that the mode of illumination is governed by the ratio S of the numerical aperture of the condenser to that of the objective. Incoherent, partially coherent, and coherent illumination is obtained when the value of this ratio is respectively infinity(nominally), finite,and zero. This method of specifying the coherence of the illumination is useful in systems where the object is placed between a condenser and an objective, as in the microscope. For the system in figure 5:1

the effective numerical aperture of the condenser is equal to the radius of the aperture K divided by the focal length of the field lens (condenser) L, which is 2/340 , $\simeq$ 0.006. The numerical aperture of the objective is equal to the radius of the objective N (17 mms.) divided by the distance to the object (5220 mms.), i.e ; about 0.003. Thus the ratio S is approximately 2 and this can be taken as near enough incoherent illumination. It is assumed here that the aperture K is incoherently illuminated, which is near enough true for the large condenser used.

The system on the left of figure 5:1, by means of which the comparison slit was produced for making the visual photometric matching, was the same as that used in chapter III, but the reflecting surface in the present system was fixed; it produced an image on a strip of white paper which was placed vertically at the centre of the black paper in the first image plane of the system on the right. Each region of the image of which the brightness was measured was brought in line with this white strip, for the greatest accuracy in brightness matching.

## 5:3 Measurements and Results.

Each photographic plate was observed with an unrestricted eye pupil, i.e ; without an artificial pupil.

Since the aperture of the objective of the telescope was 3.4 cms., the exit pupil of the system was then big enough to cover the whole area of the pupil. The luminance of the bright area of the plate was again measured with the S.E.I. photometer. The size of the eye pupil could be obtained from the table of pupil diameters at various luminances tabulated by LeGrand in 1957, and it could also be measured with the aid of a semi-reflecting surface and a scale as shown in figure 5:5. While light from the system under examination is shining upon the eye, and while the observer is looking through the semi-reflecting surface R, the image of the eye is seen on the scale S; thus the size of the eye pupil can be read off. In the present work, the measurement of the eye pupil size was done by the above-mentioned method. The eye pupil was found to be 3.0 mms. in diameter. It has been noticed that, in this method, the pupil of a brown eye is more difficult to measure than that of a blue eye. The size of the eye pupil was then checked by Le Grand's table. The luminance of the light from the system measured by the photometer was 343 cd./$m^2$ ; according to the table a pupil diameter of about 2.8 mms. would be obtained.

The widths and positions of the bands seen on the plates were measured and the brightnesses were visually matched with those of the comparison slit. Each distribution pattern was obtained from the results of 10 sets of

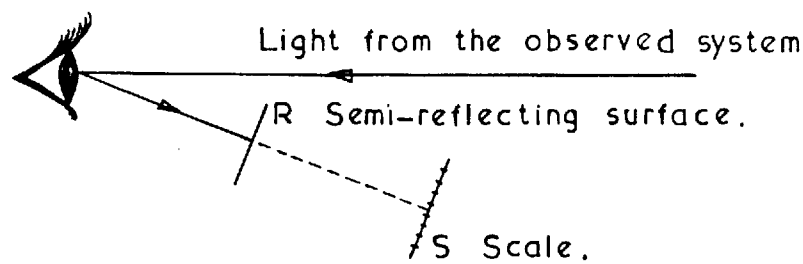



Fig. 5:5. Direct measurement of the eye pupil size.

measurements. Measurements for the widths and positions of the bands were made starting from the outer end of the dark region, and, moving across towards the dark band, and so on, until the far border of the bright band in the bright region was reached. The results were as follows:-

1). Luminance gradient. The first set(A) of five plates of which luminances were shown on figure 4:9 were observed from a constant distance. The distance from the final image plate to the eye was 5.22 metres. The luminance on the uniform bright region of each plate measured with the S.E.I. photometer was 343 candelas per square metre. With the eye pupil of 3.0 millimetres, which corresponded to this luminance level, the retinal illumination would be about 2425 trolands. The Mach bands seen on each plate were measured. The results are shown in figures 5:6 to 5:10 where the second derivative curves and three of the predicted luminance distributions are also drawn so that the comparisons can be easily made. These three predicted luminance distributions were obtained from the last chapter where various models were applied to luminance distributions of produced gradients on ten photographic plates. It was also mentioned in the same chapter that with an eye pupil of 3.0 mms. and a distance between the observer and the plate of 5.4 metres, the retinal image which was obtained by the convolution of the

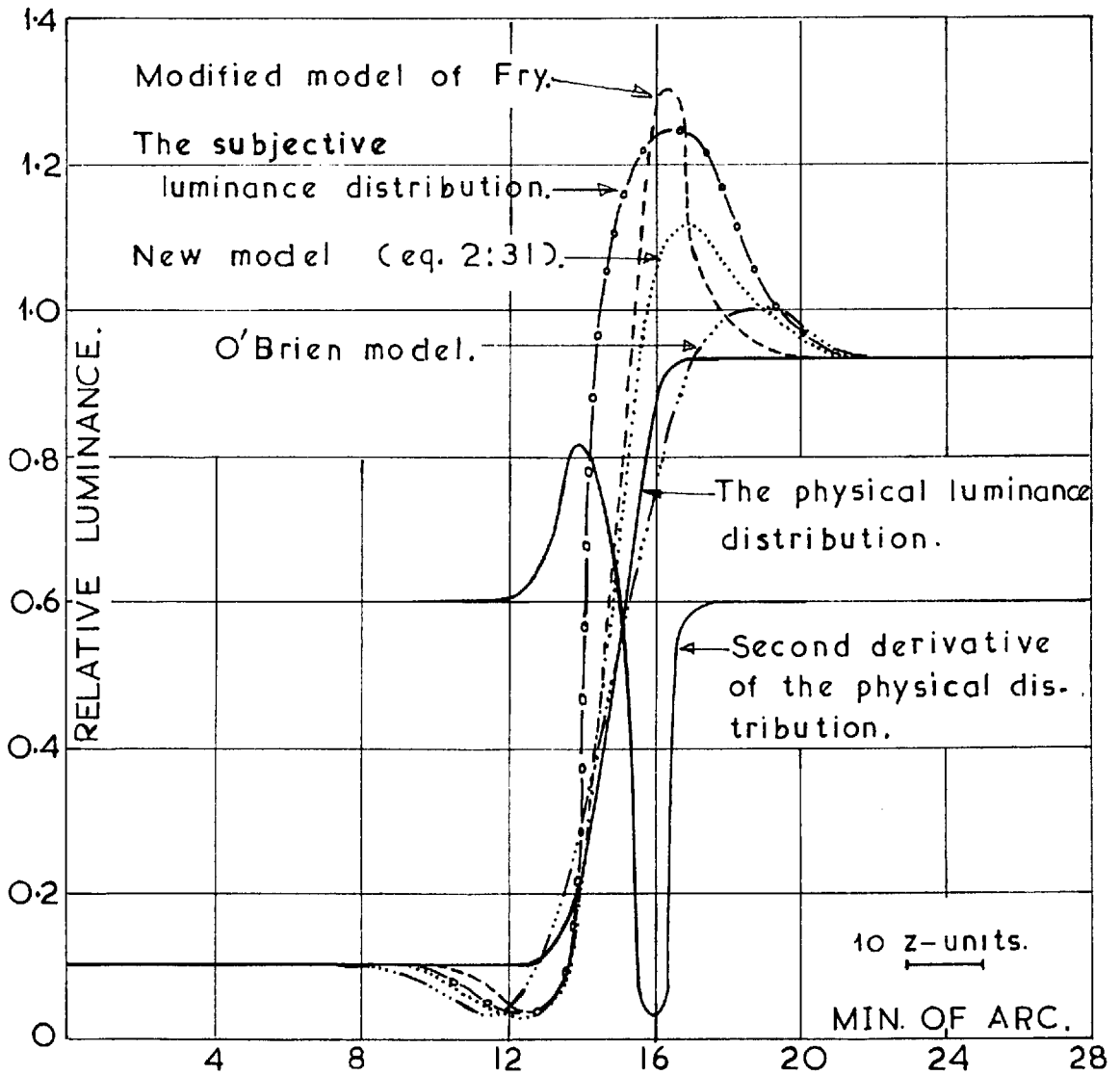



Fig. 5:6. The subjective luminance distribution seen on plate 1A, compared with some of the mathematical models.

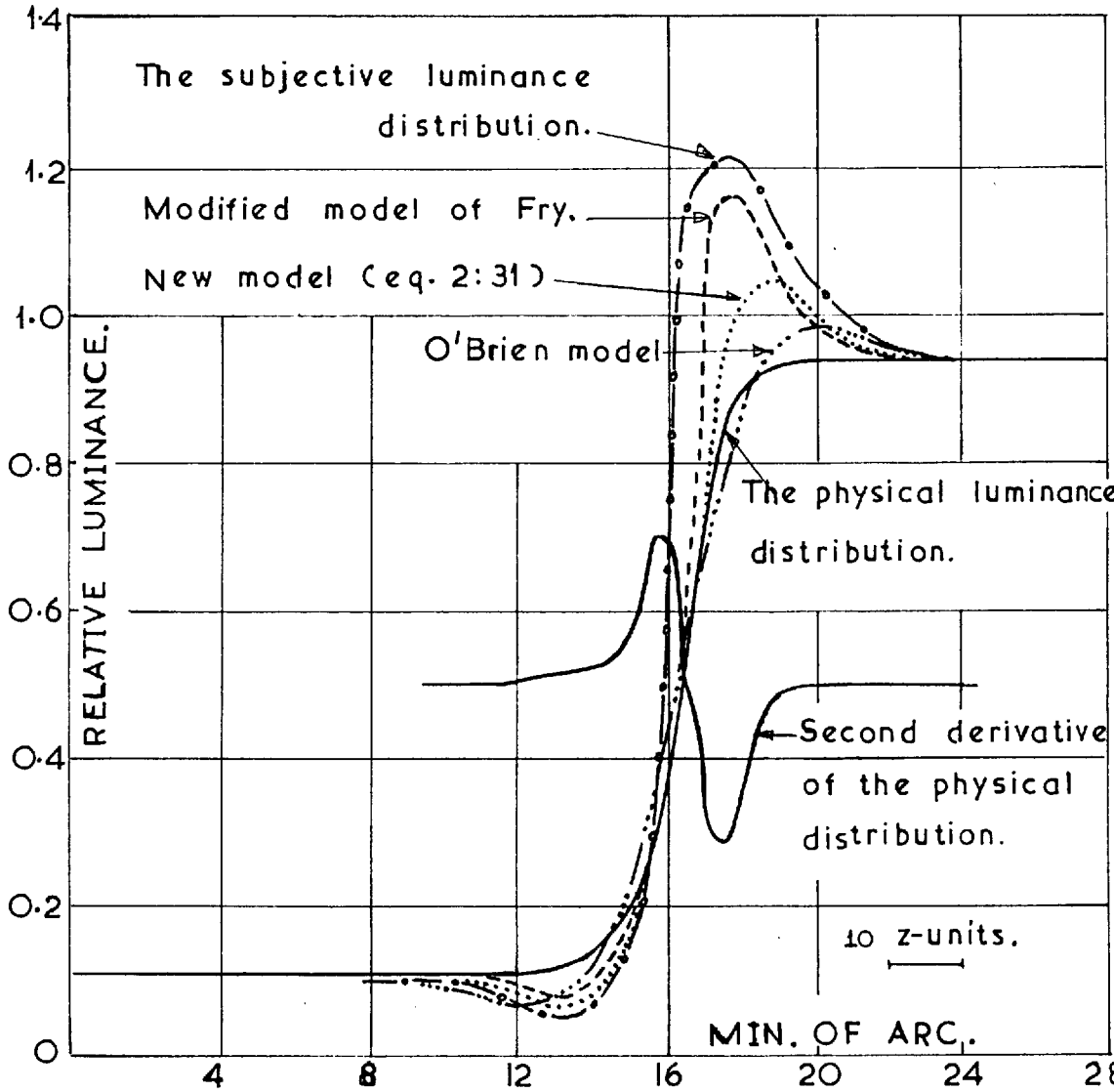



Fig. 5:7. The subjective luminance distribution seen on plate 2A, compared with some of the mathematical models.

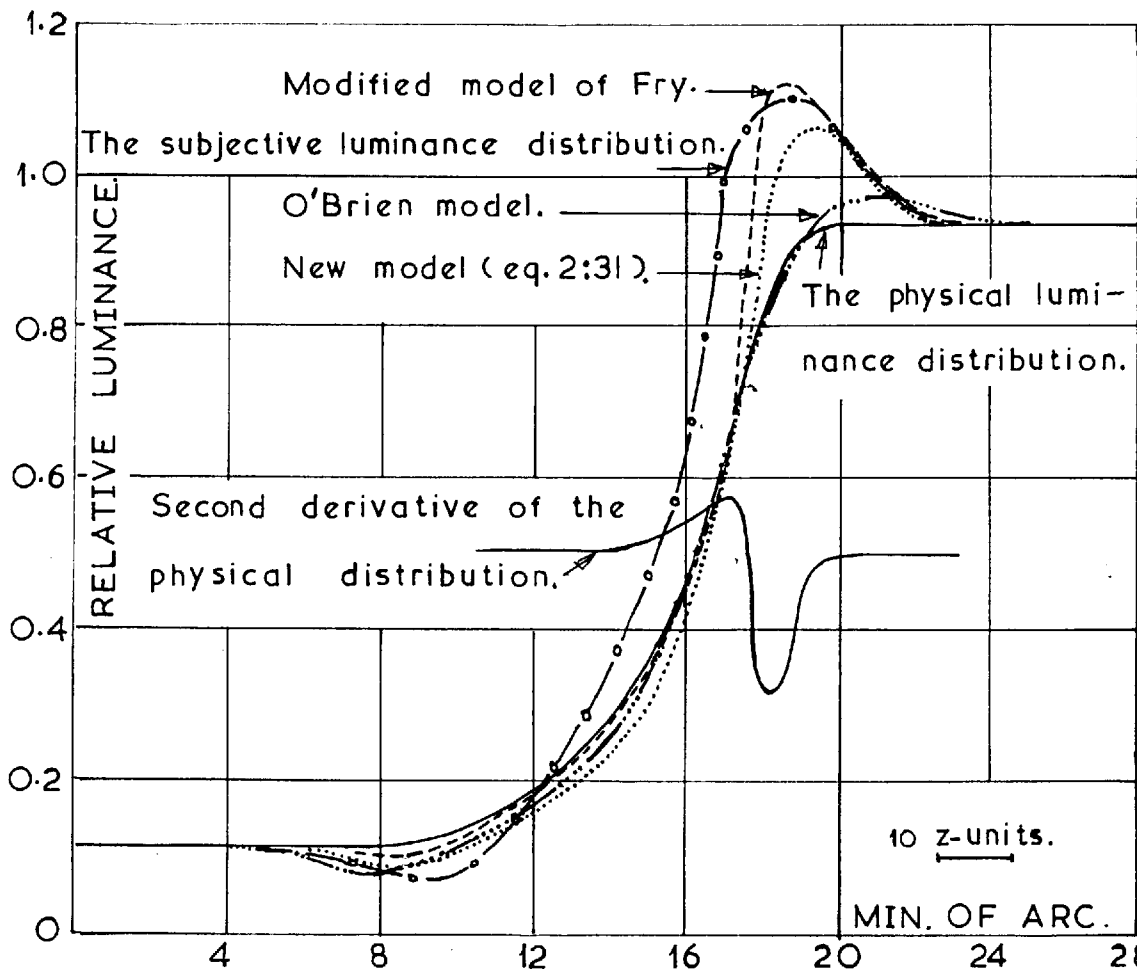



Fig. 5:8. The subjective luminance distribution seen on plate 3A, compared with some of the mathematical models.

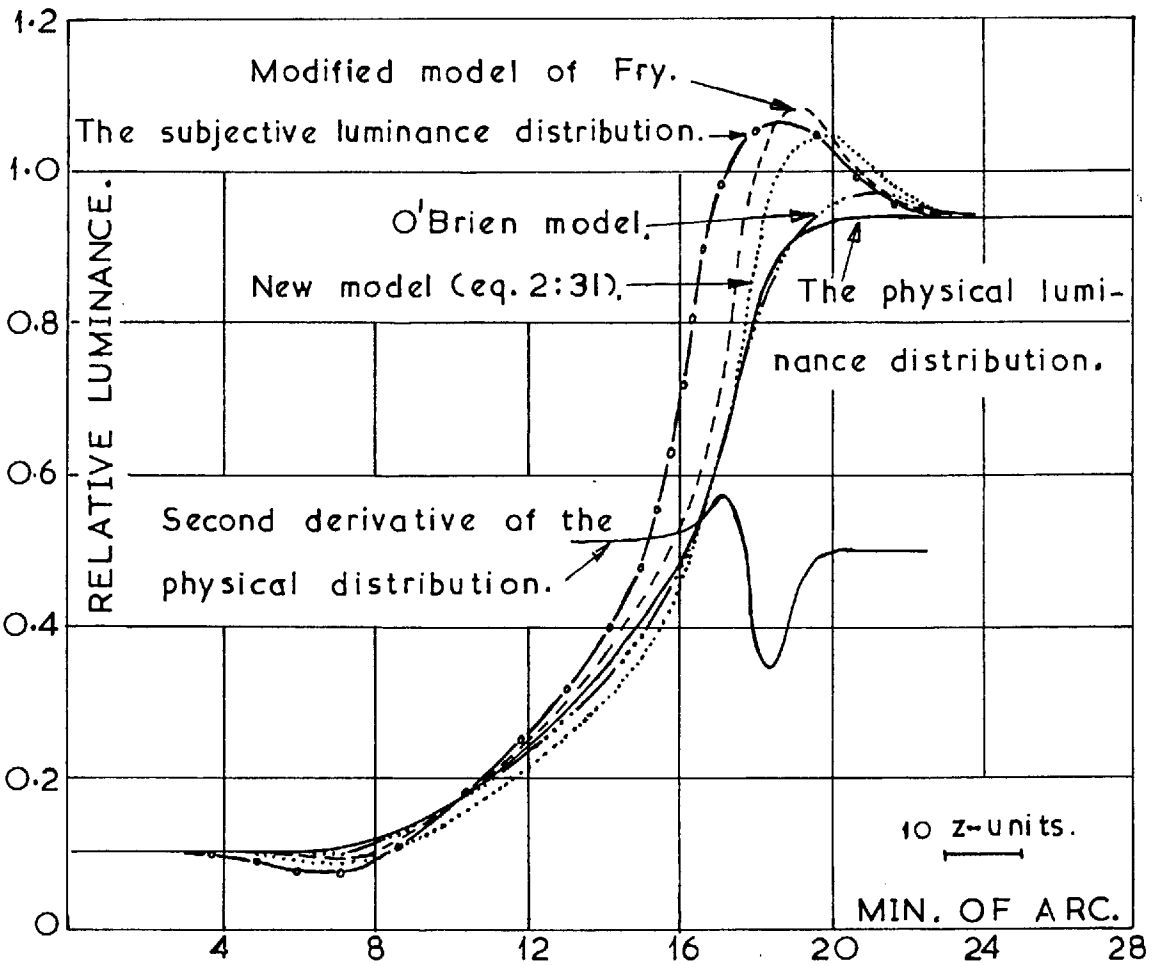



Fig. 5:9. The subjective luminance distribution seen on plate 4A, compared with some of the mathematical models.

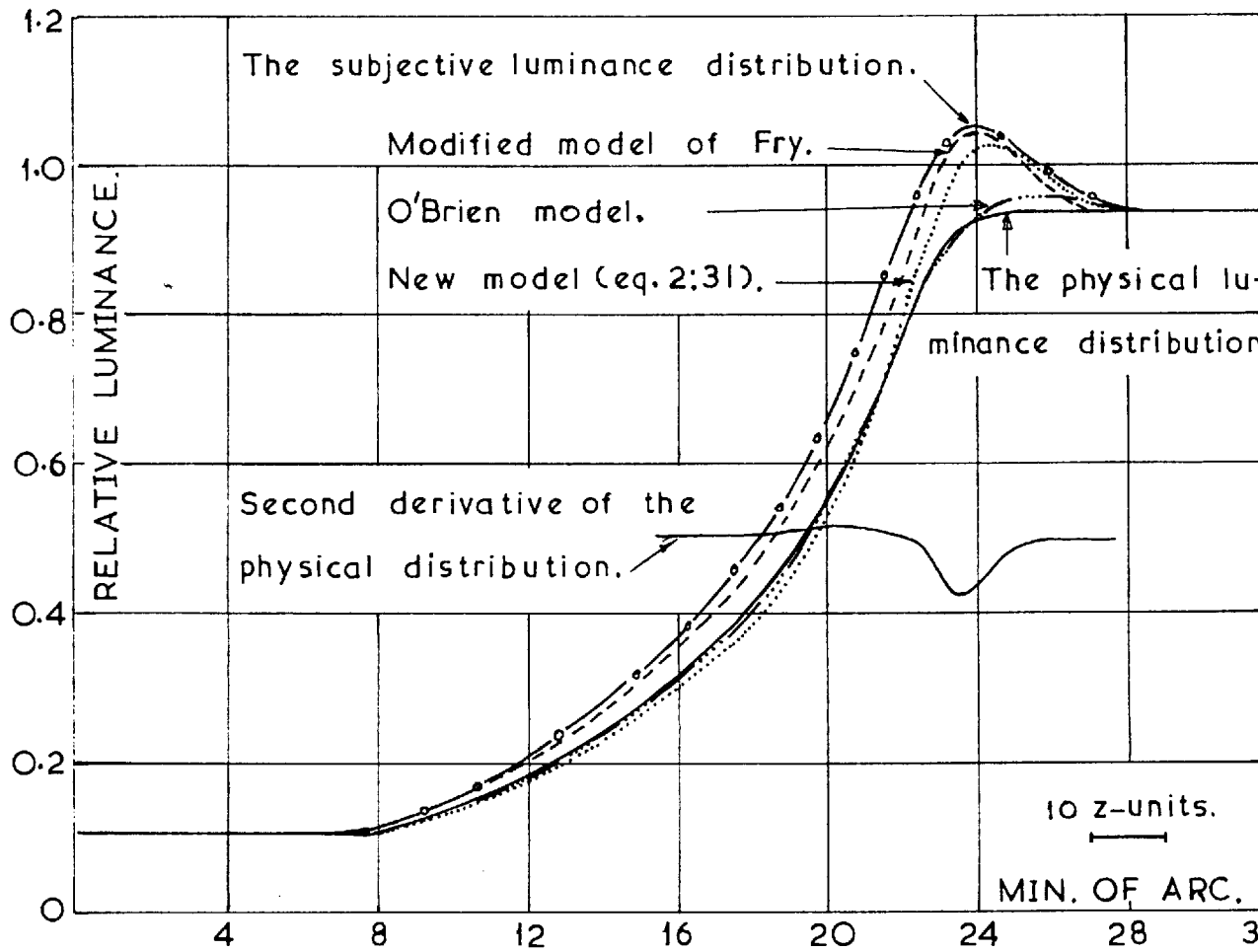



Fig. 5:10. The subjective luminance distribution seen on plate 5A, compared with some of the mathematical models.

object luminance distribution with the line spread function was not much different from the luminance distribution of the object itself. Therefore, instead of using the retinal luminance distribution in the calculation for the predicted one, the luminance distribution of the object was used.

The results from the observations showed that the bands were hardly visible for the plate with the slowest varying luminance (figure 5:10). A grey strip, lighter than the uniform dark area and darker than the uniform bright area could be seen between the dark and bright bands when the luminance gradient occupied a space greater than 6 minutes of arc, as in plates 4A and 5A.

2). Luminance contrast. Using the same conditions under which the set A of plates were observed, the second set B of five plates was examined. The plates of this set had various contrasts, the upper luminance level on them being constant (see fig. 4:10). The results are shown in figures 5:11 to 5:15. The strength of the dark band seems to increase slightly when the contrast decreases from 74% to 36%. A grey strip could be seen on plate 1B where the width of the luminance gradient was about 8 minutes of arc.

It should be noted that the contrast C is defined as,

$$C = \frac{I_{max} - I_{min}}{I_{max} + I_{min}} .$$

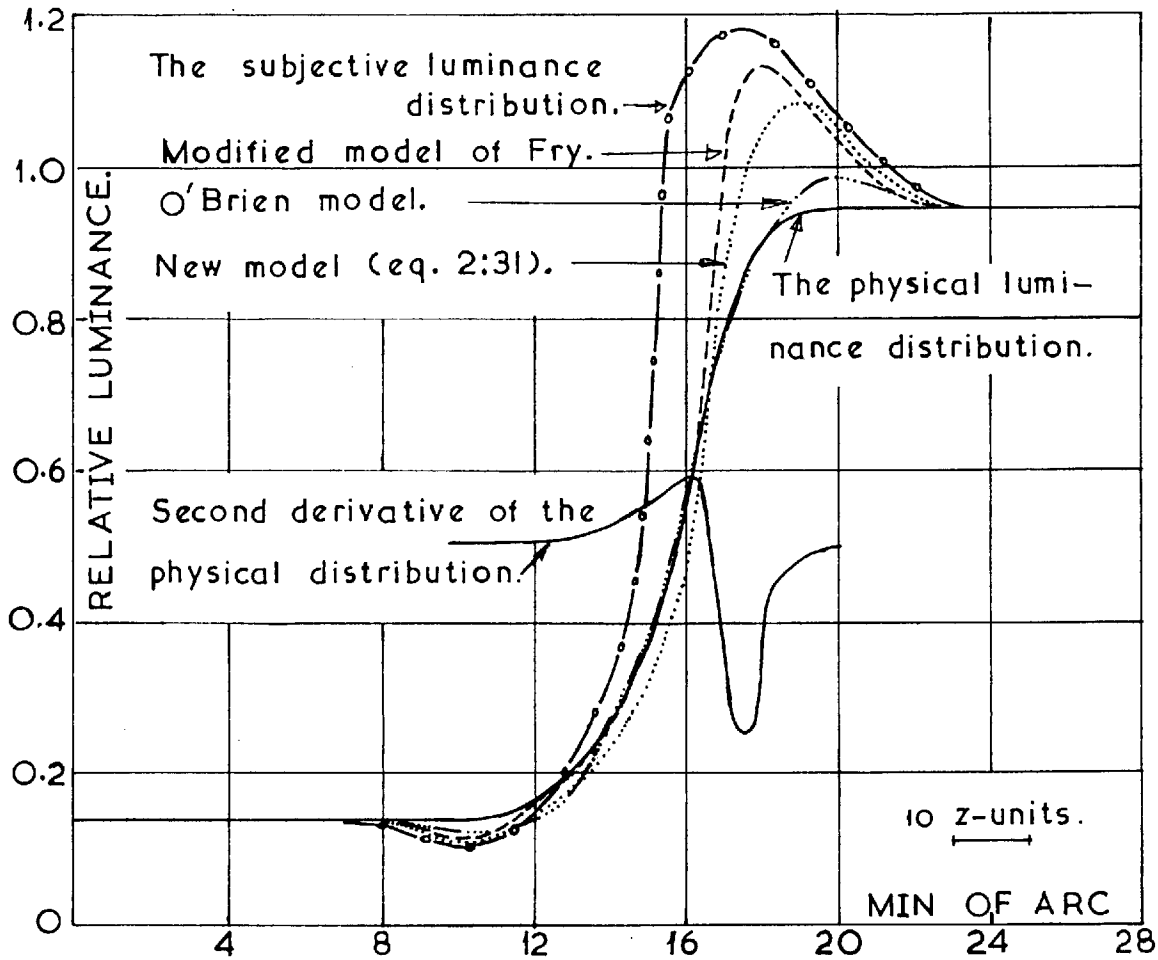



Fig. 5:11. The subjective luminance distribution seen on plate 1B (74 % contrast), compared with some of the mathematical models.

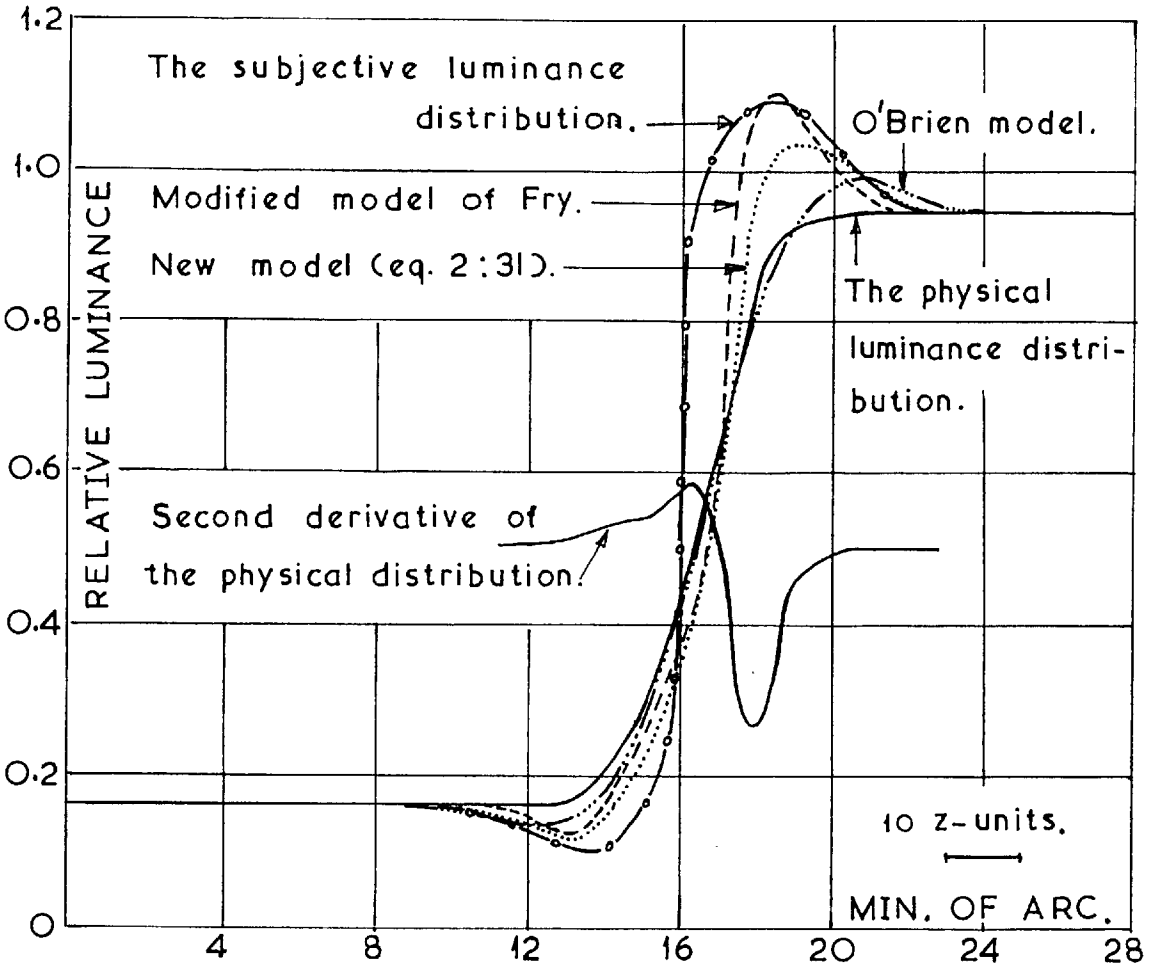



Fig. 5:12. The subjective luminance distribution seen on plate 2B (69 % contrast), compared with some of the mathematical models.

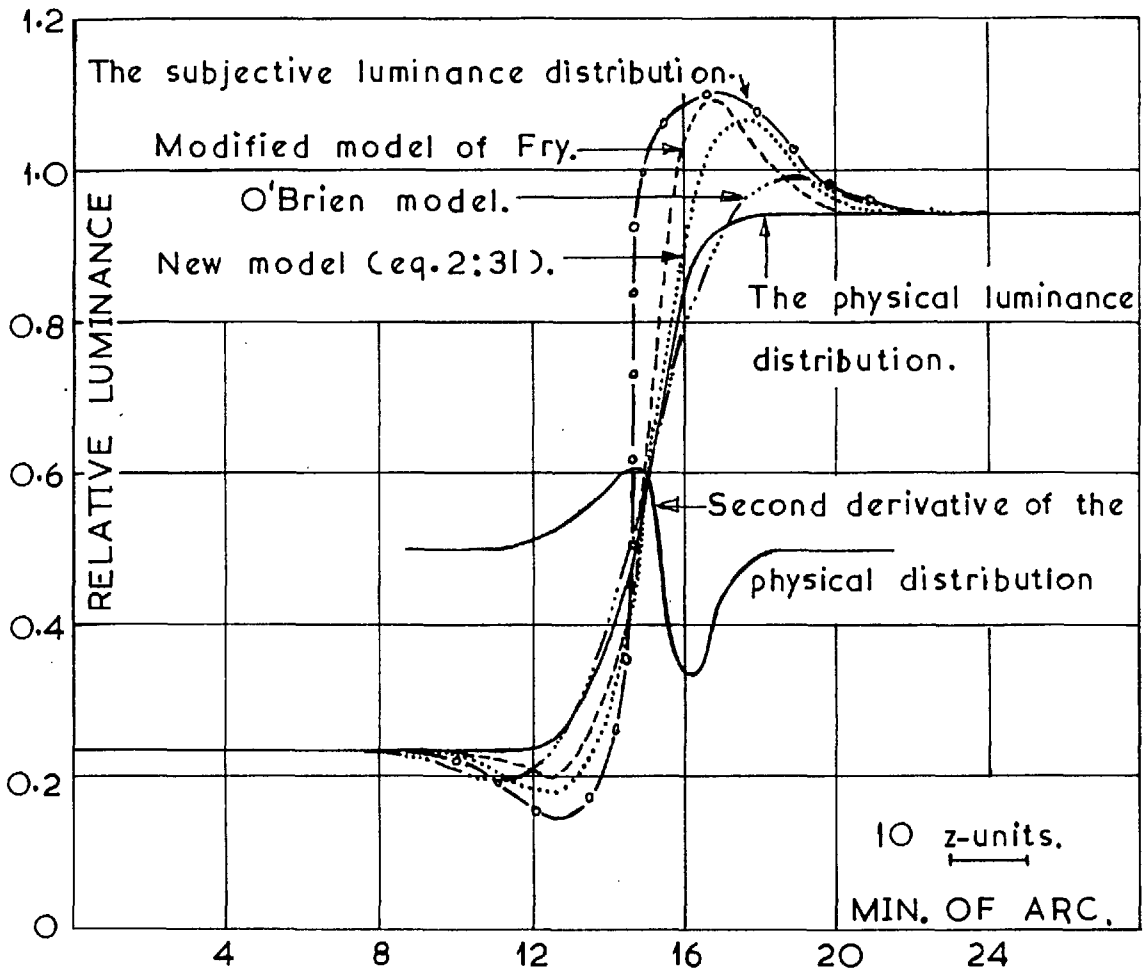



Fig. 5:13. The subjective luminance distribution seen on plate 3B (60 % contrast), compared with some of the mathematical models.

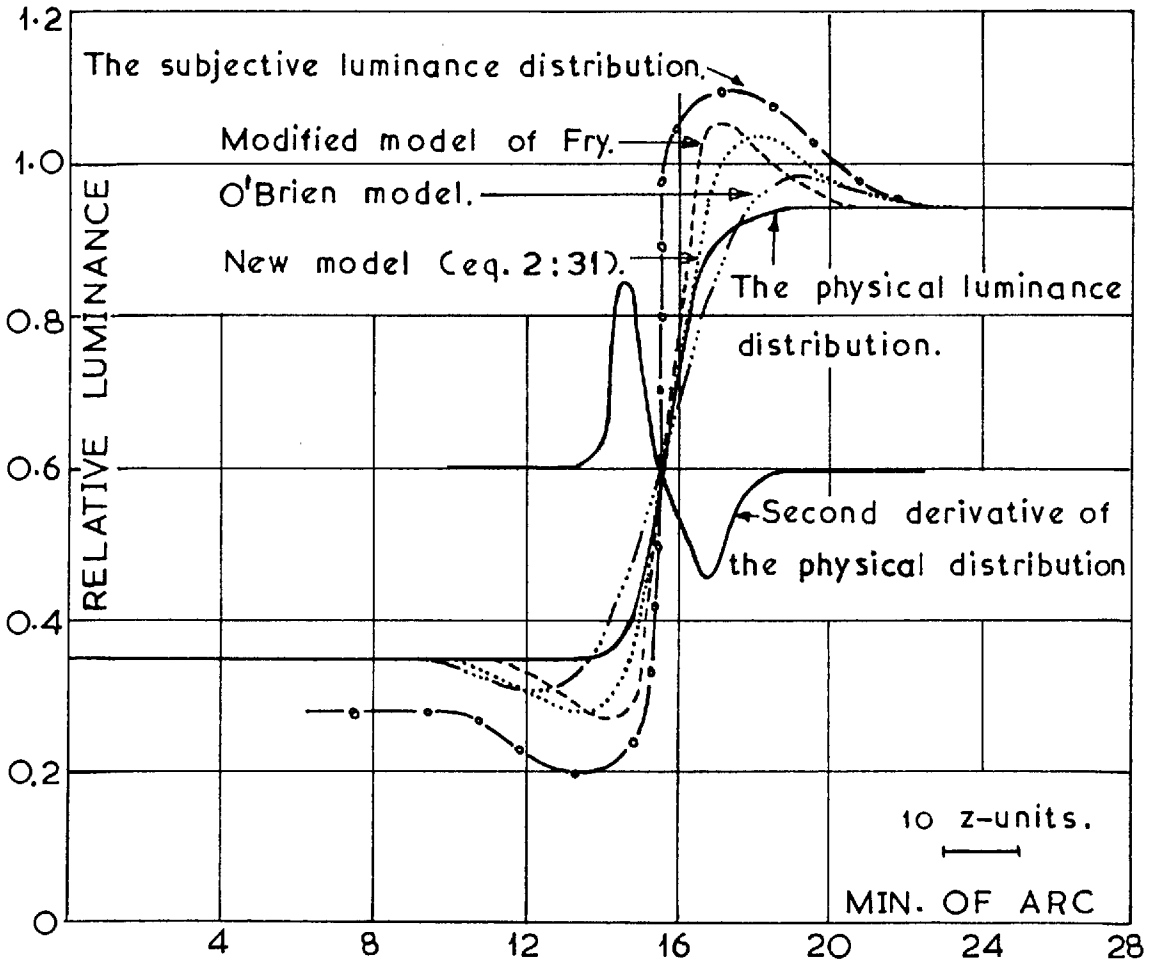



Fig. 5:14. The subjective luminance distribution seen on plate 4B (46% contrast), compared with some of the mathematical models.

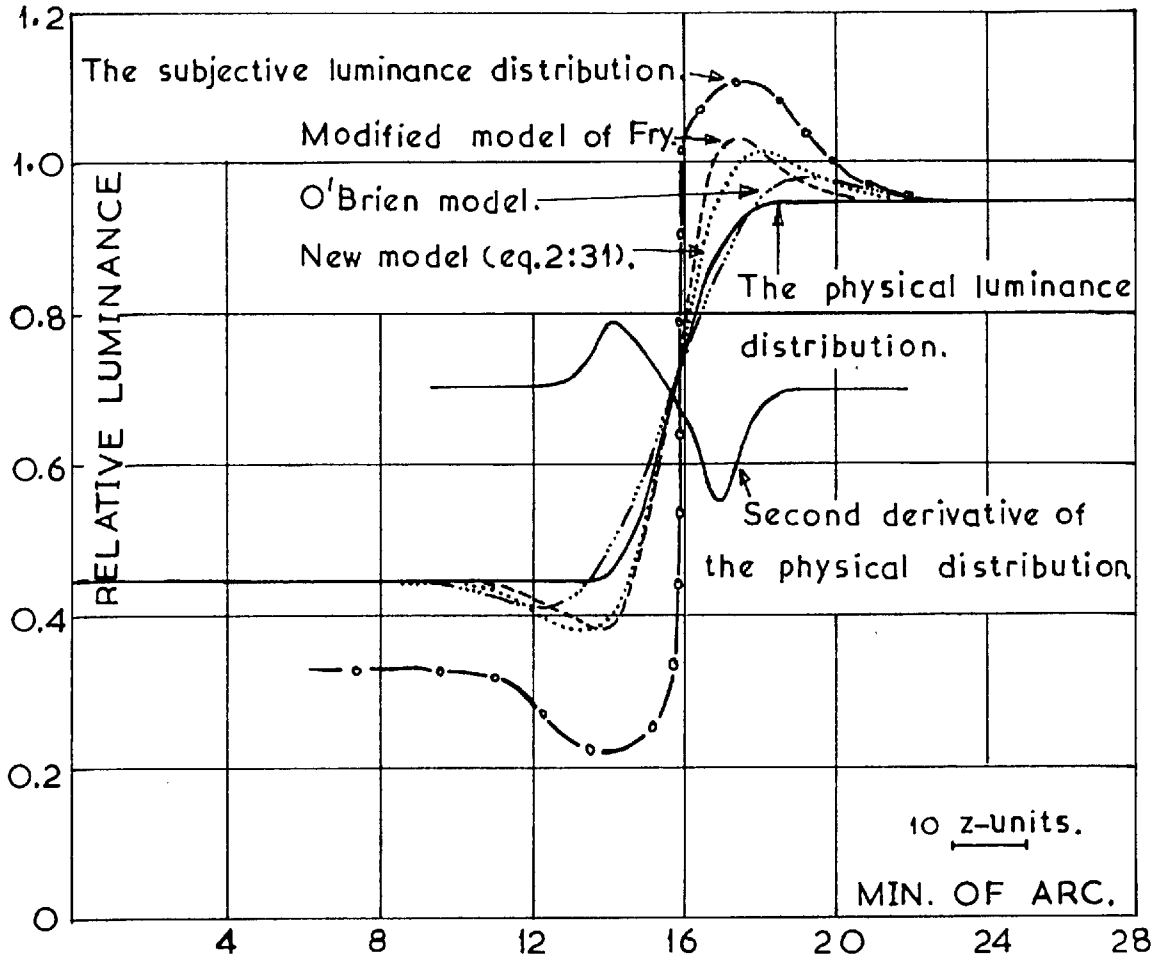



Fig. 5:15. The subjective luminance distribution seen on plate 5B (36% contrast), compared with some of the mathematical models.

3) Luminance level. Plates 1A and 1B were observed under the luminance levels of 1744, 715, 343 and 220 cd./$m^2$ (the luminances were measured on the uniform bright fields of the plates). Various levels of illumination on the plates were obtained by means of inserting neutral density filters into the illuminating system. An artificial eye pupil of 2.4 mms. was used since the diameter of the eye pupil corresponds to 1744 cd./$m^2$ is about 2.4 mms. (from Le Grand's table), and will be bigger when the luminance is decreased. The retinal illuminations were then, 7983, 4526, 1552 and 996 trolands respectively. The distance between the image and the observer for each plate was 520 cms. as in the former measurements.

From figures 5:16 and 5:17, it is clearly seen that the change in the strength of the bright band with respect to the luminance level is more marked than in the case of the dark band. There are also small shifts of the bands towards the dark side when the luminance level is increased. Furthermore, when the luminance was made less than 100 cd/$m^2$, it was found that the bands became very faint, and finally they disappeared completely with further decrease of luminance.

4) Viewing distance. The distance between the image and the observer was now altered. The largest distance which

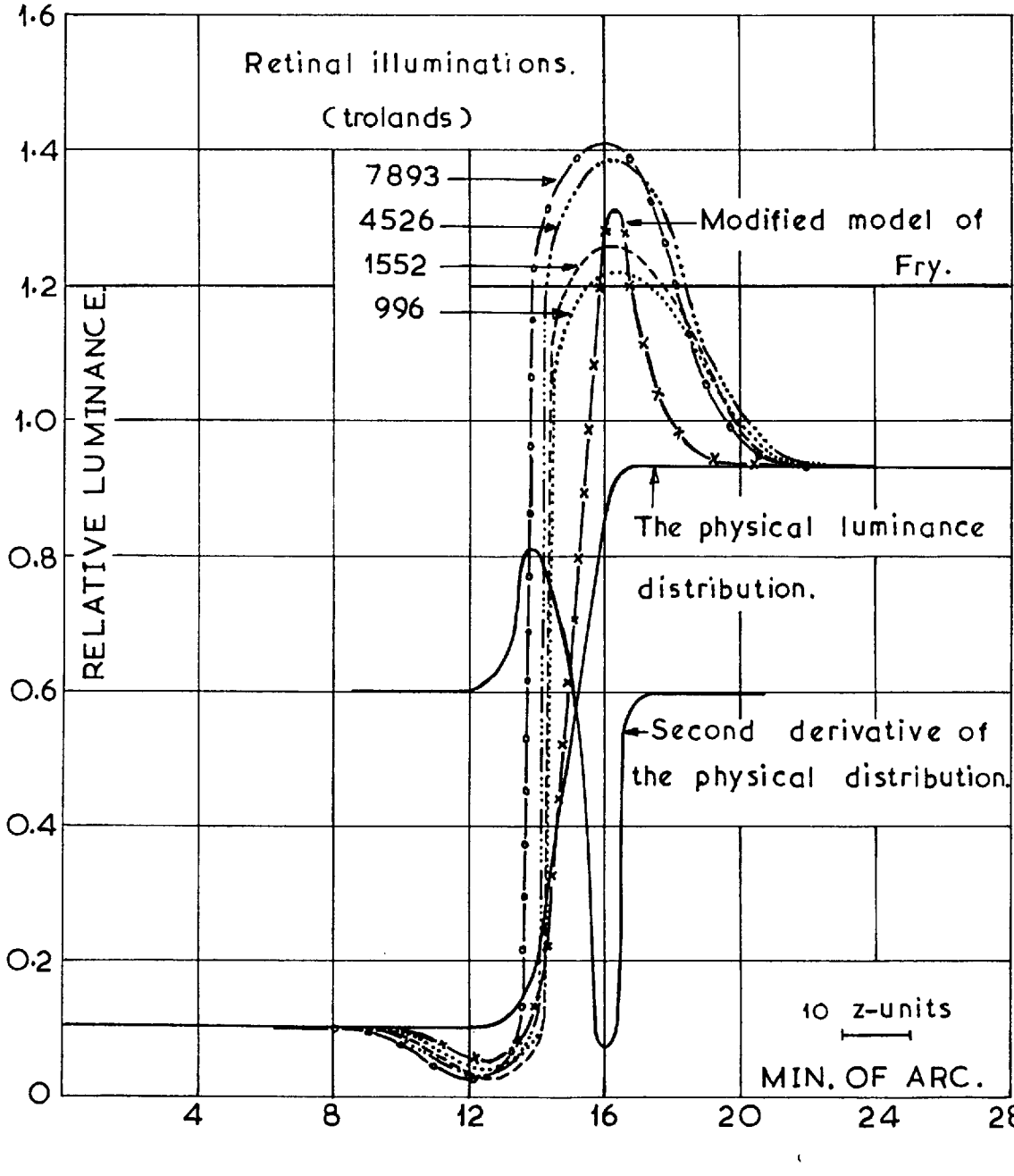



Fig. 5:16. The subjective luminance distributions on plate 1A observed under various luminance levels.

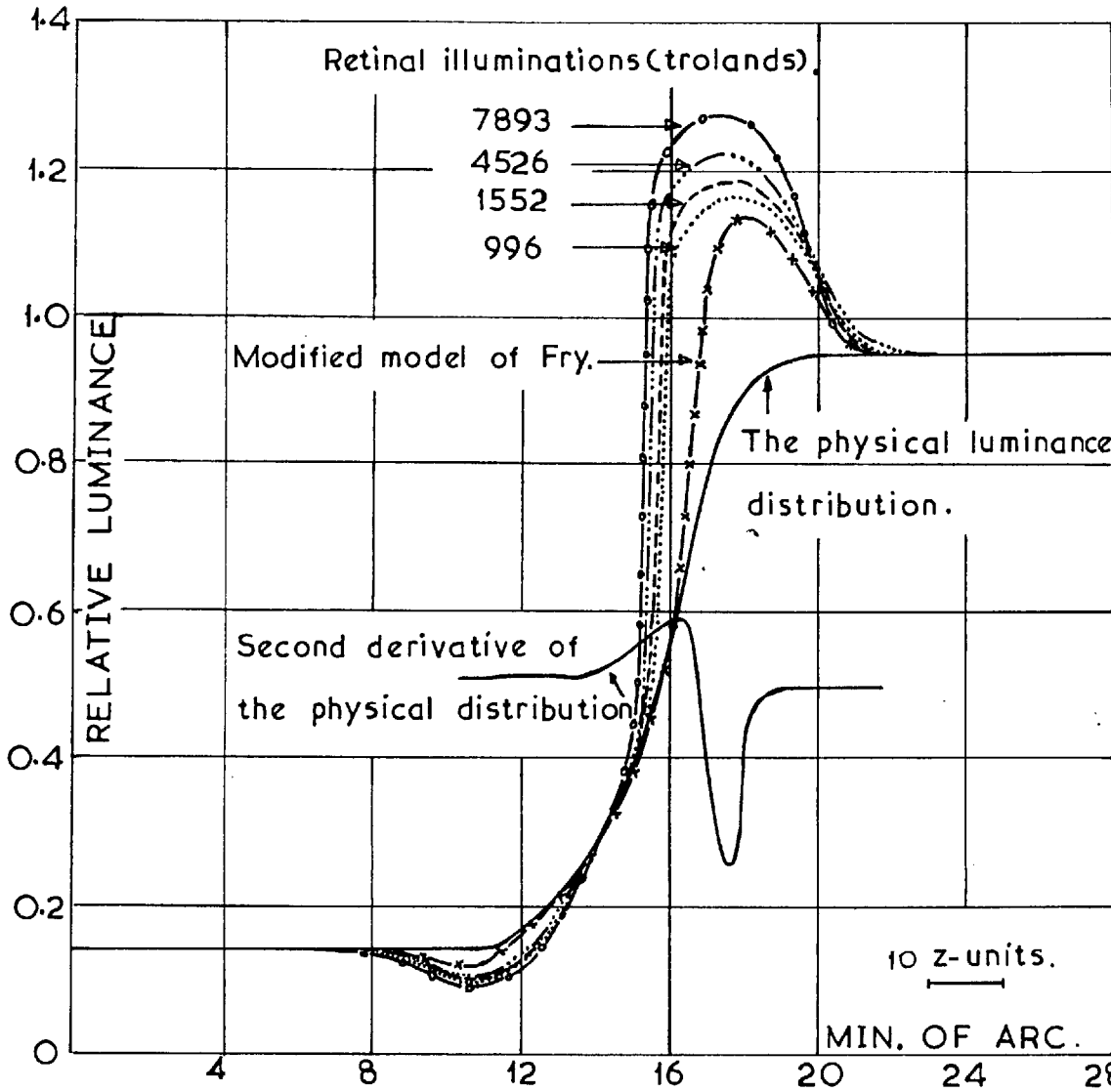



Fig. 5:17. The subjective luminance distributions on plate 1B observed under various luminance levels.

could be accommodated in the laboratory was 5.22 metres. Plates 1A and 1B were observed with the telescope of unit magnification at distance 5.22, 4.22 and 3.22 metres away from the objective. During measurements, the retinal illumination remained constant. The results are shown in figures 5:18 and 5:19. There are no significant differences in the sizes and brightnesses of the bands seen at each distance.

5:4 Discussion.

For clarity, only the second derivative curve and three of the predicted luminance distributions (two of them are from non-linear models and one from one of the linear models) obtained from chapter IV were drawn with each measurement of the visual luminance distribution. The results clearly show that the second derivative theory of Mach band perception is not sufficient to predict the positions of the bands since it gives only approximate positions. The position of the bright band is in good agreement with the position of the minimum of the second derivative of luminance with respect to the distance along the retina. However, the dark band does not occur at the maximum of the second derivative unless the luminance gradient is sufficiently steep.

The two non-linear models (the modified model of Fry and that represented by equation 2:30) chosen in

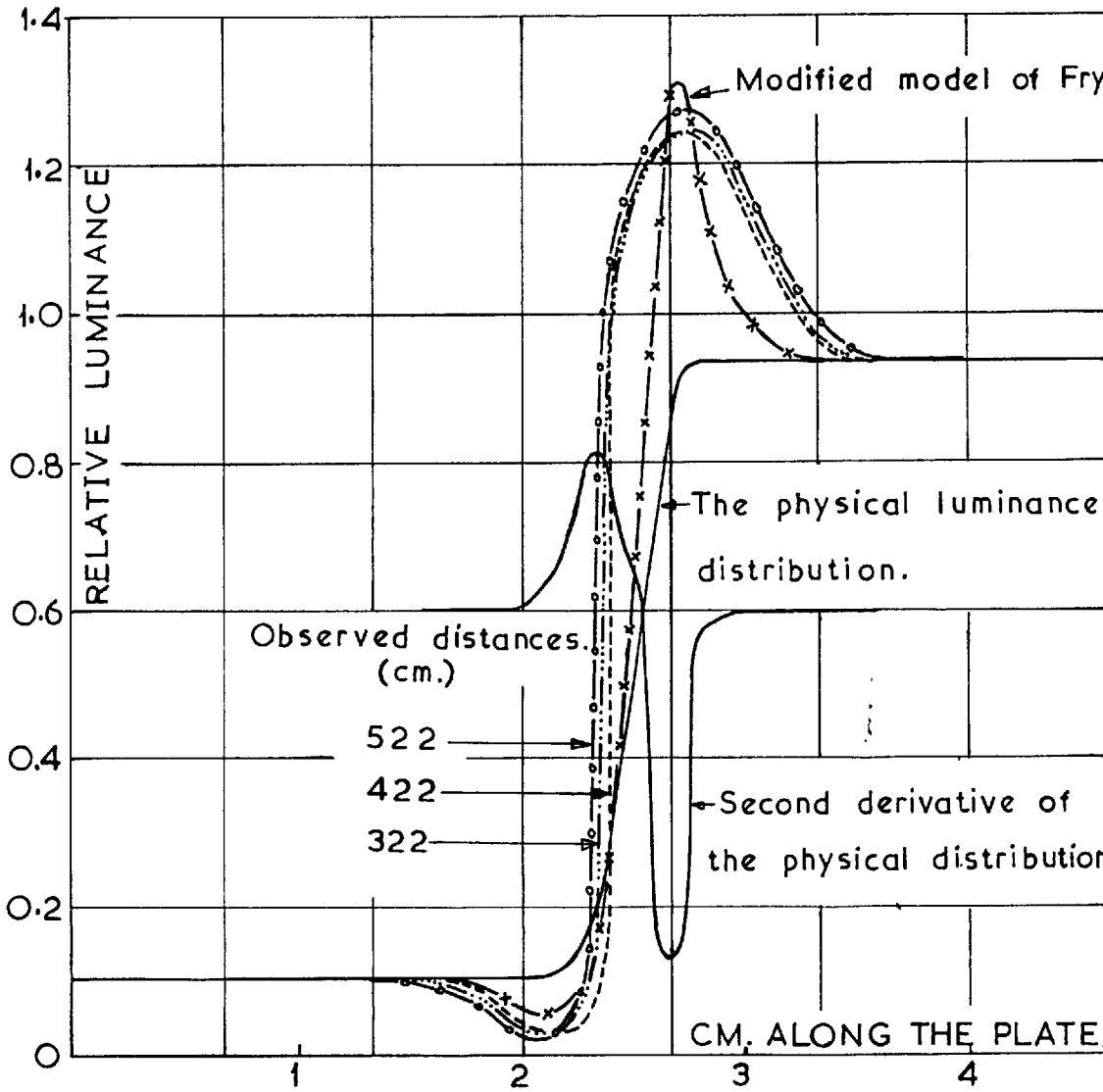



Fig. 5:18. The subjective luminance distributions on plate 1A seen at various distances.

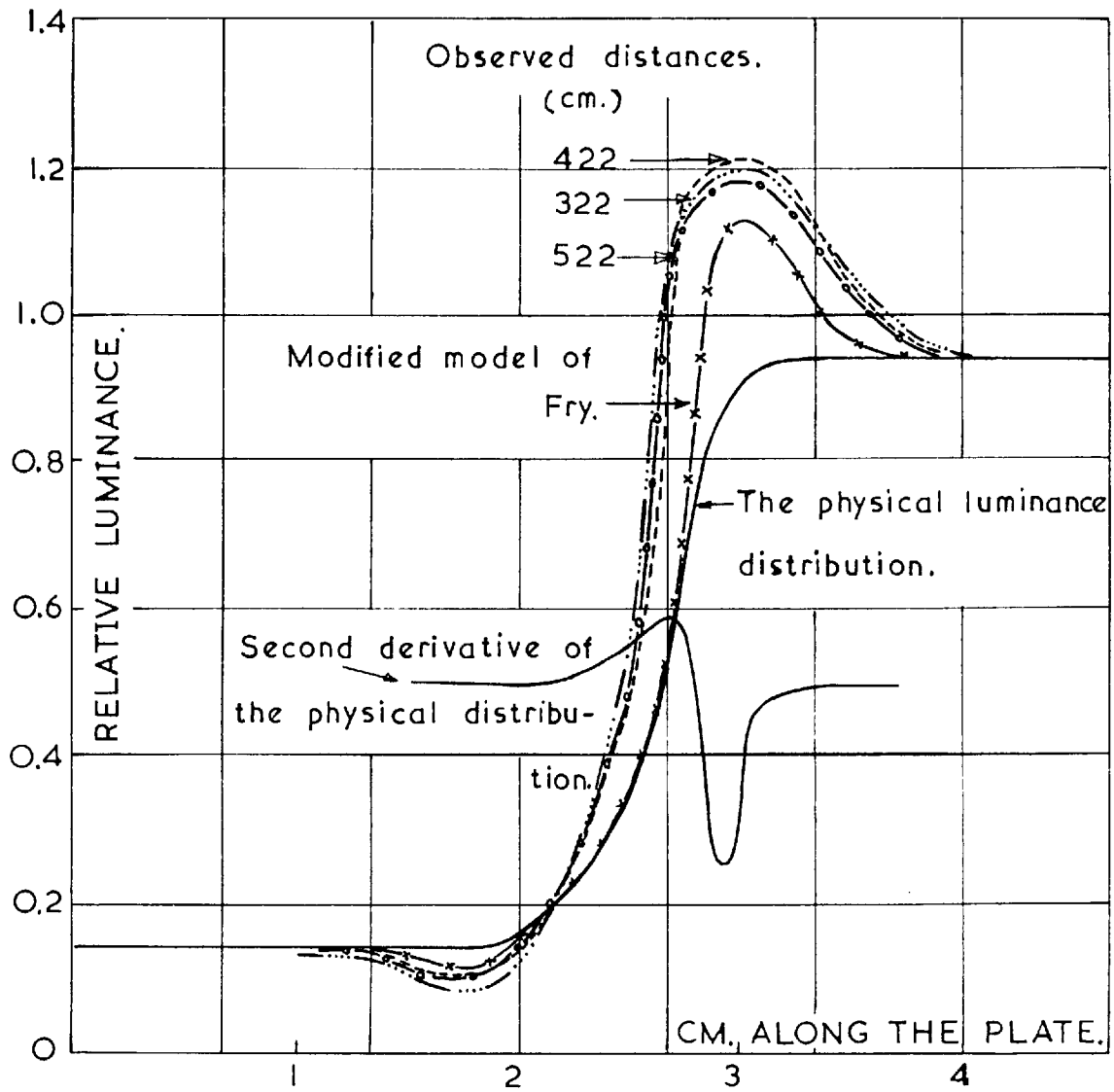



Fig. 5:19. The subjective luminance distributions on plate 1B seen at various distances.

each diagram give approximately the same positions of the bands as those from observation. If we look at the calculated results in the last chapter (see figures4:16 to 4:25) we will see that all the non-linear models predict the same positions of the Mach bands. Therefore, it can be said that any one of the non-linear models is good for prediction purposes.

The O'Brien model (a linear model) which is also given in each of figures 5:6 to 5:15 shows less agreement with the measurement than do the others.

However, from figures 4:16 to 4:25 we can see that all the models predict different widths of the bands. The brightnesses of the predicted bands can be brought close to those of the visual bands by adjusting the parameters in the equation concerned; but nothing can be done to increase the widths of the predicted bands. The visual Mach bands are always broader than the ones predicted. Clearly the models tested are all inadequate in this respect.

# CHAPTER VI

## DISCUSSION AND CONCLUSION.

The investigations described in this thesis have drawn the author's attention to a number of unsolved questions, some of which have indeed hardly been asked as yet. Two of these are concerned with, respectively, the nature of the subjective luminance scale and the method of convolving the physical image formation of the eye with a proposed mathematical model of the Mach effect.

As regards the first of these questions, it is usual to plot retinal illumination linearly as ordinate and to assume that this represents a suitable physical magnitude on which to base the theory; however, one could make a good case for taking a logarithmic scale of illumination, since most sensations, including vision, seem to be logarithmic over an extended range. This was tried out during the present research (see sect.2:8) but the results were inconclusive. A related question is that of the zero of the ordinate scale in graphs illustrating the Mach effect; in some of the models it is necessary to have a non-zero luminance level on the darker side of an edge in order to give sensible results and it is conceivable that one could obtain from a model a level in the dark bands lower than this dark

side level; it may be asked what is the significance of such a result and whether it could happen in practice. To settle the latter question a simple experiment was set up in a dark room as in figure 6:1.

Black bellows were used to prevent scattered light from reaching the eye. Half of an aperture A at one end of the bellows was covered with a razor blade which was illuminated with a bulb S through a ground glass plate G. The bulb S was placed in an enclosure so that no light could escape into the room. After being dark adapted for half an hour, the observer looked at the edge of the incoherently illuminated blade through a metal hole B which was at the other end of the bellows. This hole was about 0.5 mm in diameter and had been honed clean with a needle. A dark adapted-eye will give a much greater response to a given stimulus than a light adapted-eye, that is, with a dark adapted-eye a much smaller amount of light can be detected.

The multiple Mach bands showed up very well under these conditions of observation. No measurement was needed; the aim was merely to observe if the dark band seen through the system appeared darker than the dark area present behind the blade. A few subjects were asked to observe the phenomenon occurring on the knife edge; they all agreed that the intensity of the dark band in the dark area was

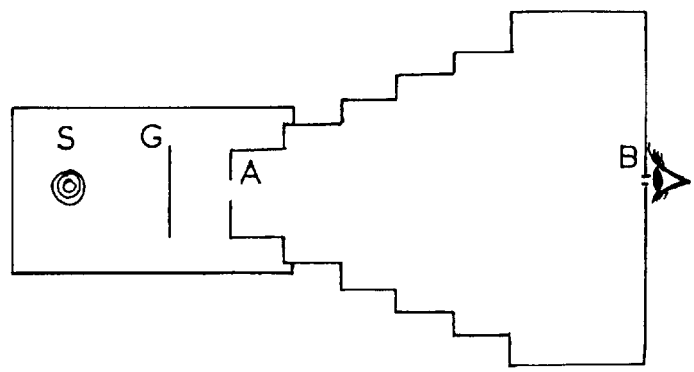



Fig. 6:1. Apparatus used in observing Mach bands.

about the same as that of the surroundings. A fine bright line separated it from the rest of the dark area. This enables us to consider it clearly as a 'dark band'. The bright band in the bright region was, of course, brighter than the bright area itself.

Hartline and Ratliff, in their model formulation, pointed out that the output frequency in the response of the eye cannot be negative since a negative frequency has no meaning; however, this seems a very forced approach to the question of negative intensities.

The second major question mentioned above, that of the convolution of the physical response of the eye with a Mach effect model, involves the question, what is to be taken as the actual retinal illumination distribution? There are two cases to consider; in the first case the effective pupil is very small ($<<$ 1 mm.) as in the studies in chapter III and in ordinary microscopy, and in this case it might seem reasonable to treat the eye as a diffraction limited optical system, as was done in this thesis. The second case involves pupils of 2-3 mms., as in ordinary vision and in the experiments of chapter IV; here there are a few experimental measurements of the spread function of the eye as an optical system ; the results of the different authors quoted are not in agreement and also they do not agree with what one would expect in the diffraction

limited case. Unfortunately it is not known whether the wider spread is due to aberrations or scatter or both and it is also not known how much of the inconsistencies are genuinely errors on one or other side and how much is due to variations between individuals. Thus the whole question of the performance of the eye as an optical instrument,i.e; leaving aside psychophysical aspects,needs more study.

Returning now to the work of this thesis, some calculations using the modified model of Fry(eqn. 2:29) mentioned in chapter II were carried out in order to show theoretically the influences of luminance gradient and contrast on the model.

The results of these calculations are shown in figures 6:2 and 6:3. Figure 6:2 shows the obvious changes of brightness of the bands when the luminance gradient between two constant and uniform luminance levels is changed. These curves show clearly that the bands increase in their intensities as the slope of the gradient becomes steeper. Also they make their appearances at the points where the changes in the gradients of the slope take place. Finally, when the transition between two luminance levels becomes abrupt, the bands, still visible, become narrower but in fact more distinct. This agrees with the experimental work reported in chapter III where Mach bands were reported to have been seen at an abrupt edge. Furthermore, from the figure, we can also

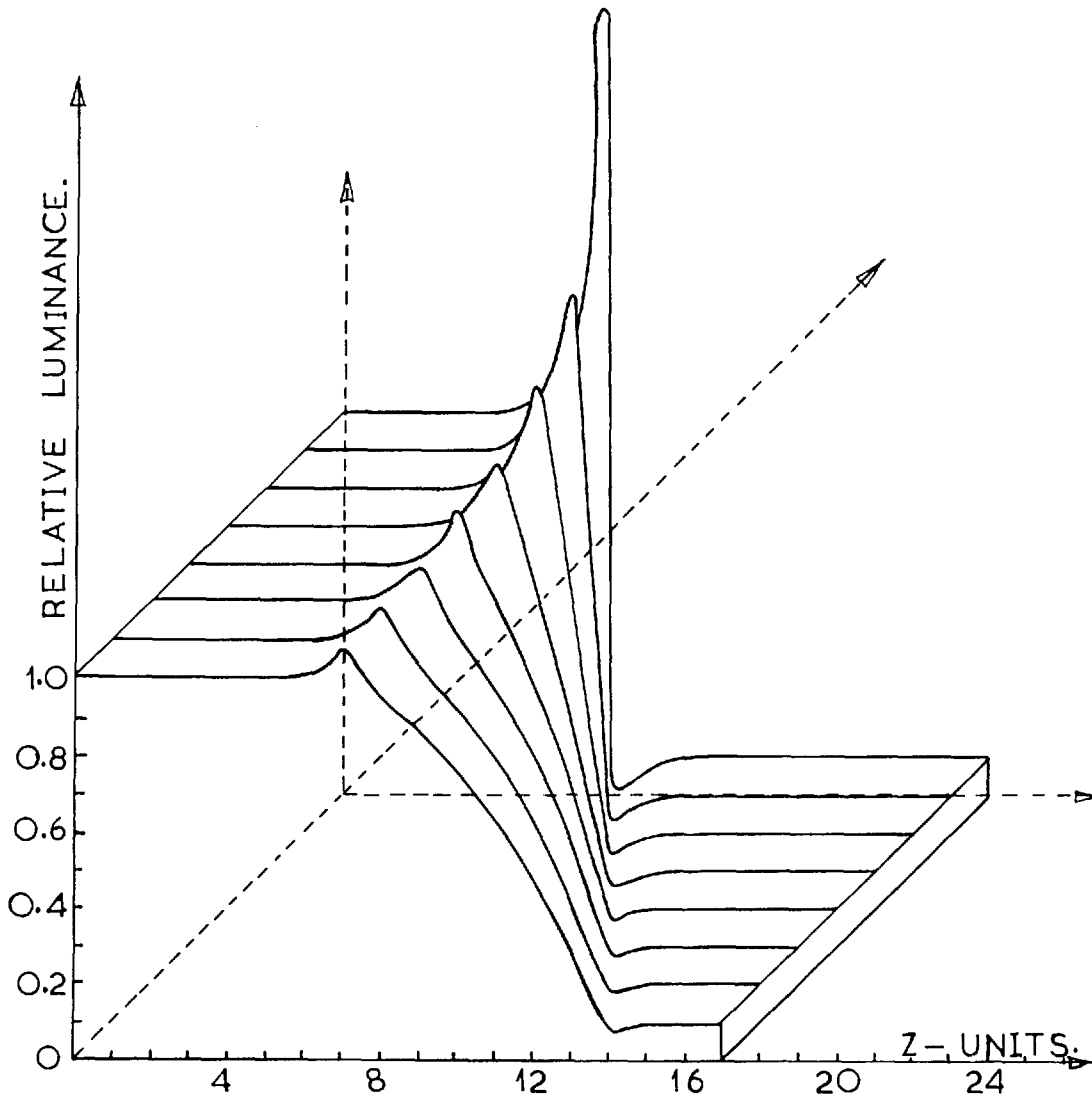



Fig. 6:2. Effect of luminance gradient on Mach bands, calculated from the modified model of Fry.

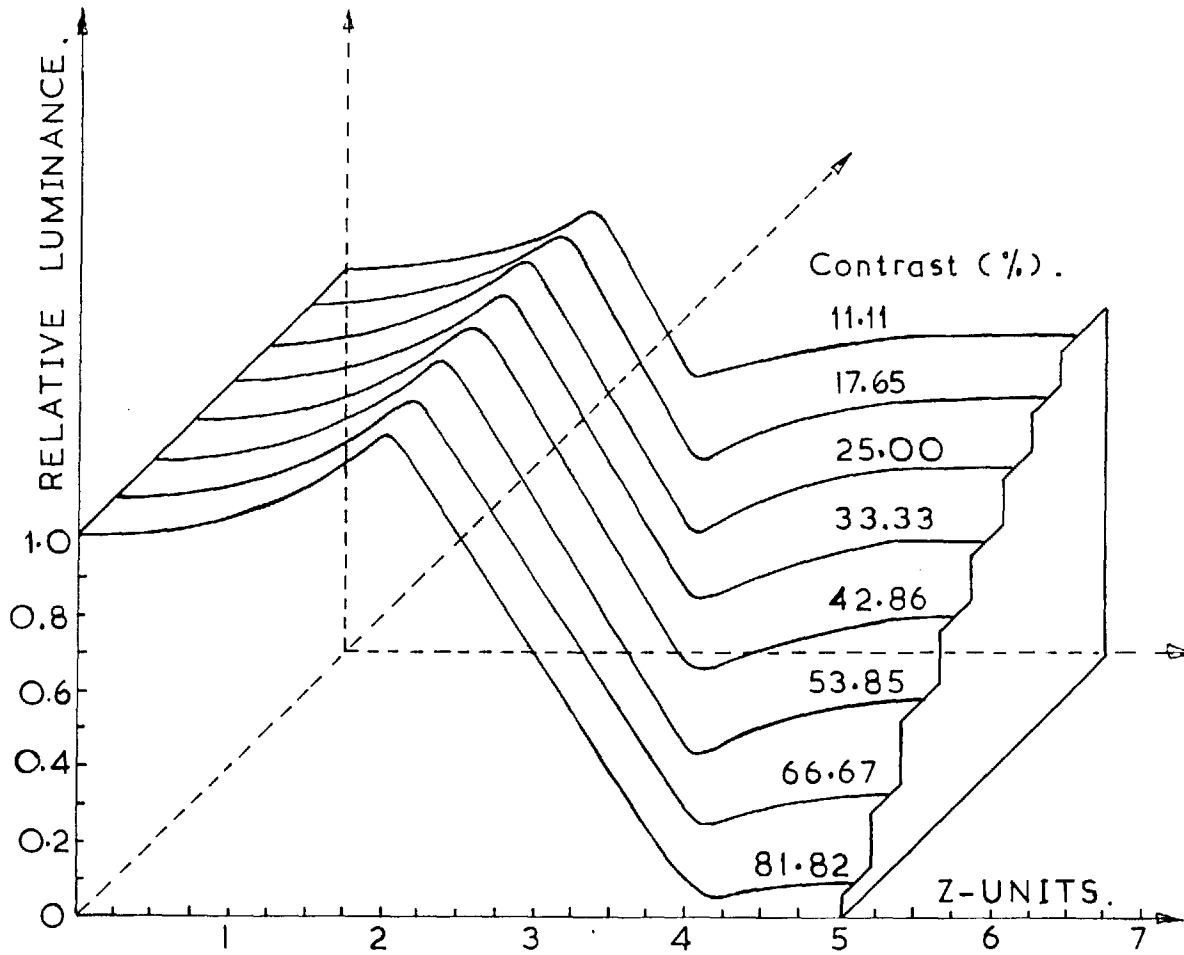



Fig. 6:3. Effect of contrast on Mach bands, calculated from the modified model of Fry.

see that the changes in brightness of the bands are more prominent than the changes in their widths.

The influence of changes in the luminance contrast is shown in figure 6:3, where the higher luminance level is kept constant but the lower one is changed. The mathematical model predicts a wider dark band when the contrast decreases, and also an increase in the amount of the undershoot. This seems to agree with the results shown in the last chapter and also with those reported by Watrasiewicz(1964) who mentioned that the dark band became wider and fainter as the contrast decreased while the undershoot grew bigger at the same time.

The method employed in measuring the brightnesses of the bands, however, has yielded only crude results and it gives only approximate estimations of the brightnesses. However, visual photometric matching is the only way at present conceivable for measuring a subjective brightness.

The large number of factors,(the wavelength of light used, the mode of illumination of the object, retinal structure, retinal illumination and the size of eye pupil, on which the Mach phenomenon depends) make the mechanism for the perception of the bands highly complicated. No model goes into so much detail as to describe how these factors are involved in the mechanism. The important factors considered

in each model are the brightness at the stimulated point on the retina which sometimes is expressed in terms of frequency of impulses, and the distance from the stimulated point to the neighbouring receptor. In fact, in the inhibitory mechanism which is presumed to be essential for the Mach band perception, there are many details which are not understood. Where and how it mediates are still topics for further investigation. The significance of the individual variations in the perception of the phenomenon, which was mentioned in chapter III, makes it more difficult to determine the usefulness of any model. The intensities of the predicted bands can be brought to agree with those of the visual bands by varying the constants in the model, but the values of these parameters in every model may need to be chosen suitably for each individual. Those constants are then applied to the rest of the stimulating patterns such that the subjective patterns may be predicted. However, there are no parameters in any model which can shift the bands according to individual differences although the observed individual shifts are quite large.

Some models give fair approximations for the positions of the bands, but none gives good estimates for the widths. The widths of the predicted bands are always smaller than those of the visual bands. The newly proposed

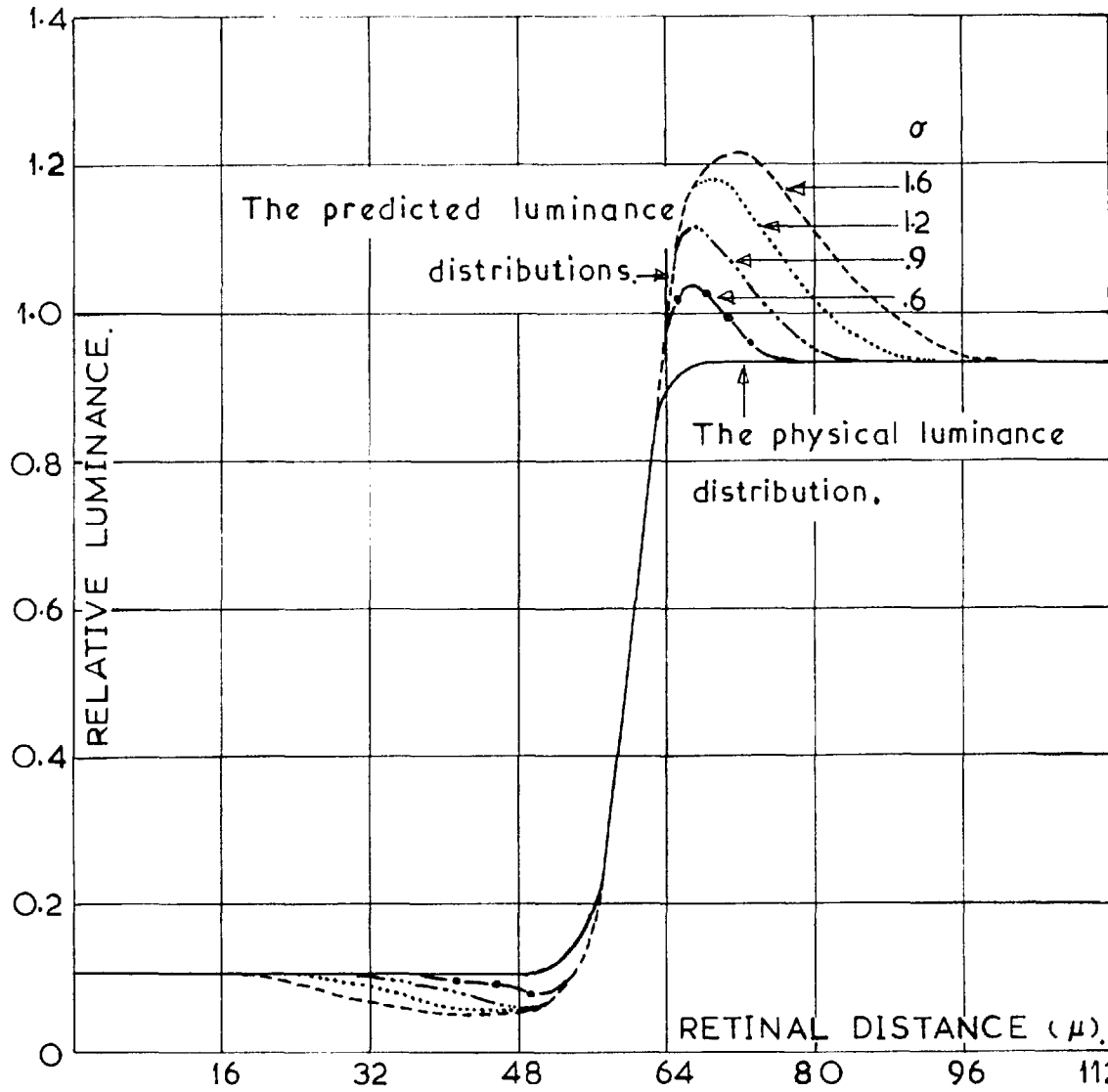



Fig.6:4. Effect of $\sigma$ on the predicted luminance distribution on plate IA, calculated from the new model (eq.2:31).

one dimensional model with the normalized function (eqn. 2:31) gives rather broad bands but their brightnesses cannot be brought higher without increasing the value of the parameter $\sigma$ . The bigger the value of $\sigma$ , the larger the inhibiting area involved (see figure 2:21) and hence, the more time needed on the computer. At the same time as the intensities of bands increase, the predicted bright band will move further into the bright area, and the corresponding dark band will shift into the dark area. Figure 6:4 expresses the changes in the subjective luminance distribution as a result of changes in the value of $\sigma$ for the plate 1A; the bands become broader and shift away from the gradient when the value of $\sigma$ increases.

If the dimensions of the predicted bands are ignored, the modified model of Fry(equation 2:29) and the proposed new model (eqn. 2:30) are the ones worth pursuing further. They give the right positions of the visual bands and the computation time needed is much less than for the model of Hartline and Ratliff.

However, a more precise model is needed so that the correct positions and widths of the bands can be obtained at the same time. It should involve all the factors which have influence on the phenomena.

# APPENDIX A

## The Intensity of the Edge Image and its Derivatives.

The values of the intensity of an image of an abrupt edge along the retina and the first to fourth derivatives are tabulated below with intervals of 0.2 Z-unit. For small values of Z (from 0 to 8.0) the calculations were done using equations 3:15, 3:9, 3:10, 3:11, and 3:12 for $I(z)$, $I'(z)$, $I''(z)$, $I'''(z)$ and $I^{IV}(z)$ respectively. The values of $H_0$ and $H_1$ were found from the tables prepared by Jahnke and Emde (1945). The asymptotic expressions (equations 3:26, 3:27, 3:28, 3:29 and 3:30) were used for the large values of Z(from 6.2 to 16.0).

| Z | I(z) | I'(z) | I''(z) | I'''(z) | $I^{IV}(z)$ |
|---|---|---|---|---|---|
| 0.0 | .50000 | .26997 | 0 | -.14399 | 0 |
| 0.2 | .55380 | .26721 | -.02854 | -.14006 | .03899 |
| 0.4 | .60647 | .25877 | -.05554 | -.13068 | .07505 |
| 0.6 | .65693 | .24520 | -.07945 | -.11137 | .10548 |
| 0.8 | .70422 | .22723 | -.09937 | -.08746 | .13264 |
| 1.0 | .74755 | .20579 | -.11409 | -.06014 | .14380 |
| 1.2 | .78634 | .18196 | -.12319 | -.03124 | .14622 |
| 1.4 | .82022 | .15690 | -.12652 | -.00268 | .13930 |
| 1.6 | .84907 | .13173 | -.12434 | .02366 | .12377 |
| 1.8 | .87295 | .10749 | -.11725 | .04619 | .10118 |

| Z | I(z) | I'(z) | I''(z) | I'''(z) | $I^{IV}(z)$ |
|---|---|---|---|---|---|
| 2.0 | .89217 | .08509 | -.10616 | .06369 | .07367 |
| 2.2 | .90715 | .06522 | -.09214 | .07541 | .04370 |
| 2.4 | .91845 | .04835 | -.07637 | .08111 | .01379 |
| 2.6 | .92670 | .03471 | -.06005 | .08094 | -.01372 |
| 2.8 | .93254 | .02430 | -.04428 | .07588 | -.03685 |
| 3.0 | .93661 | .01691 | -.02996 | .06666 | -.05417 |
| 3.2 | .93948 | .01217 | -.01778 | .05463 | -.06490 |
| 3.4 | .94163 | .00962 | -.00819 | .03122 | -.06889 |
| 3.6 | .94344 | .00871 | -.00133 | .02815 | -.06664 |
| 3.8 | .94518 | .00891 | .00288 | .01786 | -.05915 |
| 4.0 | .94804 | .00971 | .00474 | .00406 | -.04781 |
| 4.2 | .94908 | .01068 | .00462 | -.00417 | -.03421 |
| 4.4 | .95130 | .01149 | .00326 | -.00959 | -.02000 |
| 4.6 | .95364 | .01193 | .00103 | -.01224 | -.00665 |
| 4.8 | .95603 | .01188 | -.00147 | -.01240 | .00464 |
| 5.0 | .95836 | .01135 | -.00379 | -.01058 | .01301 |
| 5.2 | .96054 | .01040 | -.00560 | -.00742 | .01805 |
| 5.4 | .96250 | .00916 | -.00671 | -.00361 | .01975 |
| 5.6 | .96419 | .00777 | -.00703 | .000277 | .01847 |
| 5.8 | .96561 | .00639 | -.00662 | .00364 | .01486 |
| 6.0 | .96676 | .00516 | -.00563 | .00612 | .00976 |
| 6.2 | .96769 | .00417 | -.00425 | .00750 | .00403 |
| 6.4 | .96845 | .00347 | -.00270 | .00774 | -.00147 |
| 6.6 | .96910 | .00308 | -.00122 | .00697 | -.00605 |

| Z | I(z) | I'(z) | I''(z) | I'''(z) | $I^{IV}(z)$ |
|---|---|---|---|---|---|
| 6.8 | .96976 | .00297 | .00003 | .00542 | -.00922 |
| 7.0 | .97030 | .00307 | .00093 | .00339 | -.01074 |
| 7.2 | .97093 | .00331 | .00139 | .00123 | -.01063 |
| 7.4 | .97162 | .00360 | .00143 | -.00076 | -.00909 |
| 7.6 | .97237 | .00386 | .00111 | -.00234 | -.00630 |
| 7.8 | .97316 | .00403 | .00054 | -.00333 | -.003345 |
| 8.0 | .97397 | .00406 | -.00018 | -.00368 | -.00012 |

| Z | I(z) | I'(z) | I''(z) | I'''(z) | $I^{IV}(z)$ |
|---|---|---|---|---|---|
| 6.2 | .96804 | .00418 | -.00429 | .00783 | .00408 |
| 6.4 | .96876 | .00348 | -.00274 | .00816 | -.00141 |
| 6.6 | .96939 | .00309 | -.00124 | .00740 | -.00600 |
| 6.8 | .96999 | .00297 | .00002 | .00580 | -.00918 |
| 7.0 | .97061 | .00307 | .00092 | .00368 | -.01073 |
| 7.2 | .97128 | .00331 | .00139 | .00140 | -.01064 |
| 7.4 | .97200 | .00360 | .00144 | -.00070 | -.00911 |
| 7.6 | .97278 | .00386 | .00112 | -.00237 | -.00654 |
| 7.8 | .97359 | .00403 | .00055 | -.00343 | -.00340 |
| 8.0 | .97442 | .00406 | -.00016 | -.00382 | -.00018 |
| 8.2 | .97523 | .00396 | -.00088 | -.00356 | .00267 |
| 8.4 | .97600 | .00372 | -.00150 | -.00277 | .00480 |

| Z | I(z) | I'(z) | I''(z) | I'''(z) | $I^{IV}(z)$ |
|---|---|---|---|---|---|
| 8.6 | .97670 | .00337 | -.00192 | -.00164 | .00599 |
| 8.8 | .97731 | .00297 | -.00211 | -.00036 | .00618 |
| 9.0 | .97785 | .00255 | -.00205 | +.00086 | .00544 |
| 9.2 | .97830 | .00216 | -.00178 | .00185 | .00399 |
| 9.4 | .97869 | .00185 | -.00135 | .00249 | .00210 |
| 9.6 | .97902 | .00163 | -.00083 | .00272 | .00009 |
| 9.8 | .97933 | .00152 | -.00031 | .00255 | -.00175 |
| 10.0 | .97964 | .00150 | .00014 | .00204 | -.00316 |
| 10.2 | .97995 | .00157 | .00047 | .00129 | -.00399 |
| 10.4 | .98028 | .00168 | .00064 | .00045 | -.00416 |
| 10.6 | .98064 | .00181 | .00064 | -.00037 | -.00372 |
| 10.8 | .98102 | .00193 | .00050 | -.00105 | -.00278 |
| 11.0 | .98142 | .00200 | .00024 | -.00149 | -.00151 |
| 11.2 | .98183 | .00202 | -.00007 | -.00166 | -.00014 |
| 11.4 | .98223 | .00197 | -.00039 | -.00156 | .00113 |
| 11.6 | .98261 | .00187 | -.00066 | -.00122 | .00213 |
| 11.8 | .98297 | .00171 | -.00086 | -.00072 | .00272 |
| 12.0 | .98329 | .00153 | -.00094 | -.00014 | .00286 |
| 12.2 | .98357 | .00134 | -.00091 | .00042 | .00256 |
| 12.4 | .98381 | .00117 | -.00078 | .00088 | .00191 |
| 12.6 | .98403 | .00104 | -.00057 | .00118 | .00101 |
| 12.8 | .98422 | .00095 | -.00033 | .00129 | .00003 |
| 13.0 | .98441 | .00091 | -.00008 | .00120 | -.00088 |

| Z | I(z) | I'(z) | I''(z) | I'''(z) | $I^{IV}(z)$ |
|---|---|---|---|---|---|
| 13.2 | .98459 | .00091 | .00014 | .00094 | -.00159 |
| 13.4 | .98478 | .00096 | .000287 | .00057 | -.00202 |
| 13.6 | .98498 | .00102 | .00036 | .00015 | -.00212 |
| 13.8 | .98520 | .00109 | .00035 | -.00026 | -.00189 |
| 14.0 | .98542 | .00116 | .00026 | -.00060 | -.00140 |
| 14.2 | .98566 | .00119 | .00011 | -.00082 | -.00073 |
| 14.4 | .98590 | .00120 | -.00006 | -.00090 | -.00000 |
| 14.6 | .98614 | .00117 | -.00023 | -.00083 | .00068 |
| 14.8 | .98637 | .00111 | -.00038 | -.00063 | .00121 |
| 15.0 | .98658 | .00102 | -.00047 | -.00035 | .00152 |
| 15.2 | .98677 | .00092 | -.00051 | -.00003 | .00159 |
| 15.4 | .98694 | .00082 | -.00049 | .00028 | .00141 |
| 15.6 | .98710 | .00073 | -.00041 | .00052 | .00102 |
| 15.8 | .98723 | .00066 | -.00028 | .00068 | .00051 |
| 16.0 | .98736 | .00062 | -.00014 | .00073 | -.00005 |

# APPENDIX B

## Computer Programmes.

Besides a desk calculating machine, two computers, a National Elliot 803A and an IBM7090, were used in the present work for the theoretical calculations. The National Elliot 803A is a slow computer compared with the IBM7090. In the beginning, a program for the two-dimensional proposed new model (equation 2:31) was written for the National Elliot 803A. It was found that the running time required to obtain each point on the curve was nearly one hour (for 130 X 65 recepter units). Therefore, it became necessary to change the program to Fortran IV language for use with the IBM7090 computer, and then only 4.6 minutes were taken for the whole curve (40 points). The IBM7090 was then used for the proposed new models (equations 2:30 and 2:31) for one and two dimensions, the modified model of Fry (equation 2:29), the Hartline-Ratliff model and the Taylor model. The National Elliot 803A, however, was used for the incoherently illuminated straight edge image and its derivatives, the second derivatives of the luminance distributions of the experimentally produced gradients, the O'Brien model and the Békésy model.

In fact, for the IBM7090, two main programmes were needed, one for the Hartline-Ratliff model and another

one for the two-dimensional proposed model (equation 2:31). Then, the program for the Taylor model could be modified from the program of the Hartline-Ratliff model; and the programmes for the modified model of Fry (equation 2:29) and another proposed new model (equation 2:30) could be modified from the program for equation 2:31. Here the two main programmes are given.

1. The program for the two-dimensional proposed new model (equation 2:31).

The response of this model is given by,

$$F = \frac{I(x,y)}{1 + \dfrac{A\iint I(x-x',y-y')\left[(x-x')^2+(y-y')^2\right]\exp\left[-\dfrac{(x-x')^2+(y-y')^2}{2\sigma^2}\right]dxdy.}{\iint I(x-x',y-y').\ \exp.\left[-\dfrac{(x-x')^2+(y-y')^2}{2\sigma^2}\right]dxdy.}}$$

where A and $\sigma$ are constants. The program is as follows:-

Subroutine.

```
      SUBROUTINE SIM21(AA,N,S,E)
      DIMENSION AA(N)
      B=AA(1)+AA(N)
      M=N-1
      C=0.0
      DO 5 I=2,M,2
    5 C=C+AA(I)
```

```
      C=4.0*C
      M=N-2
      D=0.0
      DO 6 I=3,M,2
    6 D=D+AA(I)
      D=2.0*D
      E=(B+C+D)*(S/3.0)
      RETURN
      END
```

Main.

```
      DIMENSION F(250),T1(131),T2(131),T3(65),T4(65)
      READ(5,106) IF
      NF=0
  300 NF=NF+1
      IF (NF.GT.IF) GO TO 600
      READ(5,102) (F(I),I=1,250)
      WRITE(6,104) (F(I),I=1,250)
      READ(5,106) IS
      NS=0
  400 NS=NS+1
      IF (NS.GT.IS) GO TO 300
      READ(5,101) S,A,K,N1,N2
      WRITE(6,103) S,A,K
      IX=N1
  200 N3=50+IX
```

```
      DO 20 J=1,65
      JZ=J-1
      DO 13 I=1,65
      ID=66-I
      IZ=N3-I
      Z=FLOAT(I**2+JZ**2)
      Y=EXP(-Z/(2.0*(S**2)))
      T1(ID)=F(IZ)*Z*Y
   13 T2(ID)=F(IZ)*Y
      Z=FLOAT(JZ**2)
      Y=EXP(-Z/(2.0*(S**2)))
      T1(66)=F(N3)*Z*Y
      T2(66)=F(N3)*Y
      DO 15 I=1,65
      ID=66+I
      IZ=N3+I
      Z=FLOAT(I**2+JZ**2)
      Y=EXP(-Z/(2.0*(S**2)))
      T1(ID)=F(IZ)*Z*Y
   15 T2(ID)=F(IZ)*Y
      CALL SIM21(T1,131,1.0,G1)
      CALL SIM21(T2,131,1.0,G2)
      T3(J)=G1
   20 T4(J)=G2
      CALL SIM21(T3,65,1.0,H1)
```

```
      CALL SIM21(T4,65,1.0,H2)
      B=2.0*H1-T3(1)
      C=2.0*H2-T4(1)
      E=(K*F(N3))/(1+(A*B/C))
      WRITE(6,105) IX,E
      IX=IX+3
      IF (IX.LE.N2) GO TO 200
      GO TO 400
  600 CONTINUE
  101 FORMAT(3F10.5,2I10)
  102 FORMAT(50(5F10.5/))
  103 FORMAT(11H INPUT DATA/,8H SIGMA=,F10.5,3H
     A=,F10.5,3H K=,F10.5)
  104 FORMAT(7H I(X,Y)/,25(10F10.5/)//)
  105 FORMAT(4H XO=,I3,3H E=,F10.5)
  106 FORMAT(I2)
      STOP
      END
```

The subroutine program was for summing up all the areas under the curve. Simpson's rule was used. The inhibitory area on the retina was limited by the value of $\sigma$ (S, in the program). The bigger the value of $\sigma$ the bigger the inhibitory area involved. The proper parameters were chosen to give the amplitudes of the bands nearest to those obtained from the experiments. $\sigma$ =0.9 was found to give good predic-

tions on the positions of the subjective bands. A=0.2 was then found to be the suitable value when $\sigma$ =0.9. The final results were normalized to the same as the upper luminance levels of the physical distributions by the factor K in the main program. The computation time needed for one set of data was 4.6 minutes. For the one-dimensional model the time taken was 0.6 minute for the same set of data. The same amount of the time was needed when the program was adapted for equation 2:29 (the modified model of Fry) and equation 2:30. The one-dimensional model of Fry, however, gave the same results as those given by the two-dimensional newly proposed model.

2. The program for the Hartline-Ratliff model.

The program is based on the following equations:-

$$f_i = e_i - \sum_{\substack{j=1 \\ \neq i}}^{n} K_{i,j}(f_j - f^o_{i,j}),$$

where, $K_{i,j} = B/(i-j)^2$,

and, $f^o_{i,j} = C(i-j)^2$,

B and C are constants. All the limiting conditions were taken into account.

Main.

```
      DIMENSION F(150,7),V(150,7),VI(150)
      READ(5,101) B,C,IR,IP,K
      WRITE(6,102) B,C,K
      READ(5,103) (VI(I),I=1,150)
      DO 10 J=1,IP
      DO 40 I=1,IR
   40 V(I,J)=VI(I)
   10 CONTINUE
      DO 90 L=1,K
      WRITE(6,105) L
      DO 50 I=1,IR
      DO 60 J=1,IP
      Y=0.0
      DO 70 N=1,IP
      DO 80 M=1,IR
      IFOIJ=((I-M)**2)+((J-N)**2)
      IF (IFOIJ.EQ.0) GO TO 80
      AKIJ=FLOAT(IFOIJ)
      FOIJ=C*AKIJ
      AKIJ=B/AKIJ
      Z=AKIJ*(V(M,N)-FOIJ)
      IF (Z.LT.0.0) GO TO 80
      Y=Y+Z
   80 CONTINUE
```

```
 70 CONTINUE
    F(I,J)=VI(I)-Y
 60 CONTINUE
    WRITE(6,106) I,(F(I,J),J=1,IP)
 50 CONTINUE
    DO 20 J=1,IP
    DO 30 I=1,IR
 30 V(I,J)=F(I,J)
 20 CONTINUE
 90 CONTINUE
101 FORMAT(2F10.5,3I10)
102 FORMAT(3H B=,F10.5,3H C=,F10.5,3H K=,I3)
103 FORMAT(30(5F10.5/))
105 FORMAT(3H L=,I2)
106 FORMAT(1H ,I3,2X5(E12.5,3X))
    STOP
    END
```

The symbol K in the program denotes the number of iterations. The running time for one iteration was 3.1 minutes for 150 x 5 receptors. It was found that for B=0.1 and C=0.02, 10 iterations had to be carried out to obtain a solution accurate to the second decimal place. Therefore, the number of runs was limited. The values of parameters could not be chosen properly in order to bring the brightness of the bands up to the same as those obtained from experiments.

## REFERENCES.

ABRAMOWITZ,M. and STEGUN,I.A. (1965) 'Handbook of Mathematical Functions', U.S. Government Printing Office, P.495-497.

BARLOW,H.B., FITZHUGH,R. and KUFFLER,S.W. (1957) J. Physiol., 137, 338.

BÉKÉSY,G.VON. (1959) J. Acoust. Soc. Am., 31, 1236.

BÉKÉSY,G.VON. (1960) J. Opt. Soc. Am., 50, 1060.

BICKLEY,W.G. (1948) J. Math. and Phys., 27, 183.

BITTINI,M., ERCOLES,A.M., FIORENTINI,A., RONCHI,L. and TORALDO DI FRANCIA,G. (1960) Atti Fond. Giorgio Ronchi, 15, 62.

BYRAM,G.M. (1944) J. Opt. Soc. Am., 34, 571-591, 718-737.

CAMPBELL,F.W. and GUBISCH,R.W. (1966) J. Physiol., 186, 558.

CHARMAN,W.N. (1961) Ph.D.Thesis, University of London, P.82.

CHARMAN,W.N. and WATRASIEWICZ,B.M. (1964) J. Opt. Soc. Am., 54, 791.

CHEATHAM,P.G. (1952) J.Exp. Psychol., 43, 369.

CORNSWEET,T.N. (1956) J. Opt. Soc. Am., 46, 987.

DITCHBURN,R.W. (1955) Optica Acta, 1, 171.

DITCHBURN,R.W. and GINSBORG,B.L. (1953) J. Physiol., 119, 1.

ERCOLES,A.M. and FIORENTINI,A. (1959) Atti Fond. Giorgio Ronchi, 14, 230.

FENDER,D.H. (1955) Brit. J. Ophth., 39, 65.

FIORENTINI,A. (1956) 'Problems in Contemporary Optics', P.600.

FIORENTINI,A. and ERCOLES,A.M. (1957) Optica Acta, 4, 150.

FIORENTINI,A. and RADICI,T. (1958) Atti Fond. Giorgio Ronchi, 13, 145.

FIORENTINI,A., JEANNE,M. and TORALDO DI FRANCIA,G. (1955) Atti Fond. Giorgio Ronchi, 10, 371.

FRY,G.A. (1948) Am. J. Optom., 25, 162.

GRANIT,R. (1933) J. Physiol., 77, 207.

GRANIT,R. and THERMAL,P.O. (1935) J. Physiol., 83, 359.

GREEN,P.H. (1957) Bull. Math. Biophys., 19, 147.

GREEN,P.H. (1958) Factors in Visual Acuity, Aeromedical Division, U.S. Air Force of Scientific Research; AF 18 (600) 1454, Project 9777, University of Chicago.

HARTLINE,H.K. (1938) Am. J. Physiol., 121, 400.

HARTLINE,H.K. and RATLIFF,F. (1954) Science, 120, 781.

HARTLINE,H.K. and RATLIFF,F. (1957) J. Gen. Physiol., 40, 357.

HARTLINE,H.K. and RATLIFF,F. (1958) J. Gen. Physiol., 41,1049.

HARTLINE,H.K., WAGNER,H.G. and RATLIFF,F. (1956) J. Gen. Physiol., 39, 651.

HARTREE,D.R. (1952) 'Numerical Analysis', The Claendon Press.

HARTWIG,E. (1958) Optik, 15, 414.

IVANOFF,A. (1953) 'Les Aberrations de L'Oeil, Leur Role Dans L'Accommodation', Editions de La Revue d'Optique Theorique et Instrumentale, Paris 1953

IVANOFF,A. (1956) J. Opt. Soc. Am., 46, 901.

ILFORD MANUAL OF PHOTOGRAPHY 1958

JAHNKE,E. and EMDE,F. (1945) 'Table of Functions', Dover Publications, Inc., N.Y.

KEESY,U.T. (1960) J. Opt. Soc. Am., 50, 769.

KOOMEN,K., TOUSEY,R. and SCOLNIK,R. (1949) J. Opt. Soc. Am., 39, 370.

KRAUSKOPF,J. (1962) J. Opt. Soc. Am., 52, 1046.

LEELAWONGS,R. (1964) M.Sc.Thesis, University of London.

LE GRAND,Y. (1957) 'Light, Colour and Vision', Chapman and Hall, P. 104.

LOWRY,E.M. and DE PALMA,J.J. (1961) J. Opt. Soc. Am., 51, 740.

LUDVIGH,E. (1940) Arch. Ophth., 43, 397.

LUDVIGH,E. (1953) Joint Project Nos. 4 and 5, U.S. Naval School of Aviation Medicine, Pensacola, Fla.

MACH,E. (1865) Sitzungsberichte der mathematisch-naturwissenschaftlichen Classe der kaiserlichen Akademie der Wissenschaften, 52, 303.

MACH,E. (1866a) Sitzungsberichte der mathematisch-naturwissenschaftlichen Classe der kaiserlichen Akademie der Wissenschaften, 54, 131.

MACH,E. (1866b) Sitzungsberichte der mathematisch-naturwissenschaftlichen Classe der kaiserlichen Akademie der Wissenschaften, 54, 393.

MACH,E. (1868a) Sitzungsberichte der mathematisch-naturwis-

senschaftlichen Classe der kaiserlichen Akademie der Wissenschaften, 57, 11.

MACH,E. (1868b) Vierteljahresschrift für Psychiatrie in ihren Beziehungen zur Morphologie und Pathologie des Centralen Nervensystems, 2, 38.

MACH,E. (1906) Sitzungsberichte der mathematisch-naturwissenschaftlichen Classe der kaiserlichen Akademie der Wissenschaften, 115, 633.

MARIMONT,R.B. (1963) J. Opt. Soc. Am., 53, 400.

MARTIN,L.C. and JOHNSON,B.K. (1958) 'Practical Microscopy', Blackie and Son Ltd., P. 33.

MATTHEWS,M.L. (1966) J. Opt. Soc. Am., 56, 1401.

McCOLLOUGH,C. (1955) J. Exp. Psychol., 49, 141.

McDOUGALL,W. (1903) Proc Physiol. Soc., 1, 19.

MEES,C.E. (1952) 'The Theory of the Photographic Process', New York, The Macmillan Company.

MENZEL,E. (1959) Die Naturwissenschaften, 46, 316.

O'BRIEN,V. (1958) J. Opt. Soc. Am., 48, 112.

RATLIFF,F. and HARTLINE,H.K. (1959) J. Gen. Physiol., 42, 1241.

RATLIFF,F., HARTLINE,H.K. and MILLER,W.H. (1963) J. Opt. Soc. Am., 53, 110.

RIGGS,L.A., RATLIFF,F., CORNSWEET,J.C. and CORNSWEET,T.N. (1953) J. Opt. Soc. Am., 43, 495.

RONCHI,L., BITTINI,M. and ADACHI,I. (1963) Optik, 20, 132.

ROWE,S.H. (1966) Microscope and Crystal Front, 15, 216.

SCHOUSTEN,J.F. and ORNSTEIN,L.S. (1939) J. Opt. Soc. Am. 29, 168.

SHERRINGTON,C.S. (1897) J. Physiol., 21, 33.

STENSTRÖM,S. (1964) 'Optics and the Eye', Butterworth, P. 105.

TAYLOR,W.K. (1956) 'Information Theory', Colin Cherry ed., New York, Academic Press.

THOMAS,J.P. (1963) J. Opt. Soc. Am., 53, 1033.

THOMAS,J.P. (1965) J. Opt. Soc. Am., 55, 521.

THOULESS,R.H. (1922-3) Brit. J. Psychol., 13, 301.

WALD,G. and GRIFFIN,D.R. (1947) J. Opt. Soc. Am., 37, 321.

WATRASIEWICZ,B.M. (1964) Ph.D. Thesis, University of London.

WATRASIEWICZ,B.M. (1963) Optica Acta, 10, 209.

WESTHEIMER,G. and CAMPBELL,F.W. (1962) J. Opt. Soc. Am., 52, 1040.

## ACKNOWLEDGEMENTS

I wish to express my gratitude and sincere thanks to Dr. W. T. Welford for suggesting the problem and for his kind guidance throughout the progress of this work.

My thanks are also due to Dr. Watrasiewicz who provided an IBM 7090 programme for the model of Hartline and Ratliff, and to friends who willingly helped by making tiresome measurements.

I am also indebted to the Colombo Plan authorities for their generous grant towards this work.